Table of contents

List of figures

Chapter 1

Chapter 2

Chapter 3

Chapter 4

Chapter 5

List of tables

Chapter 2

Chapter 3

Chapter 4

List of abbreviations

%	Percentage
λ_{em}	Emission wavelength
λ_{ex}	Excitation wavelength
γ	Gamma
$\Delta\psi_m$	Mitochondrial membrane potential
2ME	2-Methoxyestradiol
2DG	2-Deoxy-d-glucose
3-BrPA	3-Bromopyruvate
A	Ampere
Ac-DEVD-AMC	Acetyl Asp-Glu-Val-Asp 7-amido-4-methylcoumarin
Ac-IETD-AMC	Acetyl-Ile-Glu-Thr-Asp 7-amido-4-methylcoumarin
Ac-LEHD-AFC	Acetyl-Leu-Glu-His-Asp 7-amino-4-trifluoromethylcoumarin
ADP	Adenosine diphosphate
AIDS	Acquired immune deficiency syndrome
AIF	Apoptosis inducing factor
ALT	Alanine aminotransferase
α-CD3	α-Chain of cluster of differentiation protein 3
α-CD95	α-Chain of cluster of differentiation protein 95
ANOVA	Analysis of variance
ANT	Adenine nucleotide translocator
Apaf-1	Apoptotic protease activating factor 1
ARF	Alternative reading frame protein of *INK4a*
Asp	Aspartic acid
ATCC	American Type Culture Collection
Atg	Autophagy protein
ATP	Adenosine triphosphate
Bad	Bcl2-associated death promoter protein
Bak	Bcl-2 antagonist/killer

Bax	Bcl-2-associated X protein
Bcl-2	B-cell lymphoma 2 protein
Bcl-X_L	B-cell lymphoma-extra large protein
BH3	Bcl-2 homology domain 3
BID	BH3 interacting-domain protein
BRCA1	Breast cancer 1 protein
BRCA1	Breast cancer 1 gene
BRCA2	Breast cancer 2 gene
BSA	Bovine serum albumin
BW	Body weight
℃	Degrees Celsius
Ca^{++}	Calcium ion
CAD	Caspase-activated deoxyribonuclease
cAMP	Cyclic adenosine monophosphate
Caspase	Cysteine-aspartic acid proteases
CED-3	Cell death protein 3
CI	Combination Index
CICD	Caspase-independent cell death
CMFT	Combination of cyclophosphamide, methotrexate, fluorouracil and tamoxifen
CO_2	Carbon dioxide
COMT	Catechol-o-methyl transferase
CypD	Cyclophilin D
dATP	2'-deoxyadenosine 5'-triphosphate
DCFH-DA	2',7'-dichlorodihydrofluoresceindiacetate
dH_2O	Distilled water
DISC	Death-inducing signalling complex
DMEM	Dulbecco's Modified Eagle's Medium
DMSO	Dimethylsulfoxide
DNA	Deoxyribonucleic acid
ECL	Enhanced chemiluminescence

EDTA	Ethylenediaminetetraacetic acid
eIF2α	Eukaryotic translation initiation factor 2α
ELISA	Enzyme-linked immunosorbent assay
EndoG	Endonuclease G
ER	Endoplasmic reticulum
ESE-15-ol	2-Ethyl-3-O-sulphamoyl-estra-1,3,5(10),15-tetraen-17-ol
ESE-16	2-Ethyl-3-O-sulfamoyl-estra-1,3,5(10)16-tetraene
ETC	Electron transport chain
fa	Fraction affected
FADD	Fas-associated death domain protein
FAS	Fasentin
FCS	Foetal calf serum
Fe^{2+}	Ferrous iron
Fe^{3+}	Ferric iron
Fig	Figure
FITC	Fluorescein isothiocyanate
g	Gram
g	Gravity
G_1 phase	Growth 1 phase
G_2/M phase	Gap-2/mitosis
GI_{50}	50% Growth inhibitory concentration
GLUT	Glucose transporter
g/l	Grams per litre
g/mol	Grams per mole
GSH	Reduced glutathione
GSSG	Glutathione disulfide
h	Hour
H^+	Hydrogen ion
HCO_3^-	Bicarbonate
H_2O_2	Hydrogen peroxide

HbO_2	Oxygenated haemoglobin
HBSS	Hank's Buffered Salt Solution
HEPES	4-(2-hydroxyethyl)-1-piperazineethanesulfonic acid
Her2/neu	Human epidermal growth factor receptor 2
HIF-1	Hypoxia-inducible factor-1
HIF-1α	Hypoxia-inducible factor-1α
HIF-1β	Hypoxia-inducible factor-1β
HIV	Human immunodeficiency virus
HRP	Horseradish peroxidase
HSP	Heat shock protein
HSP70	Heat shock protein 70
HtrA2	High-temperature requirement protein A2
HUVEC	Human umbilical vein endothelial cell
IAP	Inhibitor of apoptosis
ICAD	Inhibitor of caspase-activated deoxyribonulease
IC_{50}	Concentration of compound which results in 50% inhibition
i.e.	Id est
IgG	Immunoglobulin G
IND	Indinavir
i.v.	Intravenous
JC-1	5,5',6,6'-tetrachloro-1,1',3,3'-tetraethylbenzimidazolcarbo-cyanine iodide
kDa	Kilodalton
l	Litre
LC3	Microtubule-associated protein 1A/1B-light chain 3
LC3-I	Cytoplasmic form of microtubule-associated protein 1A/1B-light chain 3
LC3-II	Microtubule-associated protein 1A/1B-light chain 3 with the addition of phosphatidylethanolamine
LC-MS/MS	Liquid chromatography coupled to mass spectrometry
LON	Lonidamine
MAPK	Mitogen-activated protein kinases

mCB	Monochlorobimane
MDR1	Multi-drug resistance gene 1
Mg^{++}	Magnesium ion
mg	Milligram
mg/m^2	Milligram per square meter
min	Minute
ml	Millilitre
mm	Millimeter
mM	Millimolar
MOPS	3-(N-Morpholino)propanesulfonic acid
MPP	Mitochondrial processing protease
MPT	Mitochondrial permeability transition
MPTP	Mitochondrial permeability transition pore
mtDNA	Mitochondrial deoxyribonucleic acid
mTOR	Mammalian target of rapamycin
MTS	3-(4,5-dimethylthiazol-2-yl)-5-(3-carboxymethoxyphenyl)-2-(4-sulfophenyl)-2H-tetrazolium
m/v	Unit of mass per unit of volume
MW	Molecular mass
n	Number of assays or Amount of substance
N	Normality
NADH	Nicotinamide adenine dinucleotide
NADPH	Reduced nicotinamide adenine dinucleotide phosphate
$NaHCO_3$	Sodium bicarbonate
nM	Nanomolar
NMR	Nuclear magnetic resonance spectroscopy
NSABP	National Surgical Adjuvant Breast and Bowel Project
O_2	Oxygen
O^{2-}	Superoxide radical
p53	Tumour suppressor protein 53

p53	Gene encoding for tumour suppressor protein 53
p	Probability
PARP	Poly (ADP-ribose) polymerase
PBS	Phosphate buffered saline
PBS-T	Phosphate buffered saline supplemented with Tween-20
PC	Positive control
PE	Phosphatidylethanolamine
PERK	Protein kinase-like endoplasmic reticulum kinase
pg	Picogram
pg/ml	Picogram per millilitre
pH	Negative logarithm of the hydrogen ion concentration
PI	Propidium iodide
PINK-1	PTEN-induced putative kinase-1
PlasDIC	Polarisation-optical differential interference contrast microscopy
PMSF	Phenylmethanesulfonylfluoride
pRB	Retinoblastoma protein
PS	Phosphatidylserine
PTEN	Phosphatase and tensin homologue
PVDF	Polyvinylidene fluoride
QUER	Quercetin
rads	Deprecated unit of absorbed radiation dose
ROS	Reactive oxygen species
RPMI-1640	Roswell Park Memorial Institute
RSA	Republic of South Africa
SCID	Severely combined immune-deficient
SEM	Standard error of the mean
SRB	Sulforhodamine B
T_0	Experiment performed at time zero or exposure time
TCA	Trichloroacetic acid
TEM	Transmission electron microscopy

TGF-α	Transforming growth factor-α
TNBC	Triple negative breast cancer
TNF-α	Tumour necrosis factor-α
TORC1	Target of Rapamycin complex 1
TRIS	Tris(hydroxymethyl)aminomethane
µg	Microgram
µg/ml	Micrograms per millilitre
UK	United Kingdom
µl	Microlitre
µm	Micrometer
µM	Micromolar
UPR	Unfolded protein response
USA	United States of America
V	Volts
VC	Vehicle control
VDAC	Voltage dependent anion channel
VEGF	Vascular endothelial growth factor
VEGF	Gene encoding for vascular endothelial growth factor
VEGF-A	Vascular endothelial growth factor
VEGF-R	Vascular endothelial growth receptor
v/v	Volume per volume
WHO	World Health Organisation
WT-1	Wilms' tumour protein 1
w/v	Weight per volume
w/w	Weight per weight

Chapter 1: Introduction

1.1 A brief overview of the aetiology of cancer

In order to effectively target malignancies with chemotherapy, differences between malignant and non-malignant tissue must be exploited. Despite advances in cancer research, insight into the process of oncogenesis is confounded by the intrinsic heterogeneity of tumour cells (Pelicano *et al.*, 2006). The essence of the transformation of a normal cell to cancerous tissue is the initiation of a state of unlimited proliferation (Aaronson, 1991; Schmitt, 2003). It has been suggested that the process by which normal cells transform into malignant cells with unlimited replicative potential depends on concurrent mutations in a variety of genes including proto-oncogenes and tumour suppressor genes (Hahn and Weinberg, 2002).

In early studies it was observed that the administration of a mutant strain of polyoma virus to hamsters induced neoplastic transformation (Fried, 1965). The use of deoxyribonucleic acid (DNA) viruses to study carcinogenesis, which led to the identification of oncogenes, was confounded by the involvement of the genes in viral DNA replication; a process eliminated by the use of retroviruses (Bishop, 1985). Using retroviruses, carcinogenesis could be successfully induced in chicken and murine cells and the viral genes responsible for the transformation became known as oncogenes. Oncogenes were demonstrated to be mutated versions of proto-oncogenes expressed in non-transformed cells (Bishop, 1982). This approach led to the identification of numerous oncogenes including *c-myc* (Vennstrom *et al.,* 1982)*, c-myb, c-erb* (Gonda *et al.*, 1982) and *c-raf* (Rapp *et al.,* 1983).

The complexity of human carcinogenesis was demonstrated where neoplastic transformation could not be induced in human cells with activated *v-myc, v-ras* (Stevenson and Volsky, 1986) or *c-ras* (Sager *et al.*, 1983). It was demonstrated that a combination of oncogenes were required to induce carcinogenesis in primary rodent cells (Land *et al.*, 1982; Ruley, 1983). However, similar success was not achieved in human cells suggesting that a more complicated transformation process is required (Stevenson and Volsky, 1986). Neoplastic conversion of human epithelial and fibroblast cells was finally achieved with the ectopic expression of two oncogenes and a mutation in telomerase indicating that the alteration of multiple intracellular pathways are required for human carcinogenesis (Hahn *et al.*, 1999).

In addition to the activation of proto-oncogenes, carcinogenesis depends on the inactivation of tumour suppressor genes (Weinberg, 1991). Loss of chromosomes were associated with mutagenicity in hybrid cells created from Ehrlich and A9 murine cells (Harris, 1971). It was

suggested that this chromosomal loss was involved in the development of human retinoblastoma (Knudson, 1971) and Wilms' tumour (Knudson and Strons, 1972). These observations led to the discovery of the tumour suppressor protein, retinoblastoma protein (pRB), implicated in regulation of progression through the cell cycle (Buchkovich *et al.*, 1989) and the Wilms' tumour protein, WT-1 protein, involved in transcriptional regulation of early growth response protein 1 (Madden *et al.*, 1991).

The most reported tumour suppressor gene product is tumour suppressor protein 53 (p53). A mutation in the *p53* tumour suppressor gene has been identified in more than 50% of all human malignancies (Levine, 1997). This protein, with a molecular mass of 53 kDa, was identified in immunoprecipitation studies conducted in chemically induced murine sarcoma, but was not detected in normal murine cells (DeLeo *et al.*, 1979). The expression of wild type *p53* was demonstrated to inhibit neoplastic transformation (Eliyahu *et al.*, 1989) and regulate cell proliferation (Baker *et al.*, 1990). Cell cycle progression is regulated by p53: if DNA damage is detected a cell is arrested in the G_1phase of the cell cycle (Mathupala *et al.*, 1997b).

The combined alterations in proto-oncogenes and tumour suppressor genes result in uncontrolled cell proliferation (Weinberg, 1991). The most common characteristics have been described in terms of the 'hallmarks of cancer': changes fundamental to cancerous cells, organised into a few key characteristics (Hanahan and Weinberg, 2000; Hanahan and Weinberg, 2011). These hallmarks are summarised in Figure 1.1.

In order to sustain a high rate of proliferation tumour cells manipulate numerous mitogenic signalling pathways, including the epidermal growth factor receptor pathway (Perona, 2006). The carcinogenic potential of mutations affecting tyrosine kinase receptor pathways were demonstrated to enhance cell proliferation *in vitro* (Kokai *et al.*, 1989). Replication of malignant tissue is further supported by hyperactivation of intracellular pathways regulating cell growth including the mitogen-activated protein kinase (MAPK) and Akt pathways (Tsao *et al.*, 2004). Down-regulation of endogenous inhibitors of mitogen-activated protein kinase pathways also promotes cancer cell proliferation (Kwabi-Addo *et al.*, 2004; Lo *et al.*, 2004).

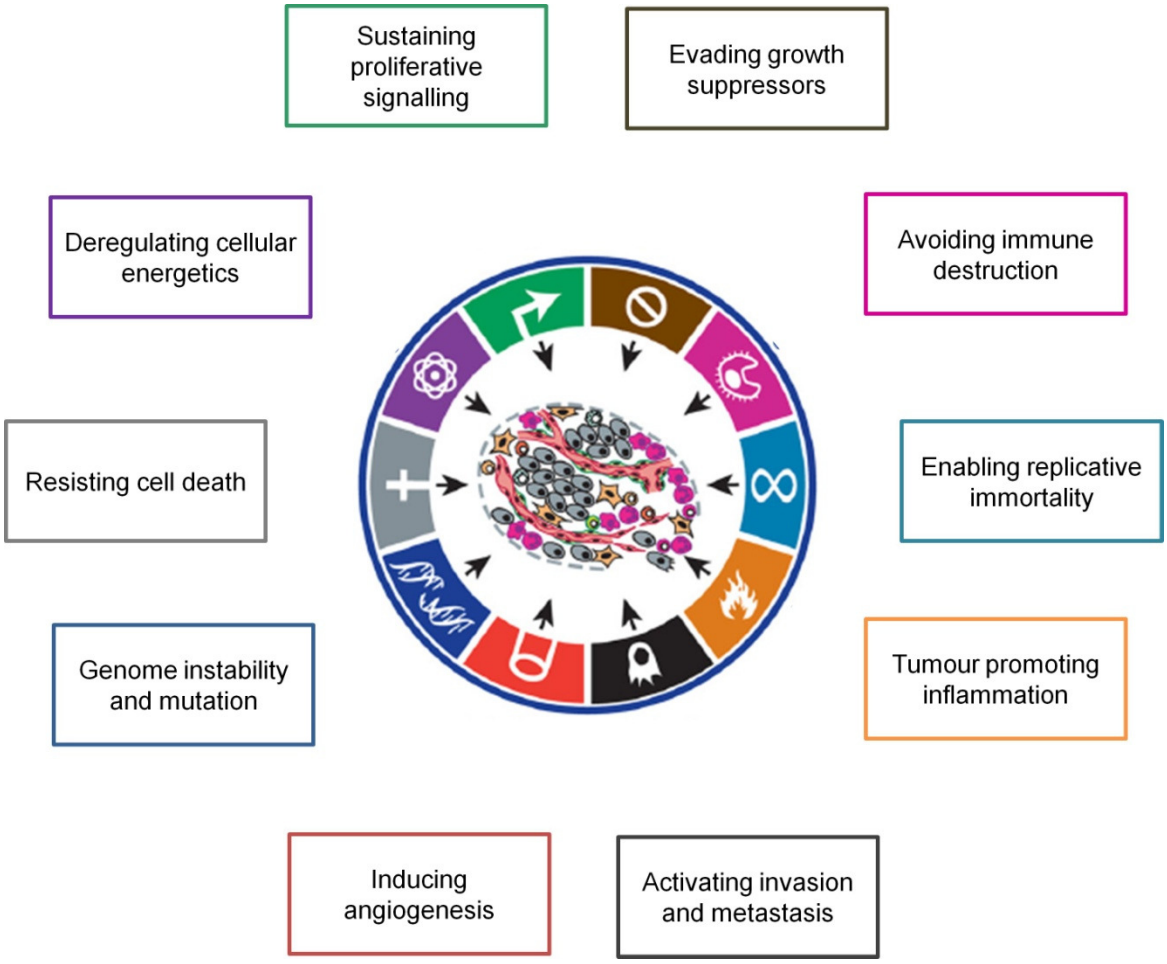

Figure 1.1: Cell characteristics referred to as the 'Hallmarks of Cancer' required for neoplastic transformation.
From (Hanahan and Weinberg, 2011), with modifications. Used with permission.

Cellular homeostasis is maintained by a balance between both proliferation and apoptosis. Deregulation of the pro-death mechanisms is associated with development of cancer (Desagher and Martinou, 2000). Tumourigenic cells may evade pro-death signals by induction of pro-survival autophagy (Gu *et al.*, 2015). Moreover, conditions of nutrient deprivation, stress or exposure to cytotoxic agents have been shown to induce autophagy which guarantees propagation of cells which may otherwise be eliminated, providing an evolutionary advantage (Jin and White, 2007).

Tumourigenic tissue employs numerous strategies to evade cell death including expression of inhibitors of apoptosis (IAP). The expression of survivin, an IAP inhibitor, in breast cancer cells is associated with a low apoptotic index and therefore poor clinical prognosis (Tanaka *et al.*, 2000). Increased expression of B-cell lymphoma 2 (Bcl-2) protein family members is

associated with evasion of apoptosis. *In vitro* over-expression of Bcl-2 in cancer cells prevented the release of cytochrome *c* from the mitochondria, a crucial step in the induction of apoptosis (Yang and Liu, 1997).

Two additional 'hallmarks' of cancer will be briefly reviewed. First the increased glucose demand and metabolism needed to supply the altered energy requirements for the high proliferation rate. Secondly the ability of tumourigenic cells to induce angiogenesis as a means to invade and establish secondary tumour sites will also be discussed.

1.2 Altered metabolism: aerobic glycolysis

Otto Warburg and colleagues first described the prevalence of aerobic glycolysis in malignant cells in 1924 and consequently this phenomenon is known as the 'Warburg effect' (Warburg *et al.*, 1924). Oxidative phosphorylation, the metabolic pathway used under normoxic conditions, produces 36 molecules of adenosine triphosphate (ATP) for every molecule of glucose consumed, whereas glycolysis yields only 2 molecules of ATP per molecule of glucose used (Pelicano *et al.*, 2006). Non-malignant cells rely primarily on glycolysis to produce ATP in the presence of oxygen (Warburg *et al.*, 1924). During the process of glycolysis, glucose is metabolised to pyruvate yielding 2 molecules of ATP. Under anaerobic conditions pyruvate is further reduced to lactic acid, while pyruvate is transported to the mitochondria for oxidation in the presence of oxygen (Pelicano *et al.*, 2006) (Figure 1.2). Oxidation of pyruvate during the tricarboxylic acid cycle produces carbon dioxide, water and 36 molecules of ATP (Gatenby and Gillies, 2004).

The first step in glycolysis is the ATP-dependent conversion of glucose to glucose-6-phosphate by hexokinases, the only rate limiting step in glycolysis (Pelicano *et al.*, 2006). Four hexokinase isozymes have been identified differing in localisation: Type I is most abundant with high expression levels found especially in the brain, Type II is mostly found in insulin-sensitive or malignant tissue whereas Type IV is mostly found in the liver (Wilson, 2003; Pelicano *et al.*, 2006). The phosphorylated form of glucose cannot be effluxed by glucose transporters (GLUT) and its accumulation results in inhibition of hexokinases Type I - III (Pelicano *et al.*, 2006). Glucose-6-phosphate may initiate the pentose phosphate pathway or glycolic pathway to generate bio-molecules, including nicotinamide adenine dinucleotide (NADH) and ribose-5-phosphate, or induce the formation of glycogen as the storage form of glucose (Wilson, 2003).

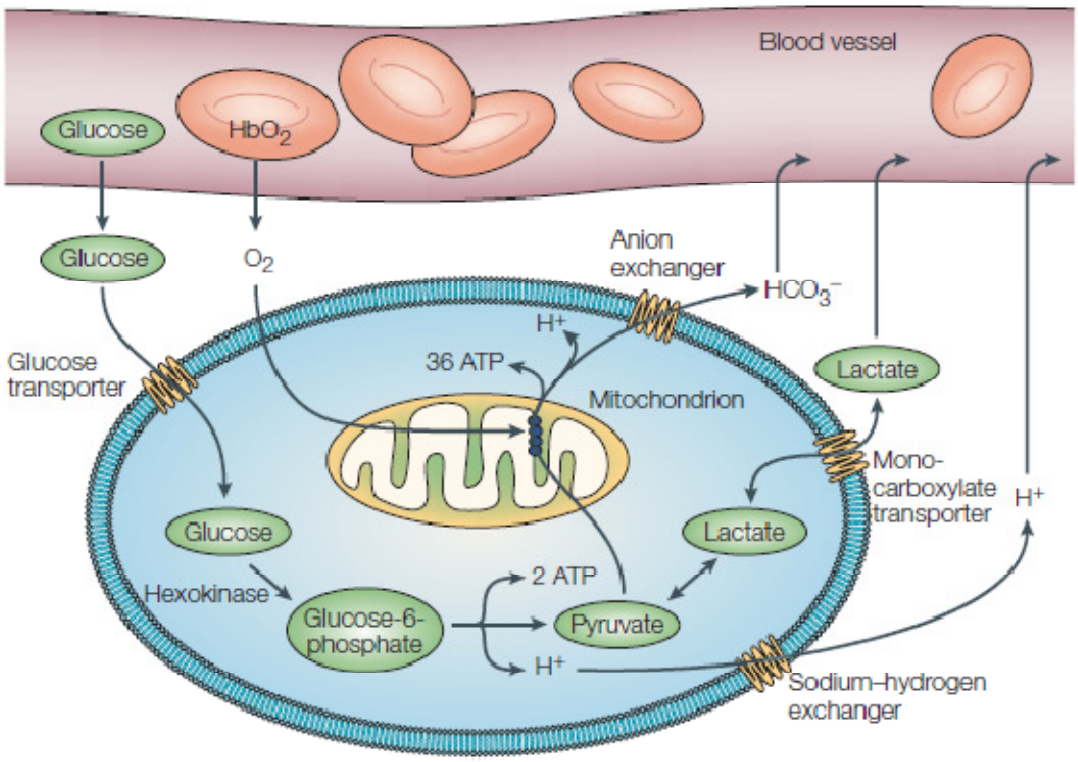

Figure 1.2: ATP production in mammalian cells. Glucose is transported into the intracellular environment by transmembrane glucose transporters. The first step of glycolysis is the conversion of glucose to glucose-6-phosphate by hexokinase, the rate-limiting step. Further metabolism of phosphorylated glucose to pyruvate generates two molecules of ATP. In the presence of oxygen oxidative phosphorylation occurs in the mitochondria where pyruvate is metabolised to generate 36 molecules of ATP. However, under hypoxic conditions pyruvate is converted to lactate.

HbO_2: oxygenated haemoglobin. HCO_3^-: bicarbonate.

From (Gatenby and Gillies, 2004), used with permission.

It has been suggested that the different isozymes of hexokinase regulate the initiation of glycolysis or the pentose phosphate pathway in response to the formation of glucose-6-phosphate (Wilson, 2003). Elevation of Type II hexokinase expression has been demonstrated in several *in vitro* cancer models (Bustamante and Pedersen, 1977; Rempel *et al.*, 1996). It is therefore not surprising that amplification in Type II hexokinasegene transcription have been reported in cancer cells (Rempel *et al.*, 1996). Transcription of the Type II hexokinasegene is stimulated by hypoxia, glucose and the tumour suppressor p53 (Mathupala *et al.*, 1997a). Several *p53* motifs are located in the Type II hexokinase promoter and mutated *p53* therefore enhance transcription of hexokinase (Mathupala *et al.*, 1997b).

Type I and Type II isoforms of hexokinase are reportedly localised to the mitochondria (Sui and Wilson, 1997). It has been demonstrated that Akt, or protein kinase B, increase the localisation of hexokinases to the mitochondria and aids in the interaction of hexokinase with voltage dependent anion channels (VDAC) in the outer mitochondrial membrane (Gottlob *et al.*, 2001). The possible involvement of hexokinases in the formation of the VDAC in the outer mitochondrial membrane suggests a link between glucose metabolism and cell death (Wilson, 2003). Indeed, hexokinases are proposed to coordinate the opening of VDAC and release of apoptogenic factors subsequent to depolarisation of the mitochondrial membrane potential (Beutner *et al.*, 1998). Inhibition of the activity of hexokinases may thus directly affect cell survival.

Aerobic glycolytic activity in cancer cells have been attributed to mitochondrial defects and adjustment to a hypoxic environment (Pelicano *et al.*, 2006). Mutations in mitochondrial DNA (mtDNA) due to oxidative damage are commonly observed in malignant tissue (Zhu *et al.*, 2005a; Cai *et al.*, 2011). As mtDNA contains genes vital to the function of the respiratory chain, mutations in these genes are likely to result in dysfunction of the respiratory chain, obliging the cell to produce ATP through glycolysis (Pelicano *et al.*, 2006).

The waste products of aerobic glycolysis, lactic acid and hydrogen ions (H^+), cause acidification of the tumour microenvironment (Schornack and Gillies, 2003). Extracellular acidosis results in elevated mutagenesis originating from impaired DNA repair mechanisms (Yuan *et al.*, 2000). Malignant cells are protected from potentially harmful acidosis through alterations in the apoptosis pathways and enhanced removal of H^+ from the cytosol to the extracellular environment. However, non-malignant cells remain vulnerable to acid-induced toxicity resulting in cell death and degradation of the extracellular matrix which may aide in tumour cell invasion (Gatenby *et al.*, 2006). Indeed, acidification of the tumour microenvironment has been reported to correlate with enhanced invasive potential (Martínez-Zaguilán *et al.*, 1996). Even though the process of aerobic glycolysis does not confer an advantage to tumourigenic cells where energy production is concerned; this process may be essential to carcinogenesis and metastasis (Gatenby and Gillies, 2004).

In order to satisfy the increased glucose demand of tumourigenic cells, expression of GLUT transporters is elevated (Grover-McKay *et al.*, 1998). The rate of glucose consumption by malignant cells correlates to metastatic potential and can therefore be used as a prognostic marker (Schwartz *et al.*, 2004; Schwarzbach *et al.*, 2005). In the MCF-7 oestrogen receptor positive breast adenocarcinoma cell line, a common non-metastatic *in vitro* model of breast cancer, the expression of both GLUT1 and GLUT12 are reported (Rogers *et al.*, 2002;

Rivenzon-Segal *et al.*, 2003). However, in the oestrogen receptor-negative MDA-MB-231 cell line GLUT1 is preferentially over-expressed (Grover-McKay *et al.*, 1998).

It has been suggested that conventional chemotherapeutic agents, which induce selective cell death of cancer cells based on their elevated proliferation rate, will not affect tumourigenic cells with decreased growth rate in hypoxic areas (Maher *et al.*, 2004). Combining inhibitor of aerobic glycolysis with conventional chemotherapy may thus provide an effective treatment strategy for neoplasms.

1.2.1 Glycolysis inhibitors

The growth of malignant cells can be effectively restricted by inhibiting excessive glycolysis at the glucose transport or phosphorylation stage (Mathupala *et al.*, 1997a; Artemov *et al.*, 1998; Rivenzon-Segal *et al.*, 2003). Aerobic glycolysis does not occur preferentially in non-tumourigenic tissue, abrogation of aerobic glycolysis present a selective target for inhibiting tumour growth (Pelicano *et al.*, 2006).

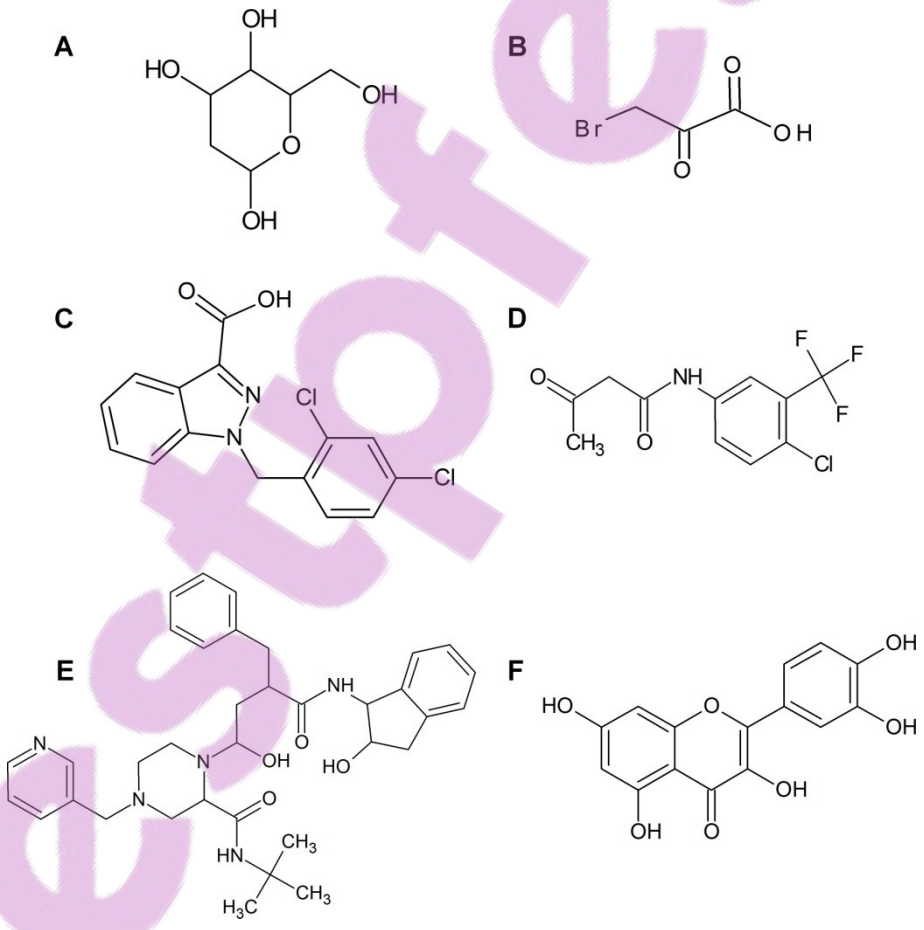

Figure 1.3: The structures of the six inhibitors of aerobic glycolysis selected for the study where (A) 2-deoxy-d-glucose, (B) 3-bromopyruvate, (C) lonidamine, (D) fasentin, (E) indinavir and (F) quercetin. Structures generated with ADC/ChemSketch Freeware version 12.01.

Six promising inhibitors of aerobic glycolysis were selected for the present study (Figure 1.3). These are discussed in more detail below.

1.2.1.1 2-Deoxy-d-glucose (2DG)

The glucose analogue 2-deoxy-d-glucose (2DG) was originally developed to elucidate glucose metabolism. It was first suggested that 2DG inhibits glucose metabolism following observation that 2DG negatively affects the intracellular transfer of glucose (Nakada and Wick, 1956). *In vitro* studies demonstrated that 2-deoxyglucose-6-phosphate was not a substrate for purified rat kidney phosphogluco-isomerase, suggesting that 2DG inhibits the glycolysis pathway at the phosphorylation step (Wick *et al.*, 1957). However, 2DG competes with glucose for phosphorylation by hexokinase (Pelicano *et al.*, 2006).

The inhibition of glycolysis by 2DG induces cell death in numerous *in vitro* models (Kaplan *et al.*, 1990; Aft *et al.*, 2002; Maher *et al.*, 2004; Cheng *et al.*, 2012). In addition to its effect on glycolysis, 2DG also affects protein glycosylation and induces endoplasmic reticulum stress (Kang and Hwang, 2006). However, induction of endoplasmic reticulum stress in response to inhibition of glycolysis may upregulate expression of P-glycoprotein, a transmembrane efflux transporter associated with drug resistance (Ledoux *et al.*, 2003).

In vivo studies with 2DG have shown that its ability to affect glucose metabolism was valid in intact organisms at sub-toxic doses (0.04% w/w) while demonstrating anti-cancer activity (Zhu *et al.*, 2005b; Papathanassiu *et al.*, 2011). The most promising *in vivo* results have been obtained where 2DG has been used in combination with other chemotherapeutic agents (Maschek *et al.*, 2004; Papathanassiu *et al.*, 2011; Cheng *et al.*, 2012). A phase I clinical trial reported tolerable side effects where 2DG was administered at a dose of 63 mg/kg/day (Raez *et al.*, 2013).

1.2.1.2 3-Bromopyruvate (3-BrPA)

3-Bromopyruvate (3-BrPA) directly inhibits hexokinase activity and mitochondrial oxidative phosphorylation resulting in cell death (Ko *et al.*, 2001; Geschwind *et al.*, 2004). 3-BrPA depletes intracellular ATP levels resulting in the dephosphorylation of B-cell lymphoma 2 (Bcl-2)-associated death promoter (Bad), translocation of Bcl-2-associated X protein (Bax) and the release of apoptogenic factors from the mitochondria (Xu *et al.*, 2005). The effects of 3-BrPA on the mitochondria have been attributed to its ability to elevate production of reactive oxygen species (Ihrlund *et al.*, 2008). It has also been proposed that 3-BrPA modulates multidrug resistance (Xu *et al.*, 2005).

In vivo studies demonstrated the potential of 3-BrPA as an anti-glycolytic agent: complete eradication of hepatocarcinoma in a rat model was reported after four doses of 3-BrPA (Ko*et*

al., 2004). This confirmed previous *in vivo* results obtained in New Zealand White rabbits with hepatocarcinoma xenografts (Geschwind *et al.*, 2002). 3-BrPA treatment also effectively limited tumour burden of aggressive lymphoma in a severe combined immunodeficient mouse model (Schaefer *et al.*, 2012).

A case study describing the treatment of a patient with fibrolamellar hepatocellular carcinoma with 3-BrPA (bolus administration of 500 mg followed by 128 mg every two weeks) showed marked tumour cell death. Unfortunately the patient suffered tumour lysis syndrome due to rapid destruction of tumour cells by 3-BrPA and inadequate capacity of the liver detoxification system (Ko *et al.*, 2012). However, this study provided proof of the clinical efficacy of 3-BrPA.

1.2.1.3 Lonidamine (LON)

Floridi and colleagues reported that the anti-spermatogenic agent lonidamine (LON) interferes with glucose metabolism (Floridi *et al.*, 1981a). Research from the same laboratory ascribed this observation to inhibition of glycolysis and hexokinase activity (Floridi *et al.*, 1981b). It has been demonstrated that LON treatment results in mitochondrial damage resulting in inhibition of glycolysis, depletion of intracellular ATP and ultimately cell death (Rosbe *et al.*, 1989; Floridi *et al.*, 1998).

Lonidamine,a derivate of indazole-3-carboxylic acid, has been used effectively in combinations with alkylating agents and anthracyclinesin an *in vitro* setting (Rosbe *et al.*, 1989; Floridi *et al.*, 1998). Numerous clinical studies followed on the *in vitro* success demonstrating potential for LON therapy in the treatment of soft tissue sarcomas, prostate carcinomas, metastatic breast cancer and advanced ovarian carcinoma (Lopez *et al.*, 1995; Dudak *et al.*, 1996; Dogliotti *et al.*, 1998; De Lena *et al.*, 2001). However, two trials investigating the potential of LON for the treatment of benign prostate hyperplasia reported elevated levels of liver enzymes (NCT00435448 and NCT00237536).

Success has been reported in an *in vivo* study where LON and paclitaxel were delivered with a non-carrier system, suggesting that potential systemic toxicity induced by LON may be reduced with a targeted carrier approach (Milane *et al.*, 2011). The decreased doses of LON required for combination therapy may thus avoid systemic toxicity.

1.2.1.4 Fasentin (FAS)

During a study aimed at identifying small molecules which sensitise resistant malignant cells via the activation of the extrinsic pathway, fasentin (FAS) was identified as a potent chemosensitiser from a library of over 50 000 compounds (Schimmer *et al.*, 2006). Gene expression studies performed to establish intracellular targets of FAS revealed its effects on

glucose metabolism and transport. It was demonstrated that at concentrations higher than 50 µM FAS inhibited GLUT1 and GLUT4 (Wood *et al.*, 2008). Numerous studies have reported using fasentin as an inhibitor of glucose transport (Liu *et al.*, 2010; Wood *et al.*, 2010; Gwak *et al.*, 2014). Its potential as anti-cancer agent has been demonstrated in *in vitro* prostate cancer and leukaemia cell lines (Schimmer *et al.*, 2006; Wood *et al.*, 2008).

To date no *in vivo*or clinical safety data on fasentin has been reported.

1.2.1.5 Indinavir (IND)

The decline in mortality rates among human immunodeficiency virus (HIV)-positive individuals in the late 1990's have been attributed to the addition of HIV protease inhibitors, such as indinavir (IND), to the standard treatment regimen (Palella Jr *et al.*, 1998). However, metabolic effects such as insulin resistance and hyperglycaemia have been associated with the use of protease inhibitors (Mulligan *et al.*, 2000). Using *Xenopuslaevis* oocyte models it was demonstrated that IND (from 10 µM) inhibits the GLUT 4 glucose transport (Murata *et al.*, 2002). It has also been reported more recently that 50 µM of IND also suppresses GLUT1 glucose transport (Hresko and Hruz, 2011).

Research into the chemotherapeutic potential of protease inhibitors begun after the publication of a report describing a 60% complete response rate in HIV-positive, protease inhibitor-naive patients with Karposi sarcoma after treatment with protease inhibitors as part of a highly active antiretroviral treatment regimen for three months (Lebbé *et al.*, 1998). The anti-cancer properties of IND were confirmed in an *in vivo* Karposi sarcoma xenograft model where administration of IND inhibited the formation of malignant lesions. In addition, results from i*n vitro* angiogenesis modelsreported anti-angiogenic potential of IND (Sgadari *et al.*, 2002). The anti-cancer activity of IND against *in vitro* and nude mouse hepatocarcinoma models (Esposito *et al.*, 2006) resulted in a pilot phase I study in dogs with stage III splenic haemangiosarcoma. All of the study animals in that study suffered fatal haemorrhages, which was attributed to the advanced stage of the disease (Spugnini *et al.*, 2006).

As the safety profile of IND had already been established in HIV patients, a clinical study to establish the effect of IND on disease progression of HIV-negative patients diagnosed with Karposi sarcoma was initiated. Favourable clinical outcome was reported in 62% of patients. No serious adverse events were reported during the study, demonstrating the potential of IND as chemotherapeutic agent (Monini *et al.*, 2009) that may or may not be related to the glycolysis inhibiting activity.

1.2.1.6 Quercetin (QUER)

Quercetin (QUER), a plant-derived flavonoid, is commonly consumed as part of the daily diet in the form of fruits and vegetables (Ross and Kasum, 2002). It is estimated that the daily dietary intake of plant-derived flavonoids like QUER range from 15 to 100 mg (Leth and Justesen, 1998; Egert *et al.*, 2008; Nishimuro *et al.*, 2015).

The ability of QUER to inhibit aerobic glycolysis and the production of lactic acid has been attributed to its inhibitory effect on the function of mitochondrial ATP synthase (Lang and Racker, 1974; Suolinna *et al.*, 1975). The effect of QUER on aerobic glycolysis is further compounded by QUER-induced competitive inhibition of glucose transport by GLUT1 and GLUT2 (Vera *et al.*, 2001; Kwon *et al.*, 2007). Apart from its effect on aerobic glycolysis, QUER influences several intracellular targets. QUER, as a tyrosine kinase inhibitor, may suppress the activity of cyclic adenosine monophosphate (cAMP)-independent kinases (Glossmann *et al.*, 1981). Additionally, QUER modulates multidrug resistance through limiting the transcription of multi-drug resistance gene 1 (*MDR1),* required for the synthesis of P-glycoprotein (Kioka *et al.*, 1992). Anti-angiogenic properties have also been attributed to QUER (Tan *et al.*, 2003; Oh *et al.*, 2010).

The anti-cancer effects of QUER has been demonstrated in numerous human *in vitro* models including gastric cancer (Yoshida *et al.*, 1990), oestrogen receptor-positive breast adenocarcinoma (Choi *et al.*, 2001) and lung cancer (Nguyen *et al.*, 2004). These effects were translated into an *in vivo* model melanoma model of syngeneic C57BL/6N mice (Caltagirone *et al.*, 2000). A phase I clinical study revealed that the administration of 1700 mg/m^2 QUER resulted in dose-limiting nephrotoxicity. The use of a bolus dose of 1400 mg/m^2 was recommended for further clinical studies (Ferry *et al.*, 1996).

1.3 The role of angiogenesis

Sustained and progressive tumour growth is dependent on neovascularisation: initially blood vessels in the surrounding tissue supply the oxygen and nutrients required for proliferation (Giaccia, 1996). However, tumour growth is limited by the supply of nutrients and oxygen: when tumour growth exceeds 1- 2 mm or the distance between neoplasms and blood vessels surpasses 150 – 200 µm, being the limit of rapid oxygen diffusion,where elevated cell death is observed (Folkman, 2003; Jin and White, 2007). Gimborne and colleagues demonstrated the dependence of tumour proliferation on vascularisation by implanting avascular tumours into rabbit cornea or iris: if vascularisation could not be initiated tumour

growth did not exceed 1 mm after 6 weeks; however when vascularisation was possible exponential tumour growth was observed in less than 24 h (Gimbrone *et al.*, 1972).

In order for tumours to proliferate and avoid entering a dormant state, restoration or establishment of oxygen and nutrient supply is crucial (Giaccia, 1996). Angiogenesis is the development of new blood vessels from existing local blood vessels (Hanahan and Folkman, 1996). This differs from vasculogenesis where the formation of new blood vessels is initiated by the differentiation of progenitor cells (Risau and Flamme, 1995). The development of adequate supply of essential nutrients and oxygen alleviates metabolic stress and permits seeding of malignant cells from the primary tumour to establish metastatic sites.

Environmental conditions resulting from insufficient oxygen supply such as metabolic stress or acidification of the extracellular matrix may activate pro-angiogenic factors, such as hypoxia-inducible factor 1 (HIF-1), initiating the process of angiogenesis (Giaccia, 1996). The balance between pro- and anti-angiogenic factors regulates the 'angiogenic switch'. Where this balance is in favour of the pro-angiogenic factors, the process of angiogenesis is initiated (Carmeliet and Jain, 2000). Pro-angiogenic triggers also include the expression of oncogenes (Rak *et al.*, 2000), the influence of cytokines such as VEGF (Fukumura *et al.*, 1998) and hypoxia-inducible transcription factors (Carmeliet and Jain, 2000) and circulating bone-marrow derived precursor cells (Lyden *et al.*, 2001).

Exponential tumour growth relies on the activation of the 'angiogenic switch' (Bergers and Benjamin, 2003)(Figure 1.4).

An association has been proposed between microvessel density in invasive breast carcinoma and prognosis: a high density of microvessels surrounding breast and prostate carcinoma has been linked with poor prognosis (Weidner *et al.*, 1992; Weidner *et al.*, 1993). Angiogenesis occurs in healthy adults predominantly during the menstrual cycle and wound healing (Hanahan and Folkman, 1996). Therefore as angiogenesis is not a ubiquitous process in healthy adults, it presents a selective target for anti-cancer therapy (Cook and Figg, 2010).

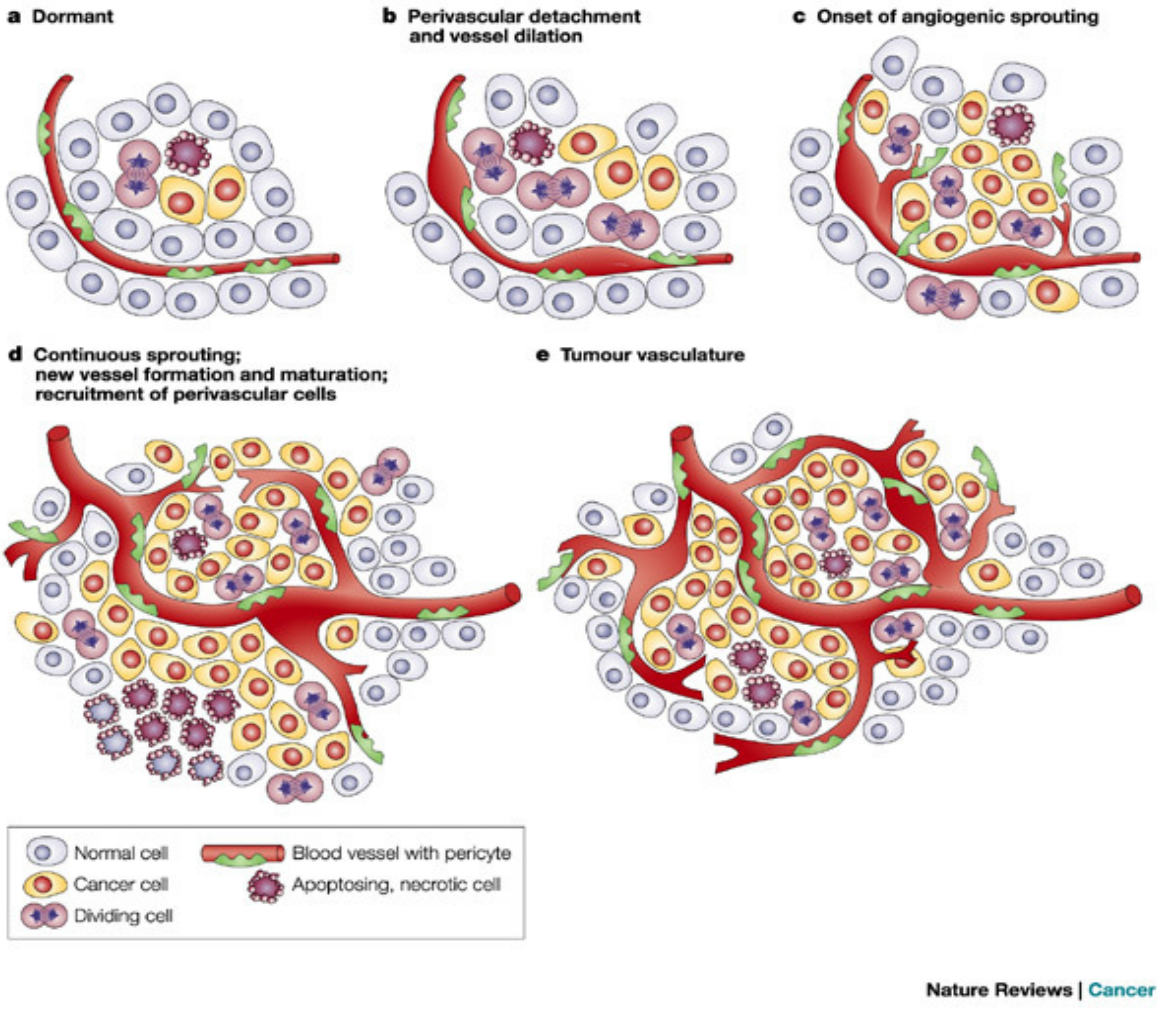

Figure 1.4: The angiogenic switch initiated by a dormant avascular tumour (a). The process of angiogenesis is initiated by the release of pro-angiogenic factors from tumourigenic cells followed by endothelial sprouts (c) and the formation of new vessels (d). Endothelial proliferation continues resulting in the development of a vasculature network supplying oxygen and nutrients to the tumour (e).

From (Bergers and Benjamin, 2003), used with permission.

1.4 Global cancer burden

The most recently published statistics on global cancer mortality estimates that approximately 8.2 million deaths and approximately 14.1 million cases of cancer were diagnosed in 2012. The most commonly diagnosed cancer (12.7%) and the leading cause of cancer-related deaths (18.2%), in both genders were lung cancer. The incidence of breast cancer ranked second at 10.9% (1.67 million) of all diagnosed cancer cases (Ferlay *et al.*, 2015).

It is estimated that approximately 600 000 deaths during 2012 in Africa were cancer-related (Parkin *et al.*, 2014). However, the situation in Africa is unique in that there is a large proportion of young people and smaller share of elderly: cancer-sufferers fall mostly in economically active age groups with significant socio-economic consequences (Sambo *et al.*, 2012; Parkin *et al.*, 2014). Among African females breast cancer has the highest incidence (27.6%) followed by cervical cancer (20.4%). Prostate cancer is most commonly diagnosed in African men (Parkin *et al.*, 2014).

The high cancer mortality rate in Africa may be due to the advanced stage of disease at the time of diagnosis (Mgbakor *et al.*, 2014). Furthermore, Africa faces unique challenges in the fight against cancer as the incidence of a number of acquired immune deficiency syndrome (AIDS)-related cancers, including Kaposi's sarcoma and non-Hodgkin's lymphoma, have been increasing in Africa since the 1990's (Chokunonga *et al.*, 1999; Parkin *et al.*, 1999). It is therefore not surprising that Africa has the highest relative risk for AIDS-associated cancers (Serraino, 1999).

Neoplastic transformation is initiated by various genetic, environmental and lifestyle factors, including infection with the oncogenic human papiloma virus resulting in the development of cervical cancer or copious alcohol consumption that has been linked to increased incidence of mouth, oropharynx and oesophageal cancers (Danaei *et al.*, 2005). Even though emphasis is often placed on hereditary factors, it is estimated that 60-90% of diagnosed cancers may be attributed to environmental factors (Lichtenstein *et al.*, 2000; Czene *et al.*, 2002). The influence of environmental factors is supported by the significant increase in breast cancer incidence in survivors of the atomic bombings of Hiroshima and Nagasaki: in a population in which breast cancer is usually rare, a four-fold increase in breast cancer incidence was reported under females exposed to more than 90 rads (Wanebo *et al.*, 1968).

Cancers due to lifestyle factors such as smoking and alcohol consumption are more commonly diagnosed in high income countries (Danaei *et al.*, 2005). Trends in cancer incidence and changing mortality rates may also be attributed to behavioural changes, progress in cancer prevention and improved care of cancer patients (Siegel *et al.*, 2015).

1.4.1 Breast cancer

1.4.1.1 Prevalence and risk factors

The global lifetime risk for developing breast cancer is approximately 12.5% (Ellsworth *et al.*, 2010). Currently it is estimated that approximately 50% of breast cancer patients will experience relapse of the disease (Akbas *et al.*, 2005). The overall 5-year survival rate of female breast cancer has been estimated at 90.3% in 2007, a marked improvement from

75% survival rate reported in 1975 (Howlader *et al.*, 2013). Improvement in survival rate may be due to the introduction of mammograms (Shapiro, 1997), resulting in early diagnosis of breast cancer.

Even though the first report suggesting a genetic predisposition to breast cancer is reputed to have been published in the eighteenth century (Le Dran, 1757), it was not until 1994 that breast cancer 1 gene (*BRCA1*) was identified and mapped. Mutations of this gene, located on chromosome arm 17q, have been linked to increased risk of ovarian and breast cancers which is not surprising as it encodes a tumour suppressor protein (Miki *et al.*, 1994). Another gene, breast cancer 2 gene (*BRCA2*), has been associated with early-onset breast cancer (Wooster *et al.*, 1995).

However, a hereditary component cannot be identified in an estimated 70% of breast cancer cases (Ellsworth *et al.*, 2010). Hormonal risk factors include elevated levels of oestrogen, prolactin and progesterone (Pike *et al.*, 1979), early menarche,late menopause and prolonged contraceptive use (Paffenbarger *et al.*, 1980). A decreased breast cancer risk is associated with first live birth at 18 years of age or younger (MacMahon *et al.*, 1970). Various lifestyle factors are also associated with increased breast cancer risk. Daily consumption of 2.4 g of alcohol is associated with a 1.7-fold increase in breast cancer risk (Longnecker *et al.*, 1988). Data from the Framingham study suggest that an increased risk for breast cancer is associated with a high central body fat distribution (Ballard-Barbash *et al.*, 1990). Bernstein and colleagues reported reduced breast cancer risk with increased physical activity in premenopausal women (Bernstein *et al.*, 1994).

1.4.1.2 Phenotypic subtypes and treatments

The term ‘breast cancer’ belies the heterogeneity of the disease: as many as 8 different cell types have been identified in excised tumours by analysing gene expression patterns (Perou *et al.*, 2000). Distinct subtypes of breast cancer were recognised as early as 1890’s at Johns Hopkins University (Halsted, 1898). Based on genetic and receptor profiling, malignant tumours are now classified into distinct subtypes (Perou *et al.*, 2000; Wirapati *et al.*, 2008):

1. Human epidermal growth factor receptor 2 (Her2/neu) positive (referred to as Her2/neu positive)
2. Oestrogen receptor-negative, basal-like (referred to as triple negative breast cancer)
3. Oestrogen receptor-positive, luminal A
4. Oestrogen receptor-positive, luminal B

Due to the overlap of genetic and receptor profiles, such classification systems may be confounding. Indeed, it has been suggested that in terms of clinical prognosis and

therapeutic strategy, classification of oestrogen receptor-positive tumours as luminal A and luminal B may be redundant (Weigelt *et al.*, 2010).

Initially therapeutic management of all breast malignancies comprised a single treatment modality: radical mastectomy (Halsted, 1898). Surgical resection of malignancies aims to remove malignant tissue as curative procedure or for further classification of malignant tissue (Leis Jr, 1981). Radical mastectomy was the mainstay of treatment of breast cancers from the late 1800's, often leaving patients permanently disfigured. However, only 50% of patients survived for more than three years after the procedure (Halsted, 1898). It was only after a study comparing the Halsted radical mastectomy to breast conserving surgery initiated in 1973 showed comparable survival rates that the Halsted procedure was abandoned (Veronesi *et al.*, 1981). The modified radical mastectomy replaced conventional radical mastectomy during the 1980's which afforded breast cancer survivors greater odds at cosmetic reconstruction (Leis Jr, 1981). A 20-year follow-up of the patients who participated in the 1973 trial comparing Halsted radical mastectomy vs. breast conserving surgery showed equivalent long-term survival rates (Veronesi *et al.*, 2002).

Approximately 70% of patients with operable disease remained disease-free 10 years after radical mastectomy. However, this success rate was reduced to 25% in patients with involvement of the axillary nodes at diagnosis (Valagussa *et al.*, 1978). This was confirmed by data gathered from approximately 24 000 patients where the involvement of the axillary nodes and tumour size correlated with prognosis (Memeto *et al.*, 1980). Superior treatment success was observed where a treatment strategy comprising surgery and chemotherapy had been used (Bonadonna *et al.*, 1995).

Histologically, oestrogen receptor-positive breast cancer is better differentiated than oestrogen receptor-negative lesions (Fisher *et al.*, 1981). The differentiation of tumours is directly associated with prognosis: a greater degree of differentiation correlates with a more favourable prognosis (Bloom and Richardson, 1957). Approximately 75% of diagnosed breast cancer is oestrogen receptor-positive (Li *et al.*, 2003). Oestrogen receptor-positive malignancies were initially treated with adrenalectomy and hypophysectomy in an attempt to reduce systemic oestrogen levels (McGuire *et al.*, 1977). Endocrine therapy was used with limited success before molecular sub-typing of tumours became the *status quo* (McGuire *et al.*, 1977).

The development of the selective oestrogen receptor modulator tamoxifen for the treatment of oestrogen receptor-positive breast cancer resulted in a marked reduction in mortality rates among breast cancer patients (Danaei *et al.*, 2005). However, treatment with tamoxifen is not without adverse effects including hot flushes, depression, weight gain and increased risk

for endometrial hyperplasia (Perez, 2007; Lorizio *et al.*, 2012). Bernard Fisher and colleagues demonstrated the benefit of tamoxifen treatment in the National Surgical Adjuvant Breast and Bowel Project (NSABP) B-14 and B-20. During the NSABP B-14 trial extended disease-free survival of patients receiving tamoxifen therapy (10 mg twice per day) was observed (Fisher *et al.*, 1989). The NSABP B-20 trial illustrated improved disease-free survival and overall survival rates in treatment groups receiving tamoxifen combined with cyclophosphamide, methotrexate and fluorouracil (CMFT) in comparison to tamoxifen alone (Fisher *et al.*, 1997). An overview of 47 clinical trials revealed that the addition of anthracyclines to a treatment regimen decreased risk of relapse and increased the 5-year survival rate (Early Breast Cancer Trialists' Collaborative, 1998). After a 15-year follow-up period the combination of tamoxifen and chemotherapy showed superior disease-free survival and an estimated 65% reduction in treatment failure (Fisher *et al.*, 2004).

Current treatment of oestrogen receptor-positive breast cancer involves combinations of endocrine therapies including ovarian suppression, selective oestrogen receptor modulators or down-regulators and aromatase inhibitors (Lumachi *et al.*, 2013). Ovarian suppression is achieved by the administration of gonadotropin-releasing hormone agonists, such as goserelin, buserelin, triptorelin, and leuprorelin, which reduce systemic oestrogen levels to postmenopausal ranges (Harvey *et al.*, 1985; Lumachi *et al.*, 2013). Due to the adverse effects associated with tamoxifen use, alternative oestrogen receptor modulators have been developed aimed at therapeutic efficacy with an improved side effect profile. The efficacy of aromatase inhibitors, which impede the synthesis of oestrogen, was compared to tamoxifen in a 10-year follow-up study (Cuzick *et al.*, 2010). Endometrial hyperplasia is not associated with the use of aromatase inhibitors which are suggested as therapy for oestrogen receptor-positive breast cancer (Goldhirsch *et al.*, 2009). However, as tamoxifen shows overall superior efficacy it remains widely used (Lumachi *et al.*, 2011).

Breast cancers displaying absence of oestrogen and progesterone receptors in addition to Her2/neu expression are classified as triple negative breast cancer (TNBC)(Shi and Wang, 2012) and comprise approximately 15% of diagnosed breast cancer cases (Abramson *et al.*, 2015). These tumours are characterised by a high proliferation rate and a poor prognostic outcome (Meyer *et al.*, 1977; Wirapati *et al.*, 2008). This aggressive breast cancer subtype shows a high rate of relapse and reduced overall survival in comparison to metastases of oestrogen receptor-positive tumours or tumours with Her2/neu amplification (Abramson *et al.*, 2015). In a retrospective study of more than 1500 breast cancer patients, survival rate of patients diagnosed with TNBC was approximately half that of other breast cancer subtypes (Dent *et al.*, 2007).

As no specific target for treatment of TNBC has been identified to date, chemotherapy is the only systemic treatment option available (Goldhirsch *et al.*, 2009).The majority of breast neoplasms with a mutation in the *BRCA1* gene present clinically as TNBC (Atchley *et al.*, 2008). Mutations in the *BRCA1* gene disrupt homologous recombination (Moynahan *et al.*, 1999). Therefore chemotherapeutics which affect DNA synthesis are proposed to effectively treat TNBC (Abramson *et al.*, 2015). Indeed, pathologic complete response has been reported where TNBC patients were treated with cisplatin (Byrski *et al.*, 2014). Due to the small sample size of this pilot study (107 patients) the 60% success rate must be confirmed in a larger study population (Byrski *et al.*, 2014). Partial response was reported in 50% of TNBC patients treated with the poly (ADP-ribose) polymerase (PARP) inhibitor olaparib (400 mg twice daily)(Tutt *et al.*, 2010).

Human epidermal growth factor receptor 2 (Her2/neu) is over-expressed in approximately 30% of breast cancers (Slamon *et al.*, 1987). Due to the homogeneity between the amino acid sequence of the product of the *Her2/neu* gene and the epidermal growth factor receptors, Her2/neu was identified as a member of the epidermal growth factor receptor family (Bargmann *et al.*, 1986). This transmembrane tyrosine kinase receptor is involved in the activation of signal transduction pathways implicated in cell proliferation and survival (Ross *et al.*, 2003). It is therefore not surprising that Her2/neu over-expression has been recognised as an unfavourable prognostic factor (Slamon *et al.*, 1987; Press *et al.*, 1997). Indeed, upon examination of more than 1 000 cases a correlation was observed between the number of Her2/neu copies and involvement of axillary nodes, disease-free survival and overall survival (Seshadri *et al.*, 1993).

A murine monoclonal antibody targeted against the extracellular domain of Her2/neu, mumAb4D5, was developed to aid in the characterisation of the expression of Her2/neu in tumourigenic cell lines (Fendly *et al.*, 1990). Available technology was used to humanise the antibody for therapeutic application (Jones *et al.*, 1986). *In vitro* testing revealed that the humanised mumAb4D5 antibody showed cytotoxicity towards the SK-Br3 cell line which over-expresses Her2 (Carter *et al.*, 1992). The addition of trastuzumab (humanised mumAb4D5) to conventional chemotherapy reduced relative risk of death by 20% in metastatic breast cancer patients. Unfortunately cardiac dysfunction was observed in patients receiving a combination of trastuzumab, cyclophosphamide and anthracyclines (Slamon *et al.*, 2001). However, due to the poor prognosis of patients with Her2/neu amplification, the low incidence of cardiac dysfunction and the reversible nature of the cardiac dysfunction trastuzumab is considered a viable therapeutic option (Suter *et al.*, 2007).

Subsequent to the success with trastuzumab, marketed under the trade name Herceptin®, numerous Her2/neu-targeted therapies have been developed. Approved Her2/neu-targeted therapies include the small molecule receptor tyrosine kinase inhibitor lapatinib and monocloncal agents pertuzumab and ado-trastuzumab emtansine (Figueroa-Magalhães *et al.*, 2014). Anti-Her2/neu therapy is routinely combined with chemotherapy (Goldhirsch *et al.*, 2009).

1.4.1.3 Limitations to successful treatment of malignancies

A major limitation to the successful treatment of malignancies is the systemic toxicity induced by many chemotherapeutic agents. Unlike the treatment modalities for many disease aetiologies, anti-neoplastic therapy is associated with high potential toxicity at therapeutic concentrations (Plenderleith, 1990). It has been estimated that more than 50% of patients will experience severe, life-threatening or fatal chemotherapy toxicity during treatment (Hurria *et al.*, 2011; Extermann *et al.*, 2012). In an cohort of 513 patients, 64% of patients experienced severe toxicity and of these 23% selected cessation of chemotherapy due to toxicity (Extermann *et al.*, 2012). The adverse effects most frequently reported induced by chemotherapy include nausea and vomiting, peripheral neuropathy,fatigue, alopecia and leukopenia (Plenderleith, 1990; Ahlberg *et al.*, 2003; Wolf *et al.*, 2008). Most of these adverse effects are due to the effects of chemotherapeutic agents on normal cells with a high proliferation rate (Plenderleith, 1990).

The use of anthracyclines, such as doxorubicin and daunorubicin, is associated with cumulative dose-dependent cardiotoxicity (Monsuez *et al.*, 2010). Chemotherapy in the treatment of breast cancer has been associated with a decline in cognitive function (Falleti *et al.*, 2005). Approximately 5% of breast cancer patients are at risk of developing secondary non-breast cancer, such as soft tissue sarcomas, and this may be due to the use of radiation therapy or chemotherapy (Schaapveld *et al.*, 2008). Despite reports of adverse effects, the benefits of treatment with chemotherapeutic agents often outweigh the risk (Plenderleith, 1990).

The limited success achieved in the treatment of TNBC has been attributed to the lack of therapeutic targets (Goldhirsch *et al.*, 2009). The advent of gene expression arrays have aided in the identification of selective therapeutic targets which are translatable into the clinical setting. Indeed, heterogeneity in gene expression profiles between the subtypes of breast cancer provides insight into potential therapeutic targets: differential expression of *AKT1*gene products and *BRCA1* and*BRCA2* mutations suggests that PARP inhibitors (Koboldt *et al.*, 2012) may show improved selectivity. Clinical trials of the PARP inhibitor

have shown success in the treatment of TNBC (Tutt *et al.*, 2010), highlighting the importance of selective therapeutic targets.

Successful treatment of neoplasms is also impeded by disease relapse. A relapse rate of approximately 20% has been reported across the phenotypic subtypes of breast cancer in patients treated with breast-conserving therapy and radiotherapy. Relapse rates are highest amongst patients diagnosed with TNBC or Her2/neu-positive breast cancer (Voduc *et al.*, 2010).

Development of multidrug resistance is a common cause for failure of chemotherapy (Riganti *et al.*, 2015). Chemo-resistance may be due to inadequate delivery of anti-cancer agents to the tumour resulting from physiological factors such as discordant blood supply to tumours (Jain, 2001) or intracellular adaptations in response to chemotherapy including the expression of transmembrane efflux pumps (Gottesman *et al.*, 2002). Multidrug resistance is implicated in treatment failure of structurally and functionally unrelated chemotherapeutic agents (Gottesman and Pastan, 1993). The first of these efflux pumps described in an *in vitro* model was P-glycoprotein, a 170 kDa transmembrane glycoprotein which confers drug-resistance to Chinese hamster ovarian cells (Juliano and Ling, 1976). P-glycoprotein belongs to the ATP-binding cassette transporter super-family (Higgins, 1991). It is proposed that transporters from this super-family is responsible for the removal of many harmful xenobiotics from the intracellular environment under normal physiological conditions as these transporters are constitutively expressed in numerous tissues including the digestive system and central nervous system (Choi, 2005).

Selective inhibitors of P-glycoprotein have been investigated with limited success. The calcium channel blocker verapamil (Tsuruo *et al.*, 1981), calmodulin inhibitor trifluoperazine (Tsuruo *et al.*, 1982) and immunosuppressant cyclosporin A (Twentyman *et al.*, 1987) reversed resistance to vinca alkaloids in *in vitro* cancer models. However, limited success in the clinical setting was achieved with these inhibitors due to dose-limiting toxicity and poor P-glycoprotein inhibitory activity (Pennock *et al.*, 1991; Bartlett *et al.*, 1994). Pharmacokinetic interactions between multidrug resistance modulators and chemotherapeutic agents further hampered clinical efficacy (Bartlett *et al.*, 1994). It has been suggested that the most simplistic solution to the problem of multidrug resistance in cancer is the use of combination therapy (Luqmani, 2005).

1.5 Drug combination therapy

The *status quo* for the management of numerous disease states including malignancies and certain infective diseases such as HIV/AIDS comprise drug combination therapy (Chou, 2006). The first successful combination therapy treatment in cancer was developed in the 1960's by Freiand colleagues. During this landmark study leukaemia patients treated with a combination of methotrexate and 6-mercaptopurine achieved higher remission rates than observed for either compound separately (Frei *et al.*, 1961a). During a presidential address, Dr Frei stipulated principles for the successful combination of chemotherapeutics (Frei, 1972):

1. Non-overlapping toxicity profiles
2. Different mechanisms of action
3. Reduced risk of development of chemo-resistance

Utilising drug combinations allow for the reduction of the dose of each compound while not compromising on therapeutic efficacy. This approach is expected to translate into a reduction in observed toxicity (Chou, 2006). Indeed, the greatest success in the treatment of breast cancer has been achieved with combinations of effective chemotherapeutics with different therapeutic targets (Goldhirsch *et al.*, 2009; Lumachi *et al.*, 2013).

Due to the heterogeneity of cancerous tissue, treatment with glycolysis inhibitors alone does not result in significant anti-tumour effect. The greatest success has been observed where glycolysis inhibitors have been used in combination with conventionalanti-cancer chemotherapeutic agents. This is potentially due to the impaired ability of ATP-deprived cancer cells to repair damage caused by chemotherapeutic agents (Gatenby and Gillies, 2007).

1.6 2-Methoxyestradiol (2ME) and analogues

Endogenous oestrogens such as 17β-estradiol are metabolised by cytochrome P450 enzymes into 2- and 4-hydroxyestradiol. The structures of these are shown in Figure 1.5 below. The enzymatic metabolism of 4-hydroxyestradiol by the enzyme catechol-o-methyl-transferase (COMT) leads to the formation of 2-methoxyestradiol (2ME)(Lakhani *et al.*, 2003). 2ME is known to protect against tumour formation and has subsequently been shown to have anti-angiogenic, anti-mitotic and pro-apoptotic effects (Salama *et al.*, 2009).

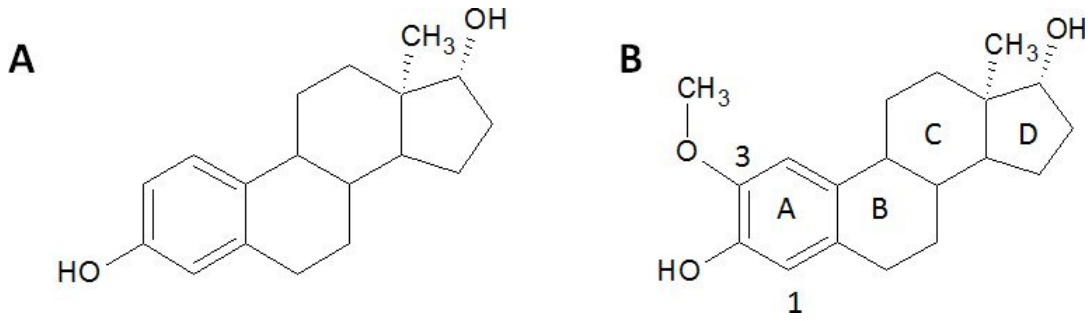

Figure 1.5: The structures of (A) 17β-estradiol and (B) 2-methoxyestradiol. Structures generated with ADC/ChemSketch Freeware version 12.01.

Cytotoxicity caused by 2ME in *in vitro* cancer models was accompanied by irregular microtubule arrangement (Seegers *et al.*, 1989). It was demonstrated that 2ME interferes with microtubule assembly through interaction with the colchicines binding site (D'Amato *et al.*, 1994a) resulting in the formation of a mitotic block and ultimately the induction of apoptosis (Attalla *et al.*, 1996). *In vitro* studies have shown that 2ME induces apoptosis in a range of cancer models including lung (Mukhopadhyay and Roth, 1997), pancreatic (Schumacher *et al.*, 1999), breast (LaVallee *et al.*, 2002) and ovarian cells (Bu *et al.*, 2006) but not in normal cells (Seegers *et al.*, 1997). It has been shown that 2ME exerts its anti-cancer effect independently of interaction with the oestrogen receptor (LaVallee *et al.*, 2002).

The anti-angiogenic effects of 2ME has been demonstrated using *in vitro* models assessing endothelial cell migration (Yue *et al.*, 1997) and invasion (Sattler *et al.*, 2003) and has been attributed to 2ME-induced apoptosis in endothelial cells (Yue *et al.*, 1997; Tsukamoto *et al.*, 1998). Furthermore, Yue and colleagues reported that 2ME inhibited neovasularisation in the well-known *in vitro* model of angiogenesis, the chicken chorioallantoic membrane (CAM) model (Klauber *et al.*, 1997; Yue *et al.*, 1997). Reports also indicated a 50% decrease in VEGF-induced corneal vascularisation in the mouse corneal micro-pocket assay at a daily dose of 150 mg/kg of 2ME (Klauber *et al.*, 1997).

Efficacy studies using the MDA-MB-435 xenograft model at concentrations of 75 mg/kg 2ME showed 60% reduction in tumour volume (Klauber *et al.*, 1997). A similar result was obtained where male severe combined immunodeficient mice inoculated with human melanoma (Dobos *et al.*, 2004). A number of clinical trials have been conducted to determine the safety and tolerability profile of 2ME in humans. A trial conducted at the Indiana University showed no potentially life-threatening toxicity in patients receiving up to 1000 mg/day and from the data gathered it was determined that the half-life of 2ME is approximately 10 hours (James*et al.*, 2007). However, a phase II clinical trial aimed at evaluating the safety of 2ME in men

found that 2ME is rapidly metabolised to 2-methoxyestrone, has poor oral bio-availability and is highly conjugated, resulting in sub-therapeutic intracellular concentrations obtained (Sweeney *et al.*, 2005). In an attempt to improve on these unfavourable characteristics, several formulations (Tevaarwerk *et al.*, 2009) and various analogues of 2ME have been developed (Cushman *et al.*, 1995; Cushman *et al.*, 1997; Tinley *et al.*, 2003; Stander *et al.*, 2011).

Initially the A-ring of 2ME was modified (Cushman *et al.*, 1995), followed by various additions to the B-ring (Cushman *et al.*, 1997) and D-ring (Tinley *et al.*, 2003). *In vitro* testing of the first generation analogues demonstrated that the most potent derivative, 2-ethoxyestradiol, had a weak affinity, comparable to that of 2ME, for the colchicine binding domain but caused inhibition of mitosis at a concentration 10 times lower than that required of 2ME to have the same effect (Cushman *et al.*, 1995). In an effort to improve on 2ME even further, modifications to the A- and B-rings were made which included the addition of an oximino group to carbon 2 (Cushman *et al.*, 1997). Even though promising results were obtained, these derivatives were not investigated further. Alterations to the D-ring led to the development of derivatives with *in vitro* anti-cancer activity in the low micromolar range. Three of these analogues proved to have better *in vivo* anti-tumour activity in comparison to 2ME in an athymic NCr-*nu* mouse model (Tinley *et al.*, 2003).

Stander et al. developed a series of 2ME analogues through *in silico* design by the addition of a sulfamoylated group to the A-ring and removing the hydroxyl group on the D-ring (Stander *et al.*, 2011) (Figure 1.6). The addition of the sulfamoylated group has been shown to improve the variable pharmacokinetic profiles of compounds with a steroid structure as first pass metabolism is avoided through interaction with carbonic anhydrase II in erythrocytes (Elger *et al.*, 1995). Two of these synthetic oestrone analogues, ESE-15-ol and ESE-16, were selected for this study.

In vitro studies have demonstrated that ESE-15-ol and ESE-16 display cytotoxic activity against breast cancer cells at nanomolar concentrations. Cell cycle kinetics assessment revealed that treatment with ESE-15-olresulted in cell cycle arrest in the Gap-2/mitosis (G_2/M) phase of the cell cycle. Exposure to ESE-15-ol and ESE-16 result in generation of reactive oxygen species, depolarisation of the mitochondrial membrane potential and abnormal spindle formation. Gene expression studies in ESE-16-treated breast carcinoma cells revealed alterations in the expression of genes involved in cell proliferation, induction of cell death and adaptation to oxidative stress (Stander *et al.*, 2012, 2013). An *ex vivo* study demonstrated that neither of the oestrone analogues caused alterations in the ultrastructure of erythrocytes suggesting a favourable toxicity profile (Repsold *et al.*, 2014a).

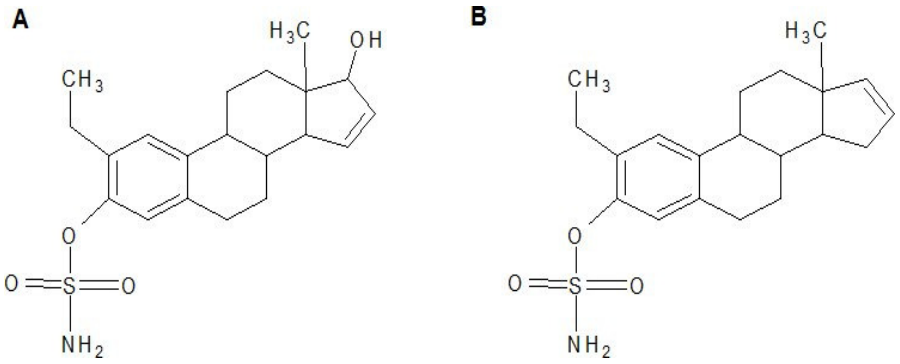

Figure1.6: The structures of (A) ESE-15-ol and (B) ESE-16. Structures generated with ADC/ChemSketch Freeware version 12.01.

An efficient tumour-eradicating strategy is to use therapeutic agents which act on vertical signalling pathways via a sequential blockade or agents which act on parallel pathways (Ocaña *et al.*, 2014). In this study the potential synergy between glycolysis inhibitors, inhibitors of ATP production from aerobic glycolysis, and oestrone analogues showing anti-mitotic effects were investigated as a form of combination therapy using three different breast cancer cell lines representing the main phenotypic subtypes of breast cancer.

1.7 Aim of the study

This study aimed at elucidating the mechanism of action of two novel oestrone analogues in context of drug combinations with selected glycolysis inhibitors in an *in vitro* setting.

1.8 Objectives of the study

1. Identify synergistic combinations of oestrone analogues and glycolysis inhibitors using *in vitro* breast cancer models and the Median Effect equation.
2. Select the most promising combinations based on the combination index values calculated from the Median Effect equation and published toxicitydata for further assessment.
3. Assess the effect of the selected synergistic combinations on intracellular indicators of toxicity including generation of reactive oxygen species, mitochondrial effects, activation of the caspase cascade and assess the induced mode of cell death.
4. Investigate the anti-angiogenic potential of the selected synergistic combinations using *in vitro* angiogenesis models.

Chapter 2: Identification of synergistic combinations

2.1 Introduction

The first attempt at accurately describing the effect of a mixture of two agents was made in 1913 when Wilhelm Frei first published on the matter. He suggested that the combination of agents 'from the same pharmacological class' were suggested to obey the principle of iso-additivism, whereas mixtures of agents from separate classes are described as hetero-additivism (Frei, 1913). However, these descriptions were continually revised. Finally Bliss described a model for classifying combination therapy (Bliss, 1939):

1. *Independent combined effect*, where two agents with different mechanisms of action are combined to yield an effect which can be estimated from the dose response curves obtained for each agent.
2. *Similar combined effect,* where agents with similar mechanisms of actions are combined in constant proportions to yield an effect which can be estimated from the dose response curves obtained for each agent.
3. *Synergistic effect,* where the effect obtained from the combination of two agents are significantly enhanced when compared to that of each agent alone, and cannot be estimated from the dose response curves obtained for each agent.

These classifications are known as the Bliss Independence theory. However, this theory is limited as it cannot be used to describe combinations of agents which do not exert a greater effect than any of the agents by itself, i.e. additive combinations. Despite this shortcoming, the Bliss Independence theory, along with the Loewe Additivity theory, remains one of the most often used models in the search for synergistic combinations.

According to Loewe's Additivity theory if two compounds have no interaction the combination would be regarded as additive, if the compounds have a negative interaction the combination would be regarded as antagonistic, and if the compounds have a positive interaction the combination would be regarded as synergistic (Loewe, 1953; Fitzgerald *et al.*, 2006). Unfortunately the contradictions between these models have muddled research into combination therapy as, in certain cases, Bliss independence can be interpreted as Loewe antagonism and vice versa. However, as the Loewe model does not require any information about the mechanism of action of the agents, it is the preferred model to identify synergy (Lee, 2010).

Originally, synergy was identified by comparing the LD_{50} obtained from dose response curves for various fixed ratios of the two components (Bliss, 1939). Even though this method

provides a precise protocol to identify synergy, it requires vast quantities of experimental reagents, animals, funds and time. Alternatively, isobolograms can be constructed based on dose-response data for each agent alone and for the mixture of agents (Martinez-Irujo *et al.*, 1996). An isobologram, or isoffective graph, is then constructed based on the curvature of the isobologram. However, this method also requires large quantities of experimental data to accurately determine synergy (Martinez-Irujo *et al.*, 1996). A more time- and cost-effective approach became possible with the development of the Median Effect equation (*Eq. 1)* of Chou and Talalay (Chou and Talalay, 1984) which is based on the Loewe Additivity model whereby the dose-effect of combinations of agents were described in terms of the combination index (CI) of the mixture.

Eq. 1

$$\frac{fa}{fu} = \left(\frac{D}{Dm}\right)^m$$

Where:

$\boldsymbol{fa}$ represents the fraction of the population affected by the concentration used

$\boldsymbol{fu}$ represents the fraction of the population which are unaffected

$\boldsymbol{D}$ represents the concentration or dose of the test compound administered

$\boldsymbol{Dm}$ represents the dose giving the median effect of that test compound

$\boldsymbol{m}$ represents the shape or sigmoidicity of the dose response curve for the test compound

According to the Chou-Talalay method, the interaction between the agents used in combination may then be described in terms of the combination index (Chou, 2006) (*Eq. 2)*:

Eq. 2

$$> 1 \; antagonism \; (negative \; interaction)$$

$$CombinationIndex = \frac{[D]_1}{[D_x]_1} + \frac{[D]_2}{[D_x]_2} = 1 \; additive \; (no \; interaction)$$

$$< 1 \; synergism \; (positive \; interaction)$$

Where:

$\boldsymbol{D_1}$ represents the percentage of the experimental population affected (x%) by the combination of drug 1 and drug 2

$\boldsymbol{D_2}$ represents the percentage of the experimental population affected (x%) by the combination of drug 1 and drug 2

$[D_x]_1$ represents the concentration of drug 1 required to affect the experimental population by x%

$[D_x]_2$ represents the concentration of drug 2 required to affect the experimental population by x%

The Chou-Talalay method relies on the assumption that the two agents in the combination exert mutually exclusive effects and CalcuSyn software, based on the Median Effect equation, relies on this assumption (Lee, 2010). These indices can be calculated for a fixed ratio, or any other combination of agents, based on as few as two data points which significantly decreases the resources required to identify synergy. Even though fewer data points are required when fixed ratios are used as simulation can be performed to identify synergy over a range of concentrations, it is not always feasible as agents must be approximately equipotent to be combined in such a fashion. For agents which are not equipotent, the checkerboard approach or Latin square design of experimental combinations is often used (Chou, 2010).

In direct contrast to synergistic action, antagonism may also be elicited when agents are combined. In such cases the action of the two agents interfere with each other resulting in a decreased effect (Bliss, 1939). In the clinical setting, agents acting antagonistically may present as ineffective combinations or combinations which induce significant toxicity (Ocaña *et al.*, 2014).

Both synergistic and additive combinations may have advantages in a clinical setting (Ocaña *et al.*, 2014). There are four possible positive clinical outcomes when combining two effective anti-cancer agents (Frei *et al.*, 1961b; Greco *et al.*, 1996; Chou, 2006). These include:

1. Enhanced cancer eradicating power
2. Reduced dosages of anti-neoplastics may achieve the same or greater therapeutic effect, decreasing the risk of unacceptable toxicity in the patient
3. Limited risk of the cancer developing drug resistance
4. Greater selectivity for heterogeneous populations of cancer cells, with differing existing resistance

The first report of the therapeutic use of combinations of anti-cancer agents was published by Frei and colleagues. In that study, patients with acute leukaemia were treated with a purine analogue, folic acid antagonists or a combination of the two with mixed success: in children the combination treatment resulted in increased remission rate but had no effect on long-term survival, whereas in adults treatment with the combination did not result in the

highest remission rate but increased the survival rate by a slight margin. It was suggested, however, that the combination of a purine analogue with a folic acid antagonist diminished the incidence of resistance to either compound (Frei *et al.*, 1961a).

From this initial study, several guidelines as to the suitable combinations of agents were suggested. The suitability of compounds for use in combination regimens and the efficacy of such a combination in the clinical setting are determined by the toxicity profiles and mechanisms of action of each drug in the combination (Frei, 1972). Compounds with overlapping cytotoxic mechanisms are generally not used in combination as this increases the likelihood of adverse side effects leading to dose reduction, and potential loss of clinical benefit (Frei, 1972). Combining compounds with differing mechanisms of action are generally used in order to avoid drug resistance.

It has been reported that 40% of breast tumours demonstrate intracellular hypoxia with a median oxygen concentration below 0.3%, whilst non-cancerous breast tissue has a median oxygen concentration greater than 9% (Nualart *et al.*, 2009). The hypoxic intra-tumour environment induces aerobic glycolysis that requires large quantities of glucose for the cell's energy requirements and therefore glucose transporter inhibitors, such as fasentin, indinavir and quercetin, and glycolysis inhibitors, including 2-deoxyglucose, 3-bromopyruvate and lonidamine, demonstrate selective cytotoxicity towards malignant cells (Gatenby and Gillies, 2007).

The anti-cancer properties of the oestrone analogues have been demonstrated in various *in vitro* cancer models including breast (Stander *et al.*, 2011; Stander *et al.*, 2012, 2013), oesophageal (Wolmarans *et al.*, 2014) and cervical adenocarcinoma (Theron *et al.*, 2013). It has been proposed that the oestrone analogues induce cell death in cancer cells by generating reactive oxygen species, dissipation of the mitochondrial membrane potential, abnormal spindle formation culminating in cell cycle arrest in the G_2/M phase and apoptosis (Stander *et al.*, 2011; Stander *et al.*, 2012, 2013).

As the oestrone analogues, ESE-15-ol and ESE-16, and glycolysis inhibitors affect different hallmarks of cancer, it is proposed that the combination of these agents will improve existing treatment strategies aimed at effectively eradicating breast cancer. Therefore this study aimed at identifying synergistic combinations of oestrone analogues and glycolysis inhibitors on *in vitro* breast cancer models.

2.2 Materials

2.2.1 Cell culture reagents

1) Dulbecco's Modified Eagle's Medium (DMEM)

DMEM medium powder (Sigma-Aldrich, St Louis, USA) (67.35 g) was dissolved in 5 l sterile, distilled water and the pH adjusted to a final pH of 7.2 by the addition of 18.5 g $NaHCO_3$. The final concentration of glucose was 4.5 g/l. The solution was sterilised by filtration using three 0.2 µm cellulose acetate filters and dispensed into sterile 500 ml bottles. A 1% penicillin/streptomycin solution was added and the medium stored at 4°C. Immediately prior to use foetal calf serum was added to the medium at a concentration of 2% or 10%.

2) Foetal Calf Serum (FCS)

Sterile foetal calf serum (Biochrom, Berlin, Germany) was heat-inactivated by incubating at 56°C for 40 min. Cell culture medium used to maintain cells was supplemented with 10% FCS, while medium supplemented with 2% FCS were used for all drug exposure experiments to minimise protein binding effects.

3) Nutrient Mixture F-12 Ham, Kaighn's Modification (Ham's F-12)

Ham's F-12 medium powder (Sigma-Aldrich, St Louis, USA) (55.5 g) was dissolved in 5 l sterile, distilled water and the pH adjusted to a final pH of 7.2 by the addition of 12.5 g $NaHCO_3$. The final concentration of glucose was 1.26 g/l.The solution was sterilised by filtration using three 0.2 µm cellulose acetate filters and dispensed into sterile 500 ml bottles. A 1% penicillin/streptomycin solution was added and the medium stored at 4°C. Immediately prior to use foetal calf serum was added to the medium at a concentration of 2% or 10%.

4) MCF-12A medium

MCF-12A medium was prepared by combining 500 ml Ham's F12 and 500 ml DMEM. The following supplements were then added:

Hydrocortisone	50 µl of a 10 mg/ml solution
Cholera toxin	100 µl of a 0.1 mg/ml solution
Insulin	500 µl of a 20 mg/ml solution
Epidermal growth factor	200 µl of a 0.1 mg/ml solution (prepared in 0.6% acetic acid solution supplemented with 1% bovine serum albumin)

All reagents were procured from Sigma-Aldrich (St Louis, USA).

5) Roswell Park Memorial Institute (RPMI) Medium 1640

RPMI 1640 powder (Sigma-Aldrich, St Louis, USA) (52 g) was dissolved in 5 l sterile, distilled water and the pH adjusted to a final pH of 7.2 by the addition of 10 g $NaHCO_3$. The

final concentration of glucose was 2 g/l.The solution was sterilised by filtration using three 0.2 µm cellulose acetate filters and dispensed into sterile 500 ml bottles. A 1% penicillin/streptomycin solution was added and the medium stored at 4°C. Immediately prior to use foetal calf serum was added to the medium at a concentration of 2% or 10%.

6) Trypsin/Versene

A sterile 0.125% trypsin/versene solution in Ca^{2+} and Mg^{2+} free PBS was obtained from Highveld Biologicals (Johannesburg, RSA), stored at 4°C and used undiluted.

2.2.2 Reagents

1) 1% Acetic acid (v/v)

A 1% acetic acid (Sigma-Aldrich, St Louis, USA) was prepared by measuring 1 ml acetic acid into a 100 ml volumetric flask and filling the flask with dH_2O to the 100 ml mark. The solution was stored at room temperature.

2) Dimethylsulfoxide (DMSO)

DMSO (Merck Chemicals, Darmstadt, Germany) was used undiluted and stored in the dark at room temperature. The final DMSO concentration did not exceed 0.6% in any cell culture experiment.

3) Hank's buffered salt solution (HBSS)

Phenol red-free HBSS (Biochrom, Berlin, Germany) was used undiluted and stored at 4°C.

4) Phosphate buffered saline (PBS)

PBS was prepared by dissolving 9.23 g of powder (Becton, Dickinson and Company, Sparks, USA) in 1 l dH_2O. Where necessary the solution was filter sterilised using a 0.2 µm syringe filter.

5) Sulforhodamine B (SRB) stain solution

Sulforhodamine B stain (Sigma-Aldrich, St Louis, USA) was prepared by dissolving 0.057 g of SRB in 100 ml of 1% acetic acid (Sigma-Aldrich, St Louis, USA). The solution was stored in the dark at 4°C.

6) Trichloroacetic acid (TCA)

A 30% trichloroacetic acid (TCA) solution was prepared by dissolving 30 g of TCA (Sigma-Aldrich, St Louis, USA) in dH_2O and made up to 100 ml with dH_2O. The solution was stored at 4°C until required.

7) TRIS buffer

A 10 mM TRIS buffer was prepared by dissolving 120 mg of tris(hydroxymethyl)aminomethane (Sigma-Aldrich, St Louis) in 100 ml dH_2O. The pH of the solution was adjusted to 10.5 with a 1M NaOH solution and the solution stored at room temperature.

8) Trypan blue

A 0.2% (m/v) trypan blue solution was prepared by dissolving 100 mg of trypan blue (Sigma-Aldrich, St Louis, USA) in 50 ml PBS. The solution was filtered using a 0.45 µm filter to remove any insoluble crystals and stored at room temperature.

2.2.3 Experimental compounds: Oestrone analogues

2.2.3.1 2-Ethyl-3-O-sulphamoyl-estra-1,3,5(10)15-tetraen-17-ol (ESE-15-ol)

ESE-15-ol is not commercially available but was synthesised from oestrone by iThemba Pharmaceuticals (Pty) Ltd (Modderfontein, Gauteng, South Africa). Purity of ESE-15-ol was greater than 95% as determined by nuclear magnetic resonance spectroscopy (NMR) and liquid chromatography coupled to mass spectrometry (LC-MS/MS). Structural confirmation was obtained by high resolution mass spectrometry. A 10 mM stock solution was prepared by dissolving 5 mg of ESE-15-ol (MW = 359.16 g/mol) in 1.42 ml DMSO. Aliquots of 2 and 10 µl were prepared and stored at -80°C until diluted to required concentrations in an appropriate cell culture medium.

2.2.3.2 2-Ethyl-3-O-sulfamoyl-estra-1,3,5(10)16-tetraene (ESE-16)

ESE-16 is not commercially available but was synthesised from oestrone by iThemba Pharmaceuticals (Pty) Ltd (Modderfontein, Gauteng, South Africa). Purity of ESE-16 was greater than 95% as determined by nuclear magnetic resonance spectroscopy (NMR) and liquid chromatography coupled to mass spectrometry (LCMS). Structural confirmation was obtained by high resolution mass spectrometry. A 10 mM stock solution was prepared by dissolving 5 mg of ESE-16 (MW = 361.50 g/mol) in 1.38 ml DMSO. Aliquots of 2 and 10 µl were prepared and stored at -80°C until diluted to required concentrations in an appropriate cell culture medium.

2.2.3.3 2-Methoxyestradiol (2ME)

A 10 mM stock solution of 2ME was prepared by dissolving 5 mg of 2ME (Sigma-Aldrich, St Louis, USA) in 1.65 ml DMSO. Aliquots of 10 µl were prepared and stored at -80°C until diluted to required concentrations in an appropriate cell culture medium.

2.2.4 Experimental compounds: Glycolysis inhibitors

2.2.4.1 2-Deoxy-D-glucose (2DG)

A 930 mM stock solution was prepared by dissolving 610 mg 2DG (MW = 164.16 g/mol) (Sigma-Aldrich, St Louis, USA) in 4 ml HBSS. Aliquots of 83 and 21 µl were prepared and stored at -80°C until diluted in the appropriate cell culture medium.

2.2.4.2 3-Bromopyruvate (3-BrPA)

A 100 mM stock solution of 3-BrPA was prepared by dissolving 6.7 mg of 3-BrPA (MW = 166.96 g/mol) (Sigma-Aldrich, St Louis, USA) in 400 µl of DMSO. Aliquots of 5 µl were prepared and stored at -80°C until diluted in the appropriate cell culture medium.

2.2.4.3 Lonidamine (LON)

A 100 mM stock solution of LON (MW = 321.16 g/mol) (Sigma-Aldrich, St Louis, USA) was prepared by dissolving 5 mg in 155.7 µl DMSO. Aliquots of 15.5 and 7.8 µl were prepared and stored at -80°C until diluted in the appropriate cell culture medium.

2.2.4.4 Fasentin (FAS)

A 100 mM stock solution of FAS (MW = 279.64 g/mol) was prepared by dissolving 5 mg of FAS (Sigma-Aldrich, St Louis, USA) in 178.8 µl DMSO. Aliquots of 15.5 and 7.8 µl were prepared and stored at -80°C until diluted in the appropriate cell culture medium.

2.2.4.5 Indinavir (IND)

A 100 mM stock solution was prepared by dissolving 10 mg of IND (MW = 711.88 g/mol) (Sigma-Aldrich, St Louis, USA) in 140 µl DMSO. Aliquots of 15.5 and 7.8 µl were prepared and stored at -80°C until diluted in the appropriate cell culture medium.

2.2.4.6 Quercetin (QUER)

A 100 mM stock solution was prepared by dissolving 10 mg of QUER (MW = 302.24 g/mol) (Sigma-Aldrich, St Louis, USA) in 330.8 µl DMSO. Aliquots of 15.5 and 7.8 µl were prepared and stored at -80°C until diluted in the appropriate cell culture medium.

2.3 Methods

2.3.1 Maintenance of cell culture

Ethical approval (307/2013) for the study was obtained from the Research Ethics Committee of the University of Pretoria (see Addendum 1). All cell lines were originally purchased from the American Type Culture Collection.

Cells were grown in a humidified incubator at 37°C and an atmosphere of 5% CO_2. The specific growth characteristics and cell culture media required are indicated in Table 1. Medium was supplemented with 10% sterile, heat-inactivated FCS and was changed every 3 – 4 days.

Table 2.1: Growth characteristics of the cell lines used in the study.

Name	Reference number	Tissue type of origin	Medium required	Growth characteristic
MCF-7	ATCC HTB-22	Human breast adenocarcinoma	DMEM	Adherent
MDA-MB-231	ATCC HTB-26	Human metastatic breast carcinoma	DMEM	Adherent
SK-Br3	ATCC HTB-30	Human breast carcinoma	RPMI-1640	Adherent
MCF-12A	ATCC CRL-10782	Human breast tissue	DMEM	Adherent

The average reported doubling time of MCF-7 breast adenocarcinoma cells is 35 h (Sutherland *et al.*, 1983; Barnes *et al.*, 2001; Kimura *et al.*, 2010), 29 h for MDA-MB-231 breast adenocarcinoma cells (Reddel *et al.*, 1985; Glunde *et al.*, 2004; Kimura *et al.*, 2010), 40 h for SK-Br3 breast adenocarcinoma cells (Lee *et al.*, 2004; Yue *et al.*, 2012) and approximately 20 h for MCF-12A non-tumourigenic cells (Pauley *et al.*, 1993; Glunde *et al.*, 2004).

Previous studies using ESE-15-ol and ESE-16 showed a marked anti-proliferative effect on various breast cancer cell lines (Stander *et al.*, 2011). In this study MCF-12A spontaneous immortalised normal breast cells were selected to provide a control for the breast cancer cell lines. The oestrogen-receptor positive MCF-7 and the oestrogen-receptor negative MDA-MB-231 breast cancer cell lines were included as it has been shown to be particularly susceptible to the oestrone analogues (Stander *et al.*, 2011). The SK-Br3 cell line, derived from breast adenocarcinoma with enhanced Her2/c-erb-2 gene expression (Trempe and Fogh, 1973), represents 20 – 30% of clinical breast cancers (Scholl *et al.*, 2001) and were thus included in these studies.

2.3.2 Preparation of cells for assays and cell counting

Cells were harvested using a 0.125% trypsin/versene solution for approximately 10 minutes at 37°C. The released cell suspension was transferred from the cell culture flask to a sterile tube containing cell culture medium supplemented with 10% FCS and centrifuged (200 *g*, 5

min) to obtain a cell pellet which was re-suspended in 1 ml of complete cell culture medium (cell culture medium supplemented with 10% FCS).

The trypan blue exclusion method was used to determine cell count by adding 20 µl of cell suspension to 180 µl of trypan blue (0.2% m/v). Viable cells were counted using a haemocytometer and a Reichert Jung MicroStar 110 microscope at 100x magnification. Thereafter dilutions of the cell suspension in the appropriate medium supplemented with 2% FCS were made to achieve the cell concentration required for the drug exposure assays.

2.3.3 Sulforhodamine B (SRB) cell enumeration assay

Cell enumeration studies were performed at T_0, immediately prior to drug exposure to account for cell growth after seeding, and after 24 or 72 h exposure to oestrone analogues and glycolysis inhibitors. The SRB assay quantifies protein based on the ability of the dye to bind to basic amino acid residues under acidic conditions, while it is released into solution under basic conditions (Vichai and Kirtikara, 2006). Vichai's method was used in this study with slight modifications to enumerate cells post drug exposure.

Cells were seeded into sterile 96-well clear microtitre plates at a density of 5 x 10^3 cells/well and incubated overnight at 37°C in a humidified incubator at 5% CO_2 to allow for attachment. Thereafter the SRB assay was performed on one plate (T_0 as in Eq. 3) in order to account for increase in cell number due to cell growth. Equivalent plates were exposed to the oestrone analogues (3.12 – 400 nM for ESE-15-ol and ESE-16, 0.08 – 10 µM for 2ME) or glycolysis inhibitors (0.22 µM– 25 mM) and re-incubated for 24 or 72 h at the abovementioned conditions. After the incubation period cells were fixed with 80 µl of 30% TCA (final concentration TCA 10%) by direct addition of TCA to the plate 4°C overnight. Thereafter the plate was washed four times using tap water, and the plate allowed to dry.

SRB stain (100 µl of 0.057% in 1% acetic acid) was added to each well and the plate incubated at room temperature for 30 min. Excess dye was then removed by washing the plate four times with a 1% acetic acid solution and the plate allowed to dry. Once dry TRIS buffer (100 µl of 10 mM at pH 10.5) was added to each well and the plate left on a shaker until all the SRB had dissolved (30 – 90 min).The absorbance of the samples was measured spectrophotometrically at 570 nm with a reference wavelength of 630 nm using a Synergy 2 plate reader (Bio-Tek Instruments Inc., Vermont, USA).

2.3.4 Assessment of synergism of combinations of oestrone analogues andglycolysis inhibitors

An individual profile for each compound was created using CalcuSyn Software Version 2.0 (Biosoft, Cambridge, UK).

Once the GI_{50} concentrations were determined for each compound, a checkerboard lay-out of the combinations of the drugs was employed to determine possible synergistic combinations between the oestrone analogues and glycolysis inhibitors using only the three breast adenocarcinoma cell lines. The compounds were combined at ¼ x GI_{50}, ½ x GI_{50}, and GI_{50} concentrations. The oestrone analogues were also used at 2 x GI_{50} and 4 x GI_{50} as these compounds are known to be active in the nanomolar concentration range (Stander *et al.*, 2011). The plate lay-out used for the checkerboard approach is shown in Figure 2.1.

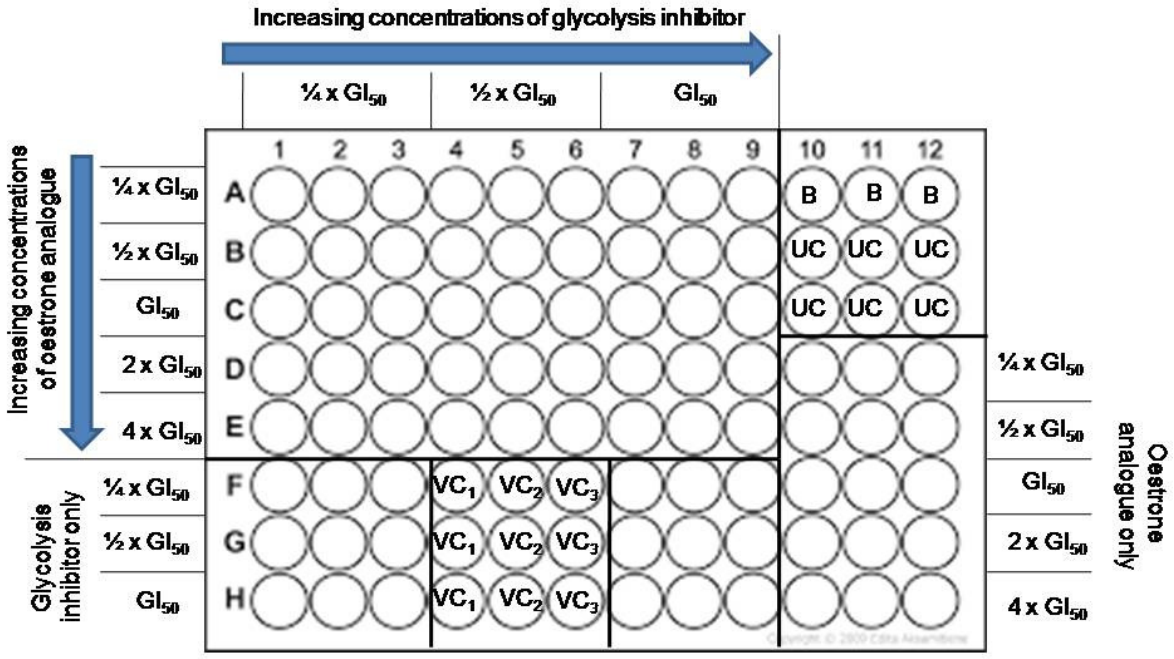

Figure 2.1: An overview of the checkerboard layout used in this study, where B represents the medium control, UC represents the untreated control, VC_1 represents the vehicle control of the glycolysis inhibitor, VC_2 represents the vehicle control of the oestrone analogue and VC_3 represents the combined vehicle of the oestrone analogue and glycolysis inhibitor.
Template of 96-well plate created by Edita Aksamitiene, open access. http://www.cellsignet.com/media/plates/96.jpg.

Briefly, MCF-7, MDA-MB-231 and SK-Br3 breast carcinoma cells were seeded into sterile 96-well clear microtitre plates at a density of 5 x 10^3 cells/well and incubated overnight at 37°C in a humidified incubator at 5% CO_2 to allow for attachment. Cells were exposed to the oestrone analogues and glycolysis inhibitors for 72 h at the abovementioned conditions. The

oestrone analogues were added to the plates first, immediately followed by the glycolysis inhibitors. After the incubation period the SRB assay was performed as described in Section 2.3.3.

2.3.5 Interpretation of results

A minimum of three independent experiments, which included internal triplicates, were conducted. The 50% growth inhibitory concentration (GI_{50}) of each compound was calculated using the formula (*Eq. 3)* as used by the National Cancer Institute (Grever *et al.*, 1992):

Eq. 3

$$\textit{Growth inhibitory effect} = 100\ X\frac{(T - T_0)}{(C - T_0)}$$

Where:

T represents the optical density of the test well after the background noise has been deducted after 24 or 72 hours incubation

T_0 represents the optical density after the background noise has been deducted at time zero (drug addition)

C represents the optical density of the vehicle treated control after the background noise has been deducted

GraphPad Prism version 4.0 for Windows (GraphPad Software, San Diego California USA, www.graphpad.com) was used for all statistical calculations and determination of the GI_{50} values. GraphPad allows for the analysis of data and calculation of GI_{50} concentrations using various curve fitting regression models. CalcuSyn Software Version 2.0 (Biosoft, Cambridge, UK) was used to analyse the results of the combination experiments and to calculate the combination index (CI) values of the drug combinations used in the study. Data was described in terms of the fraction affected (fa), limited to values between 0 and 1, in order to analyse the combinations with CalcuSyn. The following equation (*Eq. 4)* was used to calculate fa:

Eq. 4

$$fa = \frac{(A_c - A_b) - (A_e - A_b)}{(A_c - A_b)}$$

Where:

$\mathbf{A_c}$ represents the optical density of the vehicle treated control

$\mathbf{A_b}$ represents the optical density of the background

$\mathbf{A_e}$ optical density of the test well

The process used to identify synergistic combinations is summarised in Figure 2.2.

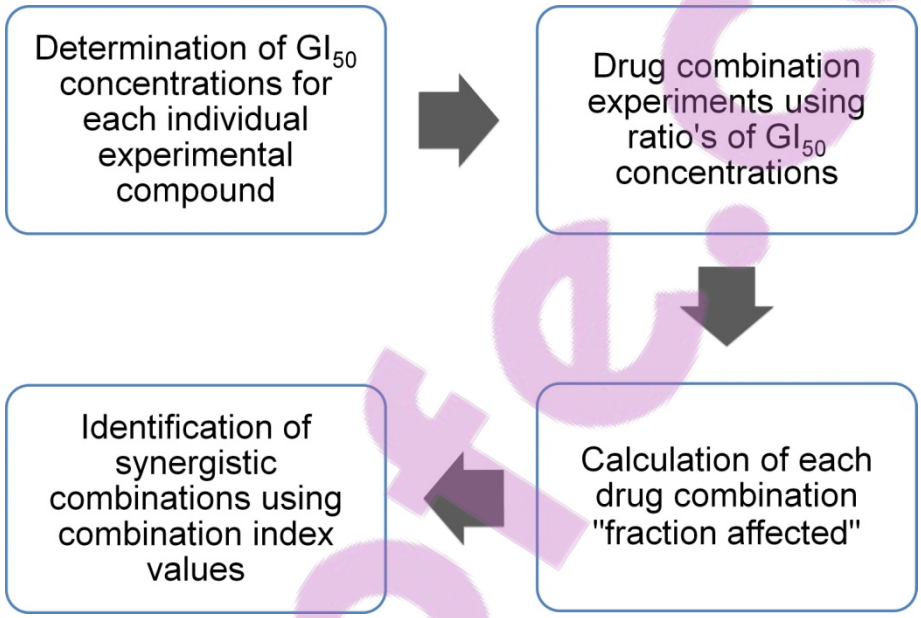

Figure 2.2: Flow diagram of the data generation and interpretation process followed in this study.

2.4 Results

2.4.1 Growth inhibition studies

The cytotoxicity of the oestrone analogues and glycolysis inhibitors were determined on the MCF-7, MDA-MB-231 and SK-Br3 breast carcinoma cells and the MCF-12A normal breast cell line after 24 and 72 h. These incubations periods allowed the study of the immediate and prolonged effect of the experimental compounds on the cell growth. GI_{50} concentrations obtained after 24 and 72 h exposure are shown in Table 2.2. Dose response curves for the oestrone analogues and 2ME on the MCF-7 breast adenocarcinoma cell line are shown in Figure 2.2.

After 24 h treatment the MCF-7 cells showed greatest sensitivity to treatment with ESE-15-ol with a calculated GI_{50} of 44.36 ± 1.13 nM, while the SK-Br3 cells exhibited the lowest GI_{50} concentration for ESE-16 at 76.40 nM (Table 2.2). The oestrone analogues were found to be at least 2.2 times more potent than 2ME. The MCF-12A cells were most susceptible to ESE-15-ol.

The glycolysis inhibitors demonstrated large susceptibility differences between cell lines and the different inhibitors. The non-tumourigenic MCF-12A and MDA-MB-231 breast adenocarcinoma cell lines were least susceptible to IND treatment after 24 h exposure with GI_{50} concentrations greater than 500 µM, the highest concentration tested. At a concentration of 500 µM of IND cell growth was not reduced by 50% and a GI_{50} concentration could therefore not be calculated. The MCF-7 and SK-Br3 cell lines were most susceptible to QUER with GI_{50} values of 108.40 and 77.90 µM, respectively).

No time-dependent decrease in the GI_{50} concentrations was observed after 72 h treatment (Table 2.2). ESE-15-ol was found to inhibit the growth of SK-Br3 cells most potently with a GI_{50} of 52.7 nM, whereas the MCF-7 cells were the most susceptible of the three breast cancer cell lines to exposure to ESE-16. ESE-15-ol again caused more growth inhibition in the MCF-12A cell line than ESE-16. Similar to the results obtained after 24 h treatment, the oestrone analogues were found to be at least 3 times more potent than the parent compound, 2ME.

The GI_{50} concentrations calculated for 2DG, 3-BrPA and FAS were found to be lower for the non-tumourigenic MCF-12A cells than for the three breast cancer cell lines tested. Comparable GI_{50} concentrations were obtained for QUER and LON on the tumourigenic and non-tumourigenic cell lines.

Of the glycolysis inhibitors, the MCF-12A cell line was most susceptible to treatment with FAS as indicated by the low GI_{50} (20.67 ±1.07 µM) obtained. The growth of the MCF-7 and SK-Br3 cell lines were also most susceptible to FAS with calculated GI_{50} concentrations of 25.15 µM and 21.10 µM respectively. The MDA-MB-231 cell line exhibited a GI_{50} of 0.64 µM for QUER.

Dose response curves for ESE-15-ol, ESE-16 and 2ME (Figure 2.3) indicate that these compounds inhibited the growth of MCF-7 cells after 24 and 72 h exposure.

Table 2.2: Effect of the oestrone analogues and six glycolysis inhibitors on the growth of **MCF-12A**, **MCF-7, MDA-MB-231** and **SK-Br3** cells after 24 and 72 h exposure expressed as GI_{50} ± SEM. Results are given in µM unless otherwise indicated. A minimum of 3 independent experiments were performed.

	MCF-12A		MCF-7		MDA-MB-231		SK-Br3	
	24 h	**72 h**	**24 h**	**72 h**	**24 h**	**72 h**	**24 h**	**72 h**
ESE-15-ol (nM)	44.36 ± 1.13	40.70 ± 1.14	48.98 ± 1.07	70.03 ± 1.11	78.07 ± 1.10	61.44 ± 1.10	60.08 ± 1.17	52.73 ± 1.01
ESE-16 (nM)	71.57 ± 1.11	62.40 ± 1.17	82.19 ± 1.09	67.05 ± 1.18	145.00 ± 1.22	142.6 ± 1.09	76.40 ± 1.20	79.76 ± 1.01
2ME	1.28 ± 1.21	1.58 ± 1.08	0.27 ± 1.06	0.49 ± 1.33	0.32 ± 1.32	0.45 ± 1.13	0.54 ± 1.19	0.76 ± 1.07
2DG (mM)	7.35 ± 2.10	4.79 ± 1.40	1.34 ± 1.59	10.76 ± 2.63	6.22 ± 1.20	6.73 ± 1.25	9.13 ± 1.28	8.00 ± 1.62
3-BrPA	77.73 ± 1.12	81.80 ± 1.11	126.90 ± 1.06	71.92 ± 1.17	210.70 ± 5.12	480.30 ± 1.70	118.70 ± 1.19	168.60 ± 1.42
LON	198.20 ± 1.26	140.40 ± 1.16	110.80 ± 1.42	153.3 ± 1.30	104.10 ± 1.35	188.30 ± 1.17	137.30 ± 1.23	165.40 ± 1.02
FAS	200.10 ± 2.01	20.67 ± 1.07	290.10 ± 7.57	25.15 ± 1.35	159.80 ± 1.06	29.89 ± 1.11	399.70 ± 3.05	21.10 ± 1.04
IND	>500	> 500	123.70 ± 1.56	230.3 ± 1.99	> 500	55.45 ± 1.08	146.20 ± 12.3	87.98 ± 1.23
QUER	189.70 ± 3.27	60.62 ± 1.15	108.40 ± 1.40	83.8 ± 4.19	269.20 ± 6.25	0.64 ± 1.42	77.90± 1.24	28.03 ± 1.31

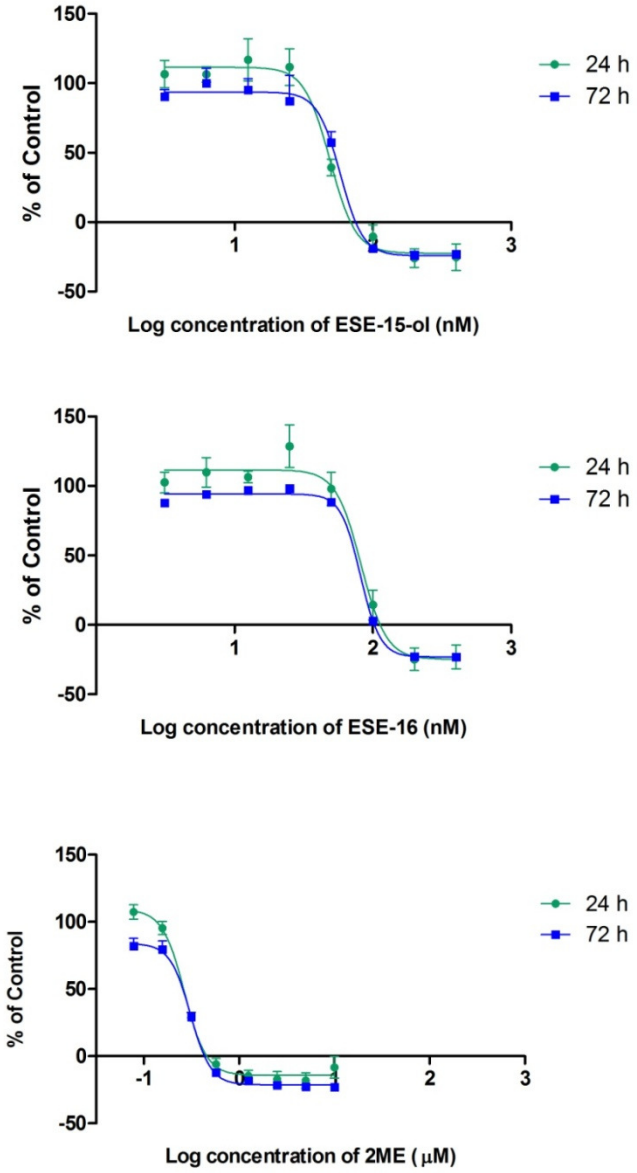

Figure 2.3: Effects of ESE-15-ol, ESE-16 and 2ME on the growth of **MCF-7** cell line after both 24 and 72 h treatment as determined using the SRB assay.Note the units for the concentration of 2ME are 1 000x the concentrations of ESE-15-ol and ESE-16.
Min n = 3

2.4.2 Identification of synergism

Oestrone analogues and glycolysis inhibitors were combined in ratios of the GI_{50}concentrations calculated for each cell line. The data generated was converted to fraction affected using *Eq.* 4 and CalcuSyn software used to assess the combinations for synergy.

An example of the graphs produced by CalcuSyn is shown in Figure 2.4. As already mentioned above, isobolograms are traditionally used to assess synergy, and as such an example of the isobolograms generated for the tested combinations is shown in Figure 2.4.

For the MCF-7 cell line synergistic combinations were identified for 2DG, IND and QUER for both oestrone analogues tested (Table 2.3). However, synergism was not identified for any combinations containing LON, and only for the ESE-16 and FAS combinations. The lowest combination index value (0.37) for the combination of 2DG and ESE-15-ol was calculated for the combination of 10.76 mM 2DG with 17.5 nM ESE-15-ol, while the combination of 10.76 mM 2DG and 134 nM ESE-16 resulted in a combination index of 0.24. Where 134 nM of ESE-16 was combined with 6.28 µM FAS a CI of 0.95 was determined. A combination index value of 0.57 was calculated for the combination of 57.5 µM of IND and 70 nM of ESE-15-ol. The combination of 57.5 µM IND and 134 nM ESE-16 also resulted in the lowest CI value determined (0.24). For the combinations with QUER tested, the lowest concentration of each oestrone analogue (17.5 nM of ESE-15-ol and 16.8 nM of ESE-16) resulted in the lowest CI values determined: 83.8 µM QUER with ESE-15-ol resulted in a CI value of 0.24 where 42 µM of QUER with ESE-16 resulted in a CI value of 0.18.

The majority of combinations tested with ESE-15-ol on the MDA-MB-231 cell line showed the lowest CI value where ESE-15-ol was used at 123.0 nM: a CI of 0.51 was identified with 188.3 µM LON, a CI of 0.69 with 55.45 µM IND and a CI of 0.56 with 132 µM of QUER (Table 2.4). For combinations with 2DG the lowest CI value (0.13) was calculated for the combination of 15.36 nM ESE-15-ol and 6.63 Mm 2DG. A CI value of 0.71 was determined where 480 µM of 3-BrPA was combined with 15.36 nM ESE-15-ol. A similar trend was observed for ESE-16 as the lowest CI values for most of the glycolysis inhibitors were calculated where 285.2 nM of ESE-16 was used: a CI value of 0.45 for the combination with 188.3 µM LON, a CI value of 0.97 where 285.2 nM ESE-16 was used with 55.45 µM IND and a CI value of 0.96 for the combination of ESE-16 and 0.64 µM QUER. For 2DG the lowest CI value (0.28) was determined where 35.65 nM of ESE-16 was used in combination with 6.73 mM 2DG, and for 3-BrPA (480 µM) where 35.65 nM ESE-16 was used (0.70).

No synergistic combinations were identified for any of the combinations tested on the SK-Br3 cell line, i.e. no combination index values of less than 1 were found for any of the combinations tested (Table 2.5).

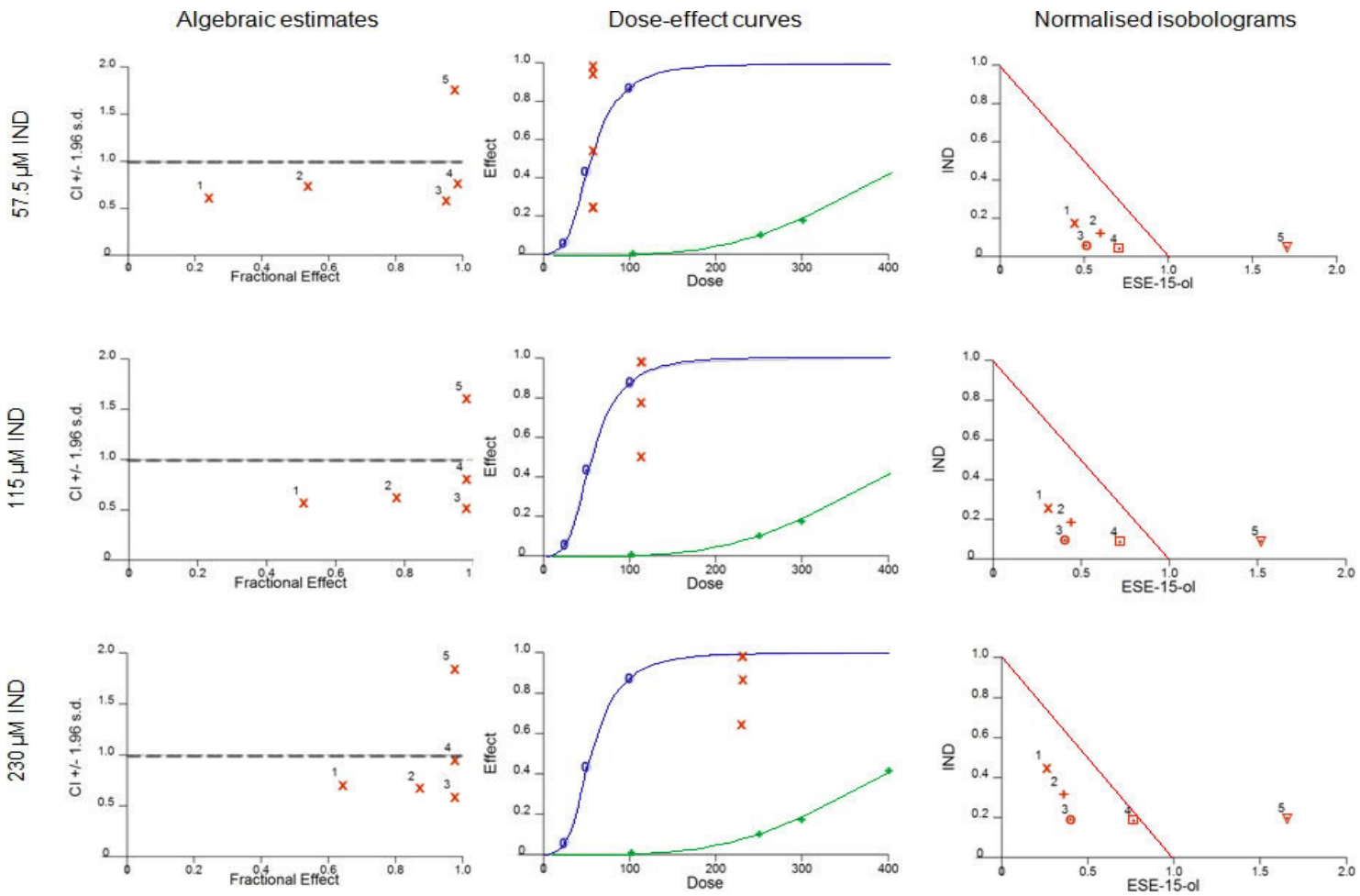

Figure2.4: Graphical representation of the combination of ESE-15-ol and IND on the **MCF-7** breast adenocarcinoma cell line. In the algebraic estimates and normalised isobolograms, combinations are indicated numerically: the lowest number corresponds to the lowest concentration of ESE-15-ol used. For dose-effect curves the blue curve represent that of ESE-15-ol the green the dose-effect curve of IND. A minimum of 3 independent experiments were performed. Note that the maximum value on the Y-axis for the algebraic estimate graphs is 2.0, while the maximum value on the Y-axis is 1.0 for the remainder of the graphs.

Table 2.3: Combination index values obtained for combination of oestrone analogues with glycolysis inhibitors and GLUT inhibitors on **MCF-7** breast adenocarcinoma cell line after 72 h incubation. Concentrations of compounds are given in µM unless otherwise indicated. Synergistic combinations (CI < 1) are indicated in blue and antagonistic combinations (CI > 1) are indicated in green. Where no CI value is shown the calculated fraction affected did not fall between 0 and 1. A minimum of 3 independent experiments were performed.

		ESE-15-ol (nM)					ESE-16 (nM)				
		17.50	**35.00**	**70.00**	**140.00**	**280.00**	**16.75**	**33.5**	**67.00**	**134.00**	**268.00**
2DG at ¼ x GI_{50}	**2.69 (mM)**	0.54	0.80	1.03	0.79	1.49	0.91	1.54	1.69	0.29	0.41
2DG at ½ x GI_{50}	**5.38 (mM)**	0.47	0.69	0.88	0.80	1.57	0.60	0.98	1.11	0.28	0.43
2DG at GI_{50}	**10.76 (mM)**	0.37	0.56	0.68	-	-	0.47	0.70	0.71	0.24	0.35
3-BrPA at ¼ x GI_{50}	**18.00**	> 10	10.00	1.39	0.48	1.21	> 10	> 10	3.99	0.26	0.35
3-BrPA at ½ x GI_{50}	**36.00**	-	6.07	1.12	0.34	1.15	> 10	> 10	2.84	0.24	0.37
3-BrPA at GI_{50}	**71.97**	7.81	2.92	0.74	-	-	1.99	2.78	0.98	0.32	0.70
LON at ¼ x GI50	**38.25**	-	-	3.13	4.5	6.46	-	-	9.67	2.36	3.11
LON at ½ x GI50	**76.50**	-	> 10	5.37	9.64	9.00	> 10	7.61	2.57	3.57	4.68
LON at GI50	**153.00**	-	> 10	-	> 10	> 10	-	7.50	6.54	> 10	> 10
FAS at ¼ x GI_{50}	**6.28**	-	> 10	1.78	2.31	3.74	> 10	> 10	2.64	0.95	4.12
FAS at ½ x GI_{50}	**12.50**	> 10	> 10	3.48	5.21	4.33	1.45	2.14	0.97	1.17	3.45
FAS at GI_{50}	**25.00**	> 10	> 10	> 10	> 10	> 10	2.87	7.08	3.30	2.90	5.60
IND at ¼ x GI_{50}	**57.50**	0.66	0.73	0.57	0.75	1.75	3.86	3.41	0.35	0.24	0.51
IND at ½ x GI_{50}	**115.00**	0.57	0.62	0.50	0.81	1.61	1.45	1.62	0.29	0.26	0.47
IND at GI_{50}	**230.00**	0.71	0.67	0.59	0.95	1.85	1.04	1.04	0.44	0.42	0.66
QUER at ¼ x GI_{50}	**21.00**	> 10	3.24	1.15	1.85	3.67	0.50	0.75	1.00	0.69	2.88
QUER at ½ x GI_{50}	**42.00**	0.35	0.57	0.99	1.99	3.68	0.18	0.38	0.59	0.92	2.63
QUER at GI_{50}	**83.8**	0.24	0.46	1.02	2.16	3.99	0.09	0.17	0.38	0.71	2.54

Table 2.4: Combination index values obtained for combination of oestrone analogues with glycolysis inhibitors and GLUT inhibitors on **MDA-MB-231** breast adenocarcinoma cell line after 72 h incubation. Concentrations of compounds are given in µM unless otherwise indicated. Synergistic combinations (CI < 1) are indicated in blue and antagonistic combinations (CI > 1) are indicated in green. Where no CI value is shown the calculated fraction affected did not fall between 0 and 1. A minimum of 3 independent experiments were performed.

		ESE-15-ol (nM)					ESE-16 (nM)				
		15.36	**30.72**	**61.44**	**123.00**	**245.76**	**35.65**	**71.30**	**142.60**	**285.20**	**570.40**
2DG at ¼ x GI_{50}	**1.68 (mM)**	> 10	> 10	> 10	1.15	2.41	> 10	> 10	3.58	1.82	2.52
2DG at ½ x GI_{50}	**3.36 (mM)**	1.95	2.73	1.89	0.87	0.82	4.60	4.29	1.57	1.44	2.11
2DG at GI_{50}	**6.73 (mM)**	0.13	0.23	0.32	0.29	0.75	0.28	0.36	0.40	0.60	1.08
3-BrPA at ¼ x GI_{50}	**120**	4.45	2.82	1.26	1.01	1.94	2.08	3.36	1.63	1.34	2.31
3-BrPA at ½ x GI_{50}	**240**	1.42	1.48	1.04	1.12	2.00	1.35	1.76	1.25	1.34	2.25
3-BrPA at GI_{50}	**480**	0.71	0.74	0.73	0.84	1.33	0.70	0.85	0.87	1.03	1.49
LON at ¼ x GI_{50}	**47.00**	> 10	> 10	6.44	0.85	2.11	> 10	> 10	6.31	1.00	2.29
LON at ½ x GI_{50}	**94.15**	6.87	6.12	2.51	0.73	1.56	6.15	5.38	2.14	0.85	1.67
LON at GI_{50}	**188.30**	1.32	1.44	1.35	0.51	0.60	1.30	1.41	0.60	0.45	1.33
FAS at ¼ x GI_{50}	**7.45**	3.63	4.93	2.80	1.16	2.34	5.69	7.04	3.93	1.85	2.64
FAS at ½ x GI_{50}	**14.90**	1.64	2.64	2.68	1.53	2.45	2.33	2.85	2.91	1.995	2.19
FAS at GI_{50}	**29.89**	1.14	2.11	2.06	1.54	1.98	1.61	2.18	2.21	1.45	1.17
IND at ¼ x GI_{50}	**13.80**	> 10	9.169	4.29	0.73	2.19	-	> 10	1.74	1.45	3.18
IND at ½ x GI_{50}	**27.70**	4.57	3.716	3.26	0.74	2.31	> 10	4.32	1.33	1.27	2.84
IND at GI_{50}	**55.45**	2.01	2.08	2.41	0.69	2.02	2.10	2.26	1.09	0.97	1.9
QUER at ¼ x GI_{50}	**0.16**	-	7.92	1.69	0.60	1.32	-	> 10	2.64	1.15	3.09
QUER at ½ x GI_{50}	**0.32**	> 10	8.57	1.11	0.56	1.38	> 10	8.36	2.27	1.00	2.37
QUER at GI_{50}	**0.64**	-	> 10	2.36	0.72	1.96	> 10	8.47	2.44	0.96	2.26

Table 2.5: Combination index values obtained for combination of oestrone analogues with glycolysis inhibitors and GLUT inhibitors on **SK-Br3** breast adenocarcinoma cell line after 72 h incubation. Concentrations of compounds are given in µM unless otherwise indicated. Synergistic combinations (CI < 1) are indicated in blue and antagonistic combinations (CI > 1) are indicated in green. Where no CI value is shown the calculated fraction affected did not fall between 0 and 1. A minimum of 3 independent experiments were performed.

		ESE-15-ol (nM)					ESE-16 (nM)				
		13.18	**26.37**	**52.73**	**105.46**	**210.92**	**19.94**	**39.88**	**79.76**	**159.52**	**319.04**
2DG at ¼ x GI_{50}	**2.00 mM**	3.58	3.98	4.43	7.38	> 10	6.68	6.02	5.16	5.57	7.06
2DG at ½ x GI_{50}	**4.00 mM**	6.85	7.54	8.00	> 10	> 10	> 10	9.76	8.88	8.95	> 10
2DG at GI_{50}	**8.00 mM**	> 10	> 10	> 10	> 10	> 10	> 10	> 10	> 10	> 10	> 10
3-BrPA at ¼ x GI_{50}	**42.15**	2.78	3.17	1.36	1.49	2.94	1.66	1.00	1.09	1.78	3.45
3-BrPA at ½ x GI_{50}	**84.30**	2.01	3.45	1.30	1.36	2.91	1.93	1.21	1.21	1.73	3.42
3-BrPA at GI_{50}	**168.6**	3.74	2.49	1.53	1.30	2.94	1.63	1.32	1.22	1.78	3.37
LON at ¼ x GI_{50}	**41.35**	1.50	1.80	1.65	2.30	4.08	7.94	7.40	6.04	5.15	6.57
LON at ½ x GI_{50}	**82.70**	1.51	1.67	1.89	2.78	4.46	> 10	> 10	> 10	9.08	9.63
LON at GI_{50}	**165.40**	1.63	1.75	2.13	2.90	3.75	> 10	> 10	> 10	> 10	> 10
FAS at ¼ x GI_{50}	**5.27**	2.97	2.79	1.78	1.87	3.64	2.22	2.29	1.72	2.16	3.92
FAS at ½ x GI_{50}	**10.55**	3.09	3.13	2.13	2.26	3.84	2.13	2.36	2.17	2.50	4.18
FAS at GI_{50}	**21.10**	2.38	2.83	2.18	2.50	3.87	1.52	2.02	1.97	2.63	4.10
IND at ¼ x GI_{50}	**21.99**	-	2.69	1.95	1.79	3.16	-	1.27	1.32	2.07	3.77
IND at ½ x GI_{50}	**43.99**	3.12	2.95	2.34	1.99	3.58	-	2.80	1.78	2.38	4.15
IND at GI_{50}	**87.98**	2.95	3.41	2.81	2.57	4.16	2.75	2.67	2.30	2.85	4.57
QUER at ¼ x GI_{50}	**7.00**	1.78	1.9	1.25	1.65	2.96	1.99	1.80	1.72	2.24	3.70
QUER at ½ x GI_{50}	**14.00**	2.47	2.38	1.37	1.99	3.19	2.64	2.21	2.03	2.47	3.81
QUER at GI_{50}	**28.00**	-	3.03	2.03	2.92	4.00	2.97	3.44	2.97	3.26	4.09

2.5 Discussion

The growth inhibition following 72 h exposure to the combinations between either of the two oestrone analogues, ESE-15-ol and ESE-16, and six glycolysis inhibitors using three phenotypically different breast cancer cell lines was assessed. These results formed the basis for the remainder of the study. In order to determine the optimal combinations of the oestrone analogues and glycolysis inhibitors to use, the effect of each compound on cell growth was determined on each cell line following 24 and 72 h treatment periods. The three breast cancer cell lines used in this study where chosen based on their differing phenotypic subtypes: the MCF-7 cell line represents oestrogen receptor positive breast carcinoma (Lippman *et al.*, 1976), the MDA-MB-231 cell line represents triple negative breast carcinoma (Cailleau *et al.*, 1974) and the Sk-Br3 cells represent Her2 positive breast cancer (Trempe and Fogh, 1973). It has been reported that the Her-2 expression in SK-Br3 cells is 18 fold higher than that of MCF-7 cells (Merlin *et al.*, 2002).

In vitro cytotoxicity studies have shown selective susceptibility of 2ME to different breast cancer cell lines. Previous studies have indicated that the SK-Br3 cell line are less susceptible to 2ME as significant growth inhibition was not observed at concentrations of 2ME below 2.5 µM, whereas 1 µM of 2ME reduced the number of MCF-7 cells by approximately 50% (Vijayanathan *et al.*, 2006). In the present study the same trend was observed when the different cancer cell lines were treated with 2ME: the observed susceptibility between the cell lines from most susceptible to least susceptible were MCF-7 ≥ MDA-MB-231 > SK-Br3. For the two test oestrone analogues the susceptibility trend changed at both incubation periods where the observed susceptibility between the cell lines from most susceptible to least susceptible were MCF-7 ≥ SK-Br3 > MDA-MB-231.

Claims have been made about the superior efficacy of the oestrone analogues in comparison to that of 2ME (Stander *et al.*, 2011; Repsold *et al.*, 2014b). Data from the present study showed that the lowest concentration of 2ME that resulted in 50% growth inhibition was 270 nM in the MCF-7 oestrogen receptor positive breast cancer cell line after 24 h exposure. In comparison to the 82 nM (ESE-15-ol) and 48 nM (ESE-16) of the oestrone analogues required to achieve the same result, the enhanced potency of the oestrone analogues is thus confirmed.

For this study the concentration of each experimental compound which results in 50% growth inhibition was determined as an indicator of each compound's potency. The GI_{50} is an indicator of cytostatic potential, and not cytotoxic ability like more commonly used indicators of potency such as the 50% inhibitory concentration (IC_{50}) or lethal dose for 50% of the study population (LD_{50}) (Grever *et al.*, 1992). It has been reported that these different

parameters, such as GI_{50} and IC_{50} concentrations, often do not correlate well (Fallahi-Sichani *et al.*, 2013). An advantage of using GI_{50} concentration assays is that the rate of cell population increase is considered (Monks *et al.*, 1991).

Cells were initially treated with the individual compounds followed by treatment with ratio's of the GI_{50} concentrations determined for each experimental compound following 72 h incubation in the presence of the drug combination. The growth inhibition data generated from these different ratios of the combination of drugs were converted to "fraction affected" (as indicated by *Eq. 4*) in order to determine the combination index for the combinations tested. The process used to identify the synergistic combinations is shown in Figure 2.2.

To facilitate the selection of synergistic combinations, the cytotoxicity of the oestrone analogues on the non-tumourigenic MCF-12A cell line was considered. The reported doubling time of MCF-12A cells are 20 hours (Pauley *et al.*, 1993; Glunde *et al.*, 2004). Previous studies have indicated that both oestrone analogues disrupt the formation of the microtubule structure essential for the progression through the G_2 phase of the cell cycle (Stander *et al.*, 2011). It is therefore expected that the oestrone analogues will have the greatest effect after at least one cell cycle has been completed. After 24 h exposure, ESE-15-ol caused 50% growth inhibition in the MCF-12A cell line at 44.36 nM, and ESE-16 at 71.57 nM. The GI_{50} concentrations calculated for the oestrone analogues decreased after 72 h treatment (40.7 nM for ESE-15-ol and 62.4 nM for ESE-16) when a larger percentage of the original cells had undergone further cell cycles.

The specificity of ESE-15-ol and ESE-16 has been reported in a number of publications from the same research group. An *ex vivo* study evaluating the effects of ESE-15-ol and ESE-16 on the ultrastructure of erythrocytes and platelets revealed that treatment with 180 nM of either ESE-15-ol and ESE-16 for 24 h did not alter the ultrastructure of these blood cells suggesting that these compounds may be tolerated at higher concentrations than the GI_{50} on the MCF-12A cells indicate (Repsold *et al.*, 2014a). The GI_{50} concentration for MCF-12A cells was reported to be in excess of 160 nM after 48 h exposure to ESE-15-ol and ESE-16 as determined by the crystal violet DNA stain technique (Stander *et al.*, 2011). However, the discrepancy in the reported and observed GI_{50} may be explained by different cell enumeration assays used (crystal violet in the 2011 study vs SRB in the present study) or the different models used to calculate the GI_{50}. Even though both studies made use of the formula developed by Grever for calculating the GI_{50} concentrations (Grever *et al.*, 1992), the present study made use of non-linear regression in order to plot the data and to determine the GI_{50} concentrations.

The crystal violet stain is useful as a nuclear stain which can be correlated to cell number. However, when cultures reach confluence cell-cell inhibition will lead to decreased cell size and this can skew the correlation between cell number and the absorbance measured (Saotome *et al.*, 1989). It is possible that MCF-12A cellcultures,seeded at 5 x 10^3 cells/well in a 96-well plate,willreach confluence after 48 h given the approximate doubling time of MCF-12A cells (Pauley *et al.*, 1993) and could also explain the discrepancy between the calculated GI_{50} results.

It is clear when comparing previous reports with the outcomes of this study that the effect of the oestrone analogues on only one non-tumourigenic cell line cannot be used as indicator of the drug selectivity or as indicator of potential systemic toxicity if these compounds to be administered *in vivo*.

It must be noted that the GI_{50} concentrations obtained after 24 and 72 h exposure to the oestrone analogues or glycolysis inhibitors (Table 2.2) do not always showa time dependent effect. This may be due to the interpretation of data as percentage growth inhibition, and not percentage cell death, as the measuredresponse. In context of growth inhibition, the similarity in GI_{50} concentrations after 24 and 72 h exposure may be indicative of a cytostatic response. The use of combinations of the test compounds may induce cytotoxic effects through enhanced metabolic stress.

Selecting suitable agents to combine to achieve a synergistic effect depends on these agents possessing different mechanisms of action (Frei, 1972) from the test compounds. In order to comply with this principle, the oestrone analogues were combined with glycolysis inhibitors that influence the energy production within the cells and the effect of these compounds as monotherapy on the cell growth of MCF-7, MDA-MB-231 and SK-Br3 tumourigenic cells and MCF-12A non-tumourigenic cells were investigated before drug combination ratios were established. Due to the heterogeneity in cancerous tissue, treatment with glycolysis inhibitors alone does not result in a significant anti-tumour effect. The greatest success has been observed where glycolysis inhibitors have been used in combination with other chemotherapeutic agents. This is potentially due to the impaired ability of ATP-deprived cancer cells to repair damage caused by chemotherapeutic agents (Gatenby and Gillies, 2007).

A number of toxic effects have been associated with the use of glycolysis inhibitors. These include hypoglycaemia and associated adverse effects including fatigue, sweating, nausea (Singh *et al.*, 2005; Raez *et al.*, 2013). The use of a combination strategy allows for the use of reduced concentrations of these compounds which could potentially minimise adverse effects experienced in the clinical setting.

A study investigating the optimal incubation period for growth inhibition studies found that the growth inhibitory effects of 20 anti-cancer compounds with known toxicity data could most reliably be determined after 48 – 96 h exposure periods (Monks *et al.*, 1991). Moreover, it has previously been suggested that compounds affecting the cell cycle, such as the oestrone analogues used in this study, should be determined after 72 – 96 hours (Fallahi-Sichani *et al.*, 2013). A 72 hexposure period was identified as the most suitable time point for evaluating agents that inhibit cell cycle progressionat a late phase. The 72 h incubation time was selected in this study as the exposure period for which synergistic effects of combinations of oestrone analogues and glycolysis inhibitors would be evaluated. Cytotoxicity results obtained after 24 h exposure periods were also collected for comparison to published results and to provide additional data for mechanistic assays performed after 24 h.

When the six selected glycolysis inhibitors were individually combined with the oestrone analogues, the synergistic combinations for further study were influenced based on the potential cytotoxicity of the compounds on the non-tumourigenic MCF-12A cell line. The concentration range of the different glycolysis inhibitors which would ensure anti-glycolytic activity was also considered. The aim of finding synergistic combinations is to decrease the risk of developing drug resistance while ensuring the maximum therapeutic response at minimum doses of each compound (Frei *et al.*, 1961a). Therefore combinations using minimal concentrations of the oestrone analogues identified as synergistic were selected for the study.

It must be considered that 2DG is a structural analogue of glucoseand is transported into the cell via the GLUT transporters acting as a competitive substrate at the different GLUT transporters. Serum glucose concentrations of a healthy adult are approximately 5.5 mmol/l. Therefore the use of 2DG in millimolar concentrations is theoretically feasible. Indeed, numerous clinical trials have reported using doses of 2DG as high as 300 mg/kg (Singh *et al.*, 2005; Dwarakanath *et al.*, 2009).

Data showed that the MCF-7 oestrogen receptor positive cell line was more susceptible to 2DG after 24 h than the SK-Br3 cell line. Previous studies using the crystal violet assay have reported that treatment with 2DG (8 mM for 72 h) reduced the cell number of MCF-7 cells by approximately 45% (Zhu *et al.*, 2005b), which correlates well with the results obtained in the present study. GI_{50} concentration for 2DG calculated in the MDA-MB-231 cell line remained approximately 6 mM atboth exposure times which may indicate a cytostatic response. Literature reports that the MDA-MB-231 cell line is less susceptible to treatment with 2DG after 6 h treatment than the oestrogen-receptor positive MCF-7 cell line when using a

clonogenic survival assay (Cheng *et al.*, 2012), and this was also observed in the present study after the 24 h treatment period.

The GI_{50} concentration of 2DG obtained for the MCF-12A cell line (4.8 mM after 72 h exposure) as well as published literature on safety data was used to select the most promising 2DG combinations. Doses of up to 300 mg/kg BW of 2DG were reportedly well-tolerated in patients diagnosed with glioblastoma multiforme (Singh *et al.*, 2005). A more recent clinical trial used 63 mg/kg/day of 2DG daily for 21 days and reported that the dose was well tolerated (Raez *et al.*, 2013) indicating low toxicity.

The oestrogen-receptor positive MCF-7 cell line showed a combination index value below 1 for the majority of combinations tested after 72 h with both the oestrone analogues. The lowest CI value calculated (0.24) was obtained for 134 nM ESE-16 combined with 10.76 mM 2DG. The CI values calculated for combinations of 2DG and oestrone analogues on the MDA-MB-231 cell line ranged from strongly antagonistic (>10) to strongly synergistic (<1.0) depending on the concentration of 2DG used in the combination: the most synergistic combinations were identified for 2DG concentrations of 6.73 mM, the maximum concentration tested.

No synergistic combinations were identified on the SK-Br3 cell line as indicated by the combination index values.

In accordance with the GI_{50} concentrations obtained for ESE-15-ol and ESE-16 on the non-tumourigenic MCF-12A cell line, the combinations where the oestrone analogues were used at concentrations below 70 nM for ESE-15-ol and 67 nM for ESE-16 were considered the most promising. Combinations where 2DG concentration exceeded 4.79 mM, the calculated GI_{50} of 2DG on MCF-12A cells, were excluded from further investigation. The combinations that were considered most promising for further assessment are indicated in Table 2.6.

The potent hexokinase inhibitor 3-bromopyruvate has been shown to reduce intracellular ATP concentrations from 100 µM in the HL-60 human leukaemia cell line and Raji human lymphoma cell line (Xu *et al.*, 2005). In the present study the GI_{50}concentrations for 3-BrPA calculated for the MDA-MB-231 and SK-Br3 cancer cell lines exceed 100 µM, but on the non-tumourigenic MCF-12A cell line a GI_{50} of approximately 82 µM was found following 72 h treatment. This suggest that the tested breast cancer cell lines are less susceptible to 3-BrPA than the non-tumourigenic cell line.

It has been reported that 300 µM of 3-BrPA reduced the viability of MCF-7 cells by more than 50% after 72 h exposure using an Alamar Blue assay (Rieber and Strasberg-Rieber,

2014). This does not correspond to the present study where a 50% cell growth was inhibited by approximately 72 µM 3-BrPA, but is must be noted that in the present study the effect of the glycolysis inhibitor was measured as a function of cell growth inhibition and not cell death. It is fairly common for concentrations of a compound which induces cell death as opposed to cell growth inhibition, not to correspond (Fallahi-Sichani *et al.*, 2013).

Cytotoxicity studies on the MDA-MB-231 cell line using the MTT assay showed approximately 40% reduction in cell viability after 24 h incubation with 160 µM of 3-BrPA (Liu *et al.*, 2014) which correlates well with the GI_{50} concentration calculated for 3-BrPA in the present study after 24 h of 210 µM. However, the results obtained for the 72 h treatment period do not correspond: the reported 50% inhibitory concentration of between 80 and 160 µM of 3-BrPA was not observed in the present study (Liu *et al.*, 2014). However, it has been reported that 3-BrPA interferes with tetrazolium-based assays like the MTT and MTS assays (Ganapathy-Kanniappan *et al.*, 2010) but not with the SRB assay (van Tonder *et al.*, 2015) which suggests that the results from the study conducted by Liu and colleagues would not correspond with results obtained in the present study.

An *in vivo* study using severely combined immune-deficient (SCID) mice reported significant weight loss in mice treated with 10 mg/kg 3-BrPA via daily intra-peritoneal injection (Schaefer *et al.*, 2012). No published clinical data is available at present.

Where the oestrone analogues were combined with 3-BrPA on the MCF-7 cell line synergism, as indicated by the calculated CI, was achieved only at the highest concentration of 3-BrPA tested. The lowest CI value (0.70) on the MCF-7 cell line was calculated for the combination of 35.65 nM ESE-16 and 480 µM 3-BrPA. Combination experiments with the oestrone analogues using 3-BrPA on the MDA-MB-231 cell line after 72 h yielded synergistic combinations at the highest concentration of 3-BrPA used. A CI value of 0.71 was obtained where 15.36 nM of ESE-15-ol was combined with 480 µM of 3-BrPA. A CI value of 0.70 was calculated for the combination of 35.65 nM of ESE-16 and 480 µM 3-BrPA.

No synergistic combinations were identified where 3-BrPA was combined with either of the oestrone analogues in the SK-Br3 cell line.

Poor tumour specificity for 3-BrPA was observed in the present study as the GI_{50} concentration calculated was at least 1.5 times lower for the non-tumourigenic MCF-12A cell line than for any of the breast cancer lines tested after both time points. The GI_{50} concentration of approximately 82 µM calculated for the non-tumourigenic MCF-12A cell line after 72 h treatment period suggest that the concentration of 3-BrPA required to achieve synergy (480 µM) may result in toxicity to non-tumourigenic cells. As relatively high

concentrations of 3-BrPA were required to achieve synergy and available *in vivo* data suggest toxicity occur at only 10 mg/kg the combinations with 3-BrPA was deemed unsuitable for further development.

The hexokinase inhibitor lonidamine (LON) has been studied extensively *in vitro* and *in vivo.* Previous studies have reported the half-maximal inhibitory concentration (IC_{50}) of LON as 170 µM on MCF-7 cells after 24 h treatment using a colony formation assay (Rosbe *et al.*, 1989). A GI_{50} concentration of 110 µMwas obtained for LON on MCF-7 cells after 24 h treatment in the present study. In a MDA-MB-231 tumour xenograft model, daily administration of LON for 28 days did not affect body weight significantly but significantly elevated liver alanine aminotransferase (ALT) levels were noted (Milane *et al.*, 2011). A pilot study in metastatic breast cancer patients where LON was combined with cisplatin and epirubicin at dosages of 450 mg of LON per day for 5 – 6 21 day cycles reported WHO grade 1 liver toxicity in 3.5% of patients (Dogliotti *et al.*, 1998). However, two trials assessing the disease improvement in benign prostatic hyperplasia using doses of up to 150 mg/day for 1 – 3 months were discontinued due to lack of symptomatic improvement and incidences of elevated liver enzyme levels (NCT00435448 and NCT00237536).

The GI_{50} calculated for LON on the non-tumourigenic MCF-12A cell line after 72 h treatment (140 µM) was used as upper limit when selecting combinations suitable for further investigation. Combination therapy identification experiments on the MCF-7 and SK-Br3 breast cancer cell lines revealed no synergistic combinations between ESE-15-ol or ESE-16 and LONafter 72 h. Synergistic combinations were identified for only the MDA-MB-231 cell line for both oestrone analogues with the lowest CI value (0.45) calculated where 285 nM of ESE-16 was combined with 188 µM LON. However, considering only combinations where LON was used at concentrations below 140 µM the combinations deemed the most promising are indicated in Table 2.6

FAShas been shown to effectively inhibit the glucose transporters GLUT1 and GLUT4 at concentrations exceeding 15 µM in a human prostatic cell line after only one hour treatment (Wood *et al.*, 2008). Data from the present study demonstrated that approximately 20 µM of FAS was required to reduce growth of non-tumourigenic MCF-12A cells by 50% after 72 h treatment period. However, after only 24 h treatment approximately 200 µM of FAS was required to achieve the same degree of cell growth inhibition. Similar time-dependent decreases in the GI_{50} concentrations calculated for the three breast cancer cell lines were also observed in the present study. Published *in vitro* data on the effect of FAS on breast cancer cells are lacking. Overnight incubation with 80 µM of FAS in DU145 prostate cancer cells, PPC-1 prostate cancer cells and U937 leukaemia cells did not reduce cell viability

below 80% as assessed with a MTS assay (Wood *et al.*, 2008). No published *in vivo* or clinical data is available at present.

As indicated by the combination index values, no synergistic combinations were identified where FAS was combined with ESE-15-ol on MCF-7, MDA-MB-231 or SK-Br3 cells for 72 h. The lowest CI value calculated for combinations with FAS and ESE-16 was 0.97 on the MCF-7 oestrogen receptor positive cell line. Even though the concentration of FAS used was below the GI_{50} concentration on the non-tumourigenic MCF-12A cell line, this combination was not deemed suitable for further assessment.

IND, a protease inhibiting antiretroviral, influences glucose homeostasis through the inhibition of predominantly GLUT4 (from concentrations between 10 – 20 µM), however GLUT1 attenuation has been reported at higher concentrations (at concentrations exceeding 50 µM) (Murata *et al.*, 2002; Hresko and Hruz, 2011). Exposure to IND for 24 h did not result in a reduction of cell growth at the highest concentration of IND tested for either non-tumourigenic MCF-12A or MDA-MB-231 breast adenocarcinoma cells. However, the calculated GI_{50} concentration for IND after 72 h exposure for the non-tumourigenic MCF-12A cell line remained above 500 µM. *In vitro* studies with IND have shown limited cytotoxicity (IC_{50}> 1000 µM) towards MCF-7 cells after 72 h exposure using the MTT assay (You *et al.*, 2010). IND was also found to have little cytotoxic effect on LNCaP prostate cancer cells after 72 h incubation using the MTT assay (Yang *et al.*, 2005). The cytotoxicity does not correlate with the GI_{50} concentrations obtained for IND, in the present study which was calculated at below 250 µM for allthree breast cancer cell lines tested after 72 h IND exposure, which would imply cytostatic activity rather than a cytotoxic effect.

As this compound has been used in the clinical setting for the treatment of HIV/AIDS, its safety profile is well established: doses of up to 400 mg twice daily were reportedly well-tolerated in HIV patients (Cressey *et al.*, 2011).

Data obtained from the combination experiments with IND on the MCF-7 cells after 72 h was conflicting between the oestrone analogues: at the highest combination of ESE-15-ol the combination index values indicated antagonistic interactions, whereas antagonistic combinations were identified only at the lowest concentrations of ESE-16. According to the CI, the most synergistic combination with ESE-15-ol and IND on the MCF-7 cell line as indicated by the CI (0.5) was at 115 µM of IND combined with 70 nM of ESE-15-ol. For the combination of 134 nM of ESE-16 and 57.5 µM IND a CI value of 0.24, the lowest for any combination with ESE-16 on the MCF-7 cell line, was calculated. Few synergistic combinations, as indicated by the CI value, were identified on the MDA-MB-231 cell line and

none on the SK-Br3 cell line. Based on the GI_{50} concentrations of IND and the oestrone analogues determined on the non-tumourigenic MCF-12A cell line and the concentrations reportedly required to achieve an anti-glycolytic effect, the combinations deemed most suitable for further development are indicated in Table 2.6.

The plant-derived flavonoid quercetin QUER has been shown to inhibit the glucose transporters GLUT1 (from approximately 100 µM) (Vera *et al.*, 2001) and GLUT2 (from approximately 10 µM) (Kwon *et al.*, 2007). QUER is found in many fruits and vegetables and the daily dietary intake of quercetin has been estimated to be approximately 100 mg/day (Kwon *et al.*, 2007). This would suggest that QUER is well-tolerated at doses exceeding the GI_{50} concentration obtained on the non-tumourigenic MCF-12A cell line (60.62 ± 1.15 µM after 72 h exposure). This is confirmed by a Phase I study which concluded that 1400 mg/m^2 of QUER administered weekly on a 3-week cycle via intravenous injection preceded by i.v.prehydration is the optimum dose of QUER for the treatment of cancer patients (Ferry *et al.*, 1996).

Reported *in vitro* data corresponds well with results obtained in the present study. Chien and colleagues reported the 50% inhibitory concentration of QUER on MDA-MB-231 cells after 24 h exposure as 278 µM as determined with the MTT assay (Chien *et al.*, 2009) which correlates with the GI_{50} concentration of approximately 270 µM calculated for the present study. The 50% inhibitory concentration of QUER on MCF-7 breast cancer cells after 24 h exposure has been reported as 88 µM as measured by the [^{3}H]thymidine incorporation assay (Wang and Kurzer, 1997). In the present study a GI_{50} concentration of 108 µM was obtained for QUER on the MCF-7 cells after 24 h exposure.

Combination experiments on the MCF-7 cell line revealed that the use of the highest concentration of QUER (83.80 µM) resulted in strong synergism with the oestrone analogues after 72 h. A CI value of 0.24 was obtained where 17.50 nM ESE-15-ol was combined with 83.8 µM QUER. Similarly the lowest CI value for combinations between ESE-16 and QUER was calculated where 83.80 µM of QUER was used in combination with 16.75 nM ESE-16. As the concentrations of the oestrone analogues used in these combinations are below the GI_{50} concentrations obtained for the compounds on the non-tumourigenic MCF-12A cell line, these combinations are considered promising.

When QUER (0.16, 0.32 or 0.64 µM) was combined with ESE-15-ol (123.00 nM) on the MDA-MB-231 cell line synergy was obtained after 72 h. The lowest CI value (0.56) was calculated for the combination of 123.00 nM ESE-15-ol and 0.32 µM QUER. As all the concentrations of QUER tested are well below the GI_{50} concentration calculated on the MCF-12A cell line, all of these combinations were considered promising. According to the CI

values, only one of the combinations of ESE-16 (285.20 nM) and QUER (0.64 µM) on the MD-MB-231 cell line were synergistic. However, the CI value for this combination, 0.96, does not indicate strong synergy and therefore this combination was not considered promising.

As observed for all the other glycolysis inhibitors, no synergy was observed between the oestrone analogues and QUER on the SK-Br3 cell line.

The overall lack of synergy observed in the present study with the SK-Br3 cell line may suggest that the treatment process should be adapted. 2DG in combination with various chemotherapeutic agents commonly used in the treatment of breast cancer have been investigated on the SK-Br3 cell line, with the difference that cells were treated with the chemotherapeutics for 20 h before a 4 h exposure to 500 µM 2DG, with promising results (Zhang and Aft, 2009). However, the study by Zhang and colleagues did not identify synergy between the compounds tested and concluded that 2DG sensitises the cells to treatment with chemotherapeutics (Zhang and Aft, 2009).

A distinguishing feature of the Sk-Br3 cells is over-expression of the Her2 receptor (Trempe and Fogh, 1973). It has been suggested that the over-expression of the c-erbB-2/neu gene product, the Her2 receptor, correlates with reduced sensitivity to anti-neoplastic agents (Yu *et al.*, 1993). The most successful treatment strategy for Her2 positive breast cancer has been combinations of chemotherapeutic agents with Trastuzumab, a humanised monoclonal antibody targeting the Her2 receptor. Further studies have shown synergy between various chemotherapeutics and Trastuzumab (Pegram *et al.*, 2004), suggesting that anti-cancer combinations designed for the treatment of Her2 expressing cancers may require selective targeting of the Her2 receptor to attain maximum efficacy.

The most promising combinations identified after 72 h on all cell lines tested are indicated in Table 2.6. In order to select combinations for further investigation the CI values and the available safety data of the combinations in Table 2.6 were considered. Furthermore, in order for the study to be clinically relevant, physiologically achievable concentrations of the compounds must be used. A myriad of clinical data is available on the safety, tolerability and physiologically achievable concentrations of 2DG, IND and QUER.

A maximal plasma concentration of 116 µg/ml (translating to 700 µM) of 2DG has been reported in patients with advanced solid tumours receiving 63 mg/kg of 2DG for 21 days (Raez *et al.*, 2013). As the doses of 2DG required for synergy are higher than 700 µM (Table 2.6), these combinations were not selected for further assessment.

It has been reported that the therapeutic serum concentration of IND falls between 0.1 – 10 mg/L, which translates to 160 µM – 16 mM (La Porte *et al.*, 2006). The combinations with IND listed in Table 2.6 are thus physiologically achievable and based on the extensive clinical safety data of IND available, these combinations were selected for further assessment. Few published reports where IND has been used in combination with anti-cancer agents are available.

Table 2.6: Most promising synergistic combinations identified during the study.

Cell line	Oestrone analogue		Glycolysis inhibitors		Combination Index
	Compound	Concentration (nM)	Compound	Concentration (µM)	
MCF-7	ESE-15-ol	17.50	2DG	2.69 mM	0.54
	ESE-16	16.75	2DG	2.69 mM	0.91
	ESE-16	134.00	FAS	6.28	0.95
	ESE-15-ol	70.00	IND	115.00	0.50
	ESE-16	67.00	IND	115.00	0.29
	ESE-15-ol	17.50	QUER	83.80	0.24
	ESE-16	16.75	QUER	83.80	0.09
MDA-MB-231	ESE-15-ol	123.00	2DG	3.36 mM	0.87
	ESE-15-ol	123.00	LON	94.15	0.73
	ESE-16	285.00	LON	94.15	0.85
	ESE-15-ol	123.00	IND	55.45	0.69
	ESE-15-ol	123.00	QUER	0.16	0.60
	ESE-15-ol	123.00	QUER	0.32	0.56
	ESE-15-ol	123.00	QUER	0.64	0.72

QUER is often present in fruit and vegetables in a glycosylated form which must be hydrolyzed in the gastrointestinal tract in order for absorption to occur. The oral bioavailability of intact flavonoids, such as QUER, consumed as part of the diet does not often reach concentrations above 1 µM but it has been suggested that repeated dosing may lead to increased serum concentrations (D Archivio *et al.*, 2007). After 10 days of daily oral QUER administration at a concentration of 1.0 g/kg, plasma concentrations of approximately 9.73 nmol/ml (9.73 µM) was reported in male Wistar rats (Nakamura *et al.*, 2000). Plasma concentrations of QUER ranging from 200 – 400 µM have been reported in a Phase I study after injection (Ferry *et al.*, 1996). These studies suggest that the concentrations of QUER found to act synergistically with the oestrone analogues are physiologically achievable.

Various *in vitro* studies on the synergistic use of QUER with anti-cancer agents have been performed. In the study done by Akbas and colleagues the combination of 0.62 µM of QUER and topotecan, a derivative of camptothecin, enhanced the cytotoxicity of topotecan on MCF-7 and MDA-MB-231 breast cancer cells after only 24 h treatment. It was postulated that the cytotoxicity observed was due elevated ROS generation (Akbas *et al.*, 2005). The GI_{50} concentration determined for QUER on the MDA-MB-231 cells in the present study falls within the sub-micromolar range and therefore the combination with the highest concentration of QUER was thus selected for further investigation. Even though the concentration of QUER required to achieve synergy with the oestrone analogues in the MCF-7 cell line is much higher (83.8 µM) this combination was deemed suitable for further study based on the clinical safety data available.

The combinations selected for further assessment are indicated in Table 2.7.

Table 2.7: Synergistic combinations selected for further study on the **MCF-7** and **MDA-MB-231** cell lines.

Cell line	Oestrone analogue		Glycolysis inhibitors		Combination Index
	Compound	Concentration (nM)	Compound	Concentration (µM)	
MCF-7	ESE-15-ol	70.00	IND	115.00	0.50
	ESE-15-ol	17.00	QUER	84.00	0.24
	ESE-16	67.00	IND	115.00	0.09
	ESE-16	17.00	QUER	84.00	0.29
MDA-MB-231	ESE-15-ol	123.00	IND	55.00	0.69
	ESE-15-ol	123.00	QUER	0.64	0.72

The potential synergy between oestrone analogues and glycolysis inhibitors was investigated in this study using a common cell enumeration method, the SRB assay, and CalcuSYN software based on the Median Effect equation of Chou and Talalay (Chou and Talalay, 1984). Three *in vitro* breast cancer models representing the phenotypic subtypes of clinical breast cancer were used. Using this method, promising combinations between oestrone analogues and the glycolysis inhibitors IND and QUER were identified on the oestrogen receptor-positive MCF-7 and triple negative MDA-MB-231 breast adenocarcinoma cell lines. No synergistic combinations were identified on the Her2-positive SK-Br3 cell line suggesting that a more targeted approach may be required for therapeutic efficacy in this subtype of breast cancer.

Combination therapy allows for the exploitation of more than one 'hallmark of cancer' with a single treatment. In the present study two of these hallmarks were targeted namely unlimited proliferative potential, with the use of oestrone analogues, and altered energy production, with the use of glycolysis inhibitors (Hanahan and Weinberg, 2000; Hanahan and Weinberg, 2011). It has been proposed that the anti-mitotic oestrone analogues, ESE-15-ol and ESE-16, exert anti-cancer activity through the production of ROS resulting in mitochondrial toxicity, activation of the caspase cascade and finally the induction of cell death via apoptosis (Stander *et al.*, 2011; Stander *et al.*, 2012, 2013). Several reports suggest that the oestrone analogues induce autophagy as possible secondary mode of cell death (Nkandeu *et al.*, 2013; Theron *et al.*, 2013; Wolmarans *et al.*, 2014).

The production of ATP using aerobic glycolysis by malignant cells results in extracellular acidosis which favours mutagenesis (Yuan *et al.*, 2000; Schornack and Gillies, 2003). Treatment of malignant cells with inhibitors of aerobic glycolysis, such as IND and QUER, will deplete intracellular ATP stores resulting in starvation. Abrogation of ATP synthesis may result in mitochondrial toxicity and the induction of cell death (Vander Heiden *et al.*, 1999). The catabolic process of autophagy may be induced under conditions of nutrient deprivation as pro-survival mechanism (Klionsky, 2005). However, if conditions do not become more favourable autophagic cell death may be observed (Schweichel and Merker, 1973; Jin *et al.*, 2007).

It has been proposed that the combination of compounds yield a third, distinct entity (Chou, 2010). In order to evaluate the effects of the synergistic combinations of oestrone analogues and glycolysis inhibitors on various intracellular parameters indicative of toxicity, a range of *in vitro* assays were conducted.

Chapter 3: Evaluation of toxicity sequence

3.1 Introduction

Cell homeostasis is a tightly regulated process with numerous checkpoints aimed at ensuring cell survival. It has been suggested that along with differentiation and proliferation, apoptosis is crucial for maintaining homeostasis (Degterev *et al.*, 2003). Compromised regulation of these processes is associated with numerous disease states such as cancer and autoimmune diseases (Desagher and Martinou, 2000). Cellular responses to stimuli have been categorised as transient, reversible events where cellular homeostasis can be restored through adaptation, or by pre-lethal events which may induce cell death by irreversible, noxious events (Figure 3.1)(van Tonder *et al.*, 2013). This suggests that cellular responses resulting in ultimate cell death are detectable prior to the endpoint of toxicity.

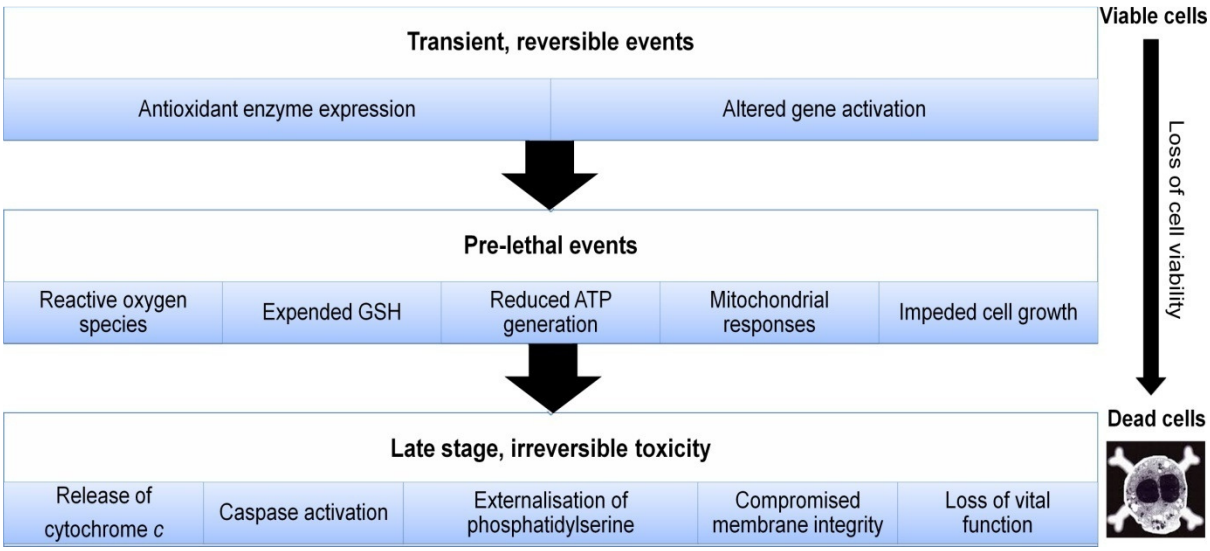

Figure 3.1: Proposed sequence of events resulting in loss of cell viability. Transient, reversible events from which the cell may recover through adaptive responses include the expression of anti-oxidant enzymes and modified gene activation. Pre-lethal events evoke responses from which the cell may recover and include retarded ATP production and impeded cell proliferation. Events which indicate that irreversible cell death has been initiated include the externalisation of phosphatidylserine and loss of vital function (van Tonder *et al.*, 2013).
(http://cdn.intechopen.com/pdfs/41961/InTechPre_clinical_assessment_of_the_potential_intrinsic_hepatotoxicity_of_candidate_drugs.pdf)
Image titled 'The real face of cell death' used with permission from D Coletti.

Anti-oxidant enzymes and molecules, including reduced glutathione (GSH), are essential to control transient events since these factors are required to maintain intracellular redox homeostasis which in turn regulates cellular functions including energy production and apoptosis. Intracellular reduced glutathione also protects against free radicals and xenobiotics, including chemotherapeutics, which may cause damage to the cell (Yeh *et al.*, 2006). It has been found that manipulation of intracellular GSH concentrations can steer cells to undergo necrosis or apoptosis in response to cytotoxic agents which would otherwise induce apoptosis (Fernandes and Cotter, 1994).

As an adaptive response to maintain homeostasis an inherent catabolic process, termed autophagy, may be activated to eliminate redundant intracellular components and foreign microorganisms (Yang and Klionsky, 2010). Under conditions of nutrient-deprivation, autophagy may serve a pro-survival role (Klionsky, 2005). During this process cellular components are degraded to provide amino acids for protein synthesis or production of ATP (Mizushima, 2005). Under persistent nutrient deprivation autophagy may initiate cell death, also referred to as type II cell death (Schweichel and Merker, 1973; Jin *et al.*, 2007). Unlike apoptosis, autophagy is thus a reversible but still regulated process (Jin *et al.*, 2007; Eisenberg-Lerner *et al.*, 2009). Molecular crosstalk between apoptosis and autophagy exist and as such it has been shown that autophagy may induce, enhance or even inhibit apoptosis. It is therefore not surprising that several gene products, including tumour suppressor protein 53 (p53), autophagy protein 5 (Atg5) and B-cell lymphoma 2 protein (Bcl-2), are involved in both pathways and that agents affecting one pathway is likely to have some effect on the other (Eisenberg-Lerner *et al.*, 2009).

If cellular adaptive mechanisms cannot restore homeostasis, cell death is initiated. Three main modes of programmed cell death have been identified: apoptosis (type I) and autophagic cell death (type II) and necrosis (type III)(Schweichel and Merker, 1973). Distinct molecular and morphological markers characterise each of these processes. During the process of apoptosis the translocation of phosphatidylserine from the inner membrane to the cell surface by flippases signals localised macrophages to eliminate the apoptotic cell through phagocytosis (Fadok *et al.*, 1992; Willingham, 1999). This elimination system reduces the risk of inflammation and tissue damage by the release of cellular components such as lysosomes (Lemasters *et al.*, 1998; Degenhardt *et al.*, 2006). Several characteristic morphological alterations occur during the apoptotic process: cells round up and contract, the endoplasmic reticulum swells to such an extent that vesicles and vacuoles are formed by the cisternae, and chromatin aggregation occurs (Wyllie *et al.*, 1980; Ly *et al.*, 2003). The nucleus disintegrates and cell membrane blebbing occurs to form apoptotic bodies (Willingham, 1999).

An infinite variety of stimuli may cause induction of apoptosis, however, many of the intracellular mechanisms identified involves mitochondrial signalling preceded by or accompanied by activation of cysteine-aspartic acidproteases (caspases)(Ly *et al.*, 2003). Based on the signalling cascades involved, induction pathways of apoptosis are classically characterised as intrinsic or extrinsic (Tsujimoto and Shimizu, 2007). The intrinsic pathway involves the mitochondria: upon opening of the mitochondrial membrane permeability pore, cytochrome *c* is released, the apoptosome is formed and executioner caspases are activated. The extrinsic pathway is initiated following binding of a ligand to a death receptor, such as the FAS receptor, which leads to downstream recruitment and activation of caspase 8 and subsequent activation of executioner caspases (Chipuk and Green, 2005). Initiator or signalling caspases, such as caspases 2, -8 , -9 and -10, are activated when apoptosis is induced and are crucial for the activation of downstream executioner caspases such as caspases 3, -6 and -7 (Slee *et al.*, 1999).

Mitochondria are essential not only for cellular respiration, β-oxidation of fatty acids and Ca^{2+} homeostasis, but also for the activation of the caspase cascade (Szabadkai and Duchen, 2010). The release of apoptogenic factors, such as cytochrome *c,* from the intermembrane space of the mitochondria is the consequence of mitochondrial membrane permeability transition (MPT)(Tsujimoto and Shimizu, 2007). MPT is induced by the opening of the mitochondrial membrane permeability transition pore (MPTP) resulting in mitochondrial membrane depolarisation (Ly *et al.*, 2003), thought to be regulated by the Bcl-2 family of proteins (Desagher and Martinou, 2000). Upon the release of cytochrome *c* from the mitochondria, a complex with apoptotic protease activating factor 1 (Apaf-1) is formed leading to the ATP-dependent activation of caspase 9 (Xiao-Ming, 2000). Activation of the executioner caspase 3 and induction of apoptosis follows (Ly *et al.*, 2003).

In contrast to the controlled process of apoptosis, necrosis has a fast onset and is characterised by the unregulated release of cytosolic contents into the surrounding extracellular environment due to loss of cell membrane integrity leading to leakage of cell content into the extracellular space where an inflammatory response is initiated. Inflammatory cells facilitate the removal of cell debris resulting in localised inflammation that may result in damage to the surrounding tissue (Willingham, 1999). Necrosis may be distinguished from apoptosis morphologically by an increase in cell volume, enlargement of organelles and random degradation of intracellular components (Galluzzi *et al.*, 2009). Not only is necrosis triggered by insufficient energy production (Jin *et al.*, 2007), but during the process ATP is expended (Osellame *et al.*, 2012).

Assessing molecular parameters of adaptive responses using endpoint assays, i.e. at cell death, may not identify subtle cellular changes that may elucidate the mechanism of action involved (O'Brien *et al.*, 2006). Therefore this study attempted to evaluate the sequential intracellular processes involved following treatment with the newly identified synergistic combinations using different cell lines.

3.2 Materials

1) 2.5% Glutaraldehyde/formaldehyde fixative

Fixative was prepared as previously described (Karnovksy, 1965). A 10% (w/v) paraformaldehyde solution (Merck, Darmstadt, Germany) was prepared by dissolving paraformaldehyde (0.4 g) in 25 ml water. The solution was heated to approximately 70°C while stirring. After cooling, the solution was stored at 4°C until required. Just prior to use 1 ml of 8% glutaraldehyde solution (SPI Supplies, Westchester, USA) was added and the volume of the solution adjusted to 100 ml using PBS. The pH of the solution was adjusted to 7.2 using sodium hydroxide (1 N, Sigma-Aldrich, St Louis, USA) if required.

2) 2-Mercaptoethanol

2-Mercaptoethanol (Sigma-Aldrich, St Louis, USA) was stored at room temperature and used undiluted in a fume hood.

3) Absolute ethanol

Absolute ethanol was obtained from Merck (Darmstadt, Germany) and used undiluted. Where diluted solutions were required for sample preparation, dilutions were made using distilled water.

4) Annexin V-FITC

Annexin V-FITC (BD Biosciences, Sparks, USA) was stored at 4°C and used undiluted.

5) Annexin binding buffer

Binding buffer was prepared by adding HEPES (10 mM), NaCl (150 mM), KCl (5 mM), $MgCl_2$ (1 mM) and $CaCl_2$ (1.8 mM) in distilled water. All reagents were procured from Sigma-Aldrich (St Louis, USA). The pH was adjusted to 7.4 with sodium hydroxide and stored at 4°C.

6) Anti-β-actin primary antibody

Anti-β-actin rabbit polyclonal antibody was procured from Santa Cruz Biotechnology Inc (Dallas, USA) and stored at 4°C. Prior to use the antibody was diluted in PBS buffer

supplemented with 2% bovine serum albuminand 0.2% (v/v) Tween-20 to a final concentration of 5 µg/ml.

7) Anti-microtubule-associated protein 1 light chain 3 II (LC3-II) primary antibody

Anti LC3-II rabbit antibody was procured from Novus Biologicals (Littleton, USA) and stored at 4℃. Prior to use the antibody was diluted in PBS-T buffer supplemented with 2% BSA to a final concentration of 1 µg/ml.

8) Bovine serum albumin (BSA)

Bovine serum albumin (Santa Cruz Biotechnology Inc, Dallas, USA) was stored at 4℃. Prior to use a 2% solution was prepared in phosphate buffered saline supplemented with 0.2% Tween-20 by dissolving 0.1 g of BSA in 5 ml PBS-T buffer solution.

9) Caspase assay buffer

Assay buffer was prepared by adding HEPES (20 mM) and EDTA (2 mM) in dH_2O. The buffer was stored at 4℃. Approximately 30 min before use the fluorescent substrates and 5 mM 2-mercaptoethanol was added to the assay buffer. All reagents were obtained from Sigma-Aldrich (St Louis, USA).

10) Caspase lysis buffer

Lysis buffer was prepared by combining CHAPS (5 mM), HEPES buffer (10 mM) and EDTA (2 mM) in dH_2O. The buffer was stored at 4℃. Approximately 30 min prior to use 1 mM PMSF, as inhibitor of serine proteases, and 5 mM 2-mercaptoethanol, to maintain the integrity of the caspase enzymes, were added to the buffer. All reagents were procured from Sigma-Aldrich (St Louis, USA).

11) Caspase 3/7 substrate

A 10 mM stock solution of the caspase 3/7-specific substrate, Ac-DEVD-AMC (Sigma-Aldrich, St Louis, USA), was prepared by dissolving 5 mg in 685 µl DMSO. Aliquots of 10 µl were prepared and stored at -70℃.

12) Caspase 8 substrate

A 10 mM stock solution of the caspase 8-specific substrate, Ac-IETD-AMC (Sigma-Aldrich, St Louis, USA), was prepared by dissolving 5 mg in 740 µl DMSO. Aliquots of 10 µl were prepared and stored at -70℃.

13) Caspase 9 substrate

A 10 mM stock solution of the caspase 9-specific substrate, Ac-LEHD-AFC (Sigma-Aldrich, St Louis, USA), was prepared by dissolving 5 mg in 653 µl DMSO. Aliquots of 10 µl were prepared and stored at -70℃.

14) Enhanced chemiluminescence reagent (ECL)

ECL substrate was purchased from Bio-Rad Laboratories Inc (Hercules, USA) and stored at room temperature.

15) EmBED812 resin

EmBED812 resin was prepared immediately prior to use by combining, in sequential order, 10.47 g EmBED812, 7.07 g nadic methyl anhydride, 2.73 g dodecenylsuccinic anhydride and 0.20 g S1-dimethylethanolamine. The mixture was stirred well before use. All reagents were procured from SPI Supplies (Westchester, USA) except S1-dimethylethanolamine which was purchased from Agar Scientific (Essex, United Kingdom).

16) Fas ligand

A 75 µg/ml stock solution was prepared by dissolving 10 µg Fas ligand (Sigma-Aldrich, St Louis, USA) in 133µl sterilised water supplemented with 0.1% BSA. Aliquots of 2 µl were prepared and stored at -80℃.

17) Gels

Mini-PROTEAN TGX precast 4-20% polyacrylamide gels with 50 µl well volume were procured from Bio-Rad Laboratories Inc (Hercules, USA) and stored at 4℃.

18) Hanks buffered salt solution (HBSS)

Phenol red-free HBSS (Biochrom, Berlin, Germany) was stored at 4℃ and used undiluted.

19) Horseradish peroxidase (HRP) secondary antibody

Goat anti-rabbit IgG-HRP (Santa Cruz Biotechnology Inc, Dallas, USA) was stored at 4℃. Prior to use the antibody was diluted in PBS-T supplemented with 2% BSA to a final concentration of 0.08µg/ml.

20) JC-1 fluorescent dye

A 1.5 mM stock solution of JC-1 (5,5',6,6'-tetrachloro-1,1',3,3'-tetraethylbenzimidazolcarbo-cyanine iodide)(Sigma-Aldrich, St Louis, USA) was prepared by dissolving 5 mg of JC-1 powder in 5.1 ml DMSO. Aliquots of 50 µl were prepared and stored at -80℃.

21) Laemmli buffer

A double concentration Laemmli buffer was purchased from Bio-Rad Laboratories, Inc (Hercules, USA), stored at room temperature and used undiluted.

22) Trans-blot membranes

Trans-Blot® Turbo™ polyvinylidene fluoride (PVDF) pre-cut membranes with 0.2 µm pore size in kits including the wick layers was procured from Bio-Rad Laboratories (Hercules, USA) and stored at 4℃.

23) Milk powder

A 2% full cream milk powder (Parmalat, Midrand, RSA) solution was prepared immediately prior to use by dissolving 0.1 g powder in 5 ml PBS-T.

24) Monochlorobimane (mCB)

A 25 mM stock solution of mCB (Sigma-Aldrich, St Louis, USA) was prepared by dissolving 2.8 mg of powder in 500 µl DMSO. Aliquots of 20 µl were prepared and stored at -80℃.

25) 3-(N-Morpholino)propanesulfonic acid (MOPS) running buffer

Running buffer was prepared by dissolving MOPS (50 mM), TRIS base (50 mM), 0.1% sodium dodecyl sulphate and ethylenediaminetetraacetic acid (1 mM) in 5 l distilled water. The pH of the solution was adjusted to 7.7 with a 1M NaOH solution. The buffer was stored at room temperature and used undiluted. All reagents were procured from Sigma-Aldrich (St Louis, USA).

26) n-Ethylmaleimide

A 50 mM stock solution was prepared by dissolving 1.5 mg n-ethylmaleimide (Sigma-Aldrich, St Louis, USA) in 250 µl DMSO. Aliquots of 10 µl were prepared and stored at -80℃.

27) Osmium tetraoxide

A 0.5% osmium tetraoxide (Sigma-Aldrich, St Louis, USA) solution was prepared from the 2% purchased solution by adding 25 ml of the 2% osmium tetraoxide solution to a 100 ml volumetric flask and filling the flask with distilled water. The solution was stored at room temperature and used in a fume hood.

28) Phenylmethylsulfonyl fluoride (PMSF)

A 100 mM stock solution of PMSF (Sigma-Aldrich, St Louis, USA) was prepared by dissolving 17 mg PMSF in 1 ml DMSO. Aliquots of 50 µl were made and stored at -70℃.

29) Phosphate buffered saline (PBS)

PBS was prepared by dissolving 9.23 g of FTA powder (BD Biosciences, Sparks, USA) in 1 l de-ionised water. The solution was stored at room temperature.

30) Phosphate buffered saline supplemented with Tween-20 (PBS-T)

PBS was prepared by dissolving 9.23 g of FTA powder (BD Biosciences, Sparks, USA) in 1 l de-ionised water. A volume of 2 ml Tween-20 (Sigma-Aldrich, St Louis, USA) was added to 1 l of PBS and stored at room temperature.

31) Ponceau S stain

Ponceau S stain (0.5% in 1% acetic acid solution) was purchased from Life Technologies (Johannesburg, RSA), stored at room temperature and used undiluted.

32) Propidium iodide (PI)

A 3 mM stock solution of PI (Sigma-Aldrich, St Louis, USA) was prepared by dissolving 10 mg PI in 5 ml dH_2O. The solution was stored at 4°C.

33) Protein standard

Novex®sharp pre-stained protein ladder standard (Life Technologies, Johannesburg, RSA) was stored at 4°C and used undiluted. The range of the standard was 3.5 – 260 kDa.

34) Reynolds' lead citrate

Reynolds' lead citrate was prepared as previously described(Reynolds, 1963). Lead (II) nitrate (1.33 g) and sodium citrate (1.76 g) was added to approximately 30 ml of distilled water in a 50 ml volumetric flask and the suspension shaken to aid in the conversion of lead nitrate to lead citrate. Approximately 8 ml sodium hydroxide (1 N) was added and the flask filled to 50 ml with distilled water. The solution was stored at 4°C and used undiluted. Reagents were procured from Sigma-Aldrich (St Louis, USA).

35) Sodium azide

A 2% stock solution of sodium azide (Sigma-Aldrich, St Louis, USA) was prepared by dissolving 2 g of powder in 100 ml distilled water. The solution was stored at room temperature and diluted in PBS-T to 0.02% prior to use.

36) Tamoxifen

A 30 mM stock solution was prepared by dissolving 5 mg tamoxifen (Sigma-Aldrich, St Louis, USA) in 448.6 µl DMSO. Aliquots of 10 µl were made and stored at -70°C.

37) Trypsin/Versene

A sterile 0.125% trypsin/versene solution in Ca^{2+} and Mg^{2+} free PBS was obtained from Highveld Biologicals (Johannesburg, RSA), stored at 4°C and used undiluted.

38) Staurosporine aglycone

A 2 mM stock solution was made by dissolving 5 mg powder (Sigma-Aldrich, St Louis, USA) in 803 µl DMSO. Aliquots of 10 µl were prepared and stored at -70°C.

39) Valinomycin

A stock solution of 15 mM was prepared by dissolving 5 mg powder (Sigma-Aldrich, St Louis, USA) in 300 µl DMSO. Aliquots of 5 µl were prepared and stored at -70°C.

3.3 Pilot study: potential interference of QUER

3.3.1 Introduction

Fluorescence analysis is a selective and very sensitive technique often used in biological assays due to the small samples required and very selective nature of the technique. Despite the many uses of fluorescence there are some limitations and considerations that must be deliberated. The most important limiting effect with fluorescence-based assays is quenching, the process whereby fluorescent intensity can be reduced. Potential interference with fluorescence-based assay may occur at:

1. *Quenching of excitation wavelength:* when an interfering compound is excited at the same wavelength resulting in reduced excitation of the analyte.
2. *Quenching of emitted signal:* the emitted signal of the analyte is absorbed by an interfering compound resulting in reduced fluorescent signal of the analyte being measured.
3. *Enhanced emitted signal:* an interfering compound emits a fluorescent signal at the same wavelength as the analyte increasing the observed signal.

The anticancer properties of the plant-derived flavanoid quercetin have been attributed to its ability to inhibit aerobic glycolysis (Lang and Racker, 1974; Suolinna *et al.*, 1975; Kwon *et al.*, 2007). During the present study synergistic combinations of oestrone analogues and QUER were identified using the MCF-7 and MDA-MB-231 breast adenocarcinoma cell lines and the sequence of toxicity induced by these combinations were further investigated. Selected responses to combination therapy were evaluated using several fluorescent-based protocols.

Reports have indicated that QUER, which shows native fluorescence, may cause interference with certain fluorescence-based assays. QUER which has been absorbed into the intracellular environment was found to produce a fluorescent signal detectable at 500 –

540 nm when excited at 488 nm (Nifli *et al.*, 2007). Another report indicated that intracellular QUER produces a similar fluorescent signal when excited between 380 - 440 nm with detection of emission at 540 nm (Baran *et al.*, 2011).

As the reported excitation and emission wavelengths of QUER corresponds to those of selected fluorometric assays used during the present study, the influence of QUER fluorescence in buffers and intracellular QUER on the data obtained during the present study was assessed.

3.3.2 Methods and materials

In order to assess the extent of interference by QUER fluorescence on experimental data generated using fluorometric assays, the fluorescent signal produced by QUER in buffer or in the intracellular environment was evaluated at the concentrations to be used in the assays.

3.3.2.1 Fluorescent signal of QUER in buffer

The fluorescent signal of QUER in a cell-free system was evaluated to determine the fluorescent signal produced by QUER at excitation and emission wavelengths used for fluorometric assays using the same instrumentation and cell culture plates as used in the mechanistic assays during the main study. Briefly, QUER was prepared in phosphate buffered saline (PBS) or Hank's Balanced Salt Solution to 84 µM, the concentration of QUER required for synergistic combinations on MCF-7 cells, or 0.64 µM, the concentration of QUER required for synergistic combinations on MDA-MB-231 cells. The final volume used was 240 µl/well.

The fluorescent signal produced by QUER was immediately assessed using the excitation (λ_{ex}) and emission wavelengths (λ_{em}) required for fluorometric assays used in the present study (Table 1). Note that the fluorescent signal produced by signal at both the emission wavelengths of the cationic dye JC-1 was evaluated as this assay uses the ratio of the emission signals. The fluorescence produced was measured using a FluoStar Optima or Synergy 2 fluorescence plate reader.

Table 3.1: Excitation and emission wavelengths used to detect the fluorescent signal produced by quercetin.

Excitation wavelength (nm)	Emission wavelength (nm)	Assay
355	460	Monochlorobimane
492	525	JC-1 monomers
545	595	JC-1 aggregates
380	505	Caspase 9
380	450	Caspase 3 and -8

3.3.2.2 Intracellular fluorescence of QUER

As it has been reported that intracellular accumulation of QUER from the extracellular buffer or matrix may produce fluorescence (Nifli *et al.*, 2007), the potential interference of intracellular QUER was investigated.

This effect was tested using the two cell lines used in the main study. Briefly, MCF-7 breast adenocarcinoma cells were seeded at a density of 5 x 10^3cells/well into sterile, 96-well white microtitre plate and incubated overnight in a humidified incubator at 37 ℃ with 5% CO_2 to allow for cell attachment. After the incubation period cells were exposed to QUER at 84 µM or 0.64 µM and incubated for a further 24 or 48 h. To simulate conditions used in the main study, cell culture medium supplemented with 2% foetal bovine serum was used for all experiments. The final volume was 240 µl/well.

After the 24 or 48 h incubation period, medium was aspirated and replaced with 100 µl PBS or HBSS. The fluorescence produced was measured using a FluoStar Optima or Synergy 2 fluorescence plate reader.

3.3.2.3 Fluorescent assays

The fluorescent assay methods used in the study for each different analyte were slightly different with respect to their excitation and emission wavelengths and the time for adding the fluorescent probes. These methods with all the concentrations of reagents and timings are described in detail in Sections 3.4.1, 3.4.4 and 3.4.5.

The monochlorobimane assay used for the detection of intracellular reduced glutathione (GSH) relies on the formation of fluorescent adducts from the non-fluorescent monochlorobimane and intracellular GSH. The assay was performed as reported by Fernández-Checa and Kaplowitz (Fernández-Checa and Kaplowitz, 1990). Briefly, after cells were seeded and exposed to QUER, the medium was aspirated cells were loaded with

monochlorobimane (10 µM in HBSS) for 1 h in a humidified incubator at 37°C with 5% CO_2. The loading solution was removed and replaced with 100 µl HBSS. Thereafter the formation of fluorescent adducts was measured at λ_{ex} = 355 nm and λ_{em} = 460 nm using a FluoStar Optima fluorescence plate reader (Bio-Tek Instruments Inc., Vermont, USA). Gain was set at 1 250.

The effect of the synergistic drug combinations on mitochondrial membrane potential ($\Delta\psi_m$) was assessed using the cationic fluorescent dye JC-1 (5,5',6,6'-tetrachloro-1,1',3,3'-tetraethylbenzimidazolcarbo-cyanine iodide). Formation of JC-1 aggregates due to accumulation in the mitochondria indicates hyperpolarisation of $\Delta\psi_m$, whereas lower concentrations of JC-1 results in monomers, suggesting mitochondrial depolarisation. The method used is based on a published method (van Tonder *et al.*, 2014). Briefly, after cells were seeded and exposed to QUER, the medium was aspirated and cells were loaded with JC-1 (10 µM in HBSS) for 2 h in a humidified incubator at 37°C with 5% CO_2. Thereafter the loading solution was removed and replaced with 100 µl HBSS. The accumulation of the monomeric form was measured at λ_{ex} = 492 nm and λ_{em} = of 525 nm, and λ_{ex} = 545 nm and λ_{em} = 595 nm for the aggregate form using a FluoStar Optima fluorescence plate reader (Bio-Tek Instruments Inc., Vermont, USA). Gain was set at 1 000 for all wavelengths.

The effect of the synergistic drug combinations on the activity of caspases 3/7, -8 and -9 was evaluated using caspase-specific fluorescent substrates which are cleaved in the presence of caspases to release the fluorophore 7-amino-4-methylcoumarin (AMC) or 7-amino-4-trifluoromethylcoumarin (AFC). The activity of caspase 3 was assessed using N-Acetyl-Asp-Glu-Val-Asp-7-amido-4-methylcoumarin (Ac-DEVD-AMC), for caspase 8 N-Acetyl-Ile-Glu-Thr-Asp-7-amino-4-methylcoumarin (Ac-IETD-AMC) was used and N-Acetyl-Leu-Glu-His-Asp-7-amido-4-trifluoromethylcoumarin (Ac-LEHD-AFC) was used to determine the activity of caspase 9. Briefly, after cells were seeded and exposed to QUER, the medium was aspirated and caspase lysis buffer was added. After 30 min incubation on ice, caspase assay buffer was added and the plate incubated for 4 h at 37°C to allow for the cleavage of the fluorescent AMC or AFC molecule. The release of AMC was measured at λ_{ex} = 380 nm and λ_{em} = 450 nm, and AFC measured at λ_{ex} = 380 nm and λ_{em} = 505 nm using a Synergy 2 fluorescence plate reader (Bio-Tek Instruments Inc., Vermont, USA).

3.3.2.4 Data interpretation

For the determination of fluorescent signal produced by QUER in a cell-free environment no data manipulation was performed. Where the intracellular fluorescence of QUER was determined, the fluorescent signal of QUER-naive cells used as the blank assays was

deducted from the fluorescent signal of QUER-treated cells. For fluorescent assays data was blank-adjusted.

GraphPad Prism 4.0 for Windows (GraphPad Software, San Diego, California, USA, www.graphpad.com). No statistical evaluation was performed. Outliers were detected using the Grubbs' test and excluded.

3.3.3 Results and Discussion

The potential interference of quercetin with fluorescence-based assays used in the present study was quantified as fluorescent signal measured at the relevant excitation wavelengths. The emitted fluorescent signal of QUER in the cell-free media as well as where QUER was internalised into the cellular environment was investigated. In general the assays performed in the main study are similar to the conditions used where the intracellular QUER fluorescence were measured, and this showed very low interference with either absorption or emission quenching nor did it contribute to increased fluorescence at the emission wavelengths in a significant manner. The experimental conditions used in the main study most closely match the studies assessing the effect of intracellular QUER.

The fluorescent signal produced by QUER excited at 355 nm and emission at 460 nm in a cell-free or intracellular environment was evaluated and compared to the signal obtained using the monochlorobimane assay (Figure 3.2). In a cell-free system the greatest signal was produced when 84 µM QUER was prepared in PBS. However, for experimental procedures HBSS was used to keep the cells hydrated prior to detection of fluorescent signal. The fluorescent signal measured at 84 µM QUER in HBSS was calculated to be 24.5% of the signal detected in the MCB assay, whereas the emitted fluorescent signal of 0.64 µM QUER in HBSS was determined to be 21.5% of the signal detected in the assay.

It must be considered that the signal produced by intracellular QUER is more comparable to that obtained during the experiments assessing the effect of QUER on the concentration of intracellular glutathione using the monochlorobimane assay (Figure 3.2). When the fluorescent intensity of intracellular QUER was evaluated, the higher signal was produced when the cells were hydrated with HBSS using the different concentrations of QUER assessed. The calculated emitted fluorescent signal of intracellular QUER was negative suggesting that quenching of excitation or quenching of emission may have occurred. The fluorescent signal of 84 µM intracellular QUER is approximately 1.2% of the signal detected during the assay. When the intracellular QUER fluorescent signal of a 0.64 µM solution was detected, it amounted to approximately 1.5% of the fluorescent signal measured during the

assay. It is therefore unlikely that the fluorescence of intracellular QUER would have interfered with the monochlorobimane assay.

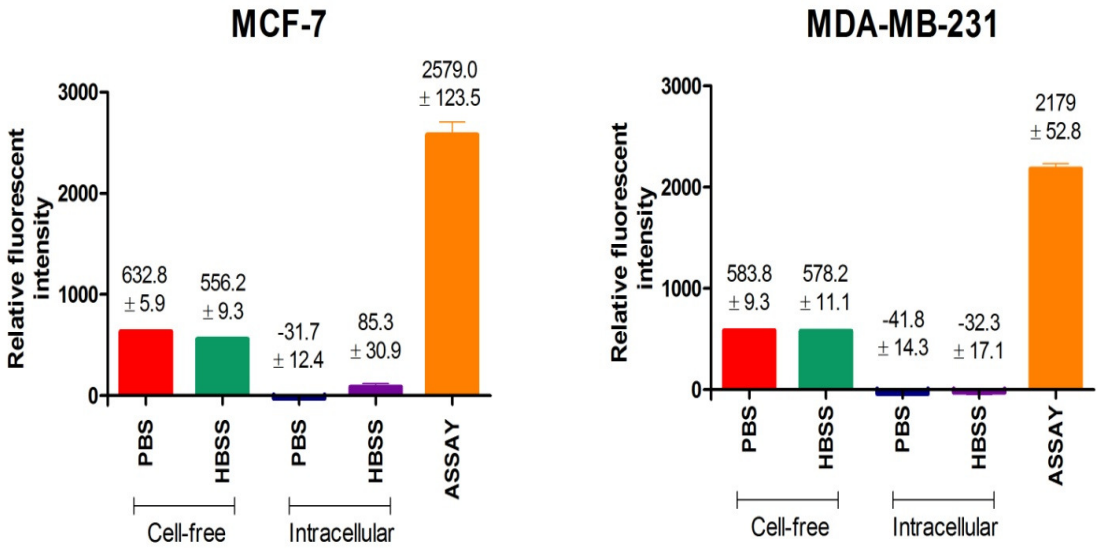

Figure 3.2: The fluorescent emission signal obtained for QUER at concentrations used in combinations with MCF-7 and MDA-MB-231 breast adenocarcinoma cells using λ_{ex} = 355 nm and λ_{em} = 460 nm. Emission was evaluated for QUER in a cell-free environment and the intracellular fluorescence of cells treated with QUER. The fluorescent signal obtained during monochlorobimane experiments is also shown (ASSAY). For MCF-7 cells 84 µM QUER was used, while 0.64 µM QUER was used for combinations with MDA-MB-231 cells. Error bars represent SEM. Where no error bars are visible the SEM was negligible.
Min n = 3

When the fluorescent signal produced by QUER in a cell-free environment was investigated at λ_{ex} = 492 nm and λ_{em} = 525 nm, as required for the measurement of JC-1 monomers, the measured fluorescent signal was comparable between QUER in PBS and QUER in HBSS (Figure 3.3). The signal produced by 84 µM QUER was marginally lower than that of 0.64 µM QUER and exceeded the measured signal detected for JC-1 as used during the mitochondrial membrane potential assay. This corresponds to the reported emitted fluorescent signal of QUER at 50 µM (Baran *et al.*, 2011).

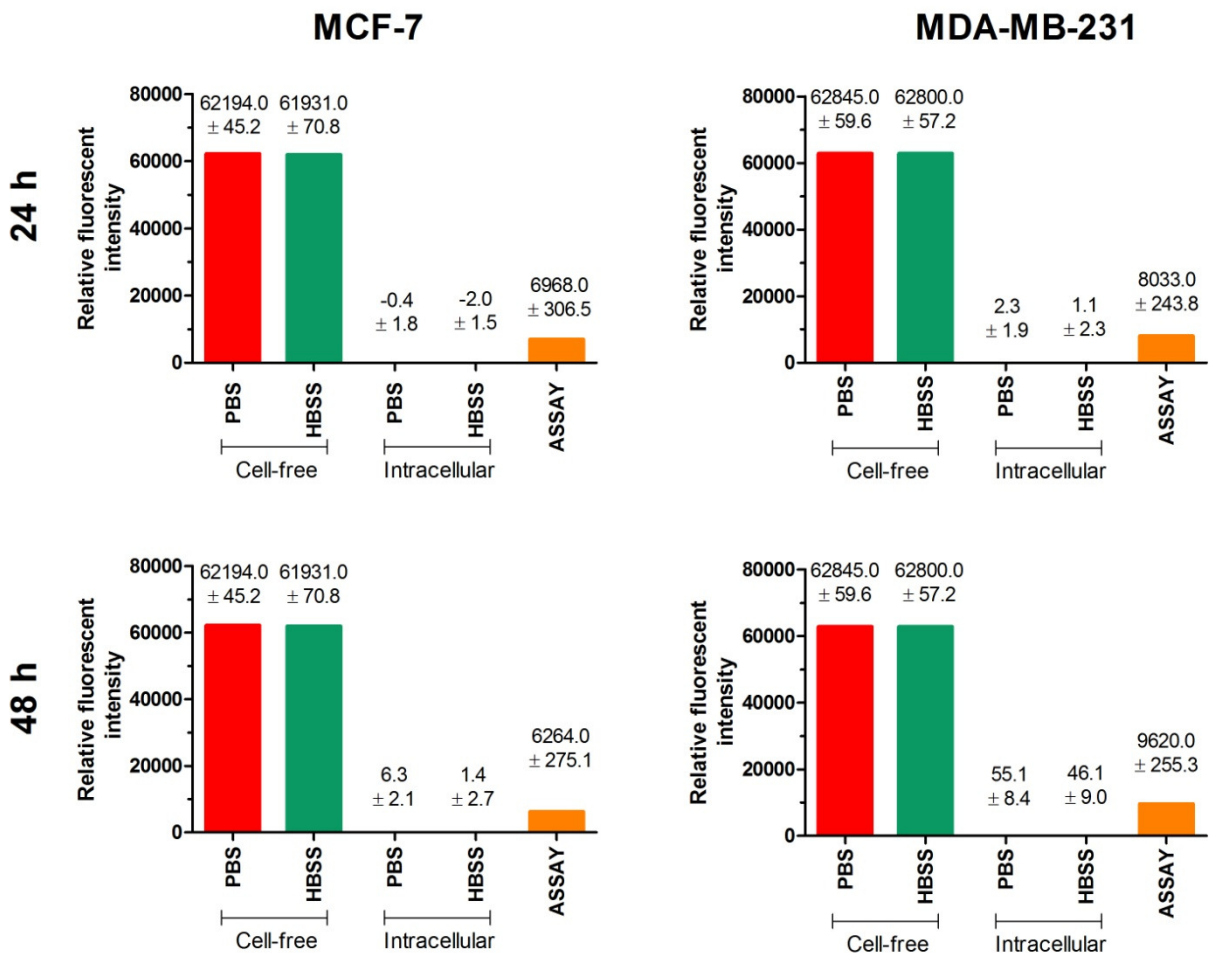

Figure 3.3: The fluorescent emission signal obtained for QUER at concentrations used in combinations with MCF-7 and MDA-MB-231 breast adenocarcinoma cells using λ_{ex} = 492 nm and λ_{em} = 525 nm. Emission was evaluated for QUER in a cell-free environment and the intracellular fluorescence of cells treated with QUER. The fluorescent signal obtained during experiments for JC-1 monomers (ASSAY) is also shown. For MCF-7 cells QUER was used at 84 µM, while 0.64 µM of QUER was used for combinations with MDA-MB-231 cells. Error bars represent SEM. Where no error bars are visible the SEM was negligible.
Min n = 3

However, the experimental conditions used during the JC-1 experiments in the present project are more comparable to those used for the intracellular fluorescence studies (Figure 3.3). During these experiments cells were hydrated with HBSS during measurement of fluorescence. When comparing the intracellular QUER fluorescence with the signal emitted at 24 h during the experiment, intracellular fluorescence of QUER amounted to 0.01% of the signal detected during the experiments for both 84 µM and 0.64 µM. The intracellular fluorescent signal emitted by intracellular QUER at 84 µM in HBSS is only 0.02% of the

signal detected during the assay, and that of QUER at 0.64 µM in HBSS only 0.48% at 48 h. This suggests that the effect of intracellular fluorescence of QUER would be negligible on the emitted fluorescence signal of JC-1 monomers.

This emission and excitation wavelengths required for detection of JC-1 aggregates were also investigated (Figure 3.4). In a cell-free system the emitted fluorescent signal from QUER at 84 µM, required for synergistic combinations on MCF-7 cells, or 0.64 µM, required for synergistic combinations with MDA-MB-231 cells, did not exceed 200 relative fluorescent units when excited at 544 nm with detection of emission at 590 nm (Figure 3.4).

When the intracellular fluorescence of QUER in HBSS was determined at the abovementioned excitation and emission wavelengths, the fluorescent signal measured from intracellular QUER did not exceed 0.97% for any of the QUER concentrations or incubation periods used (Figure 3.4). This implies that the effect of fluorescence emitted by intracellular QUER is negligible when assessing the fluorescence of JC-1 aggregates.

As data obtained using JC-1 is expressed as ratio of JC-1 aggregates: JC-1 monomers and data pertaining to the intracellular fluorescence of QUER show no definitive interference, the results obtained from the JC-1 assay were deemed to be valid.

Where the potential interference of QUER was assessed at the wavelengths (λ_{ex} = 380 nm and λ_{em} = 505 nm) required for the assessment of caspase 9 activitya greater signal was detected (approximately 19.3% of ASSAY signal) for 84 µM QUER prepared in HBSS than in PBS (approximately 13.8% of ASSAY signal) (Figure 3.5). The results obtained for fluorescence of 0.64 µM QUER in a cell-free system was similar.

Intracellular fluorescence of 84 µM QUER at 24 h excited at 380 nm with detection using emission at 505 nm, as required for was greatest when cells were hydrated with HBSS (Figure 3.5). However, this only amounted to approximately 0.86% of the fluorescent signal detected during the assay. After 48 h the intracellular fluorescence of QUER in PBS was only approximately 0.69% of the signal detected during the assay. At 84 µM the potential interference of intracellular QUER is therefore negligible.

For 0.64 nM, the concentration required for MDA-MB-231 cells, the fluorescence of intracellular QUER in HBSS was calculated to be 0.64% of the signal detected during the assay after 24 h. After 48 h the effect of intracellular QUER in PBS (approximately 1.29%) exceeded that of QUER in HBSS (approximately 0.31%). The decrease in fluorescent signal detected may be due to quenching of the excitation wavelength or emitted signal. However,

the effect of intracellular fluorescence on the data obtained for the activity of caspase 9 during this study is negligible.

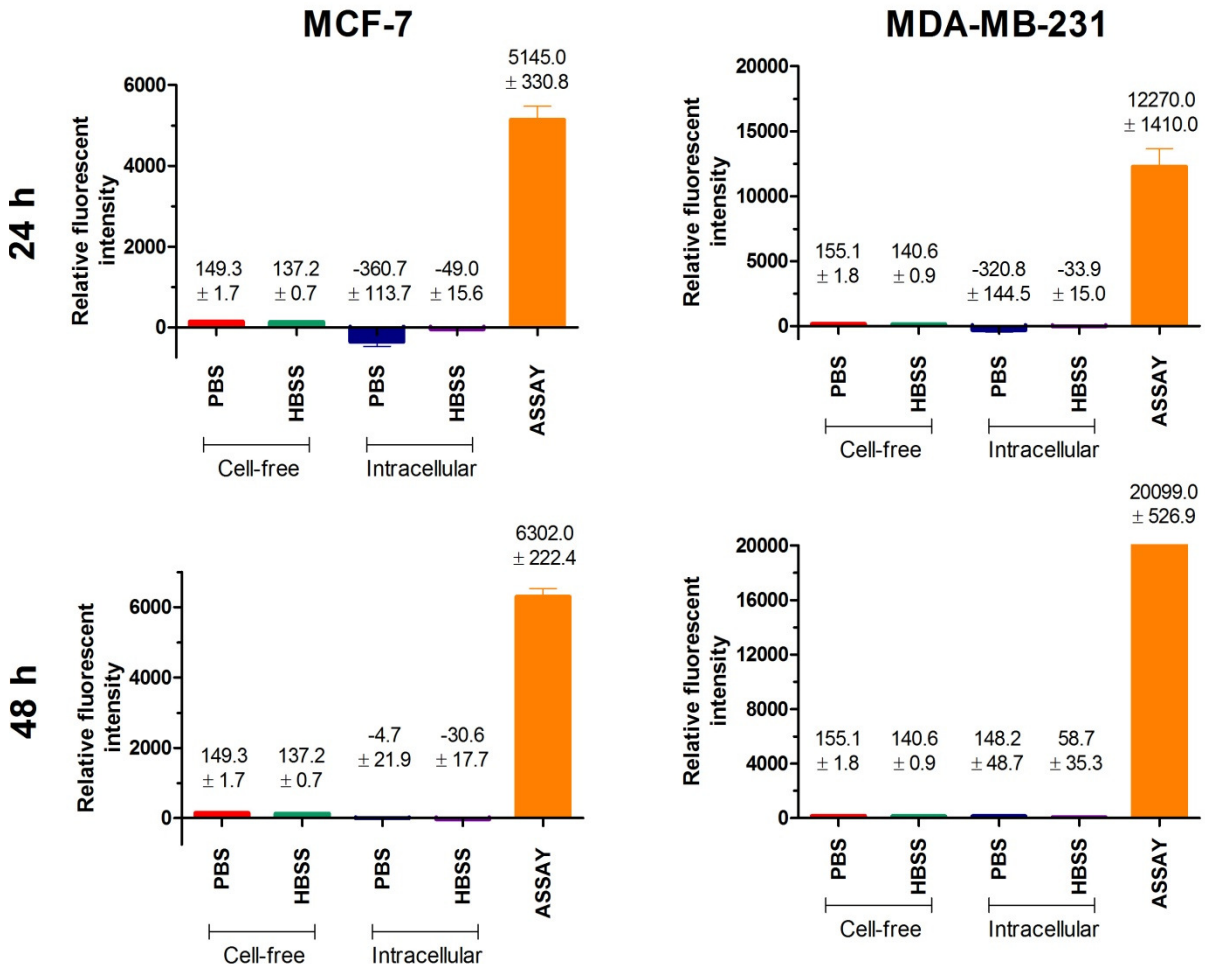

Figure 3.4: The fluorescent emission signal obtained for QUER at concentrations used in synergistic combinations with MCF-7 and MDA-MB-231 breast adenocarcinoma cells using λ_{ex} = 545 nm and λ_{em} = 595 nm. Emission was evaluated for QUER in a cell-free environment and the intracellular fluorescence of cells treated with QUER. The fluorescent signal obtained during experiments for JC-1 aggregates (ASSAY) is also shown. For MCF-7 cells QUER was used at 84 µM, while 0.64 µM of QUER was used for combinations with MDA-MB-231 cells. Error bars represent SEM. Where no error bars are visible the SEM was negligible. Note the differences in the y-axes.

Min n = 3

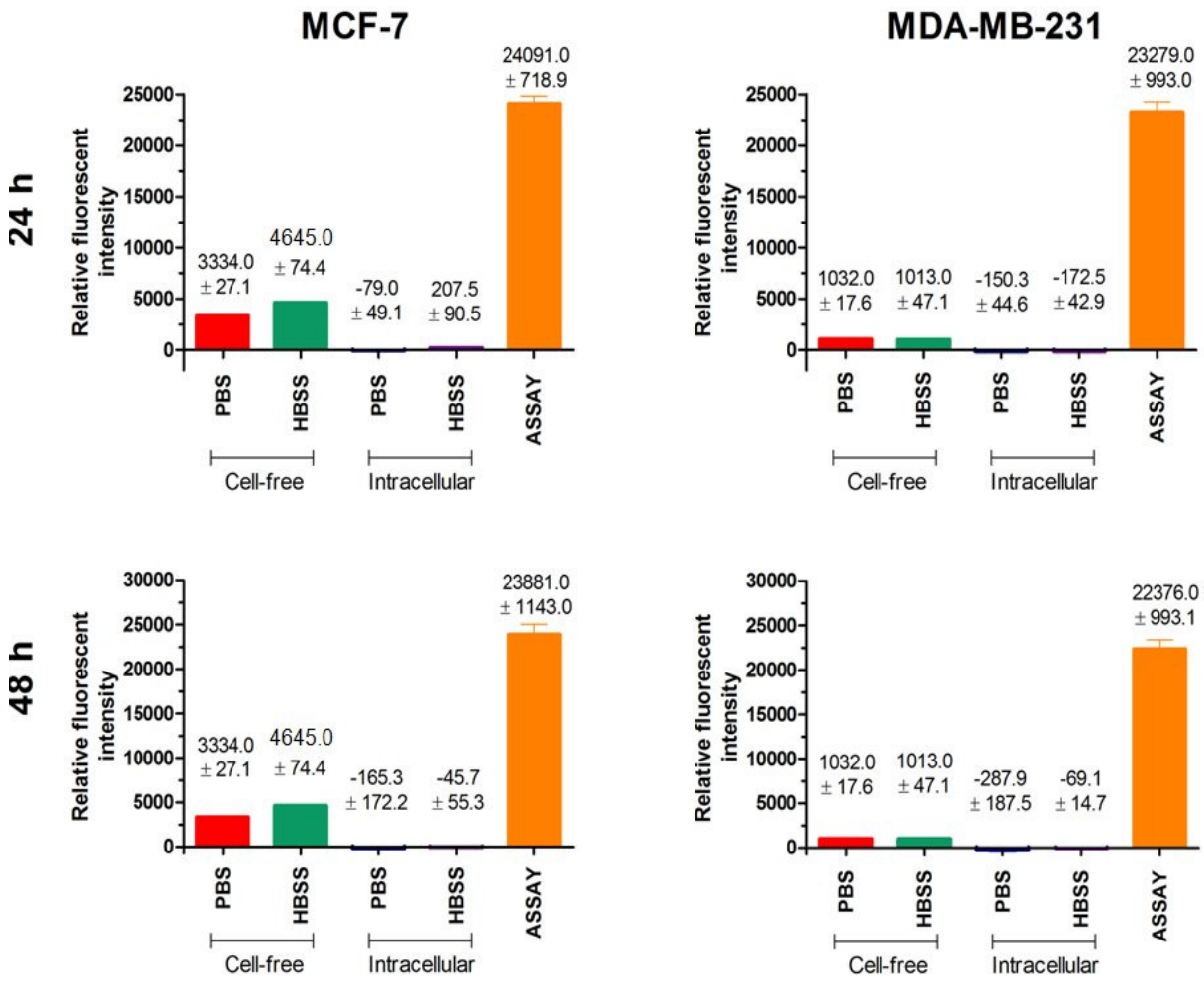

Figure 3.5: The fluorescent emission signal obtained for QUER at concentrations used in synergistic combinations with MCF-7 and MDA-MB-231 breast adenocarcinoma cells using λ_{ex} = 380 nm and λ_{em} = 505 nm. Emission was evaluated for QUER in a cell-free environment and the intracellular fluorescence of cells treated with QUER. The fluorescent signal obtained during experiments fluorescent substrate for caspase 9 is also shown (ASSAY). For MCF-7 cells QUER was used at 84 µM, while 0.64 µM of QUER was used for combinations with MDA-MB-231 cells. Error bars represent SEM. Where no error bars are visible the SEM was negligible.
Min n = 3

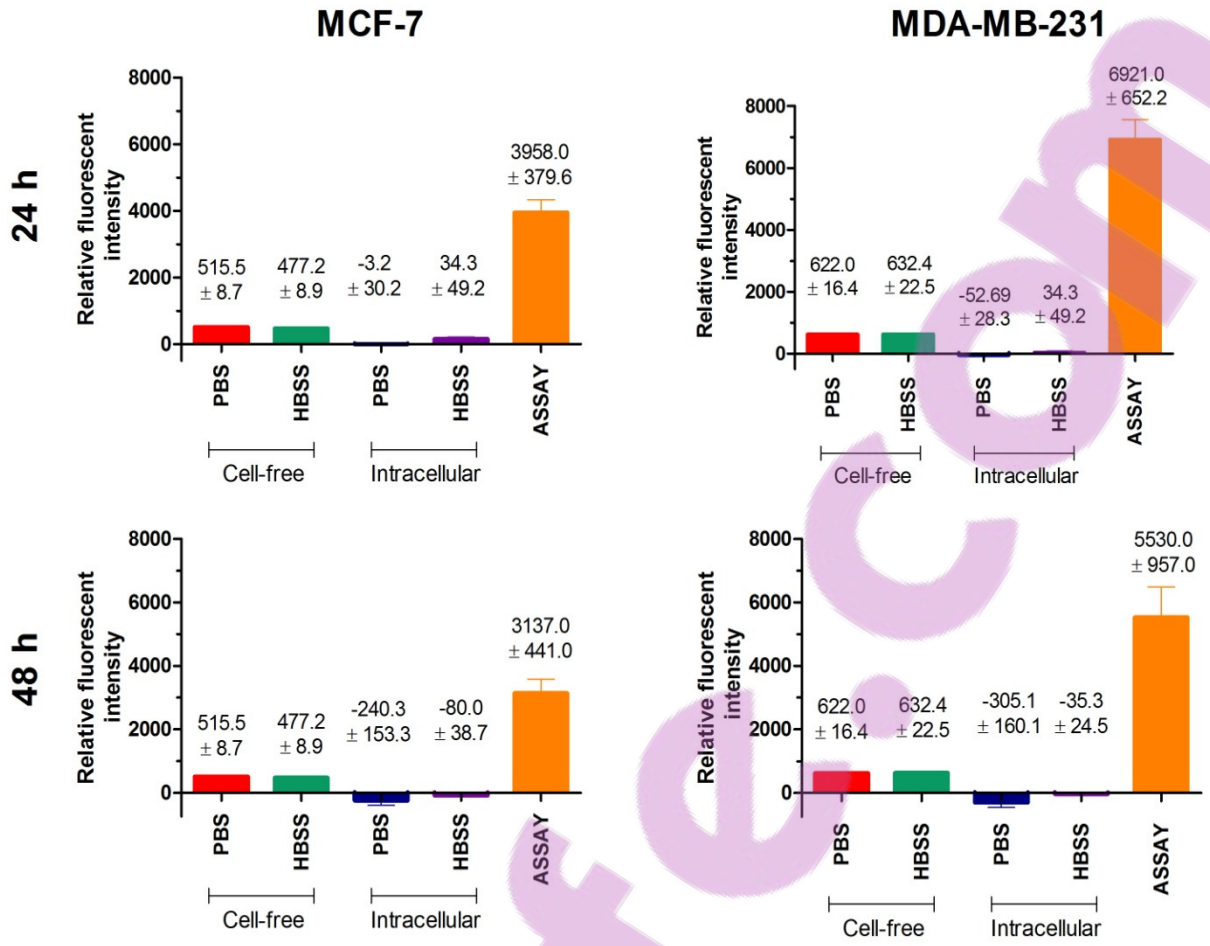

Figure 3.6: The fluorescent emission signal obtained for QUER at concentrations used in combinations with MCF-7 and MDA-MB-231 breast adenocarcinoma cells using λ_{ex} = 380 nm and λ_{em} = 450 nm. Emission was evaluated for QUER in a cell-free environment and the intracellular fluorescence of cells treated with QUER. The fluorescent signal obtained during experiments fluorescent substrates for caspase 8 and -3 is also shown (ASSAY). For MCF-7 cells QUER was used at 84 µM, while 0.64 µM of QUER was used for combinations with MDA-MB-231 cells. Error bars represent SEM. Where no error bars are visible the SEM was negligible.
Min n = 3

The activity of caspases 3 and -8 was determined using an excitation wavelength of 380 nm and emission wavelength of 450 nm. The assay was performed in caspase assay buffer which consists of HEPES and EDTA. In a cell-free system, 84 µM QUER in PBS produced a fluorescent signal of approximately 13% of the ASSAY signal which was greater than the signal detected for 84 µM QUER prepared in HBSS (approximately 12%) (Figure 3.6). For 0.64 µM of QUER, the greatest emission of fluorescence was observed where QUER was prepared in HBSS (approximately 9% of assay signal). While this data may indicate potential

for enhancing the emitted signal, it must be considered that cell-free conditions were not used in experimental setting as the cells were washed with the caspase assay buffer which removed any QUER in the media prior to the different caspase assays.

The effect of intracellular QUER on the fluorescent signal emitted during the assay was evaluated. After 24 h 84 µM QUER showed greatest potential for interference when cells were hydrated in HBSS (0.87% of ASSAY signal). However, after 48 h the fluorescent signal produced by intracellular QUER where cells were hydrated with PBS had the greatest potential for interference (7.6% of ASSAY signal).

For the concentration of QUER required for combinations on the MDA-MB-231 cells, 0.64 µM, the potential was greatest for interference where cells were hydrated with HBSS for 24 h assays (0.5% of ASSAY signal) and for 48 h assays where cells were hydrated with PBS (5.5%). Interestingly where cells were hydrated with HBSS enhanced fluorescent emission may occur while fluorescent emission of cells hydrated with PBS potential interference may be due to quenching of excitation wavelength or signal emitted.

However, even with maximal interference of intracellular QUER 7.6%, the effect on data obtained with during caspase 3 and -8 assays would be negligible.

3.3.4 Conclusion

In order to assess the potential interference of QUER with the various fluorometric assays used during the main study, the fluorescence of QUER in a cell-free and intracellular environment was assessed. The intracellular fluorescence of QUER most accurately represented the experimental conditions used in the study as the media was in all cases replaced with either HBSS or PBS, thus removing the QUER not taken up or adhering to the cells. For none of the excitation and emission wavelengths used did the emitted fluorescence of intracellular QUER exceed 7.6% of ASSAY signal suggesting negligible interference. Therefore the use of the fluorometric assays without the requirement for additional QUER controls is valid.

3.4 Methods

In an attempt to track the sequence of toxicity responses induced by the oestrone analogue and glycolysis inhibitor combinations, assays detecting specific stages in the sequence of toxicity were performed at different time points culminating in the assessment of the extent of cell death induced after 72 h (Figure 3.7). The synergistic combinations of oestrone

analogues with quercetin or indinavir identified in Stage 1 of the study are indicated in Table 2.7.

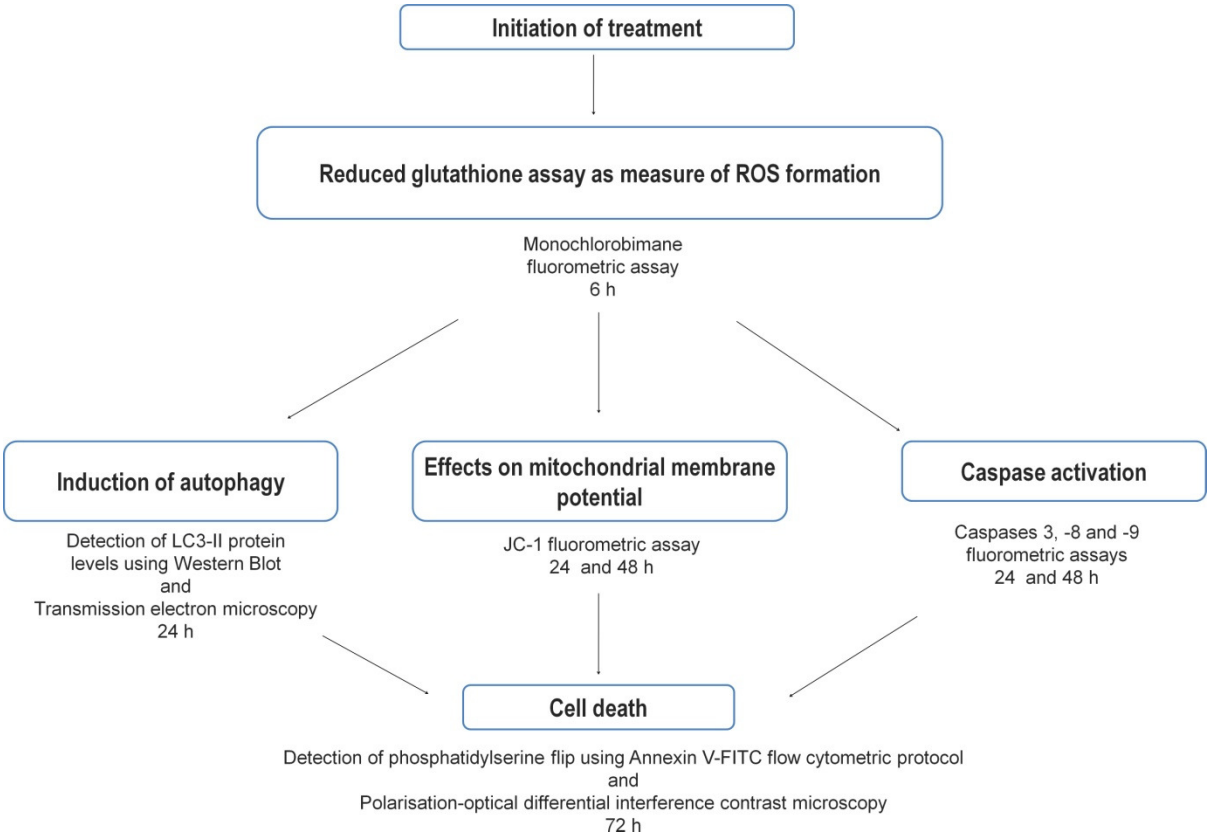

Figure 3.7: The sequence of assessment of molecular parameters followed in the present study.

As an indicator of early toxicity, the effect of the selected drug combinations on intracellular reduced glutathione concentration was assessed 6 h post exposure. Thereafter pre-lethal events including autophagy, mitochondrial effects and caspase activation were evaluated at 24 and 48 h treatment using the same synergistic combinations. Cell death, as indicator of irreversible cytotoxicity, was investigated after 72 h exposure.

3.4.1 Reduced intracellular glutathione concentration

The non-fluorescent probe monochlorobimane (mCB) was used to quantify intracellular GSH concentrations by forming fluorescent adducts with intracellular GSH which is fluorometrically quantitated (Kamencic *et al.*, 2000b). n-Ethylmaleimide (10 µM for 6 h) was used as positive control (van Tonder *et al.*, 2014).

The method used is based on the method by Fernández-Checa (Fernández-Checa and Kaplowitz, 1990). Cells were seeded at a density of 5 x 10^3 cells/well into sterile 96-well, white microtitre plate and allowed to attach overnight in a humidified incubator at 37°C and 5% CO_2. Cells were exposed to the test compounds alone and in synergistic combinations. After 6 h exposure, the medium was removed and cells loaded with mCB (10 µM in HBSS) for 1 h. The loading solution was removed and replaced with 100 µl HBSS. Thereafter the formation of adducts was monitored. Fluorescence was measured at λ_{ex} = 355 nm and λ_{em} = 460 nm using a FluoStar Optima fluorescence plate reader (Bio-Tek Instruments Inc., Vermont, USA). Gain was set at 1 250.

3.4.1.1 GSH interpretation of results and statistics

A minimum of three independent experiments were performed which included internal triplicates. All data was blank-adjusted, the area under the curve calculated and expressed as percentage of the untreated control. GraphPad Prism version 4.0 for Windows (GraphPad Software, San Diego California USA, www.graphpad.com) was used to determine statistical significance of the results obtained using a non-parametric Kruskal-Wallis with post-*hoc* Dunn's Multiple Comparison tests. A *P*-value < 0.05 was used as indicator of significance.

3.4.2 Ultrastructure studies: Transmission electron microscopy (TEM)

A previously described method was used. Tamoxifen was used as inducer of autophagy (10 µM overnight)(Theron *et al.*, 2013).

MCF-7 and MDA-MB-231 breast adenocarcinoma cells were seeded at a density of 2 x 10^6 cells into sterile 25 cm^2 flasks and allowed to attach overnight in a humidified incubator at 37°C with 5% CO_2. Cells were exposed to the test compounds alone or in combinations for 24h. Thereafter the cell culture medium in each well was transferred to sterile 15 ml centrifugation tubes. Cells were detached using trypsin/versene (0.125%) and the cell suspension added to the corresponding centrifuge tubes. A cell pellet was obtained after centrifugation (200 *g* for 5 min) which was washed once with complete cell culture medium. Thereafter the cell pellet was re-suspended in cell culture medium containing 2% FCS and transferred to sterile Eppendorf tubes.

Cells were washed once with sterile PBS before fixation in a freshly prepared 2.5% glutaraldehyde/formaldehyde fixative for 1 h at room temperature. Thereafter the cell pellet was washed three times in PBS before a second fixation in 0.5% aqueous osmium tetraoxide for 1 h. The cell pellet was again washed three times in PBS before ethanol dehydration. Ethanol dehydration was performed by incubating the cell pellet with increasing concentrations of ethanol (30%, 50%, 70%, 90% and 100%) at room temperature for 10 min each. The 100% ethanol dehydration step was performed three times. Thereafter the cell

pellet was infiltrated with increasing concentrations of EmBED812 (30%, 60% and 100% in ethanol, each for 1 h) at room temperature. An infiltration step with 100% EmBED812 and polymerisation for approximately 48 h at 60°C followed.

After polymerisation, sections of 80 µm were prepared using a DiATOME knife. The sections were mounted on copper grids and contrasted using 4% aqueous uranyl acetate for 2 min at room temperature and rinsed in water. Next the sections were contrasted in Reynold's lead citrate for 2 min at room temperature and rinsed in water. The sections were imaged using a JEM-210 0F field emission transmission electron microscope (JEOL, Tokyo, Japan) at the Laboratory for Microscopy and Microanalysis at 8 000 x and 25 000 x magnification.

3.4.3 Western blot for detection of LC3-II

The formation of autophagosomes, a crucial initial step in the macro-autophagic pathway, occurs only in the presence of the microtubule-associated protein 1 light chain 3 or LC3 protein (Cherra *et al.*, 2010). Antibody raised against microtubule-associated proteins 1A/1B light chain 3B membrane protein was used to quantify the autophagy-related (LC3) protein in western blot experiments.

Cells were seeded at a density of 2 x 10^5 cells/well into sterile 6-well microtitre plates and allowed to attach overnight in a humidified incubator at 37°C with 5% CO_2. Cells were exposed to the test compounds alone or in synergistic combinations and re-incubated for 24 h under the aforementioned conditions. After the incubation period the medium was aspirated and centrifuged (200 *g* for 5 min) in order to retain any floating cells. Wells were washed once with PBS before 150 µl Laemmli buffer, prewarmed to 90°C and supplemented with 2-mercaptoethanol, was added to each well. Cells were gently removed by scraping and transferred to Eppendorf tubes. The floating cells recovered from the medium were added to the Eppendorf tubes prior to boiling the cell lysates for 5 min at 100°C. Thereafter the cell lysates were centrifuged (14 000 *g* for 10 min) before snap-freezing at -80°C. Cell lysates were stored at -80°C.

Cell lysates (25 µl) and protein ladder (5 µl) were loaded onto polyacrylamide gels (4 – 20%) and separated at 60V for 15 min where after the voltage was increased to 120V for approximately 40 min using MOPS running buffer. The separated proteins were blotted unto polyvinylidene fluoride membranes using the semi-dry technique at 2.5 A for 7 min. Protein transfer was confirmed using Ponceau S staining. Membranes were blocked in 2% milk protein powder in PBS-T for 30 min. Thereafter the membranes were washed twice with PBS-T and incubated overnight with agitation with rabbit anti-LC3-II primary antibody (1 µg/ml) diluted in PBS-T supplemented with 2% BSA and 0.02% sodium azide at 4°C.

Membranes were washed once with PBS-T and incubated with rabbit anti-β-actin primary antibody (5 µg/ml) diluted in PBS-T supplemented with 2% BSA for 40 min at room temperature with agitation. Thereafter membranes were washed once with PBS-T and incubated with goat anti-rabbit secondary antibody (0.08 µg/ml) conjugated to HRP for 1 h at room temperature with agitation. Membranes were washed three times for 10 min each with PBS-T at room temperature. Protein bands were visualised with ECL substrate and imaged using a ChemiDOC XR+ Imager (Bio-Rad Laboratories Inc, Hercules, USA).

3.4.3.1 Western blot for detection of LC3-II interpretation of results and statistics

Band intensities were determined and normalised against housekeeping proteins using Image Lab version 5.2.1 (Image Lab Software, Bio-Rad Laboratories, Hercules, USA). GraphPad Prism version 4.0 for Windows (GraphPad Software, San Diego California USA, www.graphpad.com) was used to determine statistical significance of the results obtained using a non-parametric Kruskal-Wallis with post-*hoc* Dunn's Multiple Comparison tests. A *P* - value < 0.05 was used as indicator of significance.

3.4.4 Mitochondrial membrane potential

The accumulation of the cationic fluorescent dye JC-1 (5,5',6,6'-tetrachloro-1,1',3,3'-tetraethylbenzimidazolcarbo-cyanine iodide) in the mitochondrial membrane space is indirectly proportional to the mitochondrial membrane potential (Perry *et al.*, 2011). An increased prevalence of JC-1 aggregates is therefore indicative of a high $\Delta\psi_m$, or a hyperpolarised state, whereas more JC-1 monomers will be present with low $\Delta\psi_{m,}$ or a depolarised state (Gravance *et al.*, 2000). Valinomycin (50 µM for 24 or 48 h)(Inai *et al.*, 1997) was used as depolarisation control and tamoxifen (100 µM for 4 h)(van Tonder *et al.*, 2014) was used as hyperpolarisation control.

The method used, based on a published method (van Tonder *et al.*, 2014), is briefly described. Cells were seeded at a density of 5 x 10^3 cells/well into a sterile 96-well, white microtitre plate and allowed to attach overnight in a humidified incubator at 37℃ with 5% CO_2. Cells were exposed to the test compounds alone and in synergistic combinations and re-incubated for 24 or 48 h at the aforementioned conditions. After the incubation period the medium was aspirated and the cells loaded with JC-1 (10 µM in HBSS) for 2 h in a humidified incubator at 37℃ with 5% CO_2. The loading solution was aspirated and HBSS added to keep the cells hydrated. The fluorescence was measured using a FluoStar Optima fluorescence plate reader (Bio-Tek Instruments Inc., Vermont, USA) at λ_{ex}= 492 nm and λ_{em}= of 525 nm for the monomeric JC-1 form, and λ_{ex} = 545 nm and λ_{em} = 595 nm for the aggregated JC-1 form. Gain was set at 1 000 for all wavelengths.

3.4.4.1 $\Delta\psi_m$ interpretation of results and statistics

A minimum of three independent experiments were performed which included internal triplicates. The effect of the drug combinations on MMP was calculated using the ratio of the JC-1 aggregates: JC-1 monomers. The ratios were then normalised to a percentage of the untreated control. GraphPad Prism version 4.0 for Windows (GraphPad Software, San Diego California USA, www.graphpad.com) was used to determine statistical significance of the results obtained usinga non-parametric Kruskal-Wallis with post-*hoc* Dunn's Multiple Comparison tests. A *P* -value < 0.05 was used as indicator of significance.

3.4.5 Caspase activity

For caspase 3 activity N-Acetyl-Asp-Glu-Val-Asp-7-amido-4-methylcoumarin (Ac-DEVD-AMC) was used as fluorescent substrate and staurosporine aglycone (10 µM for 4 h)(Kirsch *et al.*, 1999) was used as a positive control. N-Acetyl-Ile-Glu-Thr-Asp-7-amino-4-methylcoumarin (Ac-IETD-AMC) was used as fluorescent substrate for caspase 8 and Fas ligand (100 ng/ml for 4h)(Li *et al.*, 1998) was used as positive control. N-Acetyl-Leu-Glu-His-Asp-7-amido-4-trifluoromethylcoumarin (Ac-LEHD-AFC) was used as substrate to probe for caspase 9 and staurosporine aglycone (10 µM for 4 h)(Chandele *et al.*, 2004) was used as positive control.

Briefly, cells were seeded at a density of 5 x 10^3 cells/well in a sterile 96-well, white microtitre plate and allowed to attach overnight in a humidified incubator at 37°C with 5% CO_2. Cells were exposed to the test compounds alone, the synergistic combinations or the various positive controls and re-incubated at the aforementioned conditions for 24 or 48 h. After the incubation period the plate was placed on ice for 2 min to cool, the medium aspirated and caspase lysis buffer added. The plate was incubated on ice for a further 30 min on a shaker. Caspase assay buffer was added to the plate and the plate incubated for 4 h at 37°C to allow for the cleavage of the fluorescent AMC or AFC molecule. The fluorescent intensity was measured using a Synergy 2 fluorescence plate reader (Bio-Tek Instruments Inc., Vermont, USA) at λ_{ex} = 380 nm and λ_{em} = 450 nm for caspases 3 and -8, and λ_{ex} = 380 nm and λ_{em} = 505 nm for caspase 9.

3.4.5.1 Interpretation of caspase assay results and statistics

A minimum of three independent experiments were performed which included internal triplicates. All data was blank-adjusted and expressed as percentage of the untreated control. GraphPad Prism version 4.0 for Windows (GraphPad Software, San Diego California USA, www.graphpad.com) was used to determine statistical significance of the results obtained using a non-parametric Kruskal-Wallis with post-*hoc* Dunn's Multiple Comparison tests. A *P* -value < 0.05 was used as indicator of significance.

3.4.6 Polarisation-optical differential interference contrast microscopy (PlasDIC)

PlasDIC is a microscopy technique where light passes through the objective before conversion to linearly polarised light (Wehner, 2003). This allows for the generation of images with enhanced detail from which information can be gathered.

Cells were seeded into sterile 6-well plates at a seeding density of 6 x 10^4 cells/well in the appropriate cell culture medium supplemented with 2% FCS. After overnight incubation in a humidified incubator at 37°C with 5% CO_2 to allow for cell attachment, cells were exposed to the oestrone analogues or synergistic combinations for 72 h. After the incubation period the medium was removed and the wells washed once with sterile HBSS. Cells were kept hydrated by the addition of HBSS to each well and PlasDIC images taken at 40 x magnification using a Zeiss Axiovert-40 microscope (Göttingen, Germany) and a Zeiss AxiovertMRm monochrome camera (Göttingen, Germany). Phase contrast microscopy images were captured at 10 x magnification.

3.4.6.1 PlasDIC interpretation of results

A minimum of two independent experiments were performed with a minimum of two observations per sample. As qualitative data was obtained no statistical analyses were performed.

3.4.7 Annexin V

During the tightly regulated process of apoptosis phosphatidylserine, a phospholipid, is translocated from the inner membrane to the cell surface by flippases (Fadok *et al.*, 1992). Annexin V- FITC staining coupled to flow cytometry was used to indicate externalised phosphatidyl serine expression (Koopman *et al.*, 1994; Aubry *et al.*, 1999; Willingham, 1999). Propidium iodide staining was used as indicator of membrane compromised necrotic cells (Willingham, 1999). Staurosporine aglycone (10 µM for 24 h) was used as apoptosis control (Kirsch *et al.*, 1999), and absolute ethanol as necrosis control.

Cells were seeded at a density of 6 x 10^4 cells/well in sterile, 6-well plates and allowed to attach overnight in a humidified incubator at 37°C with 5% CO_2. Thereafter cells were exposed to the oestrone analogues or synergistic combinations for 72 h. After the incubation period, the medium in the plate was transferred to centrifuge tubes and the wells trypsinised. The trypsinised cells were added to the centrifuge tubes, and the cell suspension washed with PBS supplemented with 1% FCS. For the necrosis control absolute ethanol (20%) was added drop wise before incubating the tube at 4° for 10 minutes and continuing with a second wash step with PBS supplemented in 1% FCS. The cell pellet was re-suspended in annexin V binding buffer and undiluted annexin V-FITC added (2 µl). The tubes were incubated for 10 minutes in the dark. Thereafter PI (2 µl, 3 mg/ml) was added to each tube

and the contents of the tubes transferred to flow cytometer tubes. The samples were analysed with a Beckman Coulter FC 500 Series flow cytometer (Beckman Coulter SA (Pty) Ltd.) using FL1 (525 nm) and FL3 (620 nm). A total of 10 000 events was recorded per sample.

3.4.7.1 Interpretation of mode of cell death results and statistics

A minimum of three independent experiments were performed. Quadrant analysis was performed using CXP software to characterise a percentage of cells as viable, in early apoptosis, late apoptosis or necrosis. Data is reported as mean ± SEM for each quadrant. GraphPad Prism version 4.0 for Windows (GraphPad Software, San Diego California USA, www.graphpad.com) was used to determine statistical significance of the results of treated groups in comparison to untreated control obtained using a non-parametric Kruskal-Wallis with post-*hoc* Dunn's Multiple Comparison tests. A P -value < 0.05 was used as indicator of significance.

3.5 Results

3.5.1 Reduced intracellular glutathione concentration

The immediate effect of the synergistic combinations on the concentration of reduced intracellular glutathione was determined using a fluorometric monochlorobimane protocol.

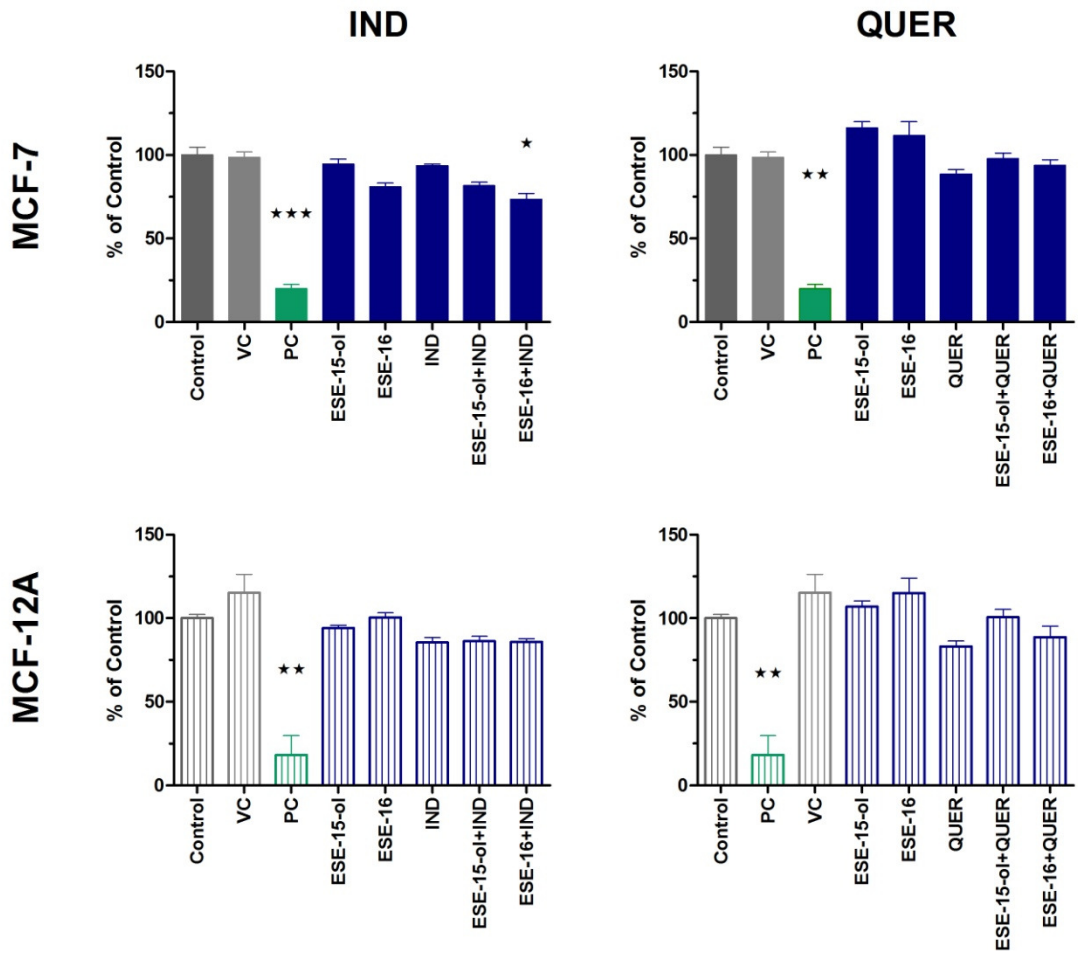

Figure 3.8: The effect of synergistic combinations of the oestrone analogues with indinavir (IND, 115 µM) and quercetin (QUER, 84 µM) on intracellular reduced GSH concentrations in **MCF-7** breast adenocarcinoma and **MCF-12A** non-tumourigenic cells after 6 h exposure using a fluorometric monochlorobimane protocol. VC indicates DMSO-treated cells. n-Ethylmaleimide (10 µM for 6 h) was used as positive control (PC). ESE-15-ol was used at 70 nM for combinations with IND and 17 nM for combinations with QUER. ESE-16 was used at 67 nM for combinations with IND and 17 nM for combinations with QUER. Error bars represent SEM.
n = 3; * $p < 0.05$ ** $p < 0.01$ *** $p < 0.001$

A significant reduction ($p < 0.01$) in GSH was observed in MCF-7 breast adenocarcinoma and MCF-12A non-tumourigenic cells treated with n-ethylmaleimide indicating that a decrease in GSH concentration could be detected using the assay (Figure 3.8).

Combinations with IND seemed to have the greater effect on GSH concentration in the MCF-7 breast adenocarcinoma cell line (Figure 3.8). A significant 20% reduction in GSH

concentrations were observed in the MCF-7 cell line exposed to 67 nM ESE-16 (for the concentration used in combinations with IND) as well as for all the drug combinations with IND. The greatest depletion of GSH concentration, approximately 27%, was achieved with the combination of ESE-16 and IND. In the non-tumourigenic MCF-12A cell line exposed to combinations with IND, GSH depletion did not exceed 15% for any of the treatment groups.An increase in GSH concentration of approximately 15% was observed where MCF-12A non-tumourigenic cells were exposed to the DMSO vehicle (Figure 3.8).

Where MCF-7 breast adenocarcinoma cells were exposed to combinations with QUER the effect was less pronounced: the greatest effect was observed where cells were exposure to the combination of ESE-15-ol and QUER which resulted in a 13% reduction in GSH concentration (Figure 3.8). Similar results were observed in the MCF-12A non-tumourigenic cell line where reduction of GSH concentration did not exceed 15%. However, an increase between 11 and 16% in GSH was observed where MCF-7 breast adenocarcinoma cells were exposed to ESE-15-ol (17 nM) or ESE-16 (17 nM), respectively. Similarly a 15% increase in GSH concentration was seen where MCF-12A non-tumourigenic cells were exposed to ESE-16 (17 nM).

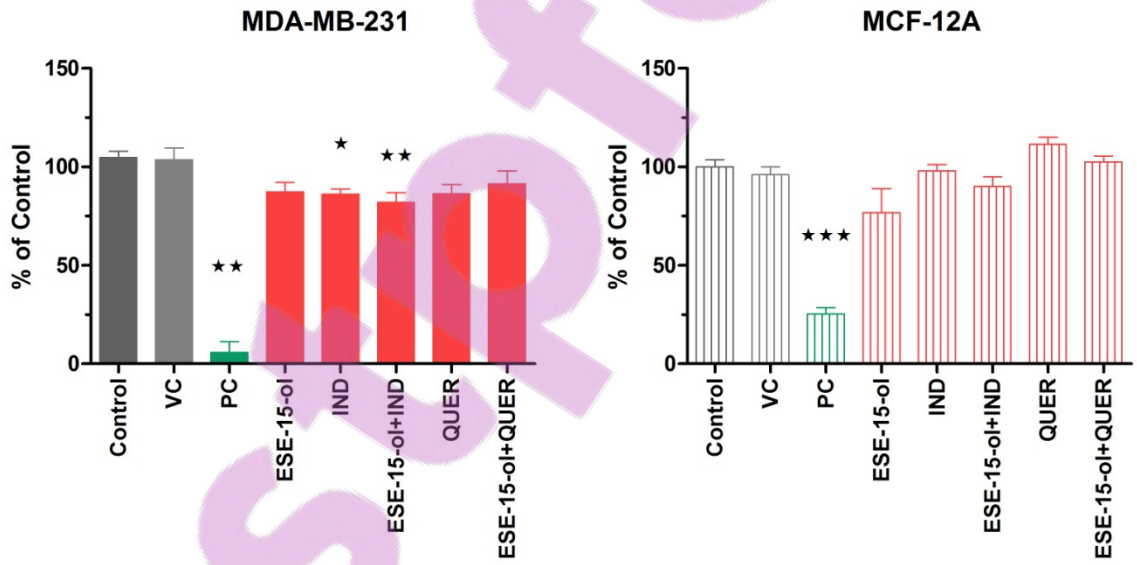

Figure 3.9: The effect of synergistic combinations of the oestrone analogue ESE-15-ol (123 nM) with indinavir (IND, 55 µM) and quercetin (QUER, 0.64 µM) on intracellular reduced GSH concentrations in **MDA-MB-231** breast adenocarcinoma and **MCF-12A** non-tumourigenic cells after 6 h exposure using a fluorometric monochlorobimane protocol. VC indicates DMSO-treated cells. n-Ethylmaleimide (10 µM for 6 h) was used as positive control (PC). Error bars represent SEM.

n = 3; * $p < 0.05$ ** $p < 0.01$ *** $p < 0.001$

A significant reduction in GSH was observed in MDA-MB-231 breast adenocarcinoma and MCF-12A non-tumourigenic cells treated with n-ethylmaleimide indicating that the assay could detect a decrease in GSH concentration (Figure 3.9). All treatment groups resulted in GSH depletion in the MDA-MB-231 breast adenocarcinoma cell line but the only significant depletion observed was after treatment with IND (55 µM) or the combination of ESE-15-ol (123 nM) and IND. A 25% reduction in GSH concentration observed in MCF-12A cells treated with ESE-15-ol (123 nM). However, an 11% increase in GSH concentrations was observed where MCF-12A cells were exposed to QUER (0.64 µM).

3.5.2 Ultrastructure studies: Transmission electron microscopy

The ultrastructure of MCF-7 and MDA-MB-231 breast adenocarcinoma cells was studied after 24 h exposure to the combinations of oestrone analogues and glycolysis inhibitors.

The ultrastructure of MCF-7 breast adenocarcinoma cells exposed to combinations of oestrone analogues and IND for 24 h revealed vesicle formation, membrane blebbing and decreased cell size (Figure 3.10).

The ultrastructure of MCF-7 breast adenocarcinoma cells exposed to combinations of oestrone analogues and QUER for 24 h revealed vesicle formation and membrane blebbing (Figure 3.11).

The ultrastructure of MDA-MB-231 breast adenocarcinoma cells exposed to combinations of oestrone analogues and glycolysis inhibitors for 24 h revealed vesicle formation, hypercondensed chromatin and membrane blebbing (Figure 3.12).

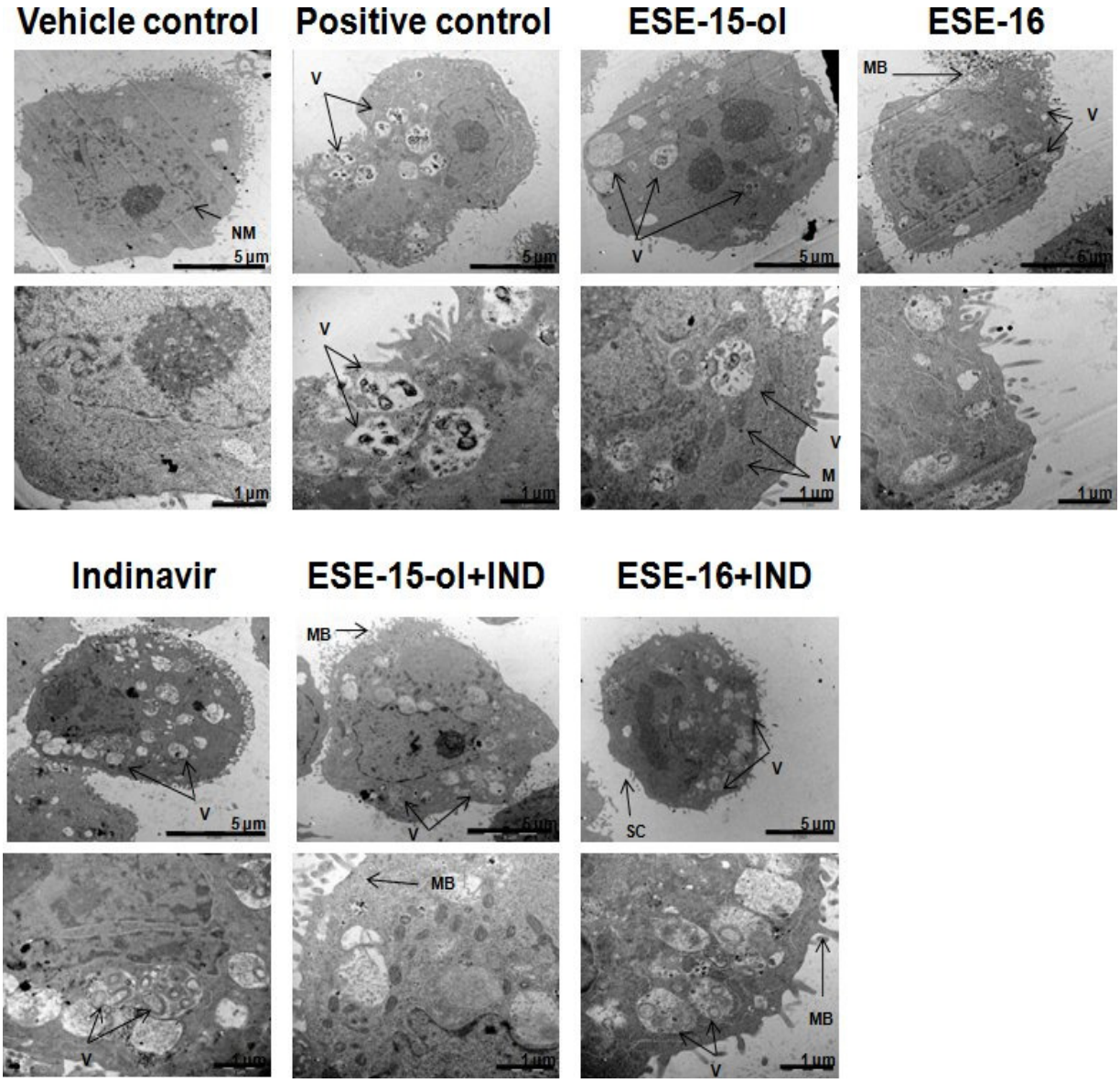

Figure 3.10: Photomicrographs of the ultrastructure of **MCF-7** breast adenocarcinoma cells after 24 h exposure to combinations of oestrone analogues and indinavir (115 µM) as observed by TEM. Tamoxifen (10 µM for 24 h) was used as positive control. ESE-15-ol was used at 70 nM for combinations with IND. ESE-16 was used at 67 nM for combinations with IND. Scale bars represent 5 and 1 µm as indicated on photomicrographs.NM: nuclear membrane. MB: membrane blebbing. SC: shrunken cell. V: vesicles.

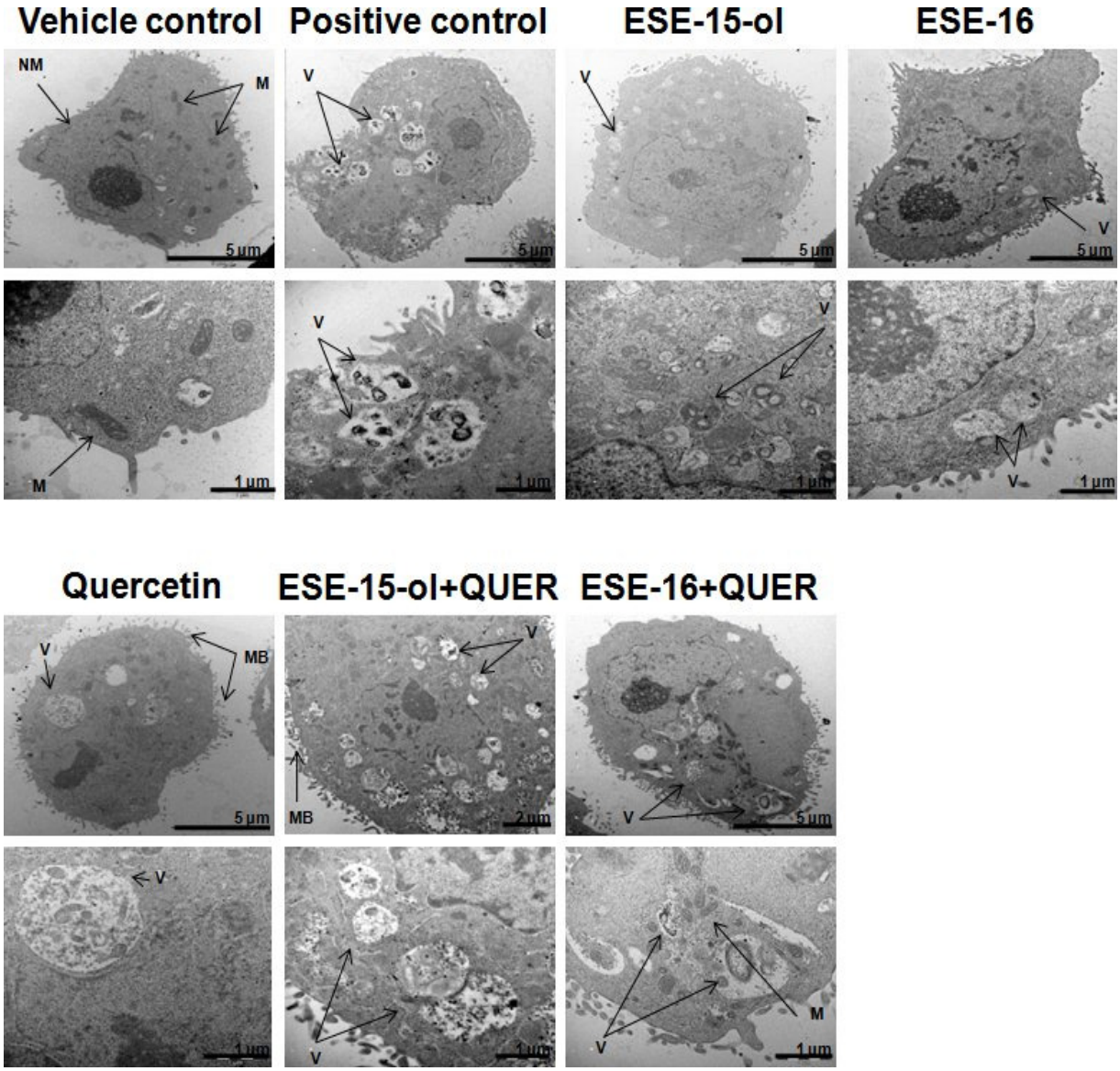

Figure 3.11: Photomicrographs of the ultrastructure of **MCF-7** breast adenocarcinoma cells after 24 h exposure to combinations of oestrone analogues and quercetin (84 µM) as observed by TEM. Tamoxifen (10 µM for 24 h) was used as positive control. ESE-15-ol was used at 17 nM for combinations with QUER. ESE-16 was used at 17 nM for combinations with QUER. Scale bars represent 5 and 1 µm as indicated on photomicrographs. NM: nuclear membrane. MB: membrane blebbing. M: mitochondria. V: vesicles.

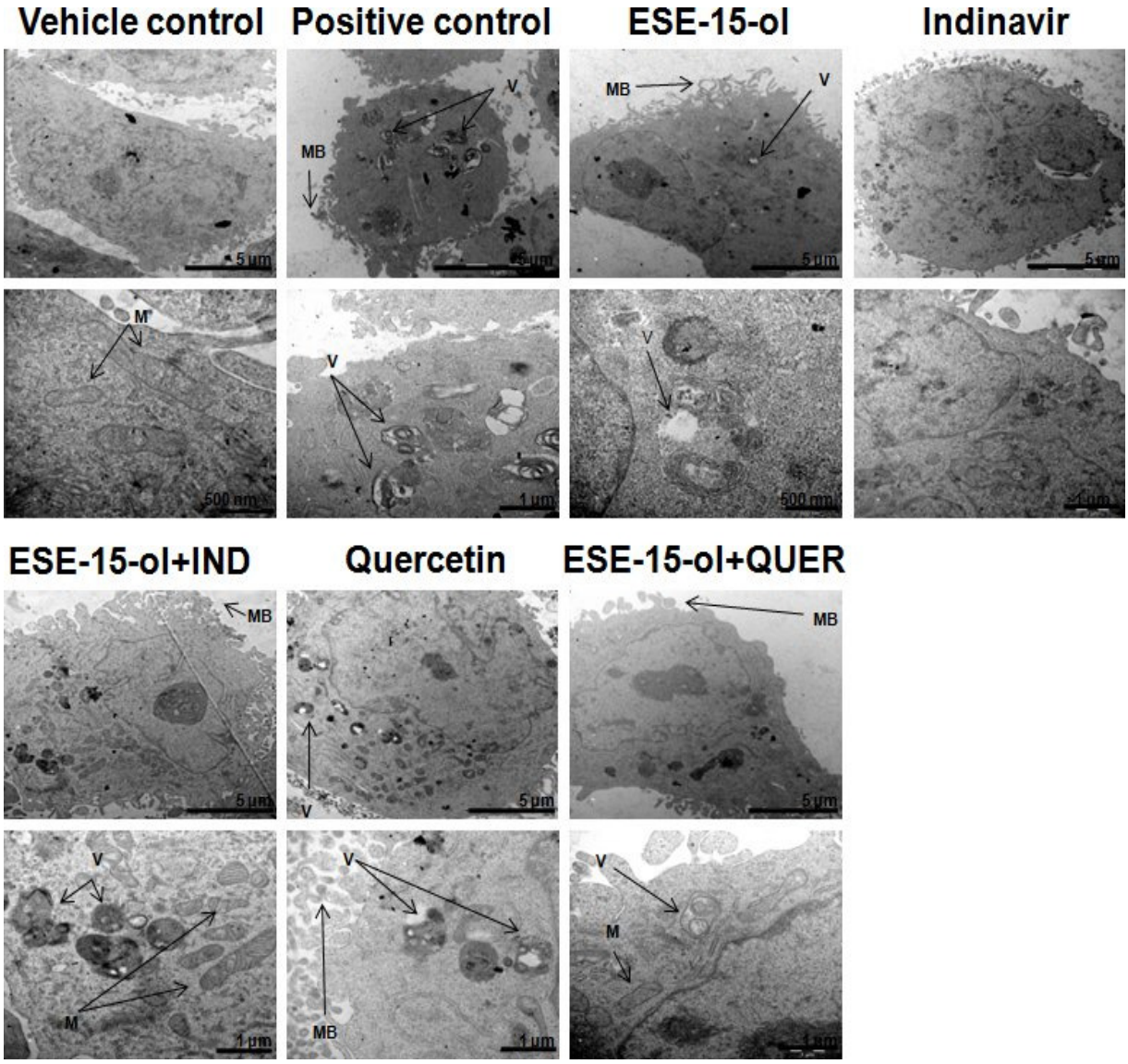

Figure 3.12: Photomicrographs of the ultrastructure of **MDA-MB-231** breast adenocarcinoma cells after 24 h exposure to combinations of ESE-15-ol (123 nM), indinavir (IND, 55 µM) and quercetin (QUER, 0.64 µM) as observed by TEM. Tamoxifen (10 µM for 24 h) was used as positive control. Scale bars represent 5 and 1 µm as indicated on photomicrographs. MB: membrane blebbing. M: mitochondria. V: vesicles.

3.5.3 Western blot for detection of LC3-II

The effect of 24 h exposure to the synergistic drug combinations on the expression of LC3-II as indicator of autophagy was assessed with Western blot.

Exposure of MCF-7 breast adenocarcinoma cells to the autophagy-inducer tamoxifen resulted in a pronounced but non-significant increase in LC3-II expression indicating that

LC3-II was detectable with the optimised protocol (Figure 3.13 B). A non-significant increase in LC3-II expression was observed in DMSO vehicle-treated cells. Treatment with ESE-15-ol (70 nM) resulted in reduced expression of LC3-II. Increased LC3-II expression was observed in cells treated with ESE-16 (67 nM) and IND (115 µM), however LC3-II expression was suppressed where these compounds were combined.

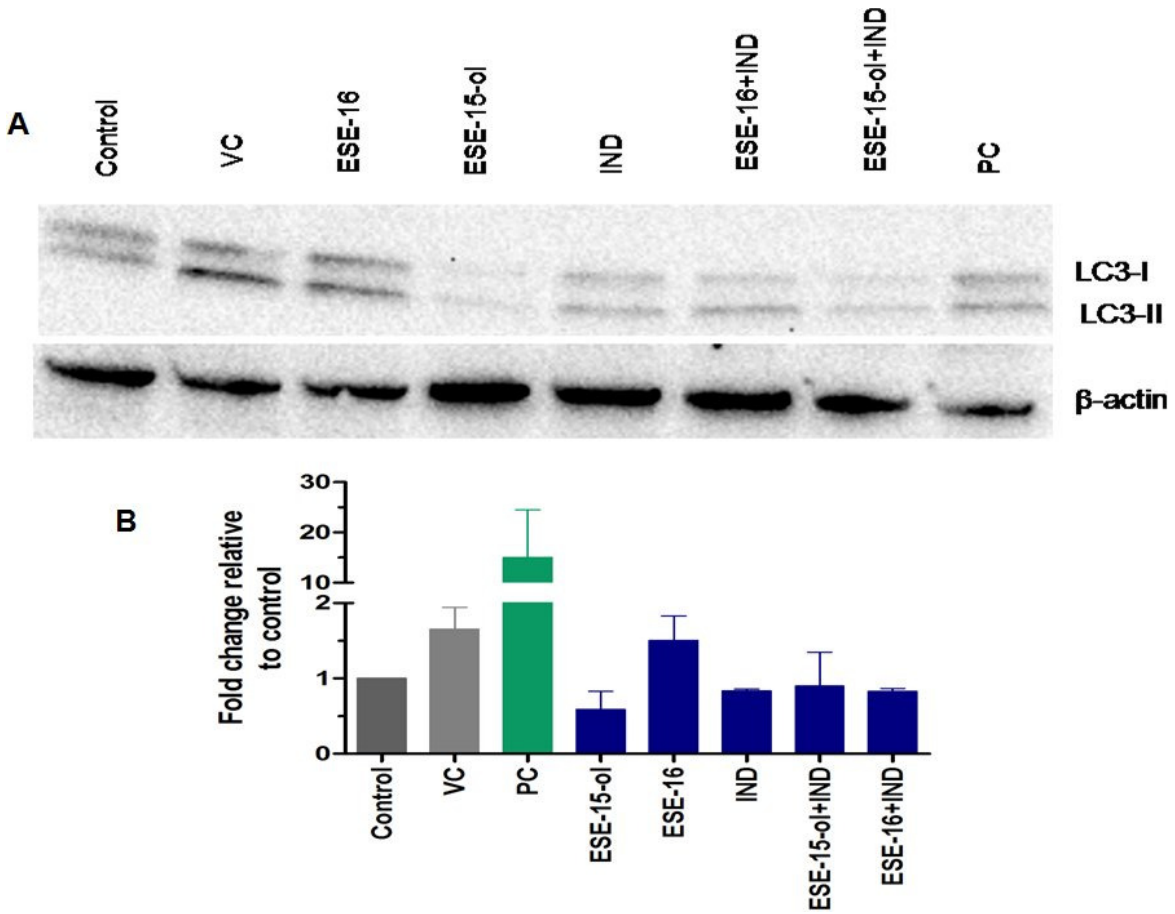

Figure 3.13: The effect of synergistic combinations of the oestrone analogues, ESE-15-ol (70 nM) and ESE-16 (67 nM) with indinavir (IND, 115 µM) on the expression of LC3-II in **MCF-7** breast adenocarcinoma cells after 24h exposure detected using Western blot. (A) Blot is representative of three independent experiments. (B) Protein normalisation to β-actin of controls and treatment groups present cumulative data of three independent experiments. VC indicates DMSO-treated cells. Tamoxifen (10 µM for 24 h) was used as positive control (PC). Error bars represent SEM. No statistically significant differences were detected.
n = 3

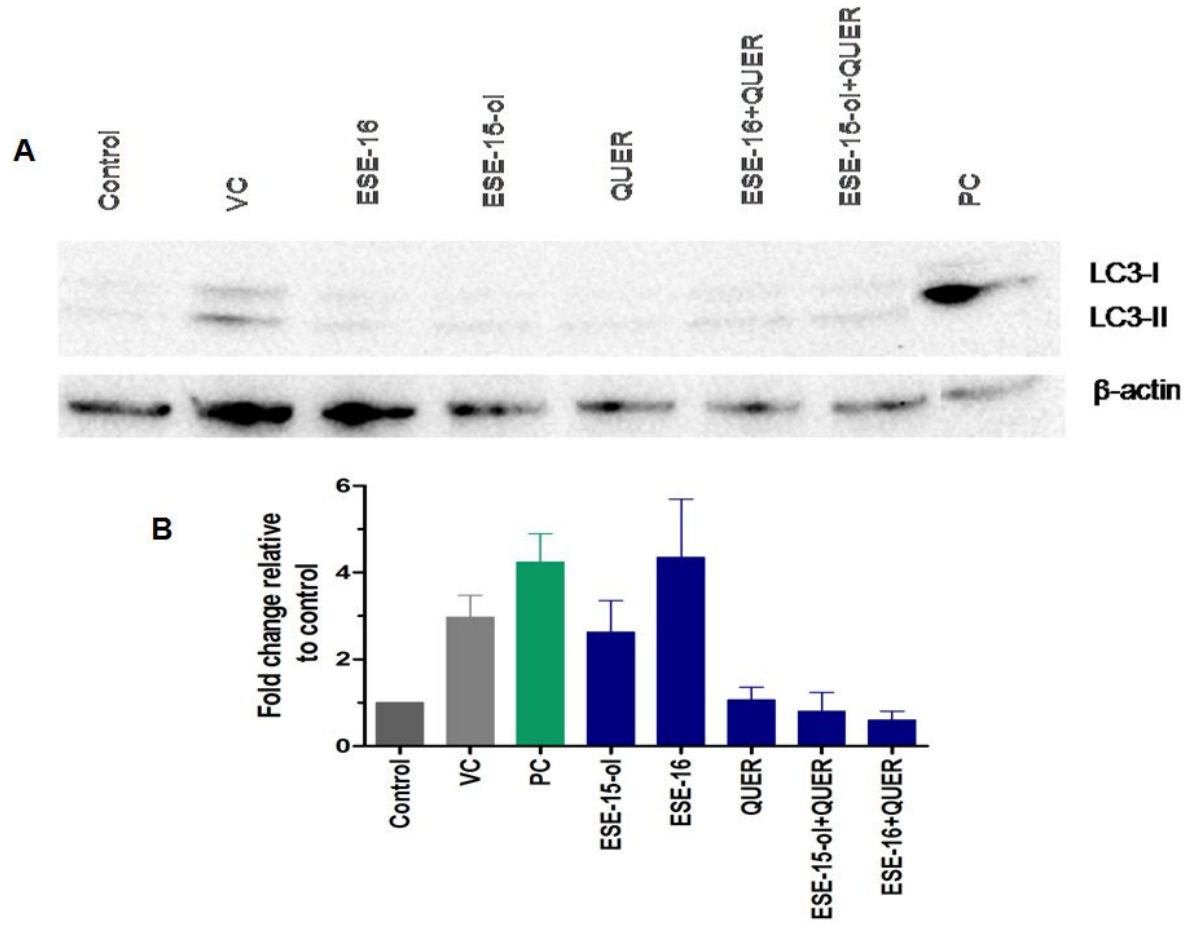

Figure 3.14: The effect of synergistic combinations of the oestrone analogues, ESE-15-ol (17 nM) and ESE-16 (17 nM) with quercetin (QUER, 84 µM) on the expression of LC3-II in **MCF-7** breast adenocarcinoma cells after 24h exposure detected using Western blot. (A) Blot is representative of four independent experiments. (B) Protein normalisation to β-actin of controls and treatment groups present cumulative data of three independent experiments. VC indicates DMSO-treated cells. Tamoxifen (10 µM for 24 h) was used as positive control (PC). Error bars represent SEM. No statistically significant differences were detected.
n = 4

Exposure of MCF-7 breast adenocarcinoma cells to the autophagy-inducer tamoxifen resulted in a marked increase in LC3-II expression indicating that LC3-II was detectable with the optimised assay protocol (Figure 3.14 B). Elevated LC3-II levels were observed in DMSO vehicle-treated cells. Increased LC3-II expression was also observed where cells were treated with the oestrone analogues. These increases were not statistically significant. However, where the oestrone analogues were combined with QUER marked suppression of LC3-II expression was seen. The combination of ESE-16 and QUER showed the greatest reduction of LC3-II expression (approximately 0.4 fold reduction in comparison to the

control). However, statistically significant differences in the LC3-II expression of treatment groups in comparison to the untreated control were not observed.

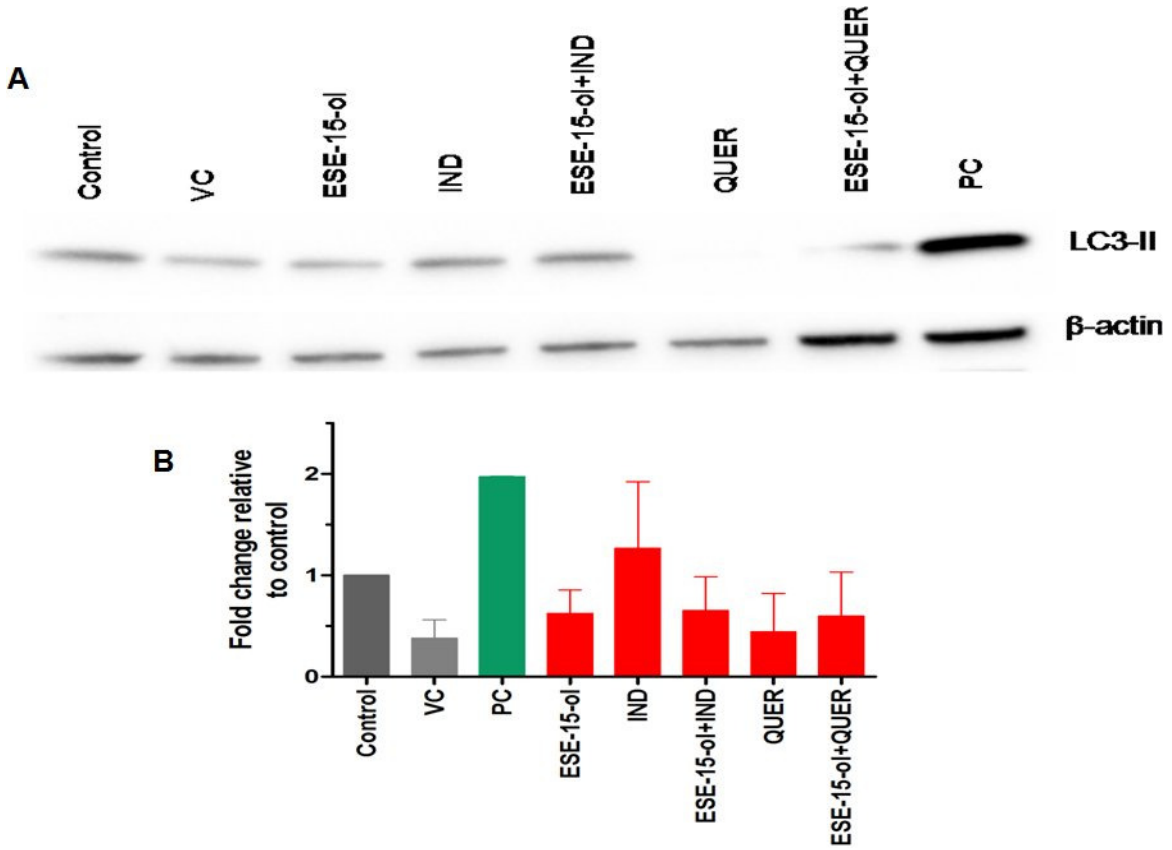

Figure 3.15: The effect of synergistic combinations of the oestrone analogue ESE-15-ol (123 nM) with indinavir (IND, 55 µM) and quercetin (QUER, 0.64 µM) on the expression of LC3-II in **MDA-MB-231** breast adenocarcinoma 24h exposure detected using Western blot. (A) Blot is representative of three independent experiments. (B) Protein normalisation to β-actin of controls and treatment groups present cumulative data of three independent experiments. VC indicates DMSO-treated cells. Tamoxifen (15 µM for 18 h) was used as positive control (PC). Error bars represent SEM. Where no error bars can be seen the SEM was negligible. No statistically significant differences were detected.
n = 3

Exposure of MDA-MB-231 breast adenocarcinoma cells to the autophagy-inducer tamoxifen resulted in a pronounced but non-significant increase in LC3-II expression indicating that LC3-II was detectable with the optimised protocol (Figure 3.15 B). DMSO vehicle-treated cells also showed elevated LC3-II expression. The elevation in LC3-II expression induced by treatment with IND only was suppressed by the addition of ESE-15-ol with an approximately 0.4 fold reduction in LC3-II expression in comparison to the control. Treatment with QUER

and the combination of ESE-15-ol and QUER resulted in reduced LC3-II levels in comparison to the control. However, changes in LC3-II expression in treatment groups in comparison to the untreated control were not statistically significant.

3.5.4 Mitochondrial membrane potential

The effect of 24 or 48 h exposure to the synergistic combinations on fluctuations of the mitochondrial membrane potential was investigated using a JC-1 fluorescent ratiometric protocol.

Exposure of MCF-7 breast adenocarcinoma and MCF-12A non-tumourigenic cells to tamoxifen resulted in a significant hyperpolarisation of the mitochondrial membrane while marked yet non-significant depolarisation of the mitochondrial membrane potential was observed in response to treatment with valinomycin indicating that the assay functioned correctly (Figure 3.16 and 3.17).

Exposure of MCF-7 breast adenocarcinoma cells to ESE-15-ol (70 nM) or ESE-16 (67 nM) resulted in significant hyperpolarisation after 24 h. After 48 h treatment with the oestrone analogues non-significant hyperpolarisation of the mitochondrial membrane potential was observed in the MCF-7 cell line. These were the concentrations showing synergistic combinations with IND (Figure 3.16). When the oestrone analogues were combined with IND the hyperpolarisation caused by the oestrone analogues alone is attenuated at 24 h. This effect was not observed at 48 h.

Non-significant depolarisation of the mitochondrial membrane potential was observed in the non-tumourigenic MCF-12A cells exposed to IND after 24 and 48 h. Where MCF-12A cells were exposed to ESE-15-ol (70 nM) or ESE-16 (67 nM) for 48 h, statistically significant hyperpolarisation was observed. Hyperpolarisation of the mitochondrial membrane in response to treatment with combinations of oestrone analogues and IND were observed after 24 h in MCF-12A non-tumourigenic cells. After 48 h MCF-12A cells treated with ESE-15-ol and IND showed a statistically significant increase of approximately 30% in mitochondrial membrane potential in comparison to the untreated control.

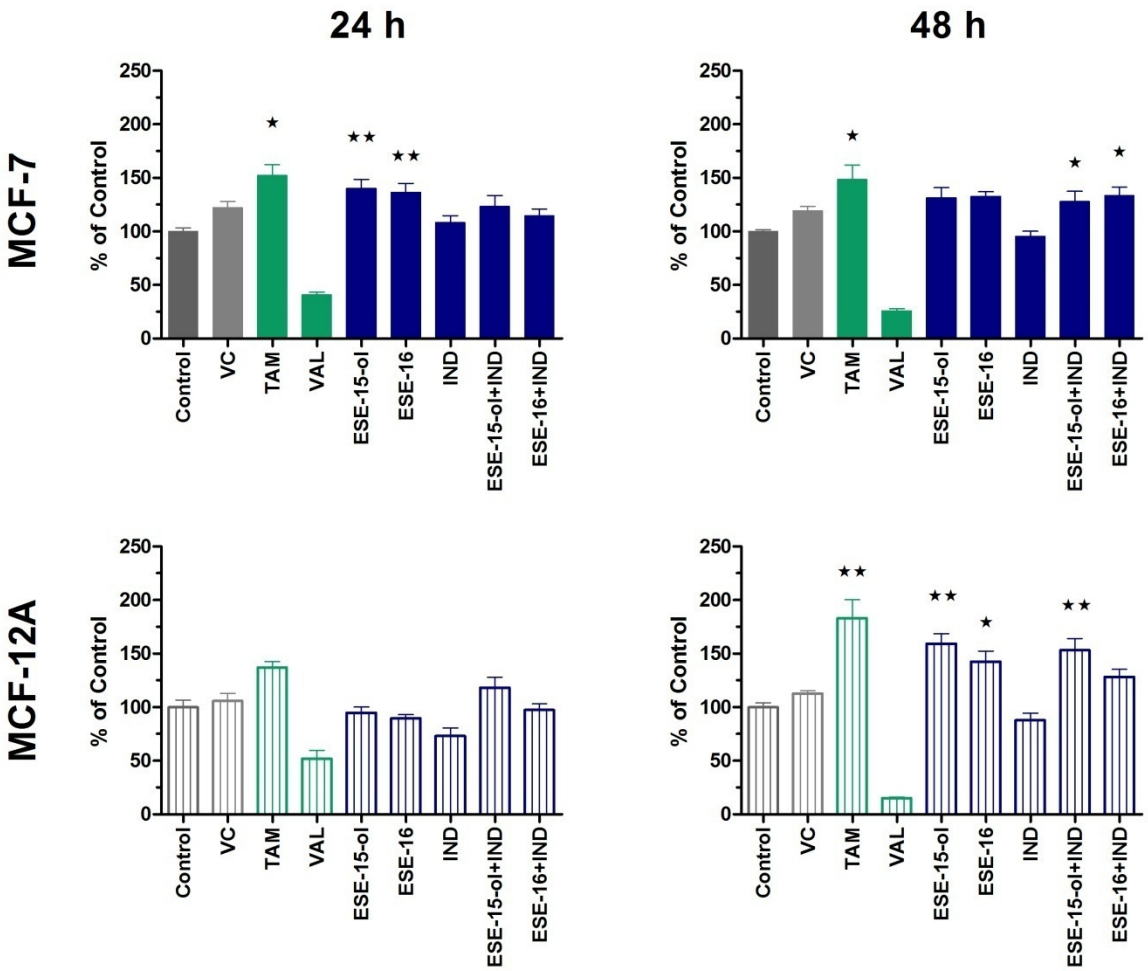

Figure 3.16: The effect of synergistic combinations of ESE-15-ol (70 nM) and ESE-16 (67 nM) with indinavir (IND, 115 µM) on the mitochondrial membrane potential in **MCF-7** breast adenocarcinoma and **MCF-12A** non-tumourigenic cells after 24 or 48 h exposure using a JC-1 fluorometric protocol. VC indicates DMSO-treated cells. Valinomycin (VAL, 50 µM for 24 or 48 h) and tamoxifen (TAM, 100 µM for 4 h) were used as positive controls. Error bars represent SEM. n = 3; * $p < 0.05$ ** $p < 0.01$ *** $p < 0.001$

Treatment of MCF-7 breast adenocarcinoma cells with the oestrone analogues (17 nM as required for combinations with QUER) alone did not affect the mitochondrial membrane potential after 24 h (Figure 3.17). However, after 48 h non-significant depolarisation was observed for treatment with ESE-15-ol (17 nM) and ESE-16 (17 nM). Significant depolarisation of the mitochondrial membrane was observed after exposure to QUER after 24 h (approximately 57% reduction) and 48 h (approximately 48% reduction). Exposure to combinations of oestrone analogues and QUER resulted in significant depolarisation of the mitochondrial membrane potential: after 24 h treatment reduction in the mitochondrial membrane potential exceeded 55%, whereas an approximate reduction of 47% was

observed after 48 h treatment. Similar resultswere observed for MCF-12A non-tumourigenic cells exposed to the combinations for both time points (Fig 3.17). Note that after 48 h exposure QUER (84 µM) reduced mitochondrial membrane potential to 37.4%, while the combinations of ESE-15-ol (17 nM) and QUER resulted in less extensive depolarisation at 37.6 and 38.2%, respectively.

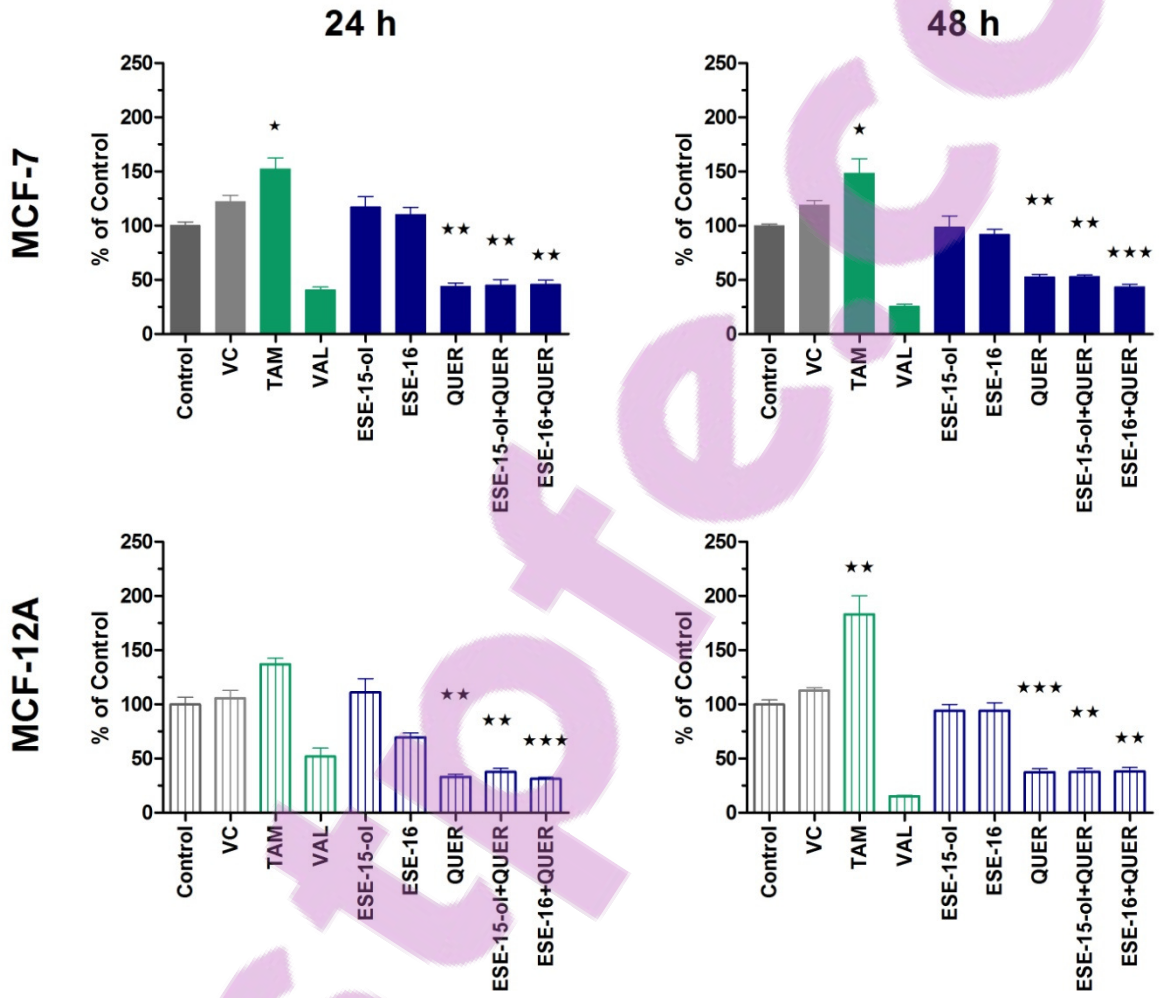

Figure 3.17: The effect of synergistic combinations of ESE-15-ol (17 nM) and ESE-16 (17 nM) with quercetin (QUER, 84 µM) on the mitochondrial membrane potential in **MCF-7** breast adenocarcinoma and **MCF-12A** non-tumourigenic cells after 24 or 48 h exposure using a JC-1 fluorometric protocol. VC indicates DMSO-treated cells. Valinomycin (VAL, 50 µM for 24 or 48 h) and tamoxifen (TAM, 100 µM for 4 h) were used as positive controls. Error bars represent SEM. Min n =3; * $p < 0.05$ ** $p < 0.01$ *** $p < 0.001$

Exposure of MDA-MB-231 breast adenocarcinoma and MCF-12A non-tumourigenic cells to tamoxifen resulted in a hyperpolarisation of the mitochondrial membrane while significant depolarisation of the mitochondrial membrane potential was observed in response to treatment with valinomycin indicating that the assay functioned correctly (Figure 3.18).

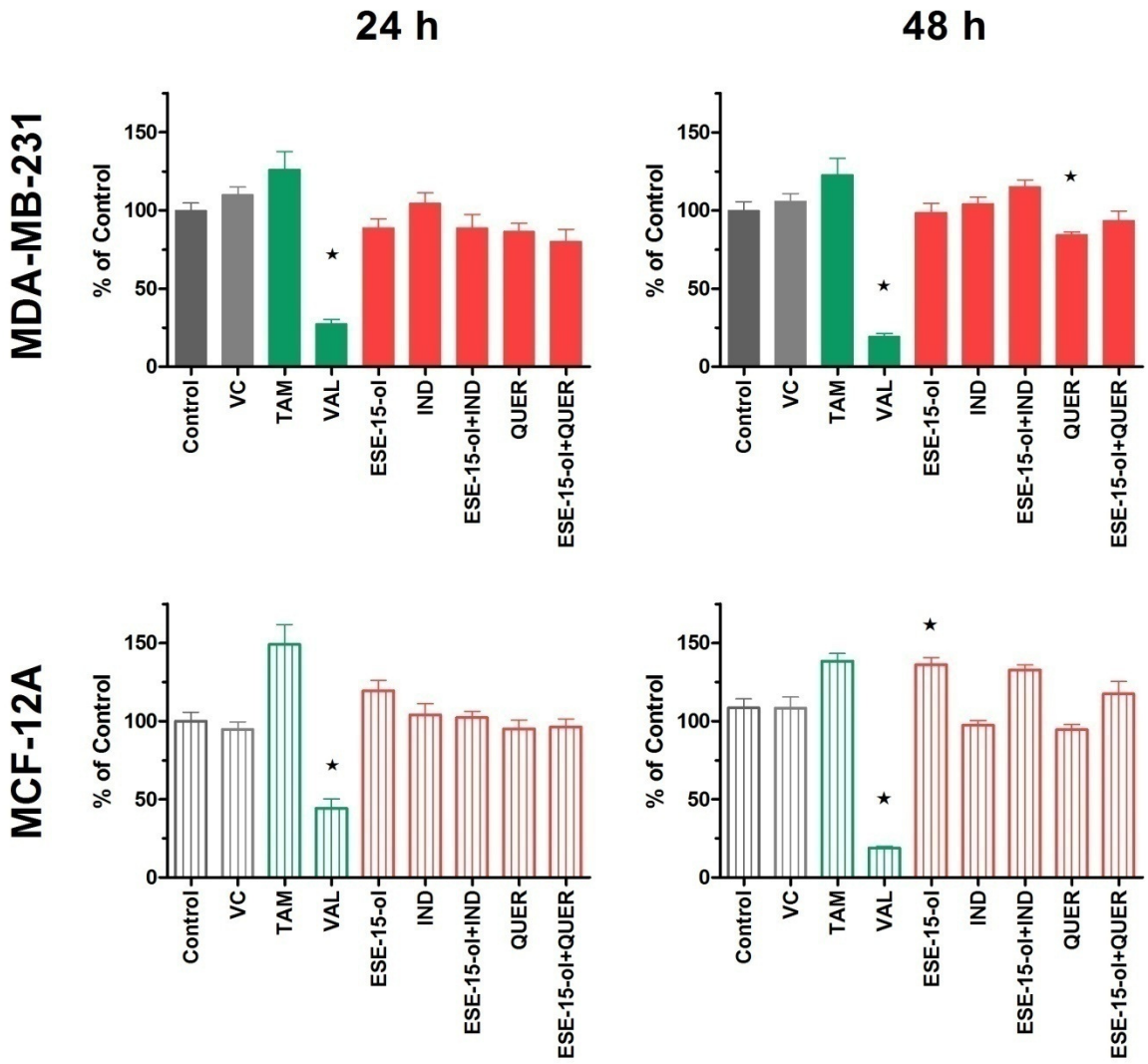

Figure 3.18: The effect of synergistic combinations of ESE-15-ol (123 nM) with indinavir (IND, 55 µM) and quercetin (QUER, 0.64 µM) on the mitochondrial membrane potential in **MDA-MB-231** breast adenocarcinoma and **MCF-12A** non-tumourigenic cells after 24 or 48 h exposure using a JC-1 fluorometric protocol. VC indicates DMSO-treated cells. Valinomycin (VAL, 50 µM for 24 or 48 h) and tamoxifen (TAM, 100 µM for 4 h) were used as positive controls. Error bars represent SEM.

Min n = 3; * $p < 0.05$ ** $p < 0.01$ *** $p < 0.001$

Non-significant depolarisation of the mitochondrial membrane observed in MDA-MB-231 breast adenocarcinoma cells exposed to combinations with IND or QUER after both time points resulted in a maximum of 20% reduction in the mitochondrial membrane potential (Figure 3.18). Depolarisation of mitochondrial membrane potential was greatest where cells were treated with the combination of ESE-15-ol and QUER for 24 h. Statistically significant depolarisation was observed where MDA-MB-231 cells were exposed to QUER (0.64 µM) for 48 h.

Non-significant hyperpolarisation of the mitochondrial membrane potential (approximately 20%) was observed in the MCF-12A non-tumourigenic cell line upon exposure to ESE-15-ol after 24 h. Statistically significant hyperpolarisation of the mitochondrial membrane potential was observed when MCF-12A cells were exposed to ESE-15-ol after 48 h. The combination of ESE-15-ol and IND caused non-significant hyperpolarisation in the MCF-12A cells after 48 h.

3.5.5 Caspase activity

The effect of treatment with the drug combinations on the activity of the initiator caspases, caspase 8 and -9, as well as the executioner caspases 3/7 was investigated with fluorometric substrates.

Caspase 8 activity was successfully induced with Fas ligand as a statistically signficant1.5-fold increase was observed in the MCF-7 breast adenocarcinoma cell line (Figure 3.19).A slight increase in caspase 8 activity was detected in MCF-12A non-tumourigenic cells, indicating that increases in caspase activity could be detected with this assay (Figure 3.19). Statistically significant increases in the activity of caspases 3/7 and -9 were induced by staurosporine treatment in both cell lines, implying that elevated caspase activity could be detected with these assays.

The activity of caspase 8 was increased by approximately 30% when MCF-7 cells were treated with ESE-15-ol (70 nM) for 24 h (Figure 3.19). Treatment with the drug combinations resulted in elevation in caspase 8 activity in the MCF-7 cell line. No marked change in caspase 8 activity was observed in the MCF-12A non-tumourigenic cell line after 24 h exposure to the drug combinations. No statistically significant changes in caspase-8 activity were observed after 24 h treatment with the combinations in MCF-7 breast adenocarcinoma or MCF-12A non-tumourigenic cells.

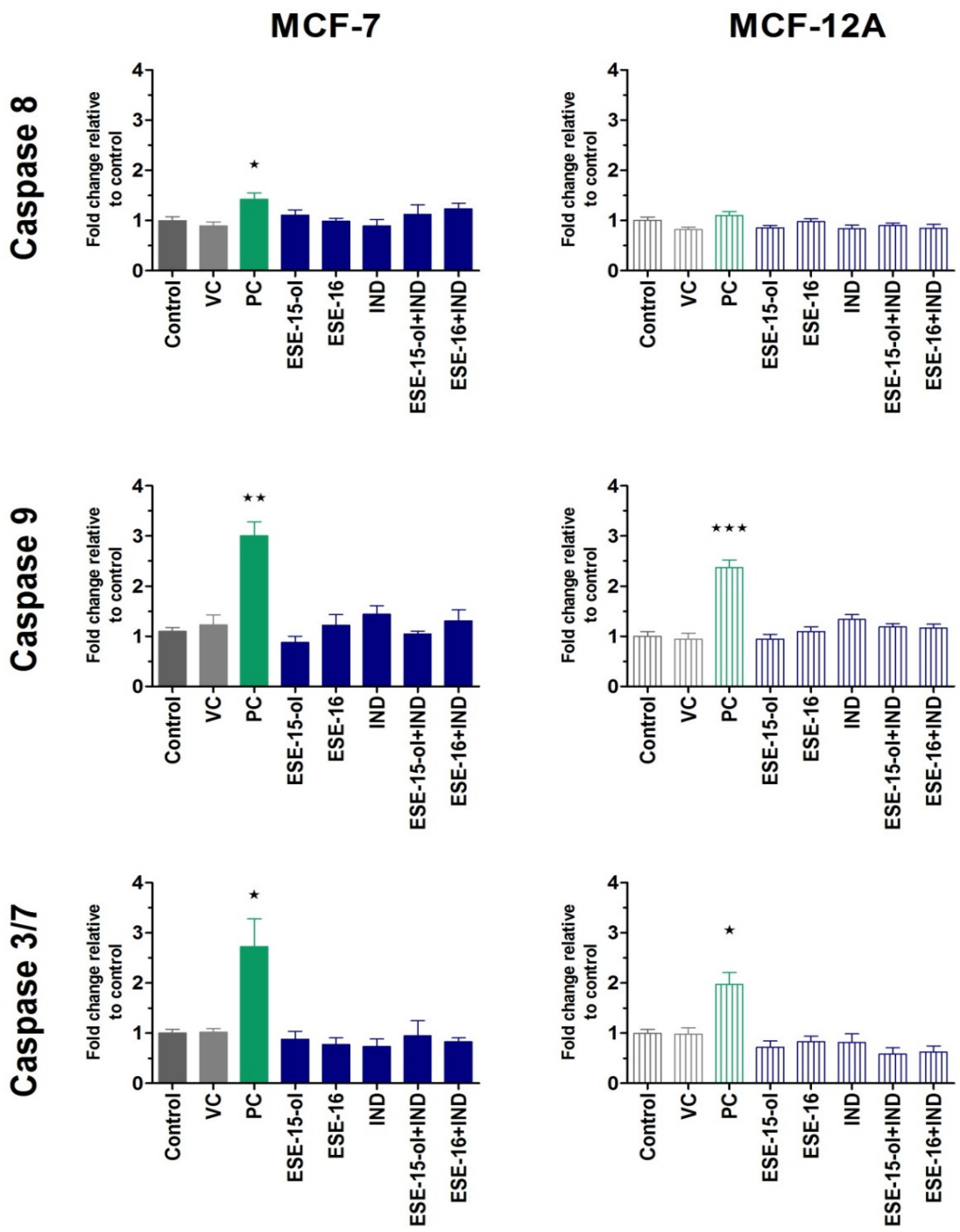

Figure 3.19: The effect of synergistic combinations of ESE-15-ol (70 nM) or ESE-16 (67 nM) with indinavir (IND, 115 µM) on the activity of caspases 8, -9 and -3/7 in **MCF-7** breast adenocarcinoma and **MCF-12A** non-tumourigenic cells after 24 h exposure using fluorometric, caspase-specific substrates. Fas ligand (100 ng/ml for 4 h) was used as positive control for caspase 8, while staurosporine (10 µM for 4 h) was used as positive control for caspase 3/7 and -9. VC indicates DMSO-treated cells. Error bars represent SEM.

Min n = 3;* $p < 0.05$ ** $p < 0.01$ *** $p < 0.001$

Exposure to IND (115 µM) elevated the activity of caspase 9 after 24 h in both cell lines tested (Figure 3.19). Increased caspase 9 activity (approximately 1.2-fold) was observed following exposure to the combination of ESE-16 and IND in the MCF-7 cell line. However in the MCF-12A non-tumourigenic cell line activity of caspase 9 was enhanced after treatment with combinations with ESE-15-ol or ESE-16 and IND after 24 h. The fluctuations in caspase 9 activity induced by treatment with the combinations for 24 h were not statistically significant in either of the cell lines.

A slight reduction in the activity of caspase 3/7 was observed where MCF-7 cells were treated with IND for 24 h (Figure 3.19). Treatment with combinations of oestrone analogues and IND resulted in a decrease in the activity of caspase 3/7 in MCF-7 breast adenocarcinoma cells. However, reduced activity of caspase 3/7 activity was observed in the MCF-12A non-tumourigenic cell line exposed to combinations with IND after 24h. However, no statistically significant effect on the activity of caspase 3/7 was observed.

Where MCF-7 breast adenocarcinoma or MCF-12A non-tumourigeniccells were exposed to Fas ligandan approximate 1.1-fold increase in the activity of caspase 8 was observed (Figure 3.20). Statistically significant increases in the activity of caspases 3/7 and -9 were induced by staurosporine treatment in both cell lines. This implies that elevated caspase activity can be detected with these assays.

When MCF-7 breast adenocarcinoma cells were treated with ESE-15-ol (70 nM) and the combination of ESE-15-ol and IND for 48 h, caspase 8 activity was decreased (Figure 3.20). Treatment with the combination of ESE-16 and IND resulted in approximately 20% reduction in caspase 8 activity in the MCF-7 breast adenocarcinoma cell line. Statistically significant suppression of caspase 8 activity was observed in the MCF-12A non-tumourigenic cell line in all treatment groups except where cells were exposed to IND only.

The activity of caspases 9 and -3/7 was reduced after 48 h treatment with the synergistic drug combinations with IND in both MCF-7 and MCF-12A cell lines after all treatments except for treatment with IND only (Figure 3.20). The greatest attenuation of caspase 9 activity was observed where MCF-7 breast adenocarcinoma cells were treated with the combination of ESE-15-ol and IND for 48 h. A non-significant elevation in caspase 3/7 activity was seen where MCF-12A non-tumourigenic cells were exposed to the combination of ESE-16 and IND.

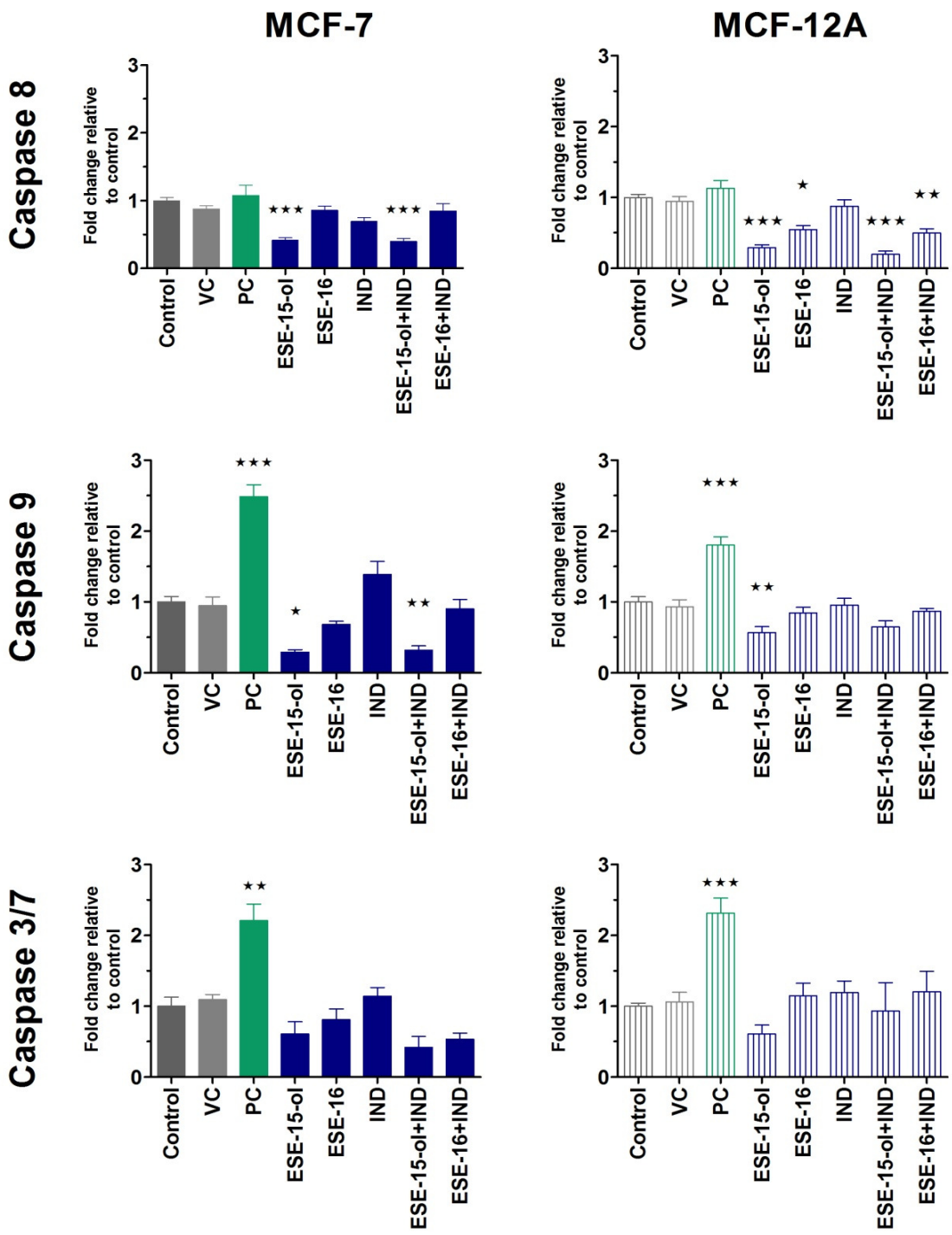

Figure 3.20: The effect of synergistic combinations of ESE-15-ol (70 nM) or ESE-16 (67 nM) with indinavir (IND, 115 µM) on the activity of caspases 8, -9 and -3/7 in **MCF-7** breast adenocarcinoma and **MCF-12A** non-tumourigenic cells after 48 h exposure using fluorometric, caspase-specific substrates. Fas ligand (100 ng/ml for 4 h) was used as positive control for caspase 8, while staurosporine (10 µM for 4 h) was used as positive control for caspase 3/7 and -9. VC indicates DMSO-treated cells. Error bars represent SEM.

Min n = 3;* $p < 0.05$ ** $p < 0.01$ *** $p < 0.001$

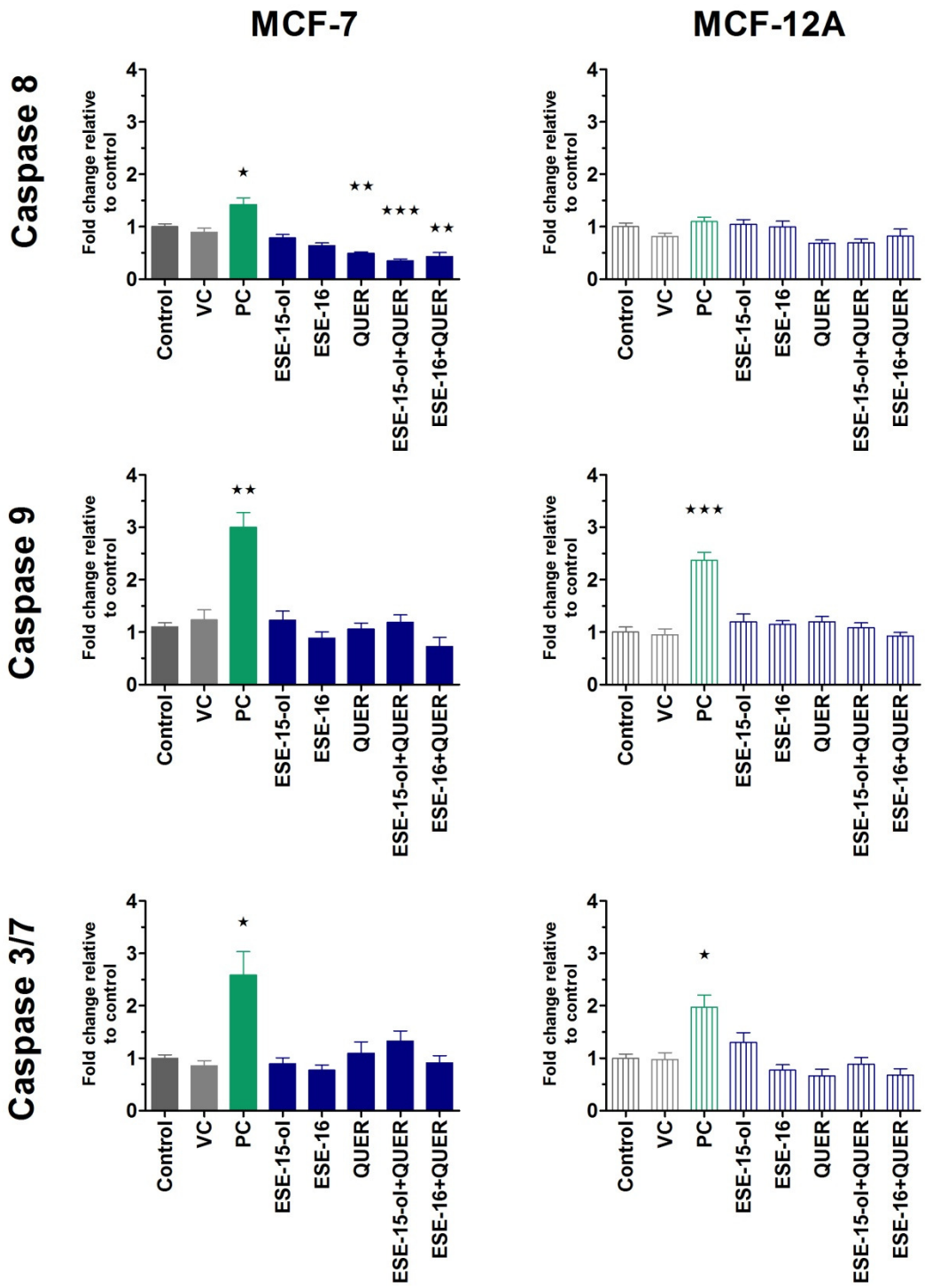

Figure 3.21: The effect of synergistic combinations of ESE-15-ol (17 nM) or ESE-16 (17 nM) with quercetin (QUER, 84 µM) on the activity of caspases 8, -9 and -3/7 in **MCF-7** breast adenocarcinoma and **MCF-12A** non-tumourigenic cells after 24 h exposure using fluorometric, caspase-specific substrates. Fas ligand (100 ng/ml for 4 h) was used as positive control for caspase 8, while staurosporine (10 µM for 4 h) was used as positive control for caspase 3/7 and -9.VC indicates DMSO-treated cells. Error bars represent SEM.

Min n = 3;* $p < 0.05$ ** $p < 0.01$ *** $p < 0.001$

The activity of caspase 8 was attenuated by treatment with QUER (84 µM), ESE-15-ol (17 nM), ESE-16 (17 nM) or combinations thereof in the MCF-7 breast adenocarcinoma cell line after 24 h treatment (Figure 3.21). When MCF-7 breast adenocarcinoma cells were exposed to QUER or combinations of QUER and oestrone analogues statistically significant reductions in the activity of caspase 8 were observed. In the MCF-12A non-tumourigenic cell line caspase 8 activity was reduced where cells were treated with QUER or combinations with QUER for 24h.

When MCF-7 breast adenocarcinoma cells were treated with ESE-16 or the combination of ESE-16 and QUER for 24 h a reduction in caspase 9 activity was observed (Figure 3.21). This was not seen where cells were treated with ESE-15-ol or its combination with QUER. A slight but statistically non-significant elevation in caspase 9 activity was noted where MCF-12A non-tumourigenic cells were exposed to ESE-15-ol, ESE-16 and QUER. However, the effect on the activity of caspase 9 resulting from exposure to the oestrone analogues, QUER or the combinations did was not statistically significant.

Elevated caspase 3/7 activity was observed where MCF-7 breast adenocarcinoma cells were treated with the combinations of ESE-15-ol and QUER (approximately 1.5-fold) and ESE-16 and QUER for 24 h (Figure 3.21). A similar trend was not observed in the MCF-12A cell line. Where MCF-12A cells were exposed to ESE-15-ol (17 nM) a 1.5-fold elevation in the activity of caspase 3/7 was observed. The elevation in caspase 3 activity observed was not statistically significant.

Statistically significant reduction of caspase 8 activity was observed in MCF-7 breast adenocarcinoma and MCF-12A non-tumourigenic cells after 48 h treatment with QUER or combinations with QUER (Figure 3.22). A similar yet less pronounced trend was noted in the activity of caspases 9 and -3/7. The activity of caspase 3/7 was slightly increased after treatment with ESE-16 (17 nM) for 48 h in the MCF-7 cell line.

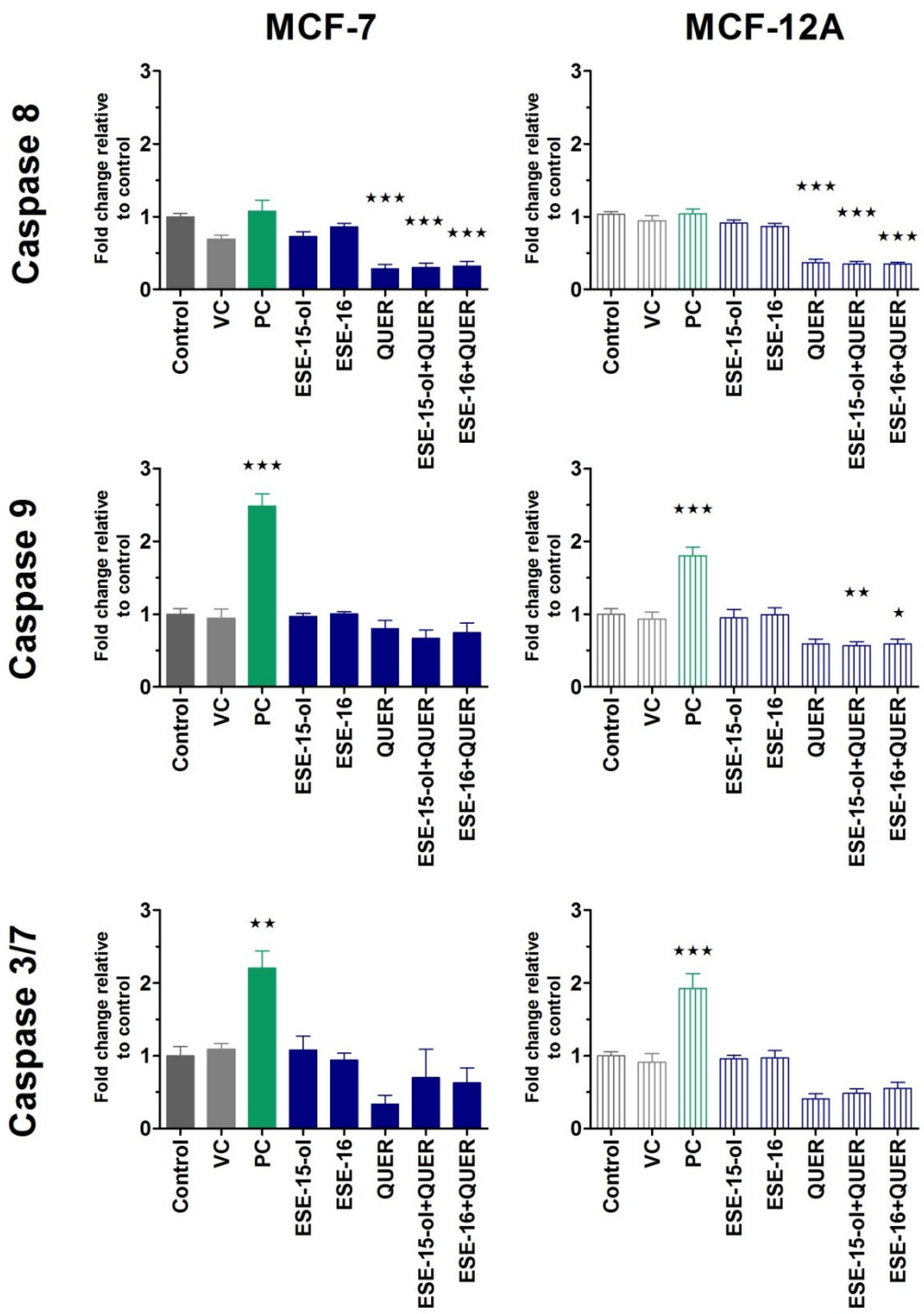

Figure 3.22: The effect of synergistic combinations of ESE-15-ol (17 nM) or ESE-16 (17 nM) with quercetin (QUER, 84 µM) on the activity of caspases 8, -9 and -3/7 in **MCF-7** breast adenocarcinoma and **MCF-12A** non-tumourigenic cells after 48 h exposure using fluorometric, caspase-specific substrates. Fas ligand (100 ng/ml for 4 h) was used as positive control for caspase 8, while staurosporine (10 µM for 4 h) was used as positive control for caspase 3/7 and -9.VC indicates DMSO-treated cells. Error bars represent SEM.

Min n = 3;* $p < 0.05$ ** $p < 0.01$ *** $p < 0.001$

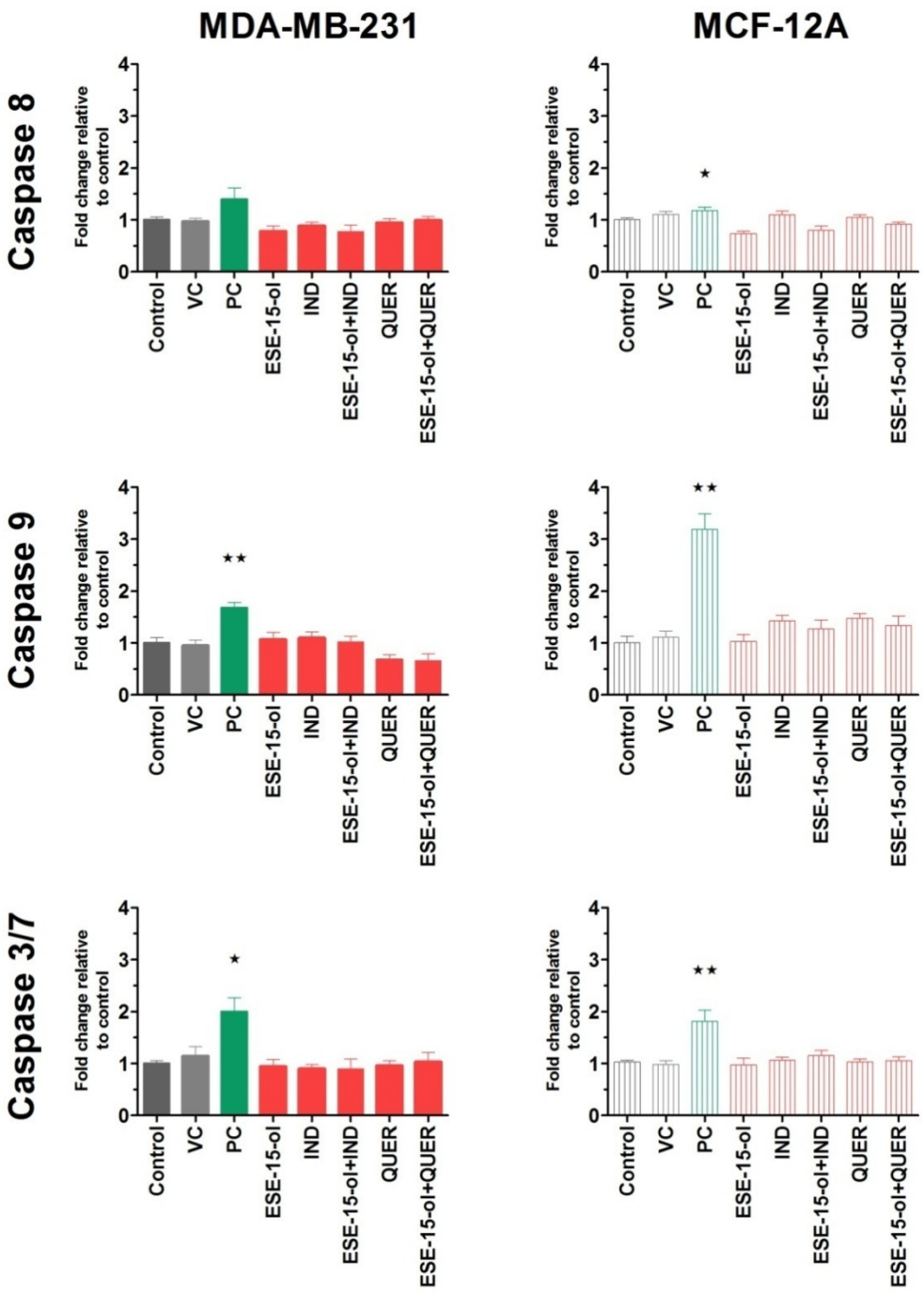

Figure 3.23: The effect of synergistic combinations of the oestrone analogue ESE-15-ol (123 nM) with indinavir (IND, 55 µM) and quercetin (QUER, 0.64 µM) on the activity of caspases 8, -9 and -3/7 in **MDA-MB-231** breast adenocarcinoma and **MCF-12A** non-tumourigenic cells after 24 h exposure using fluorometric, caspase-specific substrates. VC indicates DMSO-treated cells. Fas ligand (100 ng/ml for 4h) was used as positive control for caspase 8, while staurosporine (10 µM for 4h) was used as positive control for caspase 3/7 and -9. VC indicates DMSO-treated cells. Error bars represent SEM.

Min n = 3;* $p < 0.05$ ** $p < 0.01$ *** $p < 0.001$

A 1.5-fold increase in caspase 8 activity was observed in the MDA-MB-231 breast adenocarcinoma cell line and a statistically significant elevation in the activity of caspase 8 was observed in the non-tumourigenic MCF-12A cell line (Figure 3.23) implying that an increase in caspase 8 activity could be detected with this assay. The activity of caspases 3/7 and -9 were significantly elevated by staurosporine treatment in both cell lines, indicating that elevated activity of caspases 3/7 and -9 could be detected with these assays.

The activity of caspase 8 was reduced by approximately 20% by treatment with ESE-15-ol (123 nM) and combinations of ESE-15-ol and IND for 24 h in the MDA-MB-231 breast adenocarcinoma and MCF-12A non-tumourigenic cells (Figure 3.23). The activity of caspase 8 was essentially unaffected in both cell lines after treatment with the combination of ESE-15-ol and QUER for 24 h. No statistically significant elevations in caspase 8 activity were observed in MDA-MB-231 or MCF-12A cells.

A slight increase in the activity of caspase 9 was observed where MDA-MB-231 cells were treated with ESE-15-ol, IND or the combination of ESE-15-ol and IND for 24 h (Figure 3.23). This effect was more pronounced in the MCF-12A non-tumourigenic cell line. Suppression of caspase 9 activity was seen in the MDA-MB-231 cell line after treatment with QUER (0.64 μM) and the combination of ESE-15-ol and QUER. In contrast elevated caspase 9 activitywas demonstrated in the MCF-12A cell line after treatment with QUER or the combination of ESE-15-ol and QUER for 24 h. However, the effects on the activity of caspase 9 induced by exposure to the oestrone analogues, glycolysis inhibitors or selected synergistic combinations after 24 h were not statistically significant in the MDA-MB-231 breast adenocarcinoma or MCF-12A non-tumourigenic cell lines.

Treatment of MDA-MB-231 breast adenocarcinoma cells with the combination of ESE-15-ol and IND for 24h resulted in a slight increase in the activity of caspase 3/7. The combination of ESE-15-ol and QUER did not greatly affect caspase 3/7 activity. A similar trend in the activity of caspase 3/7 was observed in the MCF-12A non-tumourigenic cells. The activity of caspase 3/7 was not affected significantly by exposure to the oestrone analogues, glycolysis inhibitors or synergistic combinations after 24 h.

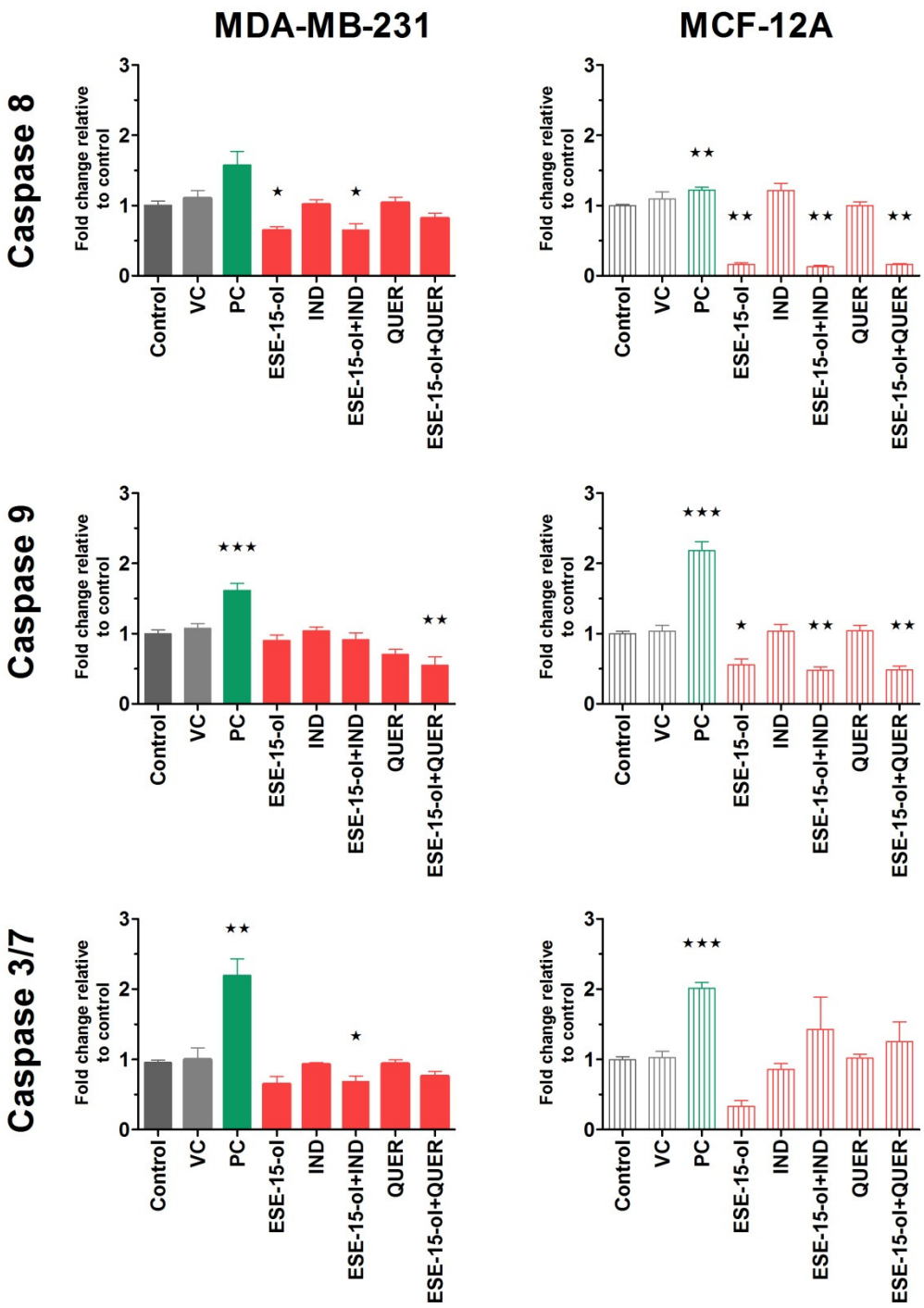

Figure 3.24: The effect of synergistic combinations of the oestrone analogue ESE-15-ol (123 nM) with indinavir (IND, 55 µM) and quercetin (QUER, 0.64 µM) on the activity of caspases 8, -9 and -3/7 in **MDA-MB-231** breast adenocarcinoma and **MCF-12A** non-tumourigenic cells after 48 h exposure using fluorometric, caspase-specific substrates. Fas ligand (100 ng/ml for 4 h) was used as positive control for caspase 8, while staurosporine (10 µM for 4h) was used as positive control for caspase 3/7 and -9. VC indicates DMSO-treated cells. Error bars represent SEM.
Min n = 3;* $p < 0.05$ ** $p < 0.01$ *** $p < 0.001$

A 1.6-fold elevation in caspase 8 activity was observed were MDA-MB-231 breast adenocarcinoma cells were exposed to fas ligand (Figure 3.24). A statistically significant increase in caspase 8 activity was observed where MCF-12A non-tumourigenic cells were exposed to fas ligand. This implies that increases in caspase activity could be detected. Treatment with staurosporine induced statistically significant elevation of the activity of caspases 3/7 and -9 in both cell lines, implying that increased caspase activity could be detected with these assays.

The activity of caspase 8 was reduced where MDA-MB-231 breast adenocarcinoma cells were exposed to ESE-15-ol or combinations with ESE-15-ol and IND or QUER for 48 h (Figure 3.24). In the MCF-12A non-tumourigenic cell line the suppression of caspase 8 activity was statistically significant where ESE-15-ol or combinations with ESE-15-ol was used. Treatment of MCF-12A cells with IND (55 µM) for 48 h resulted in a 1.2-fold elevation in caspase 8 activity.

A similar trend was observed in the activity of caspases 9 and -3/7 in the MDA-MB-231 cells after 48 h treatment with ESE-15-ol or combinations with ESE-15-ol (Figure 3.24). Activity of caspase 9 was significantly reduced where MDA-MB-231 cells were treated with the combination of ESE-15-ol and QUER. In the MCF-12A cell line the activity of caspase 3/7 was increased with at least1.2-fold by treatment with combinations of ESE-15-ol and IND or QUER for 48 h.

3.5.6 Morphology studies: Phase contrast microscopy and PlasDIC

The effect of treatment with the combinations on the cell morphology was assessed using phase contrast microscopy and plasDIC.

Phase contrast microscopy assessment of MCF-7 breast adenocarcinoma cells revealed that 72 h exposure to the combinations with IND resulted in reduced cell density (Figure 3.25). This was most notable where cells were treated with oestrone analogues or combinations of the oestrone analogues and glycolysis inhibitors. Cell rounding was observed especially in MCF-7 cells treated with the drug combinations. IND-treated samples showed a marked reduction in cell number. PlasDIC studies revealed the presence of structures resembling vacuoles in MCF-7 cells treated with ESE-15-ol and IND.

Phase contrast studies of MCF-12A non-tumourigenic cells after 72 h demonstrated reduced cell density where cells were treated with the oestrone analogues or drug combinations with IND (Figure 3.26). IND (115 µM) did not have such a marked effect on cell density.

Treatment with the oestrone analogues or combinations resulted in rounding of cells and the formation of possible vesicles in MCF-12A cells as observed with plasDIC. Cell debris was also observed in treated MCF-12A cells.

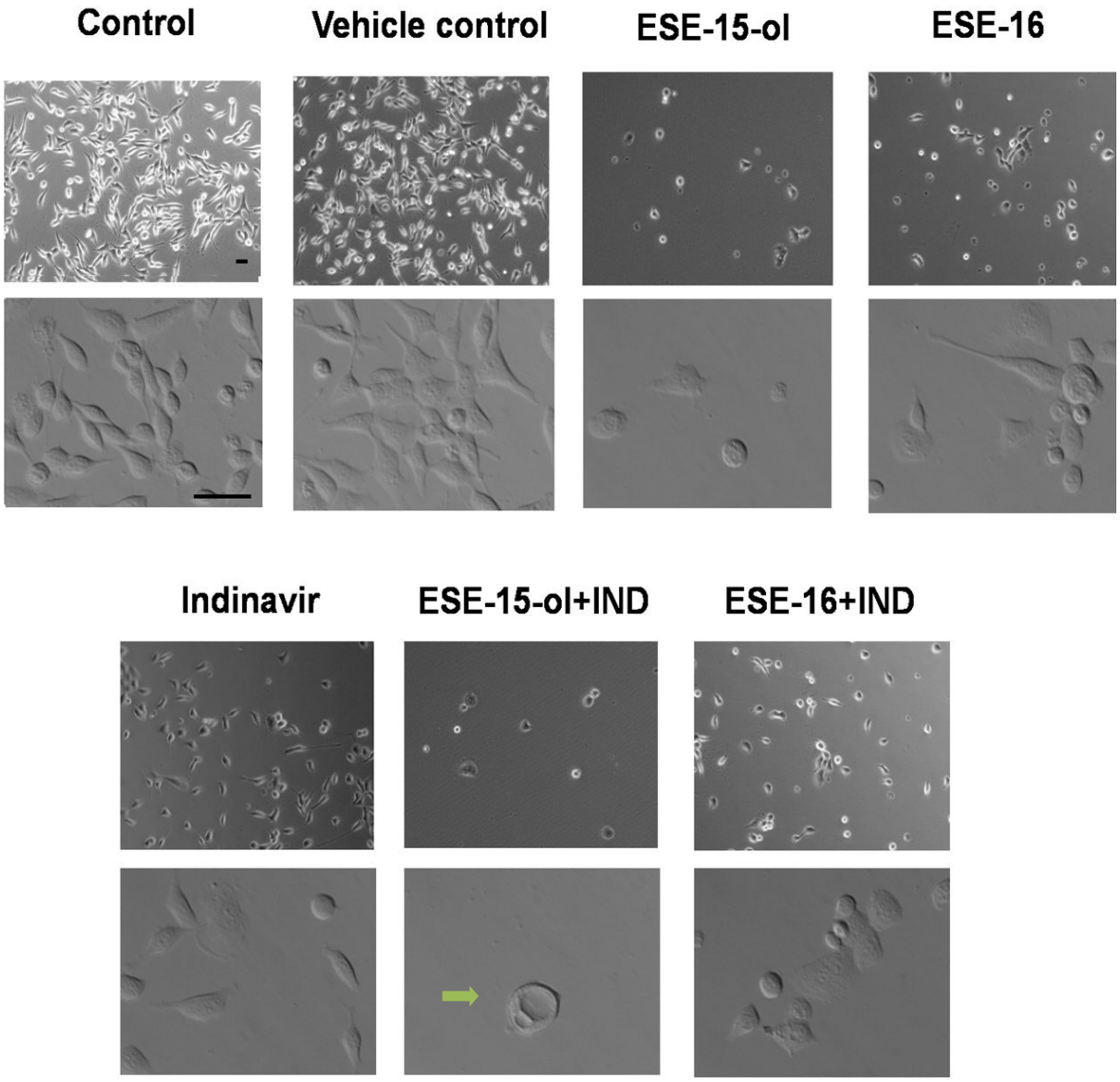

Figure 3.25: The effect of synergistic combinations of the oestrone analogues, ESE-15-ol (70 nM) and ESE-16 (67 nM) with indinavir (IND, 115 µM) on the morphology of **MCF-7** breast adenocarcinoma cells after 72 h incubation. Phase contrast microscopy images are shown in the upper panel and plasDIC images are shown in the lower panel for each sample. Vacuole-like structures are indicated by green arrows. Scale bars in control images indicate 20 µm.

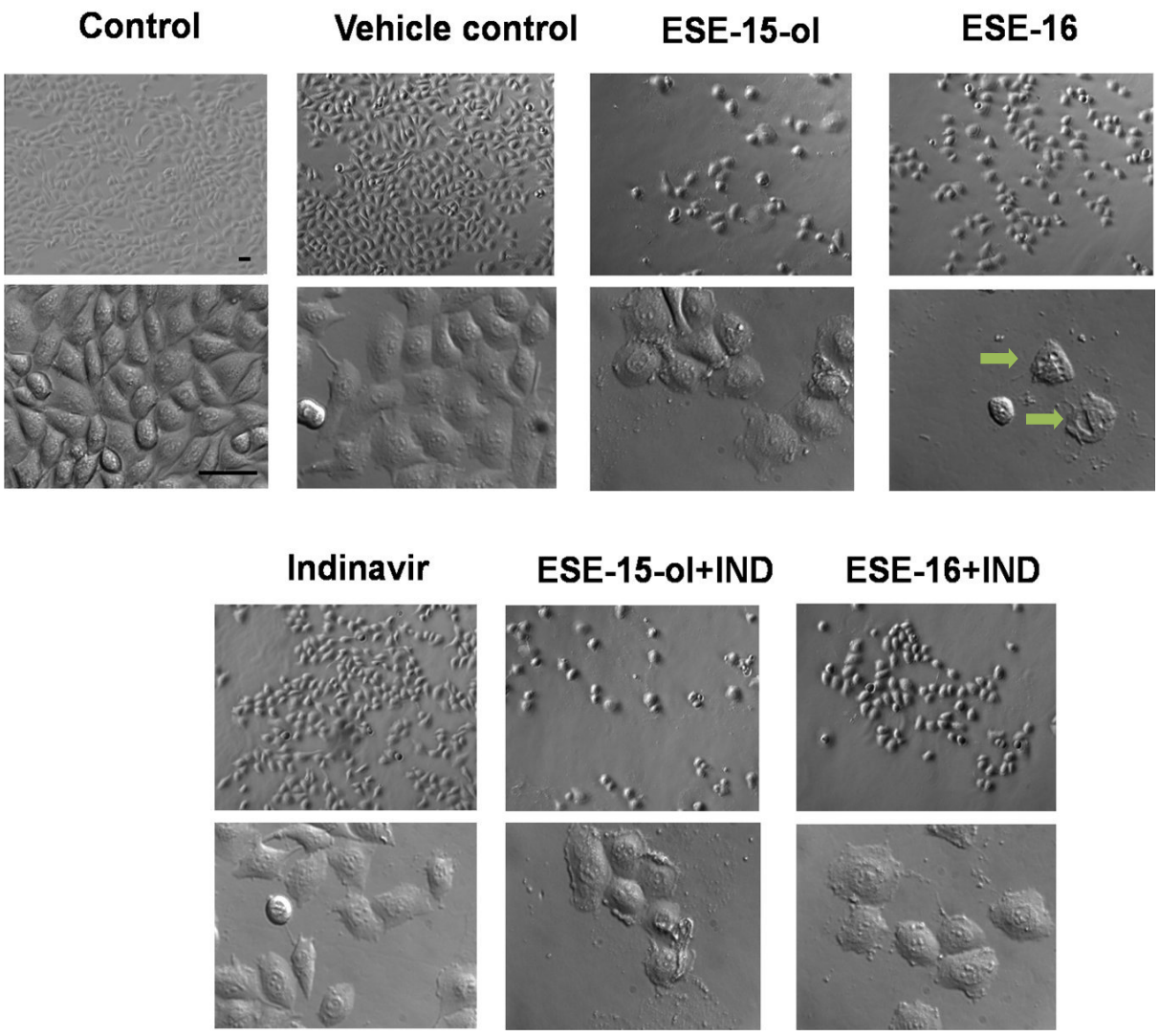

Figure 3.26: The effect of synergistic combinations of the oestrone analogues, ESE-15-ol (70 nM) and ESE-16 (67 nM) with indinavir (IND, 115 µM) on the morphology of **MCF-12A** non-tumourigenic cells after 72 h incubation. Phase contrast microscopy images are shown in the upper panel and plasDIC images are shown in the lower panel for each sample. Vacuole-like structures are indicated by green arrows. Scale bars in control images indicate 20 µm.

Morphology of MCF-7 breast adenocarcinoma cells treated with combinations with QUER (84 µM) (Figure 3.27) revealed decreased cell density, formation of vacuole-like structures and rounding of cells. The greatest reduction in cell number was observed where cells were treated with QUER. The rounding of cells was most prominent where MCF-7 cells were treated with combinations of oestrone analogues and QUER.

Photomicrographs of MCF-12A non-tumourigenic cells exposed to combinations of oestrone analogues and QUER (Figure 3.28) revealed a reduction in cell density. This was most evident where cells were treated with QUER (84 µM) and the combination of ESE-16 (17

nM) and QUER. The formation of vacuole-like structures was observed in cells exposed to QUER or the combinations of oestrone analogues and QUER.

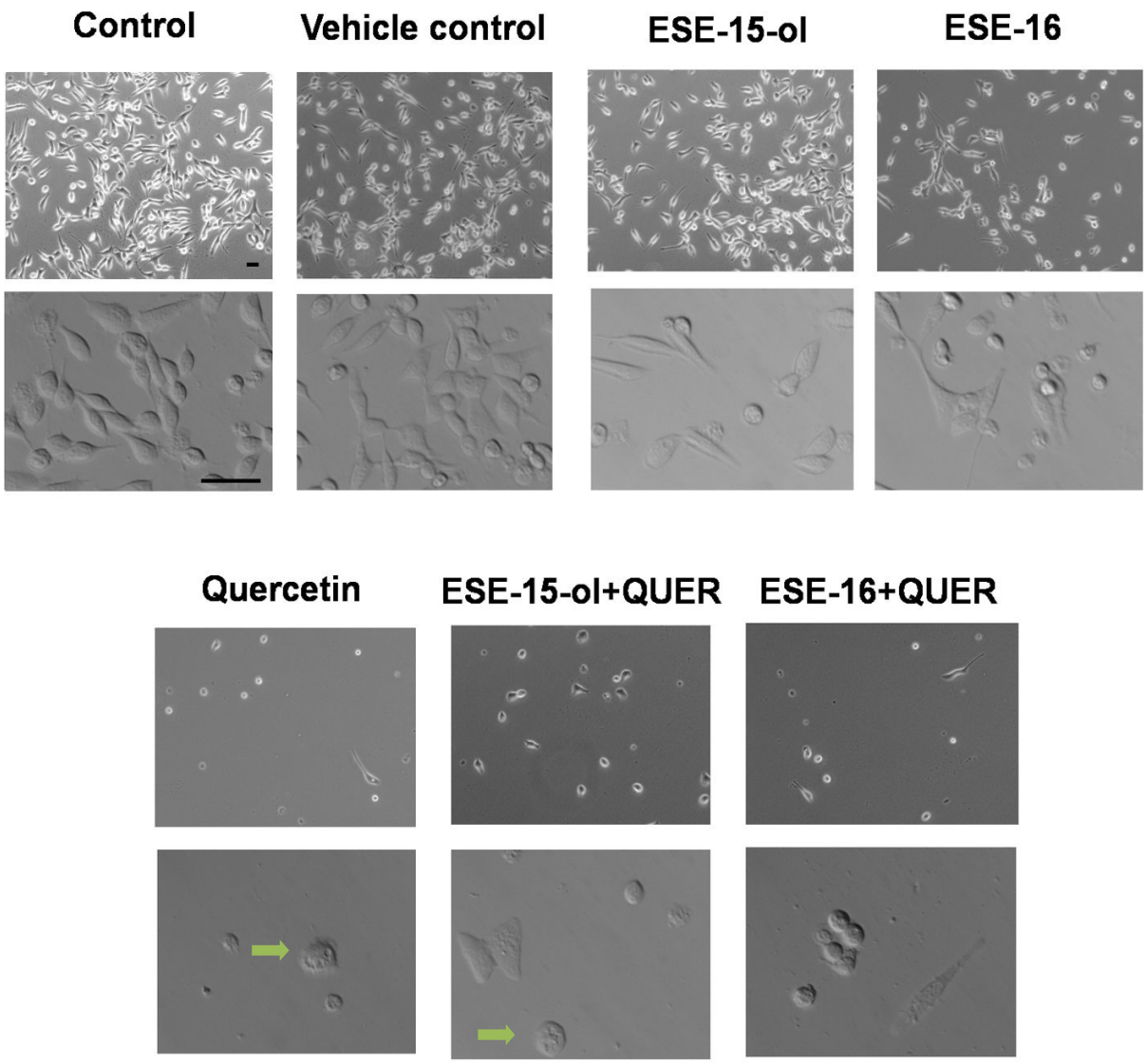

Figure 3.27: The effect of synergistic combinations of the oestrone analogues, ESE-15-ol (17 nM) and ESE-16 (17 nM), with quercetin (QUER, 84 µM) on the morphology of **MCF-7** breast adenocarcinoma cells after 72 h incubation. Phase contrast microscopy images are shown in the upper panel and plasDIC images are shown in the lower panel for each sample. Vacuole-like structures are indicated by green arrows. Scale bars in control images indicate 20 µm.

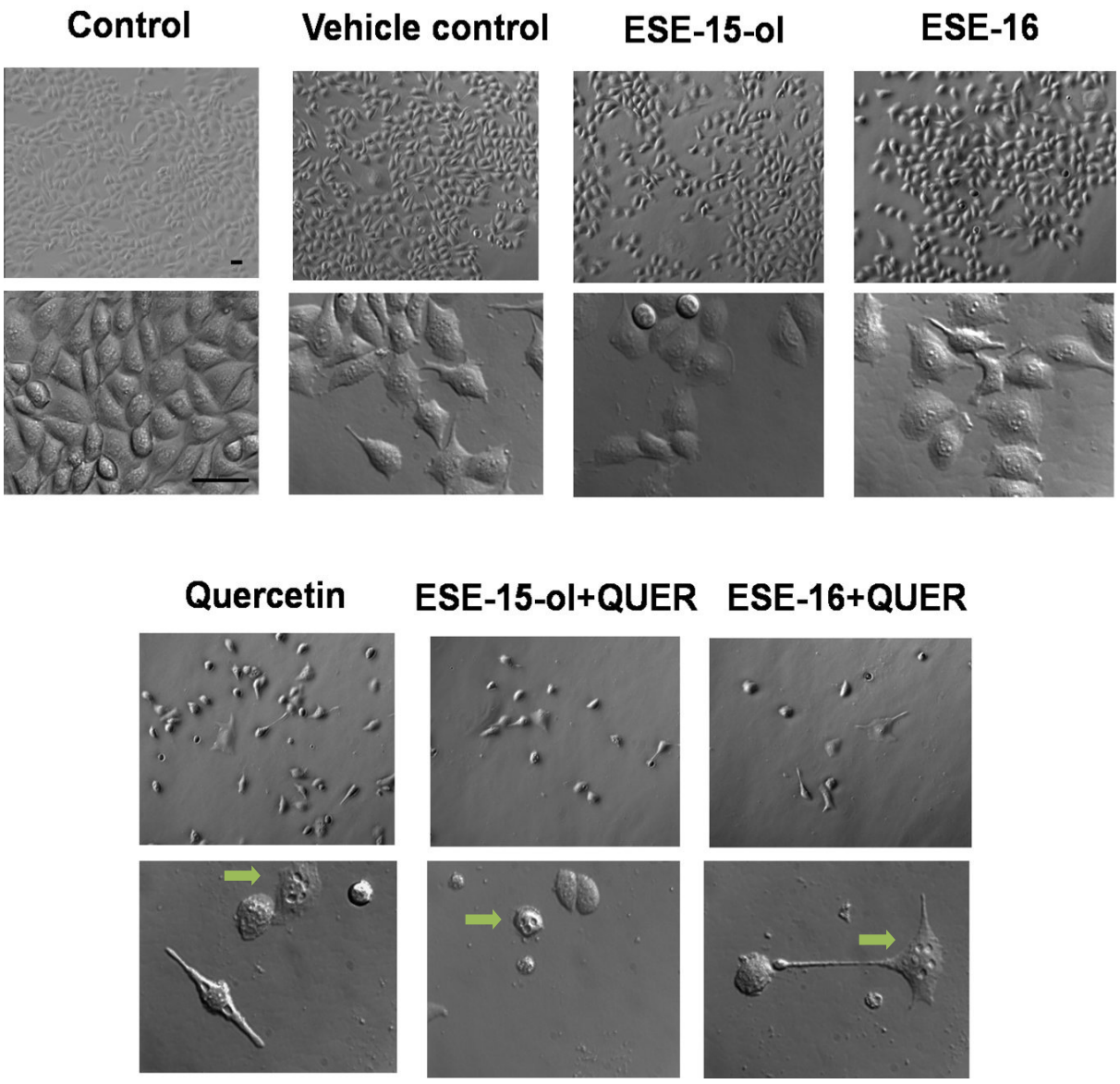

Figure 3.28: The effect of synergistic combinations of the oestrone analogues, ESE-15-ol (17 nM) and ESE-16 (17 nM), with quercetin (QUER, 84 µM) on the morphology of **MCF-12A** non-tumourigenic cells after 72 h incubation. Phase contrast microscopy images are shown in the upper panel and plasDIC images are shown in the lower panel for each sample. Vacuole-like structures are indicated by green arrows. Scale bars in control images indicate 20 µm.

Reduced cell density was observed in light microscopy images of MDA-MB-231 breast adenocarcinoma cells treated with the combinations of ESE-15-ol (123 nM) and glycolysis inhibitors for 72 h (Figure 3.29). The reduction in cell number was greatest where cells were exposed to the combinations. Treatment with QUER at 0.64 nM for 72 h resulted in a

marked decrease in cell density. The formation of possible vacuoles was observed using plasDIC in MDA-MB-231 cells treated with IND and the combination of ESE-15-ol and IND.

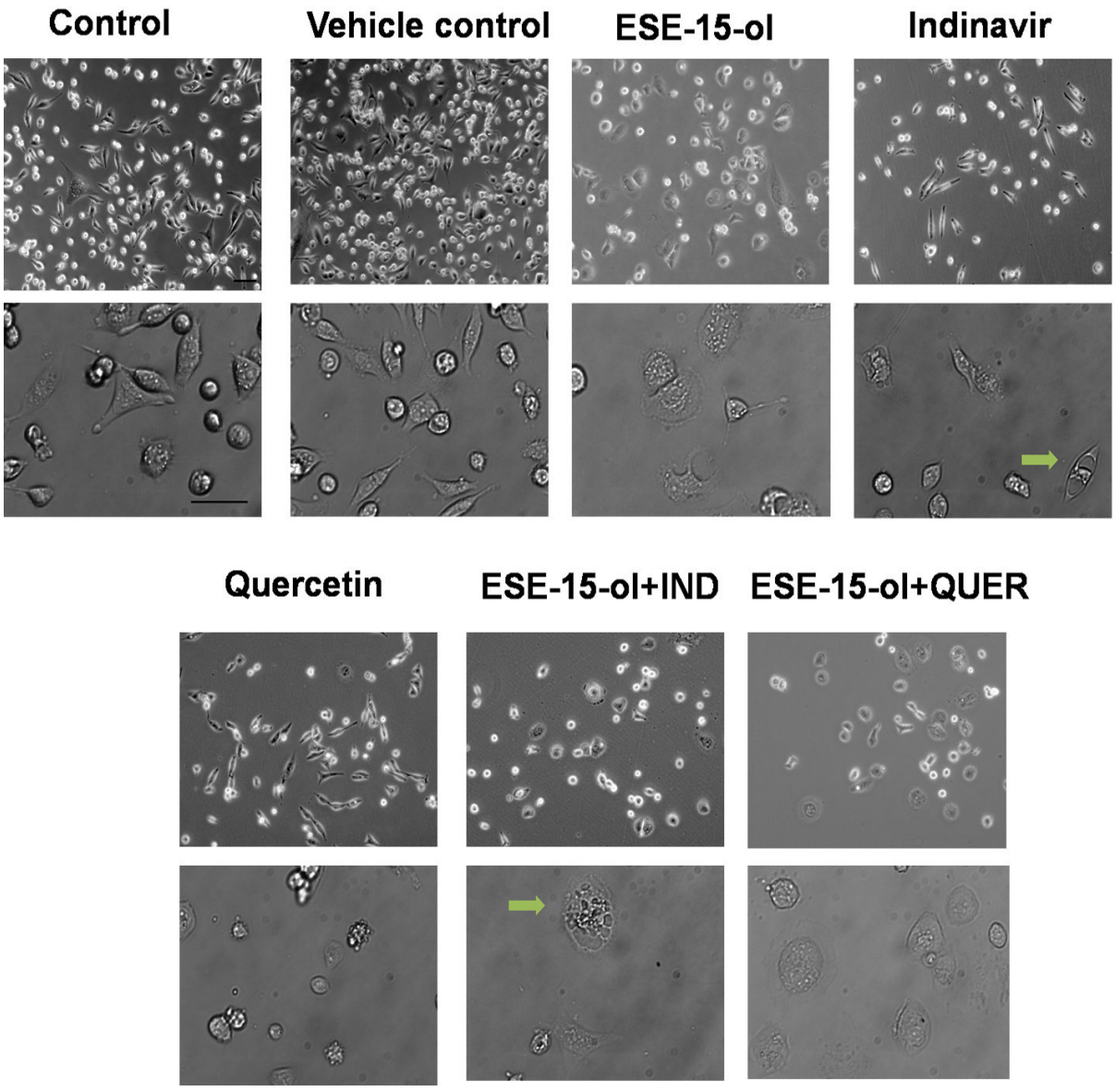

Figure 3.29: The effect of synergistic combinations of the oestrone analogue ESE-15-ol (123 nM) with indinavir (IND, 55 µM) and quercetin (QUER, 0.64 µM) on the morphology of **MDA-MB-231** breast adenocarcinoma cells after 72 h incubation. Phase contrast microscopy images are shown in the upper panel and plasDIC images are shown in the lower panel for each comparison. Vacuole-like stractures are indicated by green arrows. Scale bars in control images indicate 20 µm.

Morphological studies using phase contrast microscopy of the MCF-12A non-tumourigenic cells also showed reduced cell density (Figure 3.30). Where MCF-12A cells were exposed to ESE-15-ol (123 nM) a marked decrease in cell number was observed. Rounding of cells and cell debris was observed in plasDIC images.

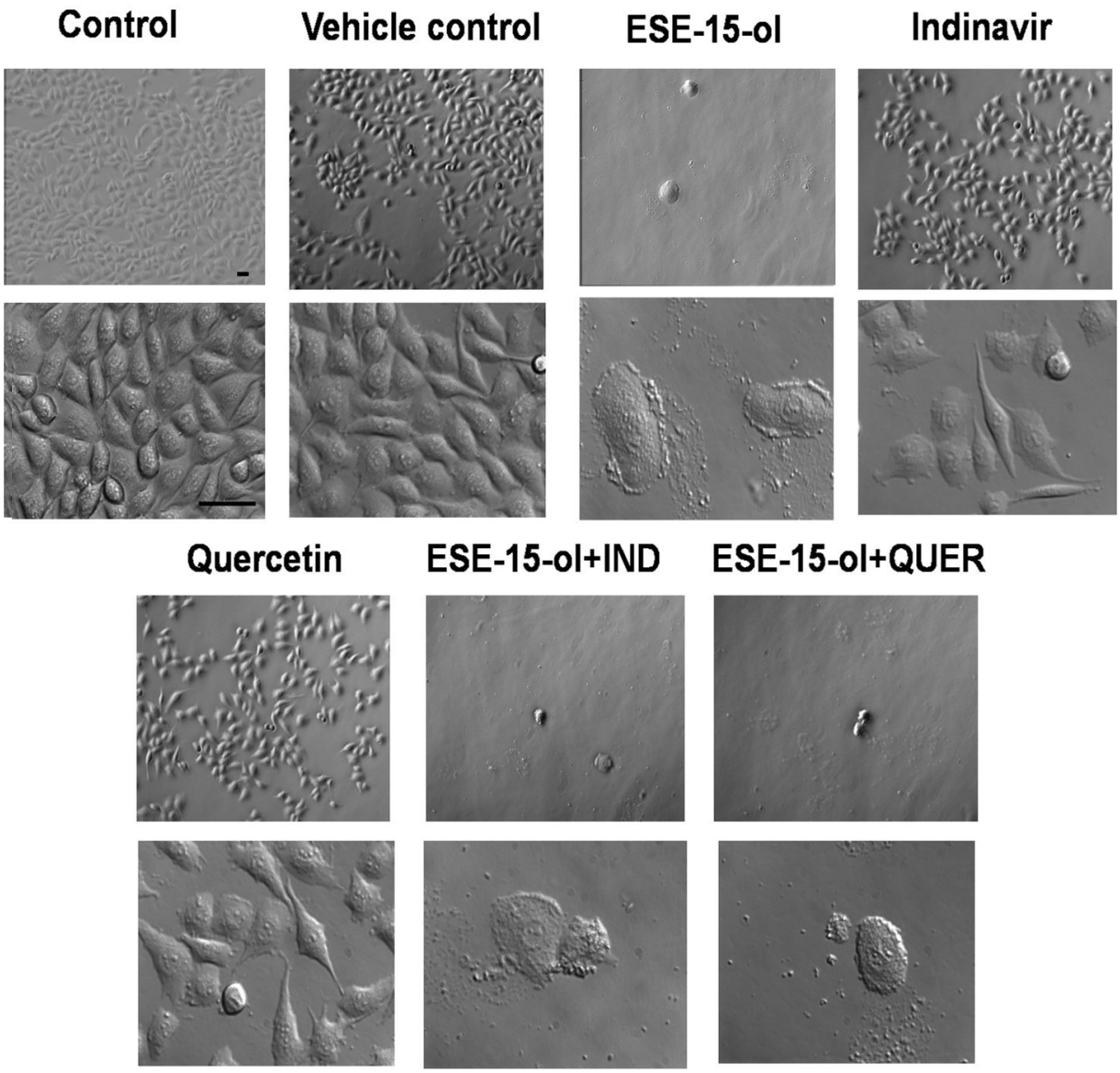

Figure 3.30: The effect of synergistic combinations of the oestrone analogue ESE-15-ol (123 nM) with indinavir (IND, 55 μM) and quercetin (QUER, 0.64 μM) on the morphology of **MCF-12A** non-tumourigenic cells after 72 h incubation. Phase contrast microscopy images are shown in the upper panel and plasDIC images are shown in the lower panel for each sample. Scale bars in control images indicate 20 μm.

3.5.7 Annexin V

The flow cytometric method proved to be an effective technique to assess mode of cell death though the comparison of the annexin V binding verses the propidium bromide uptake with clear differences observed for the control treated cells. Despite the possibility of mixed mode cell death and the potential changes in measured outcome dependant on the incubation time for the drug exposure, clear differences could be discerned. Figure 3.31 shows scatter plots for the various control and drug treated MCF-7 cell line.

Increased necrotic cell death upon treatment with ethanol and elevated apoptosis in staurosporine-treated MCF-7 breast adenocarcinoma cells indicate that the assay could detect both apoptotic and necrotic cell death (Figures 3.31 and 3.33). Following exposure to the oestrone analogues or indinavir, elevated apoptosis and necrosis was observed (Figure 3.31). This was exacerbated after treatment with combinations of oestrone analogues and IND (Table 3.2).

Where MCF-12A non-tumourigenic cells were exposed to necrosis, an increased PI-positive cell population was observed indicating that the assay could detect necrotic cell death (Figure 3.32 and 3.34). Apoptotic cell death was primarily detected where cells were exposed to staurosporine indicating that the assay could detect apoptotic cell death. After 72 h exposure to the oestrone analogues, IND or the combinations, increased apoptosis was observed in MCF-12A cells.

Elevation in the number of cells in early apoptosis was observed upon treatment of MCF-7 breast adenocarcinoma cells with ESE-15-ol (17 nM) and ESE-16 (17 nM)(Figure 3.33). Where MCF-7 cells were treated with QUER (84 μM), necrotic cell death was predominantly induced. Apoptotic and necrotic cell death was observed where cells were exposed the combinations of oestrone analogues and QUER (Table 3.2).

Exposure to ESE-15-ol (17 nM) and ESE-16 (17 nM) resulted in the induction of apoptotic cell death of MCF-12A cells (Figure 3.34). A similar response was observed where cells were exposed to QUER (84 μM) or the combinations of oestrone analogues and QUER (Table 3.2).

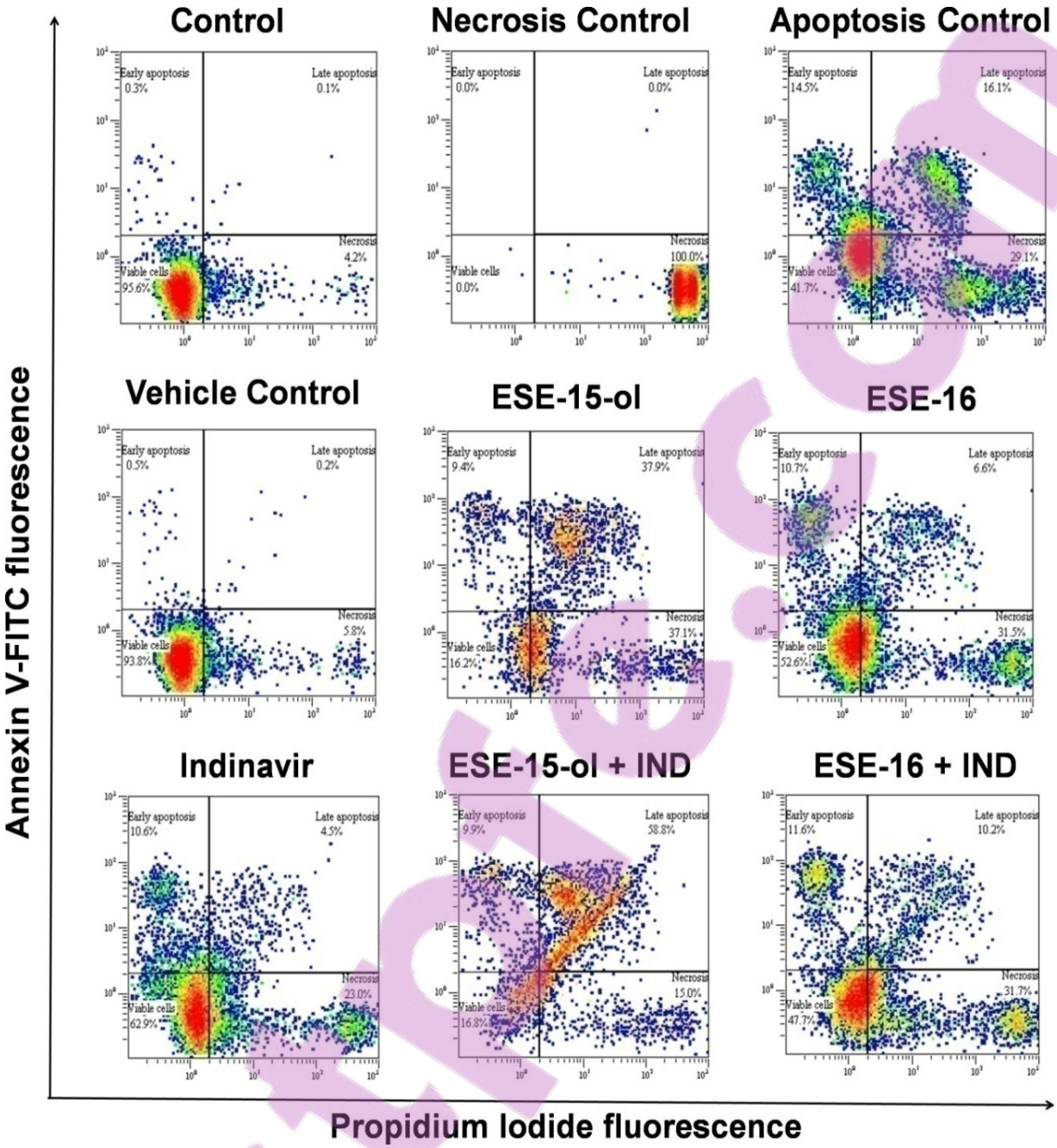

Figure 3.31: The effect of synergistic combinations of the oestrone analogues, ESE-15-ol (70 nM) and ESE-16 (70 nM) with indinavir (IND, 115 μM) on the induction of apoptosis or necrosis on **MCF-7** breast adenocarcinoma cells after 72 h incubation using a flow cytometric protocol. Staurosporine (10 μM for 24 h) was used as apoptosis control. Results are presented as scatter plots and represent one of four independent experiments.

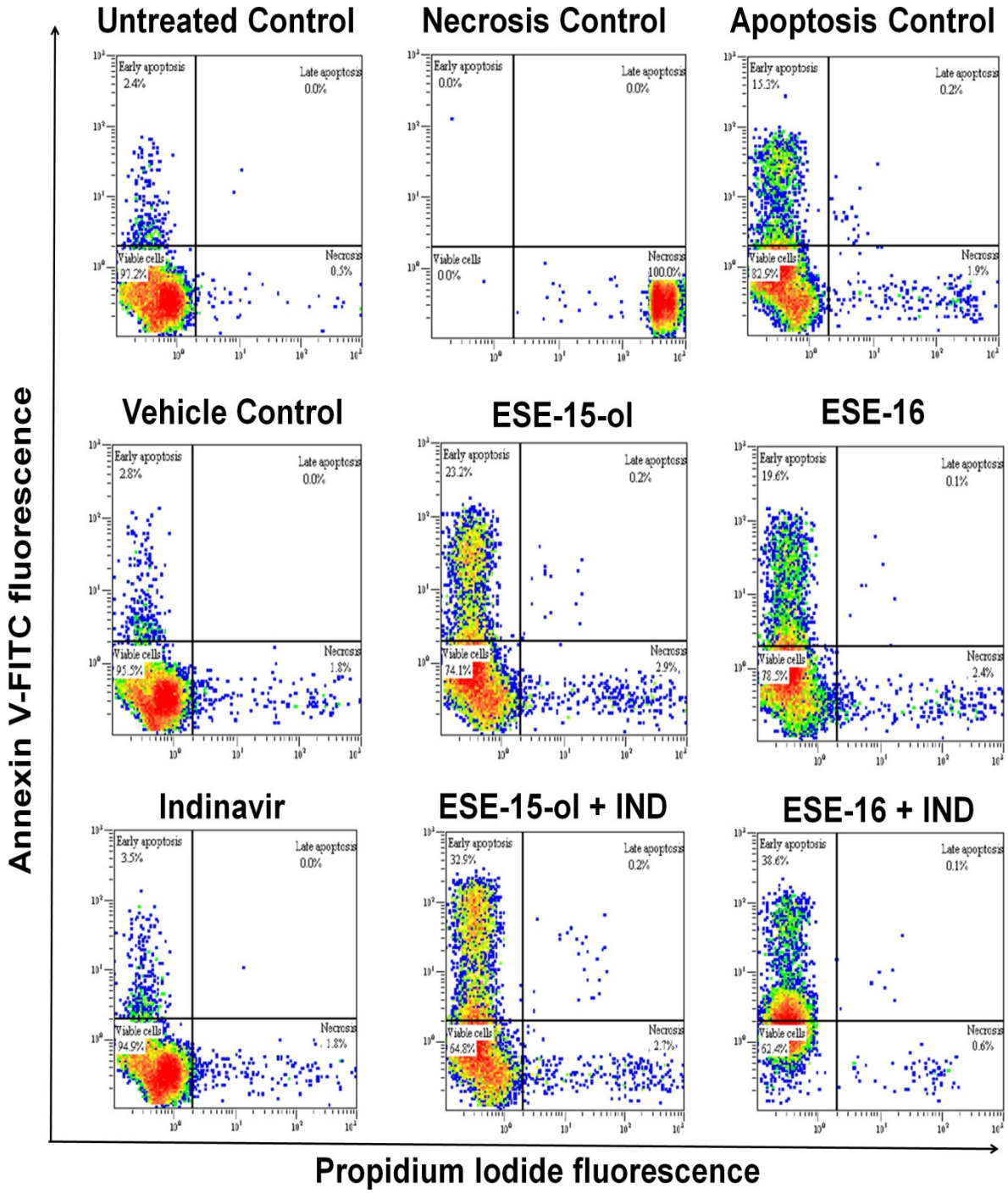

Figure 3.32: The effect of synergistic combinations of the oestrone analogues, ESE-15-ol (70 nM) and ESE-16 (70 nM), with indinavir (IND, 115 μM) on the induction of apoptosis or necrosis on**MCF-12A** non-tumourigenic cells after 72 h incubation using a flow cytometric protocol. Staurosporine (10 μM for 24 h) was used as apoptosis control. Results are presented as scatter plots and represent one of four independent experiments.

Table 3.2: The effect of synergistic combinations of the oestrone analogues with indinavir (IND) on the induction of apoptosis or necrosis on **MCF-7** breast adenocarcinoma and **MCF-12A** non-tumourigenic cells after 72 h incubation using a flow cytometric protocol. Cumulative data from four independent experiments is shown. n = 4, * $p < 0.05$ ** $p < 0.01$ *** $p < 0.001$

	Viable cells	Early apoptosis	Late apoptosis	Necrotic cells
MCF-7 breast adenocarcinoma cells				
Control	96.3 ± 1.1	1.2 ± 0.1	0.3 ± 0.2	3.6 ± 1.4
Vehicle control	94.8 ± 0.9	1.0 ± 0.3	0.3 ± 0.1	4.1 ± 0.8
Necrosis control	0.0 ± 0.0 *	0.4 ± 0.3	0.1 ± 0.1	99.9 ± 0.1 *
Apoptosis control	40.4 ± 6.8	29.6 ± 5.7	10.6 ± 2.2	20.6 ± 7.7
ESE-15-ol	25.7 ± 6.5 *	37.6 ± 15.0	20.7 ± 7.7	17.0 ± 6.9
ESE-16	51.6 ± 12.4	30.2 ± 12.6	3.1 ± 1.2	15.8 ± 6.1
IND	71.4 ± 3.5	16.3 ± 3.9	2.0 ± 0.9	11.1 ± 4.3
ESE-15-ol+IND	15.4 ± 2.9 **	45.7 ± 16.4	27.5 ± 12.0	12.0 ± 3.3
ESE-16+IND	56.0 ± 11.9	27.8 ± 13.9	3.9 ± 2.1	13.3 ± 6.2
MCF-12A non-tumourigenic cells				
Control	94.2 ± 2.6	3.8 ± 1.2	0.1 ± 0.1	2.1 ± 1.4
Vehicle control	91.4 ± 3.7	4.5 ± 2.2	0.1 ± 0.1	4.3 ± 1.7
Necrosis control	0.6 ± 0.6*	0.2 ± 0.2	0.3 ± 0.3	98.9 ±1.1*
Apoptosis control	59.9 ± 27.1	34.2 ± 25.7	0.9 ± 0.8	5.1 ± 1.6
ESE-15-ol	55.6 ± 23.7	34.1 ± 15.4	3.6 ± 3.5	7.1 ± 4.9
ESE-16	77.2 ± 7.1	18.3 ± 4.2	0.1 ± 0.0	5.0 ± 3.2
IND	77.3 ± 18.6	17.5 ± 15.5	0.1 ± 0.1	5.6 ± 3.3
ESE-15-ol+IND	49.2 ± 23.0*	43.4 ± 18.7*	1.8 ± 1.6	6.1 ± 2.8
ESE-16+IND	60.5 ± 19.0	32.6 ± 14.6	0.2 ± 0.2	7.0 ± 4.3

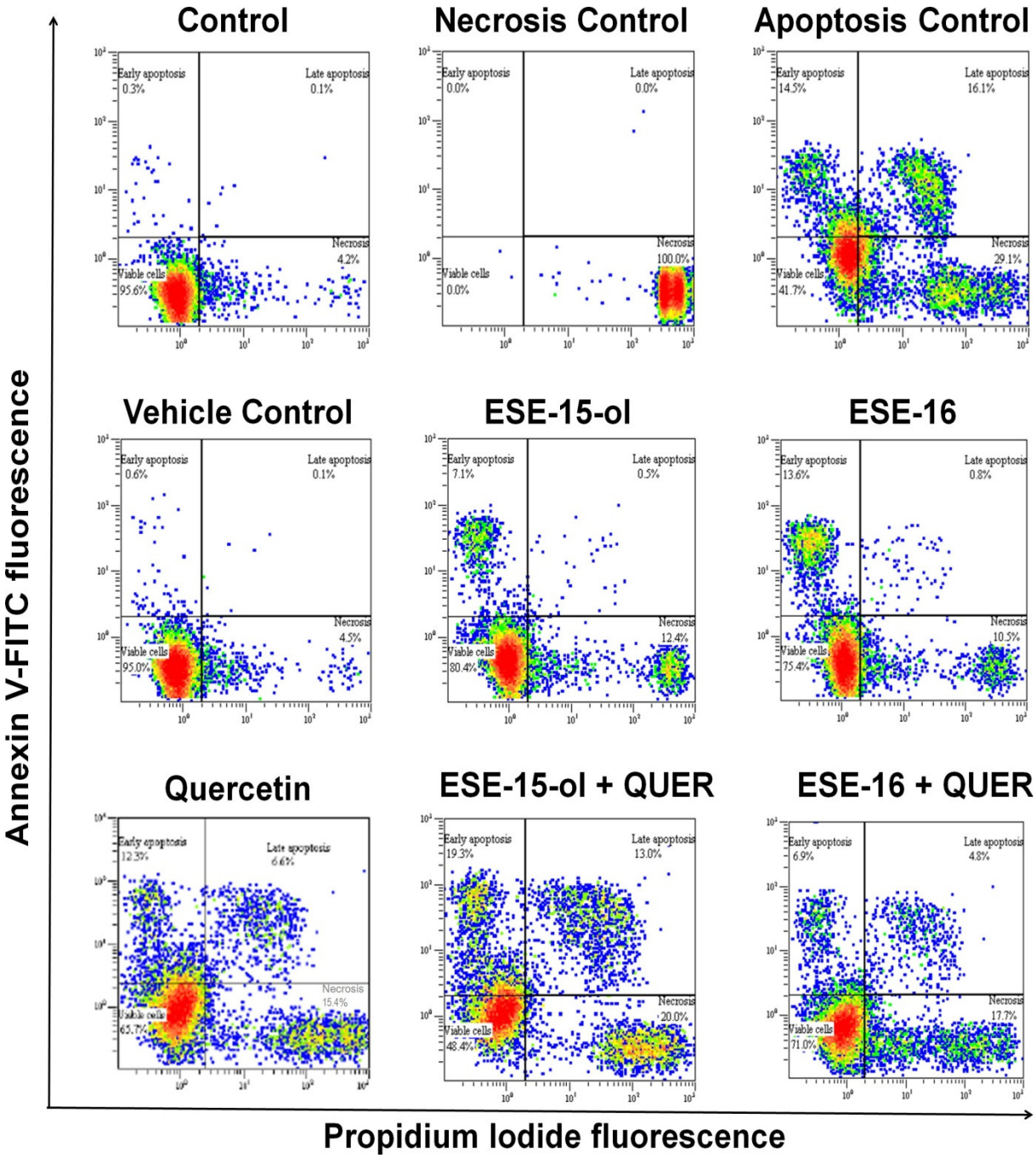

Figure 3.33: The effect of synergistic combinations of the oestrone analogues, ESE-15-ol (17 nM) and ESE-16 (17 nM), with quercetin (QUER, 84 µM) on the induction of apoptosis or necrosis on **MCF-7** breast adenocarcinoma cells after 72 h incubation using a flow cytometric protocol. Staurosporine (10 µM for 24 h) was used as apoptosis control. Results are presented as scatter plots and represent one of four independent experiments.

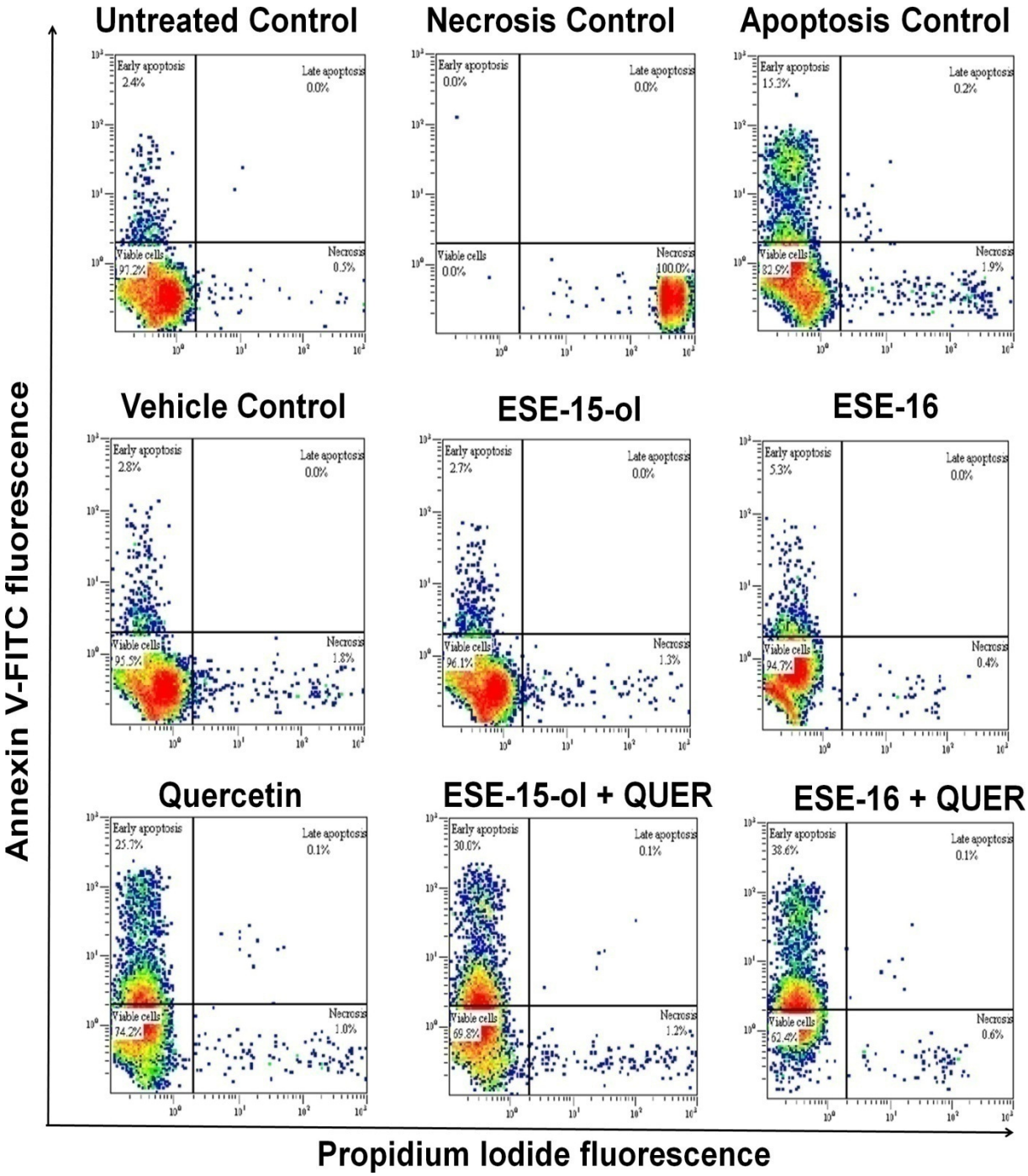

Figure 3.34: The effect of synergistic combinations of the oestrone analogues, ESE-15-ol (17 nM) and ESE-16 (17 nM), with quercetin (QUER, 84 µM) on the induction of apoptosis or necrosis on **MCF-12A** non-tumourigenic cells after 72 h incubation using a flow cytometric protocol. Staurosporine (10 µM for 24 h) was used as apoptosis control. Results are presented as scatter plots and represent one of four independent experiments.

Table 3.3: The effect of synergistic combinations of the oestrone analogues with quercetin (QUER) on the induction of apoptosis or necrosis on **MCF-7** breast adenocarcinoma and **MCF-12A** non-tumourigenic cells after 72 h incubation using a flow cytometric protocol. Cumulative data from four independent experiments is shown. n = 4, * $p < 0.05$ ** $p < 0.01$ *** $p < 0.001$

	Viable cells	Early apoptosis	Late apoptosis	Necrotic cells
MCF-7 breast adenocarcinoma cells				
Control	96.3 ± 1.1	1.2 ± 0.1	0.3 ± 0.2	3.6 ± 1.4
Vehicle control	94.8 ± 0.9	22.2 ± 13.0	0.8 ± 0.6	15.3 ± 9.7
Necrosis control	0.0 ± 0.0 *	0.4 ± 0.3	0.1 ± 0.1	99.9 ± 0.1 *
Apoptosis control	40.4 ± 6.8	29.6 ± 5.7	10.6 ± 2.2	20.6 ± 7.7
ESE-15-ol	84.3 ± 4.3	10.8 ± 4.0	0.3 ± 0.1	4.9 ± 2.5
ESE-16	78.4 ± 7.2	15.3 ± 5.5	0.4 ± 0.2	6.3 ± 2.5
QUER	28.8 ± 10.7	35.9 ± 11.5	14.4 ± 5.1	21.5 ± 4.3
ESE-15-ol+QUER	21.8 ± 9.7 *	34.6 ± 9.8	17.6 ± 4.7	26.5 ± 3.2
ESE-16+QUER	32.0 ± 14.5	32.1 ± 12.2	13.8 ± 5.0	22.6 ± 5.0
MCF-12A non-tumourigenic cells				
Control	94.2 ± 2.6	3.8 ± 1.2	0.1 ± 0.1	2.1 ± 1.4
Vehicle control	93.0 ± 3.0	5.3 ± 2.2	0.0 ± 0.0	1.9 ± 0.9
Necrosis control	0.6 ± 0.6 *	0.2 ± 0.2	0.3 ± 0.3	98.9 ± 1.1 *
Apoptosis control	59.9 ± 27.1	34.2 ± 25.7	0.9 ± 0.8	5.1 ± 1.6
ESE-15-ol	93.2 ± 3.9	4.4 ± 2.3	0.0 ± 0.0	2.7 ± 1.7
ESE-16	90.7 ± 5.3	9.4 ± 5.4	0.0 ± 0.0	0.5 ± 0.2
QUER	61.8 ± 9.7	34.1 ± 6.2	0.2 ± 0.6	1.4 ± 0.2
ESE-15-ol+QUER	61.3 ± 9.6	33.2 ± 5.9	0.5 ± 0.3	6.0 ± 3.7
ESE-16+QUER	52.6 ± 9.1	45.5 ± 6.7	0.3 ± 0.2	2.9 ± 2.1

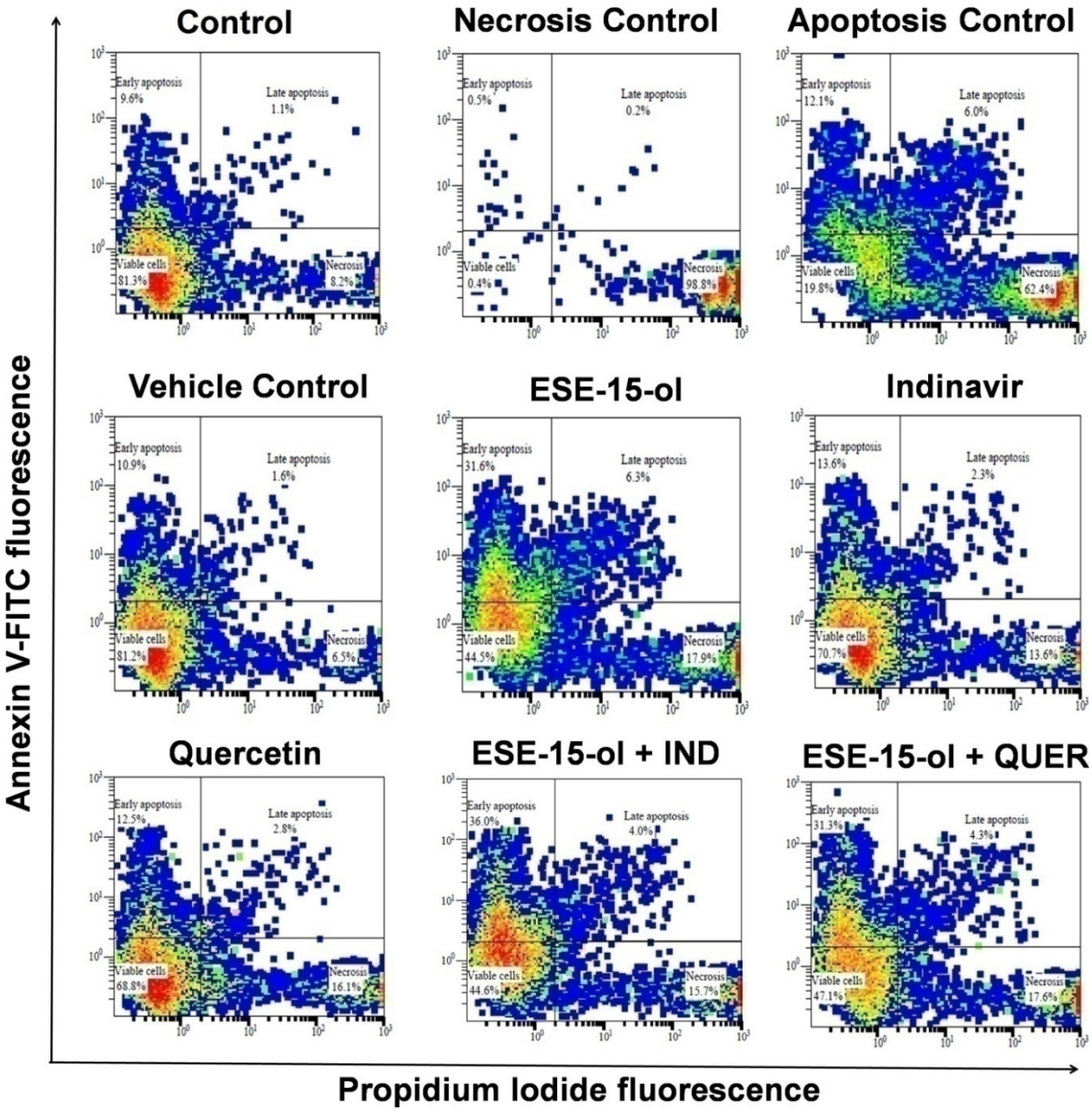

Figure 3.35: The effect of synergistic combinations of the oestrone analogue ESE-15-ol (123 nM) with indinavir (IND, 55 µM) and quercetin (QUER, 0.64 µM) on the induction of apoptosis or necrosis on **MDA-MB-231** breast adenocarcinoma cells after 72 h incubation using a flow cytometric protocol. Staurosporine (10 µM for 24 h) was used as apoptosis control. Results are presented as scatter plots and represent one of four independent experiments.

MDA-MB-231 breast adenocarcinoma cells treated with ethanol showed induction of necrosis and stimulation of apoptosis in staurosporine-treated indicate that apoptotic and necrotic cell death could be detected with the assay (Figure 3.35). Treatment of cells with ESE-15-ol and combinations with the glycolysis inhibitors showed elevation of both apoptotic and necrotic cell death (Table 3.4).

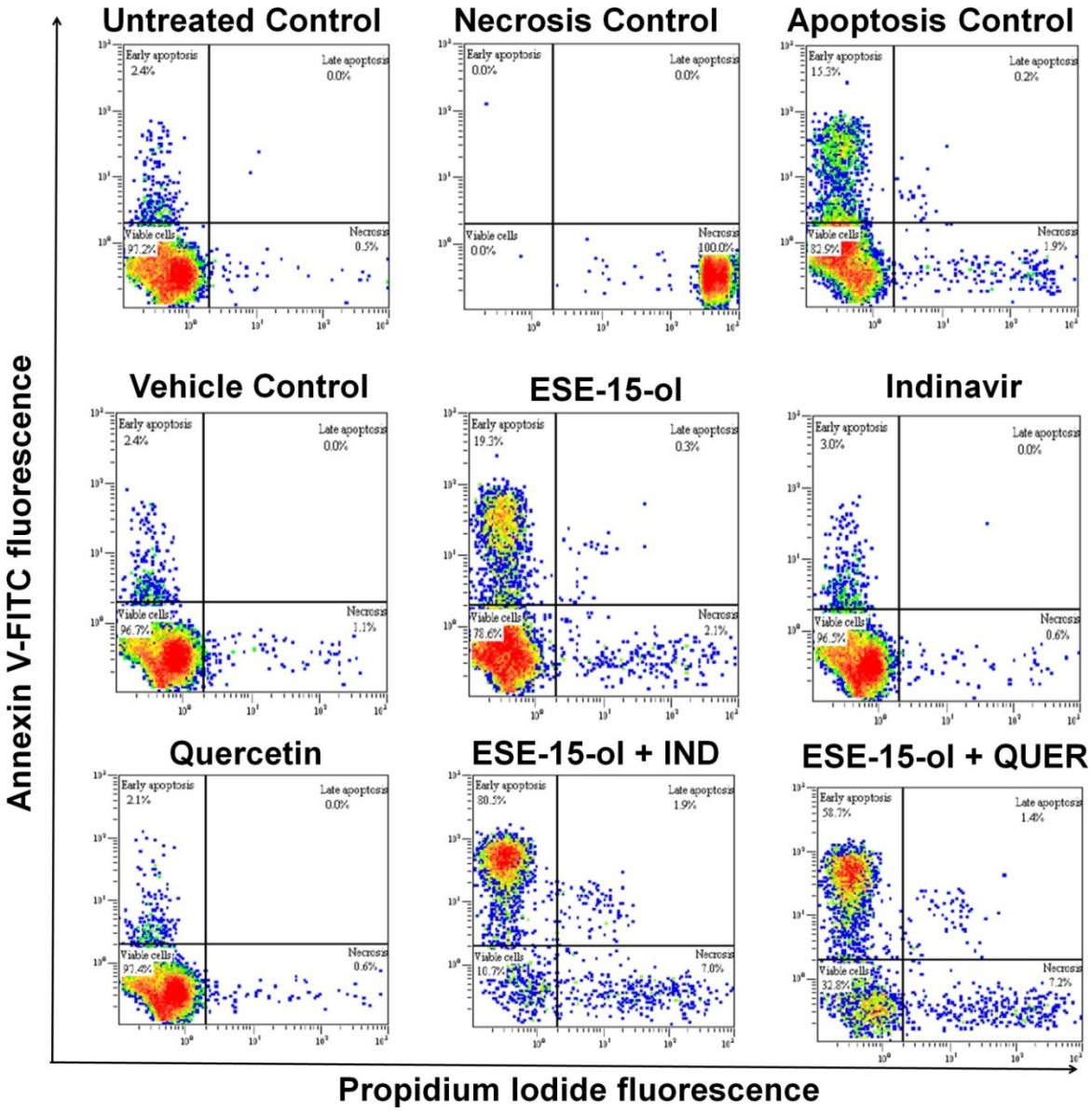

Figure 3.36: The effect of synergistic combinations of the oestrone analogue ESE-15-ol (123 nM) with indinavir (IND, 55 µM) and quercetin (QUER, 0.64 µM) on the induction of apoptosis or necrosis on **MCF-12A** non-tumourigenic cells after 72 h incubation using a flow cytometric protocol. Staurosporine (10 µM for 24 h) was used as apoptosis control. Results are presented as scatter plots and represent one of four independent experiments.

Ethanol-induced necrosis and staurosporine-induced apoptosis was successfully detected, suggesting that the assay could detect necrotic and apoptotic cell death in MCF-12A non-tumourigenic cells (Figure 3.36). Where MCF-12A cells were exposed to ESE-15-ol (123 nM) and the combinations apoptotic cell death was detected. IND (55 µM) and QUER (0.64 µM) treatment did not affect cell viability significantly. The combinations of oestrone analogues and IND or QUER induced apoptotic cell death.

Table 3.4: The effect of synergistic combinations of the oestrone analogues with quercetin (QUER) on the induction of apoptosis or necrosis on **MDA-MB-231** breast adenocarcinoma and **MCF-12A** non-tumourigenic cells after 72 h incubation using a flow cytometric protocol. Cumulative data from four independent experiments is shown. n = 4, * $p < 0.05$ ** $p < 0.01$ *** $p < 0.001$

	Viable cells	Early apoptosis	Late apoptosis	Necrotic cells
MDA-MB-231 breast adenocarcinoma cells				
Control	87.8 ± 3.4	4.5 ± 2.2	0.5 ± 0.2	6.4 ± 2.2
Vehicle control	85.9 ± 1.4	6.4 ± 1.8	0.5 ± 0.3	7.3 ± 1.5
Necrosis control	0.2 ± 0.1*	0.1 ± 0.1	0.1 ± 0.0	99.6 ± 0.2
Apoptosis control	34.4 ± 4.6	10.9 ± 4.2	2.3 ± 1.1	52.5 ± 6.7
ESE-15-ol	61.2 ± 7.5	22.1 ± 5.9	1.9 ± 1.1	14.9 ± 3.5
IND	79.4 ± 3.8	8.9 ± 1.7	0.9 ± 0.4	10.9 ± 2.7
ESE-15-ol+IND	60.6 ± 5.0	26.1 ± 4.4	1.6 ± 0.7	11.8 ± 1.9
QUER	79.8 ± 3.9	6.8 ± 2.0	0.8 ± 0.5	12.6 ± 2.4
ESE-15-ol+QUER	63.5 ± 4.7	21.8 ± 4.3	1.7 ± 0.8	13.1 ± 2.1
MCF-12A non-tumourigenic cells				
Control	95.2 ± 2.1	3.2 ± 1.0	0.1 ± 0.1	1.8 ± 1.1
Vehicle control	95.2 ± 2.2	3.1 ± 1.2	0.0 ± 0.0	1.9 ± 1.0
Necrosis control	0.5 ± 0.4*	0.2 ± 0.1	0.2 ± 0.2	99.2 ± 0.8 *
Apoptosis control	63.7 ± 19.5	32.0 ± 18.3	0.7 ± 0.6	4.2 ± 1.5
ESE-15-ol	37.3 ± 15.2	34.3 ± 13.5	3.4 ± 1.9	25.3 ± 11.0
IND	91.5 ± 5.3	6.0 ± 3.6	0.1 ± 0.1	2.8 ± 1.9
ESE-15-ol+IND	9.7 ± 1.9*	70.5 ± 3.5*	5.8 ± 2.0	14.3 ± 2.8
QUER	94.9 ± 2.3	3.5 ± 1.6	0.0 ± 0.0	1.7 ± 0.8
ESE-15-ol+QUER	18.4 ± 5.9	62.1 ± 1.5	4.1 ± 1.4	15.6 ± 3.1

3.6 Discussion

In an attempt to map the sequence of toxic effects culminating in cell death (see Figure 3.1), assays of various molecular parameters indicative of transient, reversible and irreversible toxicity were investigated on the MCF-7 and MDA-MB-231 breast adenocarcinoma cell lines. The MCF-12A cell line was used as a normal reference cell line for most assays.

It has been suggested that cell death in response to agents affecting the cell cycle may only manifest after several days (Willingham, 1999). Therefore intracellular changes that reflect adaptive responses to exposure with the combinations of oestrone analogues and glycolysis inhibitors were assessed at different time points leading up to 72 h exposure when studies of the mode of cell death induced were evaluated.

It must be considered that QUER may cause interference with certain fluorescence-based assays as the residual fluorescence of intracellular QUER is reportedly detectable at wavelengths similar to those required for the assays (Nifli *et al.*, 2007; Baran *et al.*, 2011). However, a pilot study was conducted to assess the potential interference in the same laboratory, using the same instruments as the assays performed to provide an accurate indication of the degree to which data collected with fluorescence-based assays is affected by residual intracellular QUER fluorescence. During the pilot study the greatest interference (approximately 7.6% of the signal generated during the experiment) was observed at the excitation and emission wavelengths required for caspase 3/7 and -8. However, even with maximal interference of intracellular QUER of 7.6%, the effect on data obtained with during the experiments would be negligible. Therefore under the experimental conditions used in the present study residual fluorescence of intracellular QUER was deemed negligible.

The first parameter investigated is one classified as an early, reversible response to toxic stimuli: intracellular anti-oxidant enzyme concentrations. The main endogenous anti-oxidant in mammalian cells is reduced glutathione (GSH)(Balendiran *et al.*, 2004). The majority of intracellular GSH is synthesised *de novo* from glutamic acid, cysteine and glycine (Yeh *et al.*, 2006). Conversion of reduced GSH to its oxidised form (GSSG) occurs upon contact with free radicals or where enzymes such as GSH peroxidase or GSH reductase require GSH as co-factor (Balendiran *et al.*, 2004). Glutathione reductase also aids in the maintenance of intracellular GSH levels by reducing GSSG to GSH (Fang *et al.*, 2002). Maintenance of intracellular GSH levels is crucial as GSH levels correlate with susceptibility to oxidative damage, detoxification potential and in some cases prevalence of mutations (Balendiran *et al.*, 2004).

Even though fluctuation in GSH concentration was observed in response to treatment with the combinations in the present study, statistically significant reduction in GSH was observed only where MCF-7 and MDA-MB-231 breast adenocarcinoma cells were exposed to combinations with IND (Figures 3.3 and 3.4). No statistically significant changes in GSH concentration was observed in the non-tumourigenic MCF-12A cells. However, the concentrations of IND and QUER required for synergy on the MCF-7 cell line did induce a reduction in GSH levels in the MCF-12A cells. This was most marked where the MCF-12A cells were treated with QUER (84 µM). A slight increase (11%) in intracellular GSH was observed where MCF-12A cells were treated with QUER at 0.64 µM, the concentration required for the combinations on MDA-MB-231 cells.

The contradictory anti- and pro-oxidant properties of QUER have been well-documented. It has been proposed that QUER will act as anti-oxidant against free radicals but pro-oxidant in the presence of transition metals (Cao *et al.*, 1997). In the presence of transition metal such as ferric ion (Fe^{3+}) complexes, QUER is oxidised, generating superoxide (O_2^-)(Laughton *et al.*, 1989). As with GSH an intracellular reduction of oxidised QUER by nicotinamide adenine dinucleotide phosphate (NADPH)-cytochrome P450 reductase or DT-diaphorase have been suggested (Metodiewa *et al.*, 1999). However, the cyto-protective anti-oxidant effects of QUER have been demonstrated in the presence of hydrogen peroxide (H_2O_2) (Lee *et al.*, 2003). Reports have indicated that 25 µM QUER decreased intracellular GSH as measured with the monochlorobimane assay in the human leukemic monocyte lymphoma U937 cells, but not promyelocyticleukaemia NB4 cells, after 8 h treatment. This corresponded to the degree of apoptosis induced by QUER in these two cell lines (Ramos and Aller, 2008).

Based on gene expression analysis performed on ESE-15-ol-treated (50 nM, 24 h) MDA-MB-231 cells up-regulation of several ROS-responsive genes was indicated, implying that treatment with ESE-15-ol induced ROS generation (Stander *et al.*, 2012). In the present study slight decreases in GSH concentration were observed in response to treatment with ESE-15-ol. However, the effect on GSH concentration was most notable where MCF-7 cells were treated with the lowest concentration of ESE-15-ol (17 nM)(Figure 3.8).

A statistically significant reduction in GSH was observed were MCF-7 cells were treated with ESE-16 (70 nM) alone and in combination with IND (Figure 3.8). Previous studies assessing the effect of ESE-16 on intracellular ROS levels used hydroethidine as indicator of the presence of superoxide molecules as well as 2',7'-dichlorodihydrofluoresceindiacetate (DCFH-DA) as indicator of H_2O_2 and ferrous ion (Fe^{2+}) formation (Stander *et al.*, 2013). Generation of superoxide was statistically significant after 12 h exposure to 200 nM ESE-16 in the MCF-7 cell line. After MCF-7 breast adenocarcinoma cells were exposed to ESE-16 at

200 nM for only 6 h, slight increased fluorescence was observed with the DCFH-DA assay which differed statistically from the vehicle treated control after 12 h, suggesting the production of H_2O_2 or presence of Fe^{2+} (Stander *et al.*, 2013). This corresponds to the data from the current study as a decrease in GSH concentration, as indicated by a decrease in fluorescence of the monochlorobimane derivative of GSH, suggesting increased concentrations of ROS that had depleted the GSH (Panduri *et al.*, 2004).

The irregular response to treatment with ESE-15-ol and ESE-16 observed in the MCF-7 cell line may be explained by the concentrations of the oestrone analogues required for each synergistic drug combination: for drug combinations with IND, ESE-15-ol and ESE-16 were used at concentrations exceeding 65 nM, where only 17 nM of ESE-15-ol and ESE-16 were required for drug combinations with QUER. However another possibility is increased *de novo* synthesis of GSH. The fluorescent signal detected by the monochlorobimane assay is based on the formation of monochlorobimane-glutathione adducts (Kamencic *et al.*, 2000a). When *de novo* GSH formation is elevated in response to increased ROS generation induced by a chemotherapeutic treatment, it is expected that increased adduct formation will occur. This may explain the slight increase in GSH concentration observed in MCF-7 cells treated with ESE-15-ol and ESE-16 (both at 17 nM). At higher concentrations of these oestrone analogues increased production of ROS (Stander *et al.*, 2012, 2013) resulted in increased oxidation of GSH as measured by the reduced monochlorobimane fluorescent signal.

Intracellular oxido-reductive reactions allow for the reversible conversion of Fe^{2+} ions to Fe^{3+} ions (Laughton *et al.*, 1989). In response to the potential generation of Fe^{3+} ions following treatment with ESE-16, QUER may act as pro-oxidant generating superoxide molecules. As the exposure period to the combination of ESE-16 and QUER proceeds, it is proposed that the generation of Fe^{2+} ions by ESE-16 and subsequent production of O_2^- by QUER will initiate the sequence of toxicity culminating in cell death observed after exposure to the combination for 72 h. In the presence of transition metal ions, QUER treatment will promote generation of ROS resulting in depolarisation of the mitochondrial membrane potential, as observed in the present study. Supporting this theory is the observation that the combinations of ESE-15-ol and ESE-16 with QUER enhanced the depolarisation in the MCF-7 breast adenocarcinoma cell line when compared to the effect on MMP generated by the compounds separately. However, in the absence of these transition metal ions QUER has been demonstrated to prevent hydrogen peroxide-induced apoptosis (Park *et al.*, 2003).

IND has also been shown to induce ROS generation in human subcutaneous adipocytes at 10 µM after only 24 h (Lagathu *et al.*, 2007; Apostolova *et al.*, 2011). Another study found that 5 µM IND caused elevated ROS detectable at 6 h after initiation of treatment of human

umbilical vein endothelial cells (Jiang *et al.*, 2007). IND-induced export of GSH to the extracellular space has been reported in cultured astrocytes (Brandmann *et al.*, 2012). The results obtained in the present study demonstrate the pro-oxidant properties of IND as treatment with IND and combinations with IND decreased GSH concentrations. MCF-7 cells treated with IND (115 µM), the highest concentration of IND used, did not reduce GSH concentrations as expected from the results seen with lower IND concentrations. However, increased *de novo* synthesis of GSH may account for this anomaly.

Reduced concentrations of GSH in MCF-12A non-tumourigenic cells treated with the various combinations imply that an adaptive response is elicited. Where MCF-12A cells were treated with the synergistic drug combinations specific for MCF-7 cells, the greatest GSH reductions were observed with treatment with QUER and ESE-16 separately. As for combinations specific for MDA-MB-231 cells a 25% reduction in GSH concentration was observed where cells were treated with ESE-15-ol only. As alterations in the levels of anti-oxidant enzymes are regarded as a pre-lethal, transient event (van Tonder *et al.*, 2014) the adaptive responses elicited may be sufficient to restore cellular homeostasis.

Where MCF-12A cells were treated with ESE-16 (17 nM) or QUER (0.64 µM) increased GSH was observed (Figures 3.8 and 3.9) which does not suggest the generation of reactive oxygen species. However, elevated GSH levels were observed where MCF-12A cells were treated with the DMSO vehicle (Figure 3.3). The DMSO concentration in cell culture media did not exceed 0.5%, a concentration proven to be essentially non-toxic to cell cultures (Friend *et al.*, 1971; Da Violante *et al.*, 2002; Chen and Thibeault, 2013). The concentration of DMSO used in the MCF-12A cell line is the same as that used in the MCF-7 cell line where no increase in GSH was observed. The increase in GSH concentration in the vehicle-treated samples may thus be an experimental anomaly.

Elevated levels of intracellular ROS may induce autophagy, an adaptive mechanism which allows for the removal of organelles damaged by ROS (Scherz-Shouval and Elazar, 2007). This has been demonstrated *in vitro* as the addition of an extraneous anti-oxidant limited the effect of an inducer of autophagy (Kiššová *et al.*, 2006).

Three distinct forms of autophagy have been identified: macroautophagy, microautophagy and chaperone-mediated autophagy (Cuervo and Dice, 1998). Under nutrient-rich conditions microautophagy ensures the degradation of cytosolic proteins whereas chaperone-mediated autophagy, the selective catabolism of specific proteins escorted to lysosomes, occurs under conditions of nutrient deprivation (Cuervo and Dice, 1998). Like chaperone-mediated autophagy, macroautophagy entails the catabolism of intracellular components through lysosomal degradation under conditions of nutrient deprivation (Barth *et al.*, 2010).

Macroautophagy, from here on referred to as autophagy, is the most common form of autophagy. The main function of autophagy is to generate amino acids to provide for the metabolic requirements of the cell (Mizushima, 2005). Not only does autophagy play an essential role in providing nutrients and amino acids for the production of ATP under nutrient-poor conditions, but it has been suggested that autophagy acts as checkpoint to ensure organelles are fully functional. This is of particular importance to prevent mitochondrial dysfunction as this may in turn produce damaging ROS (Jin and White, 2007).

In the context of tumourigenesis, autophagy plays a paradoxical role. One of the pro-survival mechanisms adapted by malignant cells is the evasion of apoptotic signals (Hanahan and Weinberg, 2000). When autophagy is induced, apoptotic stimuli, such as nutrient deprivation and genome instability, do not result in cell death. Generation of ATP under these conditions through autophagy ensures that vital processes are maintained leading to the survival and propagation of damaged cells (Jin and White, 2007). Autophagy may also promote survival and proliferation of malignant cells by inferring protection against necrosis (Gu *et al.*, 2015). However, extensive autophagy can also result in cell death (Bhutia *et al.*, 2013). A recent report by Gu and colleagues suggests that abrogation of autophagy may result in poor survival in breast cancer patients (Gu *et al.*, 2015). At present autophagic cell death is not completely understood: even though autophagic proteins are involved, the role of caspases in this mode of cell death is still unclear. Molecular crosstalk between autophagy and apoptosis has not been clearly defined as apoptosis often occurs concomitantly with autophagy (Bhutia *et al.*, 2013).

On a morphological level autophagy is characterised by cytoplasmic content encapsulated in multi-membranous structures (Klionsky *et al.*, 2012). These structures, termed autophagosomes were first detected with transmission electron microscopy (TEM) and this remains a commonly used technique to detect autophagy induction (Barth *et al.*, 2010). Once an autophagosome has merged with a functional lysosome, forming an autolysosome, proteolytic degradation of the sequestered contents occurs (Mizushima, 2005). However, autophagosomes may also merge with endosomes to form amphisomes (Eskelinen, 2008). Morphologically autolysomes can be distinguished from autophagosomes as autolysosomes are not contained by a double membrane, but are rather identified based on its incompletely degraded contents (Klionsky *et al.*, 2012).

A number of obstacles to the use of TEM for the detection and possibly the quantification of autophagy have been identified. Expertise in the field is required to positively identify autophagosomes (Barth *et al.*, 2010; Klionsky *et al.*, 2012) as the characteristic double sequestering membrane is not always preserved by commonly used sample preparation

techniques (Eskelinen, 2008). Furthermore distinguishing late stage autophagosomes from heterophagic vacuoles, enlarged endoplasmic reticulum or swollen mitochondria pose significant challenges (Martinet *et al.*, 2006b; Eskelinen, 2008). In TEM micrographs, the electron density of potential autophagosomal vacuoles must be similar to that of the surrounding cytoplasm (Eskelinen, 2008) and the cytoplasmic contents of autolysosomes must be identifiable (Klionsky *et al.*, 2012).

Several intracellular structures may be misidentified as autophagosomes due to the similarity in appearance. Multivesicular bodies, easily misidentified as autophagosomes, are formed during the endocytosis process when endosomes containing proteins destined for degradation form internal buds (Piper and Katzmann, 2007). Endocytic markers, such as Rabguanosinetriphosphatases, distinguish these vesicles from autophagic vacuoles (Piper and Katzmann, 2007). Confounding matters further are vesicles which may have more than one limiting membrane. Unilamellar or multilamellar vesicles, vesicles sequestered by more than one membrane, are vital to protein homeostasis as intracellular protein transport depends on proper encapsulation and trafficking within vesicles (Rothman and Wieland, 1996). Vesicles are also implicated in normal endocytosis (Verma and Roshan, 2015). The presence of vesicles or multivesicular bodies, although it may be indicative of autophagy, is thus not a specific indicator of the autophagic process.

In order to avoid misidentification of multivesicular bodies or multilamellar vesicles as autophagosomes, antibodies specific for autophagy markers can be employed. Immunogold staining using colloidal gold labelled antibodies allows for the specific identification of marker proteins during TEM studies (Horisberger and Rosset, 1977). The use of similar antibodies for the identification of the cytosolic contents of autophagosomes has been reported (Liou *et al.*, 1996). In the present study immunogold staining was not employed and therefore, even though these micrographs provide valuable information about morphological alterations induced by the combinations, conclusions cannot be drawn directly from the presence of vesicles showing autophagosome characteristics.

The photomicrographs obtained during this study for MCF-7 breast adenocarcinoma cells exposed to drug combinations (Figures 3.10 and 3.11) show the formation of vesicles in all treated samples. Vesicle formation was most evident where cells were treated with tamoxifen, a known inducer of autophagy (Theron *et al.*, 2013). A degree of similarity can be seen in the vesicles formed after treatment with tamoxifen and ESE-15-ol (17 and 70 nM), IND, QUER and combinations with IND in the MCF-7 cell line. The vesicle formation induced by ESE-15-ol was less evident where cells were treated with combinations of ESE-15-ol and IND or QUER. Interestingly, even though treatment with ESE-16 did not seem to cause

prominent vesicle formation in MCF-7 cells, vesicle formation was observed where cells were treated with combinations of ESE-16 and IND or QUER. The distinct intracellular changes induced by exposure to the two different oestrone analogues imply that these compounds may perhaps not exert their anti-cancer effect through the same mechanisms.

In the MDA-MB-231 breast adenocarcinoma cell line vesicle formation was less pronounced (Figure 3.12). Vesicles observed in tamoxifen-treated MDA-MB-231 cells resemble those observed in the MCF-7 cells. However, the vesicles seen in ESE-15-ol treated cells simulate published examples of autolysosomes, the final stage of autophagy (Nixon, 2007). Autolysosomes may contain electron dense material (Nixon, 2007) as observed in the micrographs obtained in the present study for MDA-MB-231 cells treated with the combination of ESE-15-ol and IND or QUER. The possible observation of autolysosomes may suggest that autophagy was induced by treatment with ESE-15-ol and drug combinations with ESE-15-ol before 24 h. Unfortunately, the morphological similarities between the structures of autolysosomes, lysosomes containing concentric lamellar inclusions and amphisomes complicate accurate identification of these structures (Nixon, 2007; Vergarajauregui *et al.*, 2008).

As morphology studies only provide qualitative data, cellular responses to toxicity induced by the combinations were quantified using specific intracellular markers. Assessment of molecular makers for autophagy is recommended due to the myriad of challenges of accurately detecting and quantifying autophagy based on morphological techniques (Klionsky *et al.*, 2008). A number of molecular markers of autophagy have been identified (Figure 3.37) which detect increased formation or accumulation of autophagosomes including Atg8/LC3-II, Atg 5 and TOR complex I (TORC1)(Klionsky *et al.*, 2012). Of all these markers only LC3-II is a direct molecular marker of autophagy as the extent of LC3-II expression has been directly correlated with the number of autophagosomes (Kabeya *et al.*, 2000). Once autophagy has been initiated by Atg7 and Atg3 in the presence of the Atg12-Atg5-Atg16L1 complex, LC3-I is converted to LC3-II through the addition of the lipophilic phosphatidylethanolamine (PE) group (Barth *et al.*, 2010). However, as autophagy is a dynamic process, over-expression of LC3-II may indicate induction of autophagy (Kovács *et al.*, 1988), accumulation of autophagosomes (Kovács *et al.*, 1988) or an imbalance between the formation of autophagosomes and autolysosomes (Chu, 2006).

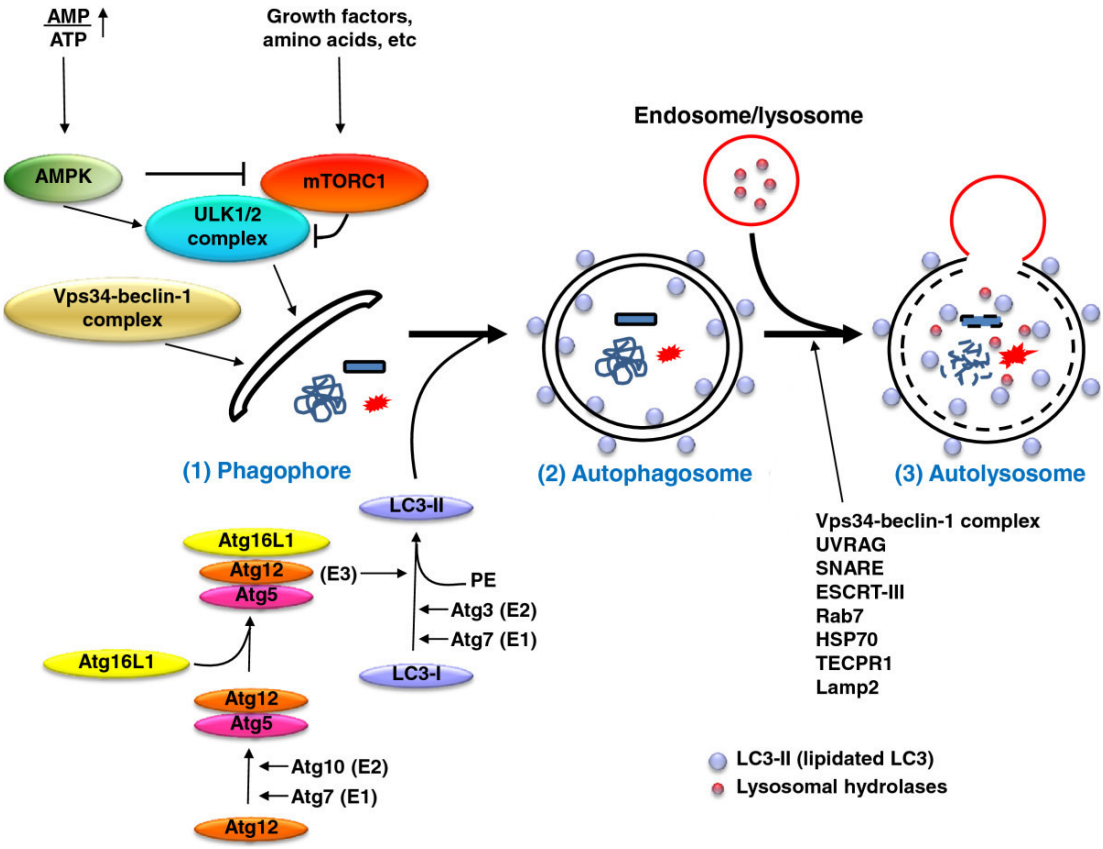

Figure 3.37: The process of autophagy with the molecular triggers for the formation of the phagophore (1), autophagosome (2) and autolysosome (3) indicated. From (Tang *et al.*, 2012), with modifications. Creative Commons Attribution License (CC-BY-2.0).

The rapid degradation of LC3-II by lysosomes during the autophagic process may pose problems for accurate detection (Martinet *et al.*, 2006b). Indeed, LC3-II can only be detected in early autolysosomes (Gukovskaya and Gukovsky, 2012). Furthermore, it has been found that due to the low abundance of the LC3-II protein detection of expression levels by Western blot are possible but other techniques, such as immunocytochemistry, may not be successful (Martinet *et al.*, 2006a). Antibodies may be less sensitive for the detection of LC3-I than LC3-II depending on tissue type and therefore normalisation of LC3-II levels should be done relative to a housekeeping protein such as β-actin and not LC3-I. However, LC3-II remains a commonly used molecular marker of autophagy (Klionsky *et al.*, 2008).

The Western blots obtained in the study (Figures 3.13 - 3.15) confirm the low abundance of LC3-II. Increased LC3-II expression was not detected in any of the treatment groups for the MCF-7 and MDA-MB-231 cell lines. From this data it is tempting to conclude that autophagy is not induced after 24 h exposure to the drug combinations. This does not exclude the possibility that autophagy may be activated earlier following drug combination exposure, as

suggested from the TEM micrographs obtained for the MDA-MB-231 cells. If the vesicles observed in the MDA-MB-231 cells are indeed autolysosomes, the degradation of LC3-II by lysosomes during such late stages of autophagy may confound Western blot results as elevated LC3-II may not be detected at this late stage of the initial response (Gukovskaya and Gukovsky, 2012). In order to fully elucidate the role of autophagy as an adaptive mechanism or in the sequence of toxicity induced by the combinations, the role of autophagy at more time points would need to be assessed.

The treatment of MCF-7 cells with the DMSO vehicle resulted in elevated levels of LC3-II which was not statistically significant (Figures 3.13 and 3.14). Vehicle-treated MDA-MB-231 cells displayed decreased levels of LC3-II (Figure 3.15). Due to the solubility profile of the compounds used during the study, a diluent was required and the commonly used amphoteric solvent DMSO was selected. For all experiments the final DMSO concentration in the cell media did not exceed 0.5%, a concentration shown to be non-toxic to cellsin culture (Friend *et al.*, 1971; Da Violante *et al.*, 2002; Chen and Thibeault, 2013). The non-significant increase in LC3-II expression due to the vehicle could potentially influence the results obtained, but as reduced LC3-II expression was observed in the majority of the treatment groups it would appear that the effect of the vehicle did not greatly influence the data obtained.

A small, non-significant increase in LC3-II expression was noted where MCF-7 cells were treated with ESE-16 (17 nM, the concentration of ESE-16 required for synergistic drug combinations with QUER, and 67 nM as required for combinations with IND)(Figures 3.13 and 3.14).This is in line with previous reports where higher concentrations of ESE-16 were used for treatment and induction of autophagy was reported:in MCF-7 breast adenocarcinoma cells after 24 h treatment with 180 nM ESE-16 (Nkandeu *et al.*, 2013), in HeLa cervical cancer cells after exposure to 500 nM ESE-16 for 24 h (Theron *et al.*, 2013) and in oesophageal SNO cells treated with 180 nM ESE-16 for 24 h (Wolmarans *et al.*, 2014). It must be noted, however, that in the present study Western blot was used, whereas flow cytometric detection of LC3-II levels and immunocytochemistry was used in the previous cited studies. In each of these reports, like in the present study, only one time point was assayed which does not fully indicate the effect of the treatments on autophagic flux. No reports on the effect of cancer cell treatment with ESE-15-ol on the induction of autophagy have yet been published.

Exposure of MCF-7 cells to IND only resulted in a slight increase in LC3-II levels (Figure 3.13). Reports on the effect of IND on autophagy are lacking; however the effect of other protease inhibitors on autophagy has been described. Nelfinavir, a potent protease inhibitor,

was shown to induce autophagy in the human oral squamous carcinoma H157 cell line at 10 μM after 16 h treatment (Gills *et al.*, 2007). However, when a combination of nelfinavir and an inhibitor of autophagy were used, increased cell death was observed suggesting a pro-survival role for nelfinavir-induced autophagy (Gills *et al.*, 2007). Similarly, induction of autophagy by another protease inhibitor, saquinavir (50 μM), was observed in ovarian cancer cell lines after only 6 h exposure (McLean *et al.*, 2009). It has been suggested that the effect of protease inhibitors on autophagy may be attributed to the induction of endoplasmic reticulum stress (Zha *et al.*, 2011).

Suppression of LC3-II expression in MCF-7 cells was observed upon exposure to the combination of ESE-15-ol and IND and ESE-15-ol only (Figure 3.13). The combination of ESE-16 and IND also resulted in reduced expression of LC3-II, suggesting that the stimulatory effect of IND on autophagy is attenuated by the addition of the oestrone analogues. A similar trend was observed in the MDA-MB-231 cell line: exposure to IND alone (55 μM) resulted in a non-significant increase in LC3-II expression while the combination of ESE-15-ol and IND caused suppression of LC3-II levels. As autophagy induced by protease inhibitors play a pro-survival role (Gills *et al.*, 2007), the inhibition of autophagy suggested by reduction in LC3-II expression by combination of oestrone analogues and IND may sensitise cells to cell death.

No changes in LC3-II levels were observed where MCF-7 cells were treated with QUER (84 μM) only (Figure 3.14). The combination of ESE-15-ol and QUER showed suppression of LC3-II expression in the MDA-MB-231 cell line in comparison to the control (Figure 3.15). Similar suppression of LC3-II expression was observed where the cells were treated with QUER only. These observations are contrary to published reports suggesting induction of autophagy after treatment with QUER (Jakubowicz-Gil *et al.*, 2010; Klappan *et al.*, 2012) and should be investigated further. However, as cell death was increased upon pre-treatment with an inhibitor of autophagy, it was proposed that QUER-induced autophagy played a pro-survival role (Wang *et al.*, 2011; Kim *et al.*, 2013). Therefore it may be deduced that abrogation of QUER-induced autophagy by the addition of oestrone analogues may sensitise malignant cells to apoptotic signals.

It must be considered that once autophagosomes merge with lysosomes during the late stages of autophagy quantification of LC3-II levels is confounded by rapid lysosomal degradation of LC3-II (Gukovskaya and Gukovsky, 2012). Therefore the increased formation of multivesicular bodies observed in the TEM micrographs for MDA-MB-231 cells exposed to combinations of QUER and IND may be indicative of the late stages of autophagy (Figure 3.12). Due to the limited sample size, variability between Western blot experiments, as seen

by the calculated standard error of the mean, may confound results. Further studies, including time course experiments, would need to be performed in order to validate this theory.

The involvement of the ROS-generating organelles, such as mitochondria and endoplasmic reticulum, in the regulation of autophagy has been elucidated (Kiššová *et al.*, 2006). In response to mitochondrial lipid oxidation by ROS, autophagy may be induced suggesting that mitochondrial ROS is instrumental in the regulation of ROS (Kiššová *et al.*, 2006). This induction of autophagy may be mediated through up-regulated expression of Beclin 1, an autophagy gene (Djavaheri-Mergny *et al.*, 2006). The role of mitochondria in autophagy induction is further supported by the observed initiation of autophagy upon accumulation of short mitochondrial form of ARF, a tumour suppressor protein (Reef *et al.*, 2006).

Mitochondria are recognised as the main producers of ATP in eukaryotic cells (Wallace and Starkov, 2000). Hydrogen ions (H^+) are transported through the electron transport chain (ETC) during the production of ATP to ultimately react with the electron acceptor, oxygen in the mitochondrial intermembrane space to form water (Osellame *et al.*, 2012). However, when electrons leak from the ETC conversion of oxygen to superoxide anion (O_2^-) occurs. $O_2^-$is the precursor for most ROS including hydrogen peroxide and hydroxyl radicals (Turrens, 2003). Due to the role of oxygen in the ETC, mitochondria are regarded as the main consumers of intracellular oxygen and decreased oxygen consumption is indicative of compromised mitochondrial function (Jiang *et al.*, 2007).

It is the inner mitochondrial membrane that is responsible for maintaining the electro-chemical proton gradient that drives the electron transport which is generally targeted by mitochondrial poisons (Wallace and Starkov, 2000). The proton accumulation across the inner membrane can be measured by the accumulation of cationic fluorescent dyes such as JC-1 (Nuydens *et al.*, 1999).The proton gradient exists as H^+ ions produced during the citric acid cycle are actively transported from the mitochondrial matrix by the electron transport chain, consisting of respiratory complexes I, II, III and IV (Hüttemann *et al.*, 2008). ATP synthase, or complex V, is connected to the ETC and utilise the influx of H^+into the mitochondrial matrix to synthesise ATP from ADP (Osellame *et al.*, 2012). The electrochemical gradient across the inner membrane is maintained using H^+ ions produced during the Krebs cycle and transport of ions and proteins into the mitochondria (Hüttemann *et al.*, 2008). It has also been proposed that protons leak into the mitochondrial matrix under normal physiological conditions (Nicholls, 1977) and that this leak is instrumental in preventing dielectric breakdown (Brand *et al.*, 1994).

Apart from its role in cellular bioenergetics, mitochondria fulfil crucial functions in the initiation of cell death: during necrosis the mitochondrial membrane permeability transition pore (MPTP) is believed to open and the irreversible commitment of cells to apoptosis are thought to be preceded by the release of cytochrome *c* from the mitochondria (Vander Heiden *et al.*, 1997; Osellame *et al.*, 2012). Theories describing the release of cytochrome *c* from the mitochondria are shown in Figure 3.38.

The depolarisation of the mitochondrial membrane often observed preceding cell death is induced by the opening of the MPTP and results in mitochondrial membrane permeability transition (Figure 3.38 b)(Tsujimoto and Shimizu, 2007). MPT occurs when the outer mitochondrial membrane becomes more permeable to solutes with molecular weights up to1 500 kDa (Ly *et al.*, 2003). The MPTP consists of the voltage-dependent anion channel (VDAC), the adenine nucleotide translocator (ANT) and cyclophilin D (CypD)(Tsujimoto and Shimizu, 2007). Once the MPTP has opened, cytochrome *c* and other apoptogenic factors including apoptosis inducing factor 1 (AIF) are released from the intermembrane space, initiating programmed cell death through the activation of the caspase cascade (Esposti and Dive, 2003).

VDAC closure has been demonstrated to cause acidification of the cytosol resulting in hyperpolarisation of the mitochondrial membrane potential (Gottlob *et al.*, 2001). The subsequent swelling and possible rupture of the mitochondria may result in the release of cytochrome *c* from the intermembrane space (Figure 3.38 a)(Desagher and Martinou, 2000). Hyperpolarisation of the inner membrane may be indicative of stimulation of the ETC, inhibition of ATP synthase (Kalbáčová *et al.*, 2003), inhibition of the inherent H^+ leak or as a result of ROS (Matsuyama *et al.*, 2000). It has been proposed that hyperpolarisation of the mitochondrial membrane potential occurs prior to release of cytochrome *c* and depolarisation of the membrane potential as indicated by the accumulation of rhodamine 123 (Vander Heiden *et al.*, 1997).

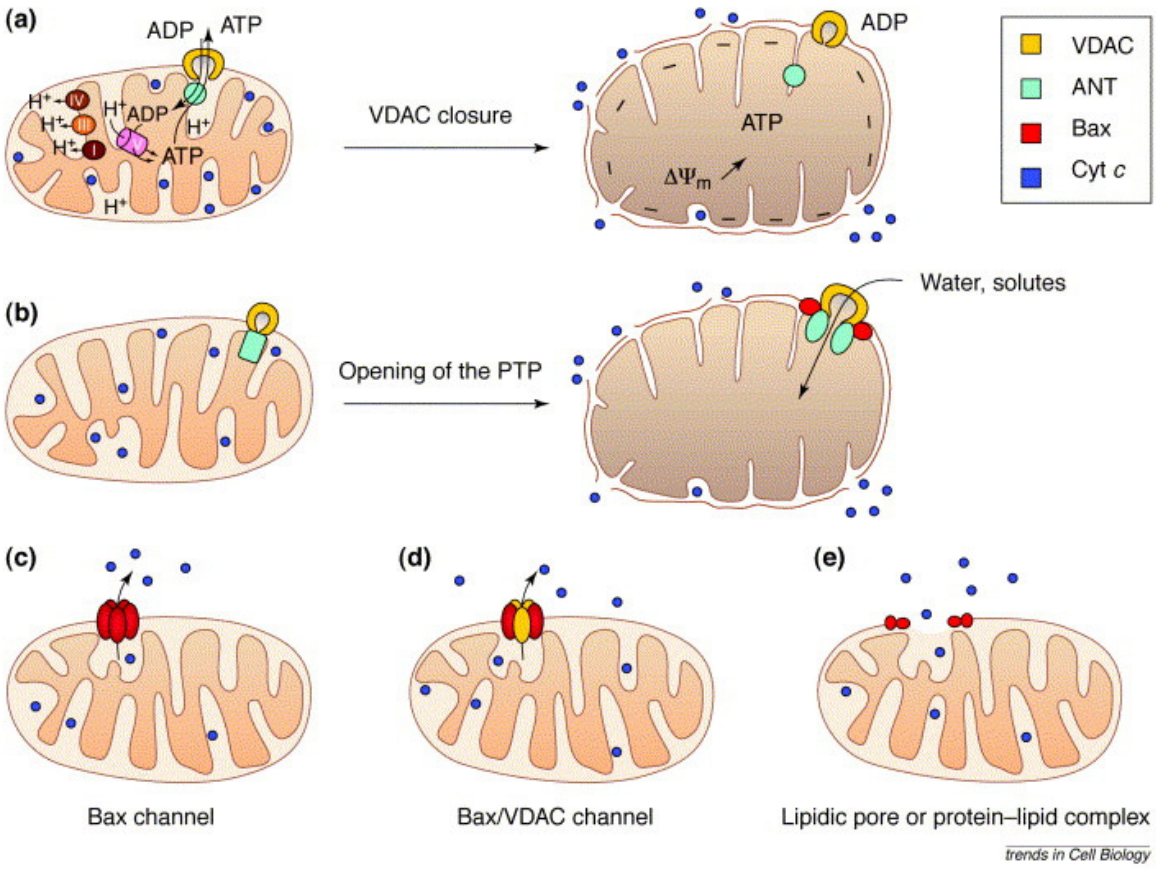

Figure 3.38: Theories on the release of cytochrome *c* from the mitochondria during apoptotic cell death. (a) Inhibition of H^+ transport from the intermembrane space to the mitochondrial matrix by complex V leads to hyperpolarisation of mitochondrial membrane potential and swelling of the mitochondria. Closure of voltage-dependent anion channel (VDAC) is also observed. When mitochondria rupture, cytochrome *c* is released from the mitochondrial intermembrane space and mitochondrial membrane potential dissipates. (b) Opening of the MPTP results in depolarisation of the mitochondrial membrane potential, swelling and rupture of the mitochondrial membrane resulting in the release of cytochrome *c*. (c-e) The formation of a channel in the outer mitochondrial membrane resulting in the release of cytochrome *c* without damage to the mitochondria. (c) Bcl-2-associated X protein (Bax) forms a channel in the outer membrane, (d) a channel is formed by the interaction of Bax and VDAC and (e) the formation of a lipid-lipid or protein-lipid channel after insertion of Bax.
From (Desagher and Martinou, 2000), used with permission. http://dx.doi.org/10.1016/S0962-8924(00)01803-1

A number of theories to explain apoptosis in the absence of hyperpolarisation of the mitochondrial membrane potential have been proposed including opening and closing of the

MPTP allowing for the release of cytochrome *c* without hyperpolarisation of the mitochondrial membrane potential (Green and Reed, 1998). It has also been postulated that members of the Bcl-2 protein family may form cytochrome *c* specific channels in the outer mitochondrial membrane which do not require opening of the MPTP and therefore do not induce loss of mitochondrial membrane potential (Desagher and Martinou, 2000; Ly *et al.*, 2003).

Depolarisation of mitochondrial membrane potential may occur upon exposure to an ETC uncoupler, due to depletion of substrates or even shortage of oxygen (Duchen, 2004). However, it is not clear whether depolarisation of the mitochondrial membrane preceding apoptosis is involved in the initiation of the process or whether it is a result of apoptotic cell death (Vander Heiden and Thompson, 1999; Sanchez-Alcazar *et al.*, 2000). Reports have shown that dissipation of the mitochondrial membrane is not required for the release of cytochrome *c* and subsequent activation of the caspase cascade (Figure 3.38 c – e)(Kluck *et al.*, 1997; Bossy-Wetzel *et al.*, 1998). Indeed, apoptosis in the presence of hyperpolarisation of the mitochondrial membrane potential has been observed *in vitro* (Sanchez-Alcazar *et al.*, 2000; Cao *et al.*, 2007). It has also been proposed that hyperpolarisation of the mitochondrial membrane due to compromised adenine nucleotide transport across the membrane occurs as a result of ATP depletion (Vander Heiden *et al.*, 1999).

Previously studies on the effect of the oestrone analogues ESE-15-ol and ESE-16 on mitochondrial membrane potential have made use of kits containing JC-1 to detect fluctuations in mitochondrial membrane potential (Stander *et al.*, 2012; Nkandeu *et al.*, 2013; Wolmarans *et al.*, 2014). JC-1 is a cationic dye and thus accumulates in mitochondria in inverse relationship to the membrane potential (Nuydens *et al.*, 1999). The use of JC-1 as a ratiometric dye has several advantages including reversible aggregate or monomer formation which is based on the state of the mitochondrial membrane (Reers *et al.*, 1991) and expanding the dynamic range available to detect fluctuations in mitochondrial membrane potential (Nuydens *et al.*, 1999).

In published reports of the effect of the oestrone analogues on mitochondrial membrane potential, sample preparation and flow cytometric detection were performed according to the manufacturer's instructions, measuring emission at only one wavelength (520 nm). Elevated levels of JC-1 monomers (λ_{em} = of 520 nm) were detected and therefore the conclusion was drawn that exposure to these compounds result in depolarization of the mitochondrial membrane (Stander *et al.*, 2012; Nkandeu *et al.*, 2013; Wolmarans *et al.*, 2014). In the present study JC-1 was also used as indicator of mitochondrial membrane potential; however the more robust ratiometric method using the emission of both the JC-1 monomers (λ_{em} = of 525 nm) and JC-1 aggregates (λ_{em} = 595 nm) detected in the same sample at the

same time was used to calculate the ratio of aggregate:monomer emission (Figures 3.16 - 3.18).

Apart from the difference in interpretation of results, previous studies based conclusions regarding the effect of the oestrone analogues on mitochondrial membrane potential using flow cytometric data with gating of the cell populations, whereas a fluorometric protocol taking all cells into account was employed in the present study. Data obtained regarding mitochondrial membrane potential from flow cytometric methods have been compared to fluorometric protocols and it has been found that even though flow cytometric methods may be more robust in detecting small changes in mitochondrial membrane potential, fluorometry provides a relatively simple method to distinguish between differences in cellular metabolism as expressed by the mitochondrial membrane potential (Kalbáčová *et al.*, 2003).

The concentrations of the oestrone analogues used in published studies differ from those in the present study: in published reports ESE-15-ol was used at a concentration of 50 nM on MCF-7 and MDA-MB-231 breast adenocarcinoma cells (Stander *et al.*, 2012), while ESE-16 was used at 180 nM on MCF-7 breast adenocarcinoma and SNO oesophageal carcinoma cells (Nkandeu *et al.*, 2013; Wolmarans *et al.*, 2014). At these concentrations depolarisation were observed in all cell lines.The highest concentration of the oestrone analogues used in the present study was 123 nM of ESE-15-ol on MDA-MB-231 cells.

In the present study mitochondrial membrane hyperpolarisation was predominant in cells treated with the oestrone analogues. Significant hyperpolarisation was observed where MCF-7 cells were treated with ESE-15-ol (70 nM) and ESE-16 (67 nM) for 24 h (Figure 3.16). After 48 h exposure hyperpolarisation was still observed, but was no longer statistically significant. In the non-tumourigenic MCF-12A cell line significant hyperpolarisation was observed after 48 h exposure to ESE-15-ol (70 nM) and ESE-16 (67 nM) (Figure 3.16). These effects were not observed where MCF-7 and MCF-12A cells were treated with the lower concentrations of ESE-15-ol (17 nM) and ESE-16 (17 nM) required for synergistic combinations with QUER (Figure 3.17). Significant hyperpolarisation of the mitochondrial membrane was not observed in MDA-MB-231 breast adenocarcinoma cells exposed to 123 nM of ESE-15-ol (Figure 3.18). However, hyperpolarisation was observed in ESE-15-ol-treated MCF-12A non-tumourigenic cells after 24 and 48 h. The hyperpolarisation became statistically significant with these cells after 48 h ESE-15-ol (123 nM) treatment.

The effect of the oestrone analogues on the mitochondria have not been studied in great detail at a molecular level, but it has been proposed that hyperpolarisation may occur in response to ROS production (Matsuyama *et al.*, 2000) as ESE-15-ol and ESE-16 reportedly increase intracellular ROS production (Stander *et al.*, 2012, 2013). This proposed effect of

ESE-15-ol and ESE-16 seem to be concentration dependent as similar observations were not made where the oestrone analogues were used at low concentrations (17 nM) as required for the synergistic drug combinations with QUER on the MCF-7 cell line.

Progressive hyperpolarisation of the mitochondrial membrane potential was observed in MCF-7 breast adenocarcinoma cells exposed to combinations with IND (Figure 3.16). A similar, but more exaggerated, hyperpolarisation was observed in samples treated with ESE-15-ol (70 nM) and ESE-16 (67 nM). However, depolarisation was observed when samples were treated with only IND which confirms previously published reports (Matarrese *et al.*, 2003; Wang *et al.*, 2009b). This suggests that the oestrone analogues abolish the effect of IND on mitochondrial membrane potential. In the absence of depolarisation of the mitochondrial membrane potential the activation of the caspase cascade may still occur as result of the interaction of Bax with the outer membrane (Figure 3.38). Antibody microarrays have indicated that ESE-16 (200 nM for 24 h) results in upregulation of Bax expression (Stander *et al.*, 2013) which indicate that the involvement of Bax in the release of cytochrome *c* from the mitochondria may be feasible but should be confirmed.

On the MDA-MB-231 cell line combinations with IND produced a different, contrasting response: after 24 h depolarisation was observed, but after 48 h hyperpolarisation of the mitochondrial membrane was observed (Figure 3.18). However, these responses were not statistically significant. For drug combination treatments on the MCF-7 cells 115 µM of IND was required, whereas only 55 µM of IND was required for drug combinations for the MDA-MB-231 cells. Even though the difference in observed effect may be attributed to differences between the cell lines used in the study, similar concentration-dependent effects on mitochondrial membrane potential have been observed for other compounds (Pasquier *et al.*, 2004; Gao *et al.*, 2005; Chatterjee *et al.*, 2008).

Hyperpolarisation of the mitochondrial membrane have been associated with inhibition of ATP synthesis (Kalbáčová *et al.*, 2003). It stands to reason that the inhibitory effect of IND on glucose transporters (Murata *et al.*, 2002; Hresko and Hruz, 2011) and the resulting depletion of intracellular glucose will result in abrogation of ATP synthesis. This effect would become more pronounced with longer exposure periods and may therefore cause the hyperpolarisation of the mitochondrial membrane observed after 48 h exposure to IND. As the concentration of IND required for synergistic drug combinations on MCF-7 cells are approximately double that used on the MDA-MB-231 cell line, cell death may be induced at different rates between the cell lines resulting in diverse observations in the intracellular parameters measured during the present study.

The decreased concentrations of oestrone analogues required for combinations with QUER elicited slight depolarisation in the MCF-7 breast adenocarcinoma cell line after 24 h which was more pronounced after 48 h incubation using drug combinations with both ESE-15-ol (17 nM) or ESE-16 (17 nM)(Figure 3.17). Significant depolarisation was observed in MCF-7 cells treated with QUER or drug combinations containing QUER after both 24 and 48 h. However, extensive depolarisation of the mitochondrial membrane potential was also observed in the non-tumourigenic MCF-12A cells treated with these compounds suggesting that the drug combinations do not exert a selective effect. The depolarisation of the mitochondrial membrane observed may precede the release of cytochrome *c* into the cytosol and the activation of the caspase cascade.

Similar results were obtained in the MDA-MB-231 breast adenocarcinoma cell line for combinations with QUER: depolarisation of the mitochondrial membrane potential was observed in QUER- or QUER drug combination-treated cells (Figure 3.18). It has been postulated that the effect of QUER on the mitochondria is due to suppression of the pro-survival Bcl-2 protein (Chou *et al.*, 2010) and up-regulation of pro-apoptotic Bax expression (Chien *et al.*, 2009). The loss of mitochondrial membrane potential was more pronounced after 24 h. It has been suggested that the activation of caspase 9 upon release of cytochrome *c* may act as a positive feedback amplification loop, resulting in further depolarisation of the mitochondrial membrane and further release of cytochrome *c* into the cytosol (Ly *et al.*, 2003). Therefore the depolarisation observed after 48 h may be a residual effect.

The Bcl-2 protein family is involved in the regulation of cell death and this relies on the interplay between pro-apoptotic, including Bax and Bcl-2 antagonist/killer protein (Bak), and anti-apoptotic signalling proteins, including Bcl-2 and B-cell lymphoma-extra large protein (Bcl-X_L)(Vander Heiden and Thompson, 1999). Bcl-2 proteins have the ability to form ion channels in lipid membranes and may therefore affect the permeability of these membranes (Schendel *et al.*, 1997). It has been demonstrated that the pro-survival Bcl-X_L proteins, such as Bcl-2, inhibit induction of apoptosis upstream of the activation of the caspase cascade by protecting the mitochondria from swelling and maintaining the integrity of the outer mitochondrial membrane (Vander Heiden *et al.*, 1997; Hitomi *et al.*, 2004). The release of cytochrome *c* therefore does not occur. The pro-apoptotic action of Bax has been attributed to its ability to induce the release of cytochrome *c* into the cytosol resulting in the activation of the caspase cascade (Rosse *et al.*, 1998). The activation of the caspase cascade is recognised as a response to irreversible cytotoxicity (van Tonder *et al.*, 2013).

The involvement of cysteine proteases in cell death was first proposed when Horvitz and colleagues successfully identified the CED-3 protein and its pivotal role in the induction of cell death in the nematode *Caenorhabditis elegans* (Yuan *et al.*, 1993). Caspases are produced as inactive pro-caspases or zymogens which are activated upon cleavage at specific aspartic acid residues (Cohen, 1997) suggesting that caspases can activate downstream zymogens. Based on the sequence of activation, caspases are referred to as initiator/signalling caspases, including caspases 2, -8, -9 and -10, or executioner/effector caspases, such as caspases 3, -6 and -7 (Figure 3.39)(Slee *et al.*, 1999).

The activation of a homogenous executioner caspases depends on the initial stimuli: the involvement of the mitochondria signals the activation of the intrinsic pathway whereas the binding of a ligand to plasma membrane receptors activates the extrinsic pathway (Degterev *et al.*, 2003). The generally accepted models of activation of the caspase cascade through the intrinsic pathway is initiated by the activation of caspase 9, while the extrinsic pathway induces caspase activation through stimulation of caspase 8 activity (Chipuk and Green, 2005).

The activation of caspase 9 is dependent on the release of cytochrome *c* from the mitochondrial intermembrane space and its interaction with Apaf-1 (Liu *et al.*, 1996; Li *et al.*, 1997). Upon binding of caspase 9 to Apaf-1 and cytochrome *c,* cleavage of procaspase 9 occurs to convert it to its active caspase 9 form. The formation of the caspase-9-Apaf-1 complex, referred to as the apoptosome, occurs only in the presence of the nucleotide precursor deoxyadenosine triphosphate (dATP) which may be substituted by ATP, suggesting that apoptotic cell death is a process during which energy is expended (Li *et al.*, 1997). Activation of caspase 9 may initiate a positive feedback loop, as it may induce depolarisation of the mitochondrial membrane potential and further activation of the caspase cascade (Ly *et al.*, 2003). The pivotal role of caspase 9 in the activation of downstream initiator caspases has been demonstrated in a cell-free system (Slee *et al.*, 1999). However, the possibility of alternative initiator caspases were demonstrated when caspase 9 deficient T-cells exposed to α-CD95 or α-CD3, T-lymphocyte specific apoptotic stimuli, resulted in apoptosis and cleavage of procaspase 3 (Hakem *et al.*, 1998).

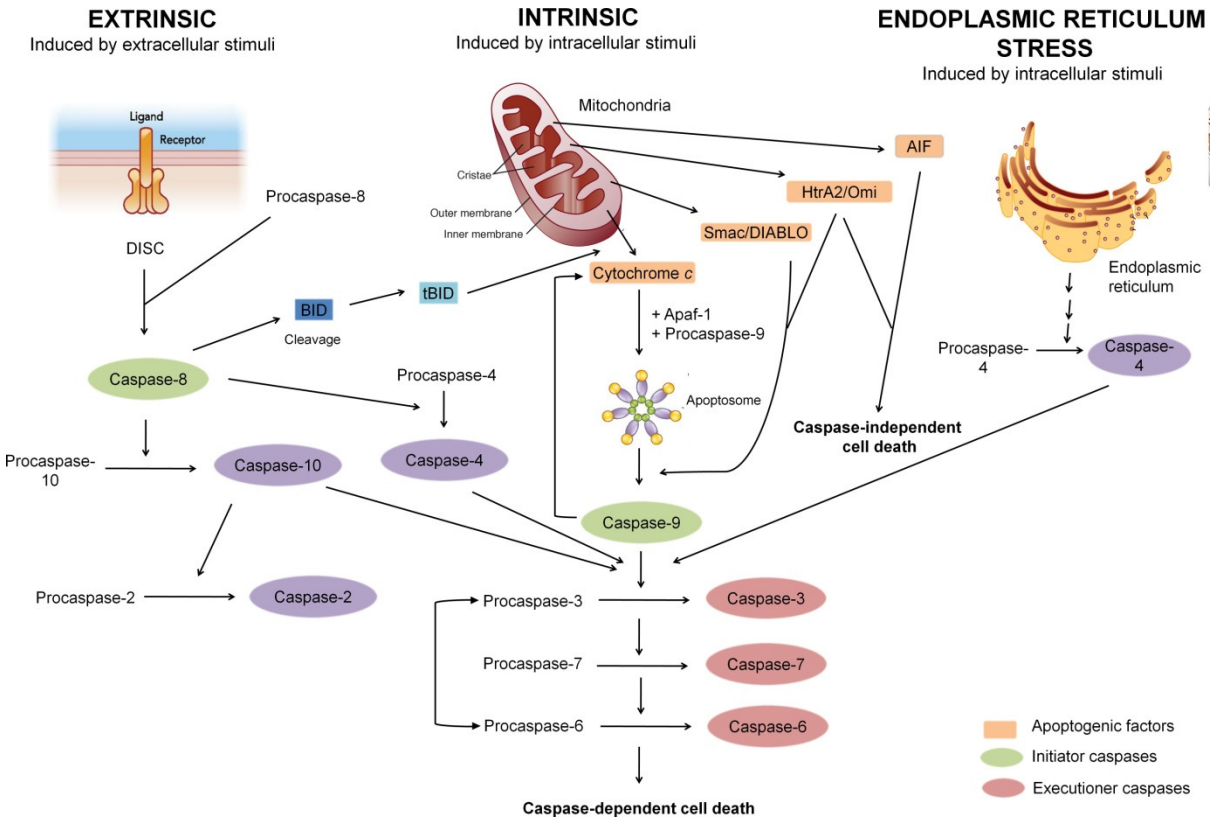

Figure 3.39: Activation of the caspase cascade. The caspase cascade may be activated by extrinsic or intrinsic stimuli. The external apoptotic pathway is induced by the binding of a ligand to a death receptor and the subsequent formation of the death-inducing signalling complex (DISC). The intrinsic apoptotic pathway is stimulated by the release of cytochrome *c* from the mitochondrial intermembrane space resulting in the activation of caspase 9 and the executioner caspases. Caspase 6 may assume the role of executioner caspase instead of caspase 3. Various other apoptogenic factors may be released from the mitochondria including Smac/DIABLO and HtrA2/Omi resulting in the activation of the caspase cascade. Endoplasmic reticulum stress may cause activation of caspase 4 resulting in activation of caspase 3. Caspase-dependent cell death, apoptosis, results from the activation of executioner caspases. Apoptotic factors released from the mitochondria, like apoptosis inducing factor (AIF), may activate the caspase cascade or cause caspase-independent cell death.

Structures of DISC and apoptosome from Sendoel and Hengartner, 2014. (Sendoel and Hengartner, 2014) with modifications. Creative Commons Attribution License (CC-BY-2.0). Structures of mitochondria and endoplasmic reticulum by Darryl Leja, NHGRI, www.genome.gov. Accessed September 2015.

The activation of the caspase cascade in the absence of cytochrome *c* has been attributed to the release of alternative pro-apoptotic factors including Smac/Diablo (Du *et al.*, 2000; Verhagen *et al.*, 2000) and high-temperature requirement protein A2 (HtrA2)/Omi (Suzuki *et al.*, 2001). Abrogation of the function of inhibitor of apoptosis proteins (IAP) by Smac/Diablo and HtrA2/Omi results in the activation of caspase 9 and the cleavage of downstream caspases (Du *et al.*, 2000; Suzuki *et al.*, 2001). HtrA2/Omi may also contribute to caspase-independent cell death (Suzuki *et al.*, 2001).

The extrinsic apoptotic pathway is initiated upon the binding of a suitable ligand to a death receptor, activation of the intracellular domain of the receptor occurs resulting in the formation of the death-inducing signalling complex (DISC)(Degterev *et al.*, 2003). DISC formation following ligand binding of the CD95/Fas receptor has been described best: the intracellular death domain of stimulated CD95/Fas receptors, Fas-associated death domain protein (FADD) and procaspase 8 are essential for the formation of DISC. Once recruited into DISC the zymogen is activated to caspase 8 (Medema *et al.*, 1997). It has been suggested that procaspase10 may alternatively be activated by recruitment into DISC (Kischkel *et al.*, 2001). Apoptosis induced by caspase 8 may be a consequence of its direct activation of downstream executioner caspases including caspase 3 and -7 or through cleavage of BH3 interacting-domain protein (BID)(Scaffidi *et al.*, 1998).

As caspases 1, -4 and -5 are not activated upon release of cytochrome *c* into the cytosol, it has been suggested that the possible involvement of these caspases in cell death relies on other stimuli (Slee *et al.*, 1999). Caspases 4 and -5 are activated by cytosolic lipopolysaccharide resulting in the induction of pyroptotis, programmed cell death induced by inflammation. Activated caspases 4 and -5 have been implicated in the cleavage of procaspase1 (Vanaja *et al.*, 2015).

Caspase 4 has been implicated in endoplasmic reticulum (ER) stress-induced apoptosis and the localisation of this protease to the ER supports this hypothesis (Hitomi *et al.*, 2004). The activation of caspase 4 occurs downstream of the mitochondria, implying that it is not activated by caspases 9 or -3, and is caused by well-known inducers of ER stress in human SK-N-SH neuroblastomacells. Other apoptotic stimuli that do not affect ER stress do not cause activation of caspase 4 (Hitomi *et al.*, 2004). However, Fas-mediated activation of caspase 8 may also result in activation of caspase 4 and downstream activation of caspase 3 (Kamada *et al.*, 1997).

During the induction of apoptosis three possible executioner caspases, caspase 3, -6 or -7 may be activated downstream of the initiator caspases (Cohen, 1997; Hitomi *et al.*, 2004). The possibility of multiple executioner caspases has been suggested as γ irradiation of

caspase 3 deficient thymocytes and splenocytes still resulted in the induction of apoptosis (Hakem *et al.*, 1998). Furthermore the externalisation of phosphatidylserine, an indicator of apoptosis, and cleavage of poly(ADP-ribose)polymerase (PARP) were detected in caspase 3 deficient mouse embryonic fibroblasts (Woo *et al.*, 1998).

Caspase 3, a key executioner caspase, is responsible for the cleavage of poly (ADP-ribose) polymerase (PARP) to form an 85 kDa fragment (Tewari *et al.*, 1995). As PARP has been implicated in DNA repair mechanisms (Miller, 1975), proteolytic cleavage of PARP results in irreversible DNA damage. Caspase 3 activity has been directly linked to not only DNA fragmentation but also to morphological features of apoptosis (Jänicke *et al.*, 1998). The contrasting role of caspase 3-induced apoptosis or survival has been demonstrated in caspase 3 deficient mouse models: caspase 3 deficient mice showed marked shortened lifespan due to impaired neural development, although the development of T- and B-cells remained unaffected (Woo *et al.*, 1998). It has recently been observed that caspase 3 is required for maintenance of neural plasticity (Lo *et al.*, 2015). Thus the role of caspase 3 is highly tissue- and cell type specific.

Due to the level of conservation in their peptide sequences, there is a high level of substrate overlap between caspases 3 and -7 (Cohen, 1997; Porter and Jänicke, 1999). In the absence of caspase 3, activation of caspases 6 and -7 may be involved in induction of apoptosis. Nuclear fragmentation and the formation of apoptotic bodies were evident in the absence of caspase 3 activation, suggesting that caspase 3 is not solely responsible for the characteristics defining apoptotic cell death (Liang *et al.*, 2001). It has been suggested that caspase 3 may be involved in the activation of caspase 6; alternatively caspase 6 may cleave procaspase 3 resulting in caspase 3 activation (Cohen, 1997).

It has been reported that MCF-7 breast adenocarcinoma cells do not express caspase 3 (Jänicke *et al.*, 1998; Jänicke, 2009). This was concluded after procaspase 3 and DNA fragmentation could not be detected after MCF-7 cells were treated with staurosporine for 16h (Jänicke *et al.*, 1998). However, several reports indicate the presence of caspase 3 in MCF-7 breast adenocarcinoma cells using Western blot (Nizamutdinova *et al.*, 2008; Yeruva *et al.*, 2008; Wang *et al.*, 2009a; Gan *et al.*, 2015; Pang *et al.*, 2015). It has been suggested that karyotype studies be performed to determine the expression of caspase 3 in the original MCF-7 breast adenocarcinoma cell line (Jänicke, 2009). However, as the substrate preference of caspases 3 and -7 overlap, the fluorogenic substrate used in the present study cannot distinguish the activity of caspase 3 from that of caspase 7 (Porter and Jänicke, 1999).

A previous study using antibody microarrays to detect protein expression levels have demonstrated that treatment with ESE-16 (200 nM for 24 h) resulted in upregulation of caspase 4 and caspase 7 in the MDA-MB-231 breast adenocarcinoma cell line (Stander *et al.*, 2013). Another study showed elevated activity of caspases 3 and -8 in HeLa cervical adenocarcinoma cells after 24 h exposure to 500 nM ESE-16 (Theron *et al.*, 2013). This suggests activation of the extrinsic pathway of apoptosis where activation of caspase 8 may result in activation of caspase 4 with the subsequent activation of the executioner caspases (Kamada *et al.*, 1997). However, activation of caspase 4 has also been identified as a consequence of ER stress (Hitomi *et al.*, 2004).

2-Methoxyestradiol (2ME), the parent compound of the oestrone analogues used in this study, has been shown to induce apoptosis via the extrinsic pathway in MDA-MB-231 breast adenocarcinoma cells (LaVallee *et al.*, 2003a). Treatment with 2ME (2 µM for 24 or 48h) resulted in elevated expression of death receptor 5, one of the death receptors involved in the activation of DISC and procaspase 8, resulting in activation of caspases 8, -9 and -3 (LaVallee *et al.*, 2003a). The activation of caspase 9 may be a downstream event initiated by the cleavage of BID by caspase 8, resulting in depolarisation of the mitochondrial membrane potential, release of cytochrome *c* and activation of caspase 9 (Li *et al.*, 1998). However, the activation of caspase 9 induced by 2ME (LaVallee *et al.*, 2003b) may indicate that both the intrinsic and extrinsic pathways are involved in 2ME-induced apoptosis.This has been demonstrated in cell-based studies (Gao *et al.*, 2005; Basu *et al.*, 2006).

In the present study the activity of the initiator caspases 8, -9 and the executioner caspase 3/7 was investigated using fluorogenic caspase substrates. A disadvantage of the use of fluorogenic caspase substrates is the overlap between substrates specificities. Commonly used substrates selective for caspase 8 (Ac-IETD-AMC), caspase 9 (Ac-LEHD-AFC) and caspase 3/7 (Ac-DEVD-AFC) were used. However, it has been shown that the IETD substrate may also be cleaved by caspases 9 and -10 and that caspases 6 and -8 may also cleave the DEVD-substrate (Stennicke and Salvesen, 1999). It has also been shown that caspase 8 has a high affinity for the LEHD-substrate (Talanian *et al.*, 1997). As many of the caspases showing overlapping substrate specificities are involved in different pathways of cell death induction, results obtained with fluorogenic substrates may confound conclusions.

It must be considered that untreated cells are not expected to exhibit extensive caspase activity and therefore the caspase activity observed in the untreated control represents the basal caspase activity. Where reduced caspase activity is observed in treated groups in comparison to the untreated control, this may indicate an experimental artefact, such as quenching or decreased cell number, or may be a true inhibition of caspase activity. In the

present study caspase activity was not standardised to protein content, but rather relied on the use of the same cell number. Based on the GI_{50} concentrations obtained for the experimental compounds after 24 and 72 h exposure (Table 2.2) it may be assumed that loss of cell number may be involved in the reduction in fluorescent signal detected with the caspase assays after 24 and 48 h. However, this must be confirmed. As it is not clear why a reduction in fluorescent signal was observed in some of the treated groups, the discussion will focus on the elevations in caspase activity observed.

The results observed in this study showed that activity of caspase 8 was elevated in the MCF-7 breast adenocarcinoma cell line exposed to ESE-15-ol (70 nM) and ESE-16 (67 nM); although these increases were not statistically significant (Figure 3.19). Exposure of MCF-7 cells to the lower concentrations of oestrone analogues as required for synergistic drug combinations with QUER for 24 h resulted in suppression of caspase 8 activity (Figure 3.21). A concentration dependent activation of caspase 8 in the MCF-7 cell line was thus observed. These results may suggest that activation of the extrinsic pathway in MCF-7 cells may be a transient response to treatment with the oestrone analogues. Increased activation of caspase 8 was not observed in the MCF-12A non-tumourigenic cell line suggesting that the extrinsic pathway was not induced and implying that the oestrone analogues induce the activation of caspase 8 selectively.

In contrast, where MDA-MB-231 cells exposed to 123 nM of ESE-15-ol, as required for synergistic drug combinations on the MDA-MB-231 breast adenocarcinoma cell line, reduced caspase 8 activity was observed (Figure 3.23 and 3.24). Even though inhibition of caspase activity should be further assessed, data suggest that the extrinsic pathway is not activated in the MDA-MB-231 cell line after exposure to ESE-15-ol. Cell line specific induction of caspases in response to treatment with the oestrone analogues has been demonstrated as the activation of caspases 4 and -7 was observed in the MDA-MB-231 cell line after treatment with ESE-16, but not in the MCF-7 cell line (Stander *et al.*, 2013).However, the difference in concentrations required for the drug combinations on the two cell lines may also affect the activity of caspase 8.

Activity of caspase 9 was suppressed after MCF-7 breast adenocarcinoma cells were treated with 70 nM ESE-15-ol, the concentration required for synergistic drug combination with IND (Figures 3.19 and 3.20). However, where MCF-7 cells were exposed to 17 nM ESE-15-ol, the drug concentration required for combinations with QUER, elevated caspase 9 activity was observed after 24 h treatment (Figure 3.21) implying activation of the intrinsic apoptosis pathway. The elevation of caspase 9 activity was not statistically significant. This correlates with the depolarisation of mitochondrial membrane potential observed when MCF-

7 cells were treated with 17 nM ESE-15-ol for 48 h: activation of caspase 9 may cause depolarisation of the mitochondrial membrane potential and subsequent cytochrome *c* release in to the cytosol (Ly *et al.*, 2003). However, the potential induction of the intrinsic pathway by ESE-15-ol may be cell line specific as caspase 9 activity in the MDA-MB-231 cell line remained largely unaffected by treatment with ESE-15-ol.

Treatment of MCF-7 cells with ESE-16 (67 nM), required for synergistic drug combination with IND, resulted in slightly elevated caspase 9 activity after 24 h (Figure 3.19). After 48 h treatment the caspase 9 activity levels were comparable to that of the untreated control. The lower concentration of ESE-16 (17 nM), required for combinations with QUER, did not induce marked fluctuations in the activity of caspase 9 in MCF-7 cells (Figures 3.21 and 3.22). It is therefore proposed that ESE-16 does not induce the activation of the intrinsic pathway.

The activity of the executioner caspase, caspase 3 was assessed. As the substrate preference for caspases 3 and -7 overlap substantially (Porter and Jänicke, 1999) the results from the present study cannot distinguish between the activation of these two executioner caspases. In the MCF-7 adenocarcinoma cell line elevated caspase 3/7 activity was only observed where cells were treated with 17 nM of the oestrone analogues, the concentrations required for synergistic drug combinations with QUER. Similarly, caspase 3/7 activity remained largely unaffected in the MDA-MB-231 cell line after exposure to ESE-15-ol. This data conflicts with published studies showing increased caspase 3/7 activity after treatment with the oestrone analogues (Stander *et al.*, 2013; Theron *et al.*, 2013). Unlike in published reports, results obtained in the present study for caspase activity assays were unfortunately not standardised to protein content and therefore the potential decrease in cell number upon extended treatment was not taken into account.

However, an alternative executioner caspase, such as caspase 6, may also be involved. As the activity of caspase 6 was not investigated during this study its involvement in cell death induced by treatment with the oestrone analogues remains unconfirmed. The activation of the caspase cascade by other apoptogenic factors may also play a role. However, the effect of ESE-15-ol and ESE-16 on apoptogenic factors such as cytochrome *c*, Smac/DIABLO, HtrA2/Omi and AIF has not been established.

Where the oestrone analogues were combined with IND the effect on caspase activity on the MCF-7 breast adenocarcinoma cells were altered compared to the effect of the oestrone analogues alone. A transient elevation in the activity of caspase 8 was demonstrated by the combinations of oestrone analogues and IND (Figures 3.19 and 3.20). After 24 h treatment a slight increase in the activity of caspases 9 and -3/7 was observed in the drug combination

treated MCF-7 cells. Upon treatment with IND or drug combinations of oestrone analogues and IND, the mitochondrial membrane potential of MCF-7 cells remained unaltered implying that cytochrome *c* had not been released, or had been released through a MPT independent mechanism (Figure 3.38). Data suggests that the extrinsic pathway may be activated resulting in the cleavage of caspase 8.

In the MDA-MB-231 cell line elevated caspase 8 activity was not observed when cells were treated with IND or the drug combinations of ESE-15-ol and IND. The activation of the extrinsic pathway by IND may thus be cell line- or concentration-dependent. Approximately double the concentration of IND used for drug combinations in the MDA-MB-231 cell line (55 µM) was required for synergistic drug combinations on the MCF-7 cell line (115 µM). Transient increases in the activity of caspases 9 and -3/7 were observed after MDA-MB-231 cells were treated with IND or the combination of ESE-15-ol and IND (Figure 3.23). The combination of ESE-15-ol and IND increased the activity of caspase 3/7 after 24 h exposure in the MDA-MB-231 breast adenocarcinoma cell line. However, the observed increase was not statistically significant.

Initially it was proposed that protease inhibitors, including IND, may inhibit the activity of the caspase cascade; however as HIV protease is an aspartyl protease and caspases are cysteine proteases this is unlikely (Badley, 2005). It has been demonstrated that activity of caspases 3, -6 and -8 was not abrogated in puromycin-induced apoptosis in human macrophage U937 cells treated with IND (100 nM for 4 h)(Ghibelli *et al.*, 2003). However, elevation of caspase activity was also not observed in that study. Another study confirmed these results: IND treatment (12.5 – 100 mM for 2 h) had no inhibitory effect on caspases 1, -3, -4, -5, -9 and -8 in Jurkat human T-cell leukaemia cells, but increased caspase activity was not observed (Chavan *et al.*, 2001). The treatment periods used in the present study before of caspase activity assessment was performed differ substantially from the treatment periods used in the aforementioned studies and may explain the dissimilar results obtained.

In contrast to IND, elevated caspase activity in response to QUER has been reported. QUER (250 µM) induces the activity of caspases 3, -8 and -9 in MDA-MB-231 cells after 24 h exposure (Chien *et al.*, 2009). Treatment of HepG2 hepatocellular carcinoma with QUER for 18 h did not induce dose dependent activation of caspases 3, -8 and -9: activation of the caspases was increased significantly after 50 µM QUER exposure but the effect was less pronounced at 75 µM QUER exposure (Granado-Serrano *et al.*, 2006).

In the present study QUER (84 µM required for combinations on MCF-7 cells) induced caspase 3/7 activation in MCF-7 cells, but not that of caspase 8, after 24 h exposure (Figure 3.21). The elevation in caspase 8 observed in QUER-treated cells was not statistically

significant. No effect on the activity of caspase 9 was observed in QUER-treated cells after 24 h. After 48 h QUER exposure reduced the activity of all the caspases tested in MCF-7 cells. The results of Granado-Serrano and colleagues suggest that activation of the caspase cascade in response to QUER treatment is influenced by the concentration of QUER used and that the concentration used in the present study may have exceeded a concentration where an effect on caspase activity may be observed (Granado-Serrano *et al.*, 2006). However, the finding of Granado-Serrano and colleagues may be a cell line specific observation. A similar lack of effect on the activity of the tested caspases was observed in MDA-MB-231 cells treated with QUER (0.64 µM) only (Figures 3.23 and 3.24). This may be explained by the low concentration of QUER used as required for synergistic drug combinations on the MDA-MB-231 cell line.

The activation of the caspase, as indicated by the elevated activity of caspases 9 and -3/7 (Figure 3.21), when QUER (84 µM) was combined with the oestrone analogues on MCF-7 breast adenocarcinoma cells result from the release of cytochrome *c* from the mitochondrial intermembrane space and the significant depolarisation of the mitochondrial membrane potential observed. Data from the present study thus indicates the activation of the intrinsic pathway of apoptosis by these drug combinations.

Where MDA-MB-231 breast adenocarcinoma cells were treated with the combination of ESE-15-ol (123 nM) and QUER (0.64 µM), decreased caspase 9 activity was observed suggesting that the intrinsic or mitochondrial pathway is not induced by the combination (Figure 3.23). However, the depolarisation of the mitochondrial membrane potential observed after MDA-MB-231 cells were treated with the combination of ESE-15-ol and QUER, suggest initiation of caspase activation through cytochrome *c* release. This may imply that caspases other than those assessed during the present study are involved in cell death induced by this drug combination, or that alternative apoptogenic factors, such as HtrA2/Omi or AIF, were released from the mitochondria resulting in cell death via caspase-independent mechanisms. The ability of QUER treatment (25 µM for 24 h) to induce the release of HtrA2/Omi from the mitochondrial intermembrane space of human leukemic monocyte lymphoma U937cells has been demonstrated (Ramos and Aller, 2008). The release of HtrA2/Omi may result in the activation of caspase 9 and cleavage of downstream caspases, or the induction of cell death via caspase-independent mechanisms (Du *et al.*, 2000; Suzuki *et al.*, 2001). Similarly the release of AIF from the mitochondria after treatment with QUER (250 µM for 24 h) has been demonstrated in MDA-MB-231 cells which may result in caspase-independent cell death (Chien *et al.*, 2009).

Several mechanisms of caspase-independent cell death have been identified. Caspase-independent cell death (CICD) has been described as the induction of apoptosis in response to apoptotic stimuli in the absence of caspase activation (Chipuk and Green, 2005). Mitochondrial membrane depolarisation may not occur during CICD; alternatively depolarisation of mitochondrial membrane potential may occur at a slower rate than during the induction of apoptosis. A number of distinct differences between apoptosis and CICD have been proposed: a cell undergoing CICD will not stain annexin V-FITC positive and may appear vacuolated (Chipuk and Green, 2005). The formation of apoptotic bodies may not occur during this mode of cell death (Jaattela and Tschopp, 2003). Crucially, the inducers of caspase-independent cell death that have been identified are regulated by various intracellular signalling pathways; thus unlike necrosis this mode of cell death is closely regulated (Bröker *et al.*, 2005).

Induction of cell death through AIF eliminates the requirement for activation of caspases (Bai *et al.*, 2015). Pro-apoptosis Bax is involved in the release of both cytochrome *c* and AIF from the mitochondrial intermembrane space, but the release of cytochrome *c* precedes that of AIF and it has been suggested that the release of these apoptotic factors are independent and occur via different mechanisms (Cregan *et al.*, 2002). The release of AIF from the mitochondria is dependent on the depolarisation of mitochondrial membrane potential (Cregan *et al.*, 2002). AIF has also been implicated in the caspase-independent externalisation of phosphatidylserine (Yu *et al.*, 2002).

Morphological assessment of cell death often underestimates the extent of cell death as the cells in the early stages of cell death may not differ in appearance from their viable counterparts and cell fractions remaining after completion of cell death pathways are not easily detectable (Galluzzi *et al.*, 2009). The plasDIC images obtained during this study (Figures 3.25 and 3.27) for MCF-7 breast adenocarcinoma cells exposed to the combinations of oestrone analogues and glycolysis inhibitors for 72 h show reduced cell density and the formation of intracellular vacuoles (especially in MCF-7 cells treated with the QUER and drug combinations with QUER). Formation of multivesicular bodies were observed using TEM after 24 h exposure to the drug combinations (Figures 3.10 and 3.11). This resembles the vacuole formation observed after 72 h exposure to the drug combinations as observed by plasDIC and may suggest the induction of autophagy after 72 h treatment.

Cell rounding observed indicate that the drug combinations induce the sequence of toxicity. Similar morphological changes were observed in MDA-MB-231 cells exposed to the drug combinations of ESE-15-ol and IND or QUER (Figure 3.29). Unfortunately decreased cell

density, cell rounding and vacuole formation is also observed in the MCF-12A non-tumourigenic cell line exposed to drug combinations with IND and QUER implying that the toxic response elicited by the combinations are not selective for cancer cells (Figure 3.30). Cell debris was also evident in treated MCF-12A cells implying cell death of some cells.

To further assess the ability of the combinations to induce cell death, the induction of apoptosis and necrosis was investigated in the present study using a flow cytometric protocol. Phosphatidylserine externalisation is regarded as a specific molecular marker of initiation of apoptosis and attracts phagocytes to removal of the dead cell without inducing inflammatory processes (Willingham, 1999). However, during the late stages of apoptosis or during necrosis membrane integrity is lost and intercellular phosphatidylserine may also be detected using labels such as annexin V-FITC (Willingham, 1999). In the present study co-staining with PI, an indicator of cell membrane integrity, was performed to address this issue.

Externalisation of phosphatidylserine (PS) is indicative of the initiation of apoptosis, but cannot provide information regarding upstream apoptosis induction (Ferraro-Peyret *et al.*, 2002). In the presence of various caspase inhibitors PS translocation was observed in peripheral blood lymphocytes treated with etoposide or staurosporine indicating that activation of the caspase cascade is not a requirement for the PS flip (Ferraro-Peyret *et al.*, 2002).

Previous reports have shown that ESE-15-ol and ESE-16 induce apoptosis in cancer cells. After MCF-7 and MDA-MB-231 breast adenocarcinoma cells were exposed to 50 nM of ESE-15-ol for 48 h, apoptotic cell death was observed in more than 60% of exposed cell populations (Stander *et al.*, 2012). Approximately 35% of MCF-7 and MDA-MB-231 breast adenocarcinoma cells exposed to ESE-16 (200 nM for 48 h) stained positive with annexin V-FITC indicating apoptotic cell death (Stander *et al.*, 2013). Similar results were observed in SNO oesophageal cancer cells after treatment with ESE-16 (180 nM for 24 h)(Wolmarans *et al.*, 2014) and in HeLa cervical adenocarcinoma cells treated with ESE-16 (500 nM for 24 h) (Theron *et al.*, 2013). Induction of cell death in response to treatment with ESE-15-ol or ESE-16 was observed in the MCF-7 and MDA-MB-231 cells in the present study, confirming published reports.

In the present study exposure of MCF-7 breast adenocarcinoma cells to ESE-15-ol (70 nM) for 72 h resulted in a 75% reduction in cell viability (Table 3.2).The lower concentration of ESE-15-ol (17 nM), as required for combinations with QUER, decreased cell viability by only 15% (Table 3.3). A similar trend was observed with ESE-16-exposed MCF-7 cells: where cells were exposed to 67 nM of ESE-16, as required for combinations with IND, cell viability was decreased by approximately 50% while a reduction of only 22% was observed at 17 nM

of ESE-15-ol. Results thus indicate that MCF-7 cells are more susceptible to treatment with ESE-15-ol. This is not surprising as the growth inhibition studies indicated superior potency of ESE-15-ol (Table 2.2).

MDA-MB-231 breast adenocarcinoma cells exposed to 123 nM of ESE-15-ol showed a reduction in cell viability of approximately 39% (Table 3.4). However, a greater reduction in cell viability was observed where MCF-7 cells were exposed to 70 nM of ESE-15-ol suggesting a cell-specific sensitivity to ESE-15-ol. These data confirm results of the SRB assay after 72 h (Table 2.2).

The cell death induced by the oestrone analogues on the MCF-7 and MDA-MB-231 cell lines was predominantly apoptosis. Approximately 58% of MCF-7 cells exposed to 70 nM of ESE-15-ol were observed to undergo apoptosis, while only 17% of ESE-15-ol-exposed cells were necrotic (Table 3.2). A similar trend was observed for MCF-7 cells exposed to 67 nM ESE-16 and MCF-7 cells exposed to 17 nM of ESE-15-ol or ESE-16 (Tables 3.2 and 3.3).

A significant reduction of approximately 85%of viable cells was observed in MCF-7 cells exposed to the combination of ESE-15-ol and IND (Table 3.2). This combination caused predominantly apoptotic cell death, which exceeded that observed in the cells treated with ESE-15-ol or IND alone: the combination of ESE-15-ol and IND reduced the viable population of MCF-7 cells from 25 to 15%.The effect of ESE-15-ol and the combination of ESE-15-ol and IND was more pronounced than that observed for ESE-16 and the drug combinations of ESE-16 and IND. Approximately 56% of the MCF-7 cells exposed to the combination of ESE-16 and IND was viable after 72 h exposure. Interestingly the necrotic population of MCF-7 cells exposed to the combination of ESE-15-ol and IND (12%) and that of the combination of ESE-16 and IND (13%) correlated well (Table 3.2).

In the MDA-MB-231 breast adenocarcinoma cell line the combination of ESE-15-ol and IND decreased cell viability to a greater extent than the compounds separately (Table 3.4). Interestingly, the necrosis induced in MCF-7 and MDA-MB-231 cells by IND was mitigated by the addition of ESE-15-ol. As necrosis is associated with inflammation and the formation of scar tissue (Willingham, 1999), mitigated necrosis may produce a more favourable response *in vivo.*

Data obtained in the present study confirms limited previously published reports on the pro-apoptotic properties of IND. It has been shown that IND at 5 – 50 µM induces apoptosis in Jurkat cells after 24, 48 or 72 h exposure (Chavan *et al.*, 2001). It has been suggested that IND treatment may induce ER stress (Zha *et al.*, 2011) and prolonged ER stress has been identified as a pro-apoptotic event (Rao *et al.*, 2006).

It has been reported that QUER treatment (12.5 – 200 µM for 72 h) induced apoptotic cell death in a dose dependent manner in the MCF-7 breast adenocarcinoma cell line (Duo *et al.*, 2012). The induction of DNA fragmentation in MDA-MB-231 cells after treatment with 200 µM QUER for 48 h suggests the induction of apoptosis (Chien *et al.*, 2009). It has been found that QUER exerts its pro-apoptotic effect via two distinct pathways: through the activation of the caspase cascade and by induction of ER stress resulting in caspase-independent apoptosis (Chou *et al.*, 2010).

The pro-apoptotic effect of QUER is confirmed by the results obtained in the present study as exposure to QUER (84 µM) resulted in the induction of apoptosis (approximately 50%) in the MCF-7 breast adenocarcinoma cell line (Table 3.3). Necrotic cell death was also observed. Even though apoptotic cell death (approximately 8%) was also observed in MDA-MB-231 cells exposed to QUER, the reduced response may be due to the lower concentration of QUER used (0.64 µM)(Table 3.4). QUER-treatment also resulted in necrotic cell death in the MCF-7 and MDA-MB-231 cell lines.

Where ESE-15-ol was combined with QUER on the MCF-7 breast adenocarcinoma cell line, cell viability was reduced from approximately 29% with QUER-treatment to approximately 22% (Table 3.4). Cell death was induced via apoptosis and necrosis. Exposure of MCF-7 cells to the combination of ESE-16 and QUER did not result in greater induction of cell death than was achieved by QUER treatment alone. The induction of cell death via apoptosis or necrosis was more pronounced in cells treated with the combination of ESE-15-ol and QUER (approximately 22% viable cells) than the combination of ESE-16 and QUER (approximately 32% viable cells). However, where cells were exposed to the combinations of oestrone analogues and QUER an increase in necrotic cells was observed in comparison to QUER-treated cells.

A similar trend was observed in MDA-MB-231 cells treated with QUER (0.64 µM): the viable cell population was reduced by approximately 20% by QUER treatment alone, but a reduction of approximately 37% was observed where cells were treated with the combination of ESE-15-ol and QUER (Table 3.4). The induction of apoptotic cell death corresponds to the activation of the caspase cascade observed, while the increased necrotic population may be the result of caspase-independent mechanisms.

Unfortunately increased cell death was observed where MCF-12A non-tumourigenic cells used as a surrogate of normal cells were exposed to the oestrone analogues or combinations of oestrone analogues and glycolysis inhibitors (Tables 3.2 – 3.4). Where MCF-12A cells were treated with ESE-15-ol (70 nM) or ESE-16 (67 nM) for 72 h cell viability was reduced by approximately 45%and 23%, respectively (Table 3.2). At the lower

concentrations of the oestrone analogues required for combinations with QUER, the viability of MCF-12A cells were reduced by approximately 10% only.

Combinations of oestrone analogues and IND reduced viability of MCF-12A cells to a greater extent than each compound by itself suggestingenhanced cytotoxicity (Table 3.2). The combination of ESE-15-ol (70 nM) and IND (115 µM) resulted in the greatest induction of apoptosis (approximately 45%) while exposure to the combination of ESE-16 (67 nM) and IND (115 µM) resulted in approximately 7% necrosis. In contrast to the combinations with IND, the combination of ESE-16 (17 nM) and QUER (84 µM) affected MCF-12A cells to the greatest extent: cell viability was reduced by approximately 50%, apoptosis induced in approximately 45% of the population and necrotic cell death induced in approximately 3% of the population (Table 3.3).

However, MCF-12A cells were most affected by the combinations required for synergy on the MDA-MB-231 cell line: the viability of MCF-12A cells were decreased by approximately 90% after exposure to the combination of ESE-15-ol (123 nM) and IND (55 µM) and approximately 80% after exposure to the combination of ESE-15-ol and QUER (0.64 µM) (Table 3.4). The greatest induction of necrosis (approximately 25%) in MCF-12A cells was caused by exposure to 123 nM of ESE-15-ol, as required for combinations on the MDA-MB-231 cell line. Data suggests that the combinations specific for the MDA-MB-231 cell line may not exert a selective effect on cancer cells and this may result in a poor side effect profile in the clinical setting.

From the data obtained in this study, a mechanism of cell death induced by the combinations of oestrone analogues with IND (Figure 3.40) and QUER (Figure 3.41) are proposed. In order to simplify the proposed sequence of toxicity induced by the drug combinations, results obtained on the MCF-7 and MDA-MB-231 cell lines from the present study were combined.

During the sequence of toxicity induced by the combinations of oestrone analogues and IND, data suggests that the induction of cell death may occur via the extrinsic apoptotic pathway and not the intrinsic pathway that appears to be activated by IND alone (Figure 3.40). Published reports indicate that the oestrone analogues induce cell death via the extrinsic pathway (Theron *et al.*, 2013). Therefore crosstalk between the intracellular death pathways induced by the oestrone analogues and IND appear to occur. The effect of combinations of oestrone analogues and IND culminated in the induction of cell death predominantly through the induction of apoptosis after 72 h.

Where oestrone analogues were combined with QUER similar intracellular signalling pathways were initiated: extensive depolarisation of the mitochondrial membrane potential

was induced by the production of ROS resulting in the activation of the intrinsic apoptotic pathway. After 72 h exposure to QUER or the combinations of oestrone analogues and QUER the induction of apoptotic and necrotic cell death was observed. For combinations of ESE-15-ol and QUER induction of cell death proceeded mainly via apoptosis, however necrotic cell death was induced predominantly by combinations of ESE-16 and QUER.

In order to further explore the activity of the combinations of oestrone analogues and glycolysis inhibitors, the potential anti-angiogenic activity of these combinations were investigated using *in vitro* models.

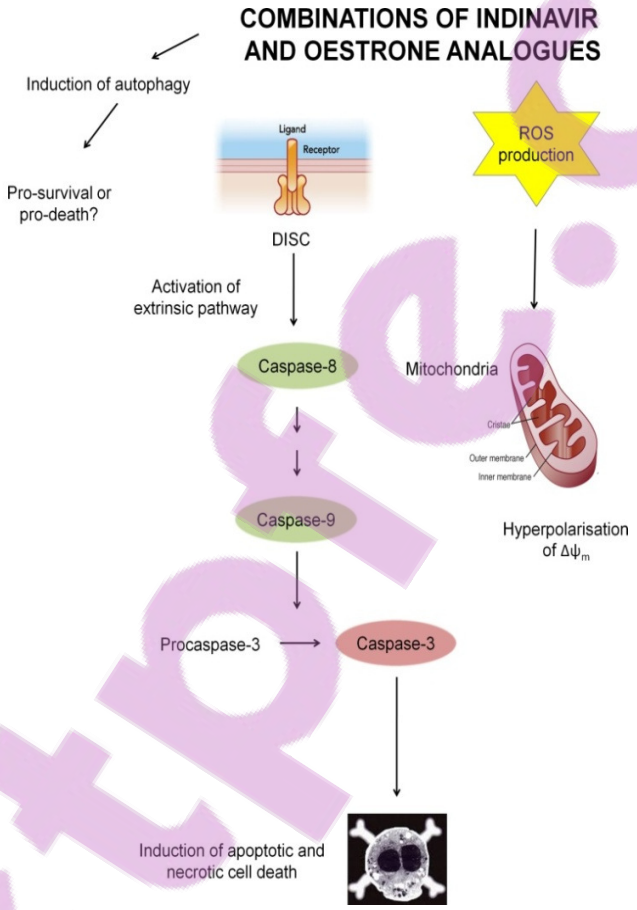

Figure 3.40: Proposed mechanism of action of synergistic combinations of oestrone analogues and indinavir based on results obtained during the study.Initiation of treatment with combinations of oestrone analogues and indinavir resulted in the generation of ROS and caused hyperpolarisation of the $\Delta\psi_m$. Based on caspase activity studies the external apoptotic pathway is activated resulting in the formation of the death-inducing signalling complex (DISC) and downstream activation of the executioner caspases. This culminates in cell death via apoptosis. However the induction of necrosis observed cannot be explained from data gathered during this study. Abrogation of autophagy was also demonstrated which may be pro-survival or pro-death.

Structures of DISC and apoptosome from Sendoel and Hengartner, 2014. (Sendoel and Hengartner, 2014) with modifications. Creative Commons Attribution License (CC-BY-2.0). Structure of mitochondria by Darryl Leja, NHGRI, www.genome.gov. Accessed September 2015. Image titled 'The real face of cell death' used with permission from D Coletti.

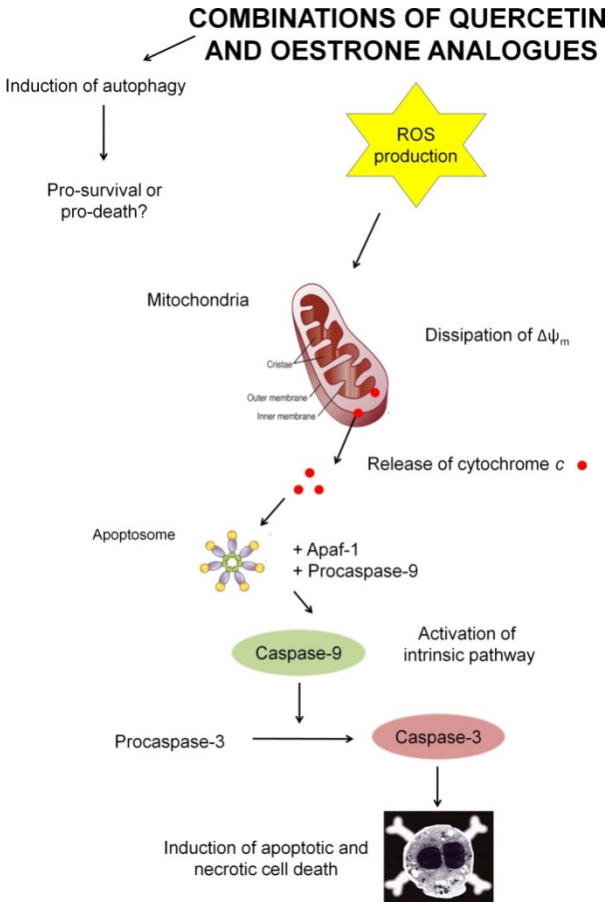

Figure 3.41: Proposed mechanism of action of synergistic combinations of oestrone analogues and quercetin based on results obtained during the study. Initiation of treatment with combinations of oestrone analogues and quercetin generates reactive oxygen species (ROS) resulting in depolarisation of mitochondrial membrane potential ($\Delta\psi_m$), activation of the caspase cascade and induction of apoptosis. However the induction of necrosis observed cannot be explained from data gathered during this study. Induction of autophagy was also demonstrated by quercetin treatment which may be pro-survival or pro-death.
Structure of the apoptosome from Sendoel and Hengartner, 2014. (Sendoel and Hengartner, 2014) with modifications. Creative Commons Attribution License (CC-BY-2.0). Structure of mitochondria by Darryl Leja, NHGRI, www.genome.gov. Accessed September 2015.
Image titled 'The real face of cell death' used with permission from D Coletti.

Chapter 4: Angiogenesis studies

4.1 Introduction

Synergistic combinations of the oestrone analogues, ESE-15-ol and ESE-16, with the glycolysis inhibitors IND or QUER were identified specific for the oestrogen receptor positive MCF-7 and triple negative MDA-MB-231 breast adenocarcinoma cells. These combinations target different characteristics distinguishing malignant cells from non-malignant cells, namely the increased proliferation rate and altered cellular energy production (Hanahan and Weinberg, 2000; Hanahan and Weinberg, 2011).

The proliferation of malignant cells is impeded under conditions of hypoxia: levels of oxygen below 1% (Kumar and Choi, 2015). It has been established that the attenuated proliferation is not necessarily due to a lack of nutrients or macromolecules required for duplication of intracellular components, but rather due to arrest of DNA synthesis during the synthesis (S) phase. DNA synthesis may resume upon alleviation of hypoxic conditions (Riedinger *et al.*, 1992; Gekeler *et al.*, 1993). To restore the supply of oxygen, and therefore to ensure the growth of malignant cells, the process of angiogenesis is initiated (Giaccia, 1996).

The process of angiogenesis occurs in a number of sequential and well regulated steps (Figure 4.1). Upon initiation of angiogenesis the extracellular matrix of the basal membrane is enzymatically degraded by matrix metalloproteases to release pericytes from the endothelium (Carmeliet and Jain, 2011). Simultaneous to degradation of the basement membrane, the permeability of the existing vasculature is modulated by vascular endothelial growth factor (VEGF or VEGF-A). This allows for the efflux of various plasma proteins which aids in the migration of endothelial cells (Bergers and Benjamin, 2003).

Endothelial cells from the existing vessels then proliferate and migrate to form new blood vessels as extensions from existing blood vessels (Hanahan and Folkman, 1996). This endothelial sprouting or tube formation is guided by pro-angiogenic factors released by tumours (Bergers and Benjamin, 2003). As tube formation is completed the new vessel is encapsulated by a basement membrane under the influence of tissue inhibitors of matrix metalloproteases (Gomez *et al.*, 1997) and plasminogen activator inhibitor type-1 (Higgins, 2002).

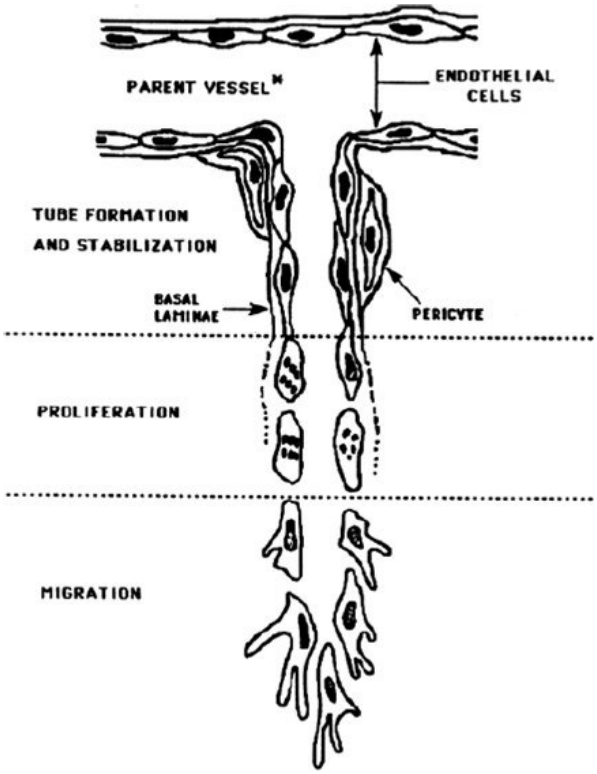

Figure 4.1: The process of angiogenesis. Angiogenesis is initiated by the enzymatic degradation of the basement membrane allowing formation of endothelial tubes. The tube formation and migration of endothelial cells are regulated by angiogenic factors. Endothelial cell proliferation and migration results in the establishment of a vasculature network which supplies oxygen and nutrients required by the tumour.
From (Stewart and Nowak, 1996), with modifications. Used with permission.

Under hypoxic conditions tumourigenic cells produce pro-angiogenic factors after formation of by hypoxia-inducible factor-1 (HIF-1) complex comprising hypoxia-inducible factor-1α (HIF-1α) and hypoxia-inducible factor-1β (HIF-1β)(Carmeliet and Jain, 2011). It has been speculated that the role of HIF-1α in a hypoxic environment is three-fold: to induce anaerobic metabolism as means to produce energy, to inhibit apoptosis and thus increase cell survival, and thirdly to attempt to establish a sufficient oxygen supply through angiogenesis (Hitchon and El-Gabalawy, 2004). The HIF-1 complex binds to the hypoxia-responsive element in oxygen-regulated genes to enhance their transcription (Distler *et al.*, 2004). The transcription of various angiogenic gene products including VEGF (Ryan *et al.*, 1998) and plasminogen activator inhibitor-1 (Kietzmann *et al.*, 2001) are also elevated by the HIF-1 complex.

As angiogenesis is not a ubiquitous process in healthy adults therefore it presents a selective target for novel anti-cancer therapy (Cook and Figg, 2010). Furthermore, the

antiangiogenic activity of IND (Sgadari *et al.*, 2002) and QUER (Tan *et al.*, 2003; Oh *et al.*, 2010) has been previously reported. Therefore the potential anti-angiogenic effects of the selected combinations of the oestrone analogues and glycolysis inhibitors were assessed using *in vitro* cell culture models.

4.2 Materials

1) 2-Methoxyoestradiol (2ME)

A 10 mM stock solution of 2ME (Sigma-Aldrich, St Louis, USA) was prepared by dissolving 10 mg powder in 3.3 ml DMSO. Aliquots of 2 µl was prepared and stored at -80°C.

2) Actinomycin D

A 1 mg/ml stock solution of Actinomycin D (Sigma-Aldrich, St Louis, USA) was prepared by dissolving 5 mg powder in 5 ml DMSO. Aliquots of 2 µl was prepared and stored at -80°C.

3) Human VEGF Quantikine® enzyme-linked immunosorbent assay (ELISA) kit

A human VEGF Quantikine® ELISA kit was procured from R&D Systems (Minneapolis, USA), stored at 4°C and used according to manufacturer's instructions.

4) Matrigel®

Matrigel® (10 ml, 9.3 mg/ml) was procured from Corning (New York, USA), defrosted overnight on ice at 4°C and transferred under sterile conditions to 1 ml aliquots. Aliquots were stored at -20°C. All pipette tips and micro-reaction tubes used were pre-cooled at 4°C.

4.3 Methods

The anti-angiogenic potential of selected combinations of the oestrone analogues and glycolysis inhibitors were assessed by evaluation of the effect on three key components of angiogenesis using the MCF-7 and MDA-MB-231 breast adenocarcinoma cells and the EA.hy926 human hybrid endothelial cell line (Figure 4.2).

The synergistic combinations of oestrone analogues with quercetin or indinavir identified in Stage 1 of the study are indicated in Table 2.7.

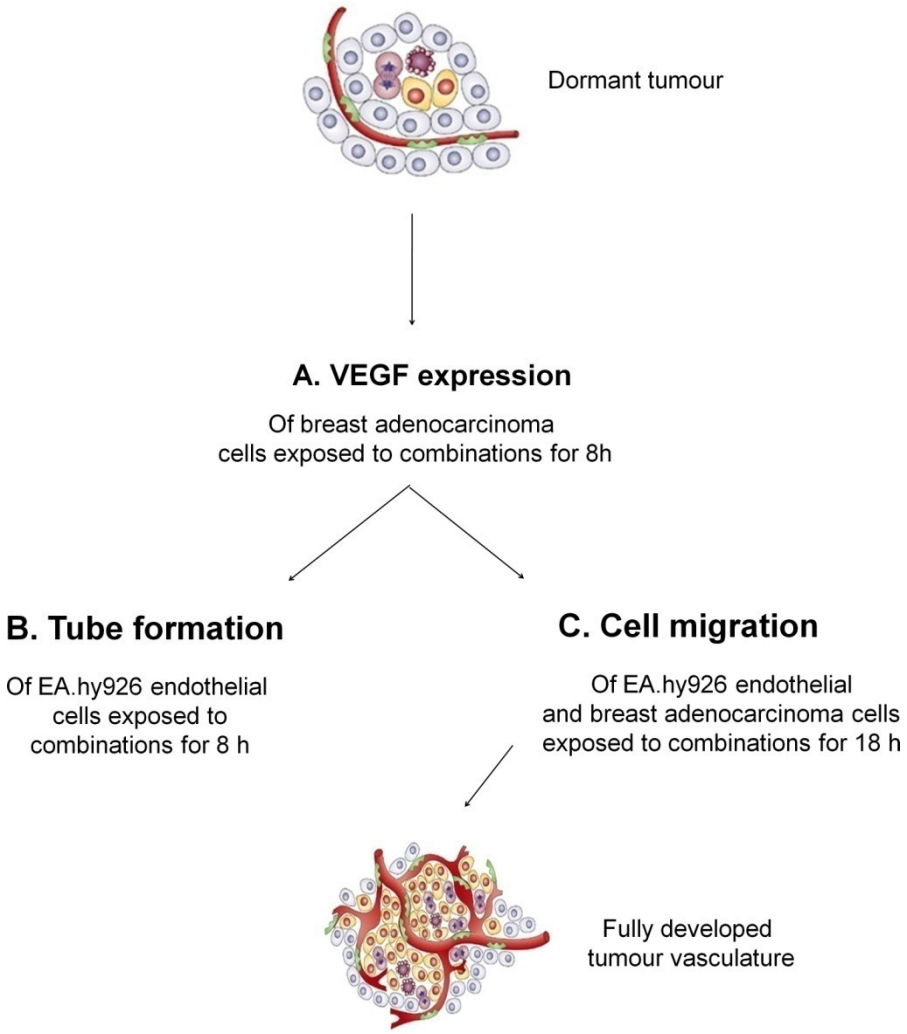

Figure 4.2: The evaluation of potential anti-angiogenic properties of combinations of oestrone analogues and glycolysis inhibitors. (A) The generation of vascular endothelial growth factor (VEGF) by MCF-7 and MDA-MB-231 breast adenocarcinoma cells exposed to drug combinations under hypoxic culturing conditions for 8 h. (B) Assessment of tube formation of EA.hy926 human hybrid endothelial cells exposed to the drug combinations for 8 h. (C) Measurement of cell migration of MCF-7 and MDA-MB-231 breast adenocarcinoma and EA.hy926 human hybrid endothelial cells exposed to the combinations for 18 h.
From (Bergers and Benjamin, 2003), with modifications. Used with permission.

The EA.hy926 human hybrid endothelial cell line was established by Dr CJ Edgell and colleagues through the fusion of human umbilical vein endothelial cells (HUVEC) with the human lung carcinoma A549 cell line. This cell line displays an elevated proliferation rate in comparison to HUVEC's while maintaining expression of factor VIII-related antigen, or Von Willebrandt Factor, unique to endothelial cells and megakaryocytes (Edgell *et al.*, 1983). The use of the EA.hy926 cell line as *in vitro* model of angiogenesis has been validated and

recommended (Bouïs *et al.*, 2001) based on expression of Von Willebrandt Factor, tissue-type plasminogen activator and plasminogen activator inhibitor type 1 (Emeis and Edgell, 1988). Furthermore the ability of EA.hy926 cells to migrate and produce VEGF is comparable to that of the well-known HUVEC cell line (Baranska *et al.*, 2005).

EA.hy926 cells and permission for the use of these cells were kindly provided by Dr Edgell before the cell line became commercially available (see Addendum 2).

EA.hy926 cells were cultured in DMEM cell culture medium supplemented with 10% FCS in a humidified incubator and atmosphere of 5% CO_2. Cell culture medium was replaced every 2 - 3 days during propagation of the cell line.

4.3.1 Determination of VEGF content using a VEGF ELISA kit

The effect of 8 h exposure to the oestrone analogues and selected combinations of oestrone analogues with glycolysis inhibitors on the expression of the pro-angiogenic factor VEGF of MCF-7 and MDA-MB-231 breast adenocarcinoma cell lines was assessed using a VEGF ELISA kit. Cell culture supernatants from cells incubated in a humidified incubator under normoxic conditions (37°C, with 5% CO_2 and approximately 21% O_2) were used as positive control.

A human VEGF Quantikine® ELISA kit was used according to manufacturer's instructions. Briefly, MCF-7 or MDA-MB-321 cells were seeded into sterile 96-well plates at a seeding density of 5 x 10^3 cells/well and incubated overnight to allow for cell attachment in a humidified incubator at 37°C with 5% CO_2. After a further 24 h incubation period cells were exposed to the oestrone analogues and selected combinations of oestrone analogues with IND or QUER and incubated in a humidified incubator under hypoxic conditions (37°C, 1.1% O_2) in an ESCO CelCulture CO_2 incubator (Horsham, USA) for a further 8 h. After the incubation period the plates were centrifuged at 1000 *g* for 20 min to remove cell debris from the cell culture supernatants. Cell culture supernatants (240 µl per sample) were transferred to micro-reaction tubes and snap frozen at -80°C until the ELISA was performed.

A calibration curve was set up for each experiment with concentrations of VEGF ranging from 15.6 pg/ml to 1000 pg/ml.

Assay diluent (50 µl) and cell culture supernatant (200 µl) were added to each well and the plate incubated at room temperature for 2 h without shaking. Thereafter the plate was washed three times with wash buffer before VEGF conjugate (200 µl) was added to each well. The plate was incubated at room temperature for 2 h. The plate was thereafter washed

three times with wash buffer and finally the substrate solution (200 µl) added to each well. The plate was incubated in the dark at room temperature for 20 min before stop solution (50 µl) was added to each well. The absorbance was measured using a Synergy 2 plate reader (Bio-Tek Instruments Inc., Vermont, USA) at 450 nm and a reference wavelength of 540 nm.

4.3.1.1 VEGF ELISA kit interpretation of results and statistics

Two independent repeats with internal duplicates were performed. Results were interpreted as fold change in VEGF concentration (pg/ml) relative to the untreated control incubated under hypoxic conditions using the calibration curve for each particular experiment. GraphPad Prism version 4.0 for Windows (GraphPad Software, San Diego California USA, www.graphpad.com) was used to determine statistical significance of the results obtained using a non-parametric Kruskal-Wallis with post-*hoc* Dunn's Multiple Comparison tests. A *P* - value < 0.05 was used as indicator of significance.

4.3.2 Tube formation assay

The effect of 8 h exposure to the combinations of oestrone analogues and glycolysis inhibitors on the formation of tubes by the EA.hy926 human hybrid endothelial cells was evaluated using a tube formation assay (Aranda and Owen, 2009).

Matrigel® was diluted to 5 mg/ml using ice cold cell culture medium. Sterile, flat-bottom 96-well plates were coated with 100 µl of the diluted Matrigel® and the plate incubated overnight in a humidified incubator at 37°C with 5% CO_2. EA.hy926 hybrid endothelial cells were plated onto the Matrigel® at a concentration of 2.5 x 10^4 cells/well and immediately exposed to combinations of the oestrone analogues and glycolysis inhibitors. 2ME (20 µM) was used as inhibitor of tube formation. The plate was re-incubated at the aforementioned conditions for 8 h. After the incubation period light microscopy was performed using a Zeiss Axiovert-40 microscope (Gottingen, Germany) at 5 x magnification.

4.3.2.1 Tube formation assay interpretation of results and statistics

Four independent repeats were performed with internal duplicates. In order to quantify the effect of the combinations of oestrone analogues and glycolysis inhibitors on tube formation of EA.hy926 cells, the number of tubes formed in each well was counted. Continuous cell-cell connections were used as indicator of tube length. The length of the longest individual tube in a sample was determined manually using AxioVision version 4.9.1.0 for Windows (AxioVision, Jena, Germany, www.zeiss.com).

GraphPad Prism version 4.0 for Windows (GraphPad Software, San Diego California USA, www.graphpad.com) was used to determine statistical significance of the results obtained

using a non-parametric Kruskal-Wallis and post-*hoc* Dunn's Multiple Comparison tests. A *P* - value < 0.05 was used as indicator of significance.

4.3.3 Assessment of cell migration using the scratch assay

The effect of 18 h exposure to the combinations of oestrone analogues and glycolysis inhibitors on cell migration of MCF-7 and MDA-MB-231 breast adenocarcinoma and EA.hy926 human hybrid endothelial cells were evaluated using a cell culture scratch assay. The method of Liang and colleagues was used (Liang *et al.*, 2007). Actinomycin D (40 nM for 18 h) was used as positive control.

Briefly, MCF-7 breast adenocarcinoma, MDA-MB-231 breast adenocarcinoma or EA.hy926 endothelial hybrid cells were plated at 1 x 10^5, 1.5 x 10^5 or 1.75 x 10^5 cells/well respectively, in a sterile 24-well plate using cell culture medium supplemented with 10% FCS and incubated overnight at 37℃ to allow for cell attachment. In order to synchronise the cells, the medium was replaced after the attachment period with medium supplemented with only 0.5% FCS and the plate re-incubated overnight.

A narrow scratch in the form of a cross was made in the monolayer using a sterile 200 µl pipette tip. Each well was gently rinsed with sterile PBS and fresh cell culture medium supplemented with 2% FCS was added to each well. Light microscopy was performed using a Zeiss Axiovert-40 microscope (Gottingen, Germany) at 5 x magnification. Sterility was maintained by imaging with the plate lid in place. The scratch in the form of a cross served as a marker for the location of the images taken. The plate was then exposed to the oestrone analogues or selected synergistic combinations for 18 h. After the incubation period the wells were gently rinsed with sterile PBS before the light microscopy at the same approximate location of the scratch was repeated.

4.3.3.1 Cell migration interpretation of results and statistics

Four independent experiments containing one repeat per sample were performed for each cell line. Two images at different locations were recorded per well. ImageJ2x software (ImageJ2x 2.1.4.9 2015, www.rawak.de/rs2012/) was used to calculate the area of the initial scratch created and the area that remained uncovered by cells after the treatment period.

GraphPad Prism version 4.0 for Windows (GraphPad Software, San Diego California USA, www.graphpad.com) was used to determine statistical significance of the results obtained using a non-parametric Kruskal-Wallis and post-*hoc* Dunn's Multiple Comparison tests. A *P*- value < 0.05 was used as indicator of significance.

4.4 Results

4.4.1 VEGF content

To assess the effect of the combinations of oestrone analogues and glycolysis inhibitors on the expression of VEGF under hypoxic conditions, conditioned medium from MCF-7 and MDA-MB-231 were analysed for VEGF content using a VEGF selective ELISA.

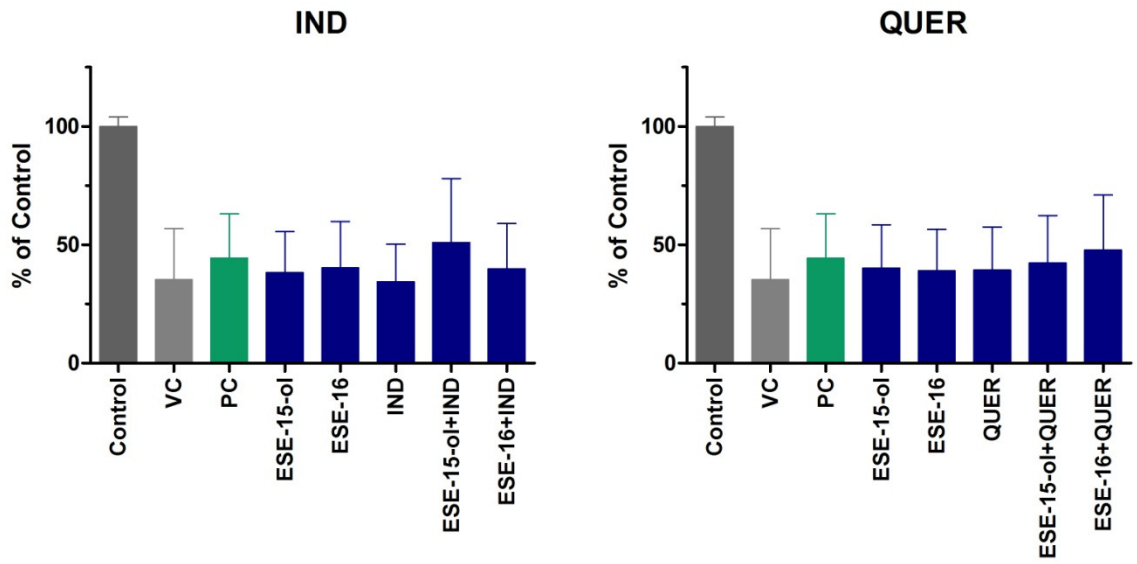

Figure 4.3: Vascular endothelial growth factor (VEGF) content of **MCF-7** cell culture supernates exposed to the combinations of oestrone analogues and indinavir (IND, 115 µM) or quercetin (QUER, 84 µM) under hypoxic conditions for 8 h. ESE-15-ol was used at 70 nM for combinations with IND and 17 nM for combinations with QUER. ESE-16 was used at 67 nM for combinations with IND and 17 nM for combinations with QUER. Control indicates untreated cells cultured under hypoxic conditions. PC indicates untreated cells cultured under normoxic conditions. VC indicates DMSO-treated cells cultured under hypoxic conditions. Error bars represent SEM. No statistically significant difference was observed.
n = 2

The effect of combinations of oestrone analogues and IND on the VEGF content of MCF-7 cell culture supernatants are shown in Figure 4.3. Where untreated cells were incubated under hypoxic conditions (1.1% O_2 for 8 h), VEGF content was elevated in comparison to the untreated cells incubated under normoxic conditions (5% CO_2 with approximately 21% O_2 for 8 h), indicating that the experimental design was appropriate and hypoxia-induced elevation in VEGF expression could be detected by the assay. Supernates collected from untreated cells incubated under normoxic conditions served as positive control. All treated samples

incubated showed a minimum decrease in VEGF content of approximately 73 pg/ml in comparison to the untreated control incubated under hypoxic conditions. VEGF content for all samples are listed in Table 4.1. The greatest reduction (approximately 76 pg/ml) was observed in MCF-7 cell culture supernatants obtained from MCF-7 cells exposed to IND. No statistically significant decreases in VEGF concentration were observed.

Table 4.1: Vascular endothelial growth factor (VEGF) content of **MCF-7** cell culture supernatants exposed to the combinations of oestrone analogues and indinavir (IND) for 8 h under hypoxic conditions. Cell supernatants incubated under normoxic conditions were used as positive control. Results are presented as mean ± standard error of the mean. Two independent experiments were performed.

	VEGF concentration (pg/ml)
Control	87.40 ± 40.46
Vehicle control	22.89 ± 5.15
Positive control	14.54 ± 1.66
ESE-15-ol	12.67 ± 0.62
ESE-16	11.93 ± 0.11
IND	11.40 ± 0.85
ESE-15-ol+IND	13.63 ± 2.41
ESE-16+IND	11.51 ± 0.82

The effect of combinations of oestrone analogues and QUER on the VEGF content of MCF-7 cell culture supernatants are shown in Figure 4.3. Where untreated cells were incubated under hypoxic conditions (1.1% O_2 for 8 h), VEGF content was elevated in comparison to the untreated cells incubated under normoxic conditions (5% CO_2 with approximately 21% O_2 for 8 h), indicating that the experimental design functioned correctly and enhanced VEGF expression could be detected with the assay.Supernates collected from untreated cells incubated under normoxic conditions served as positive control. A reduction in VEGF content was observed in all treated cell culture supernatants. MCF-7 breast adenocarcinoma cell culture supernatants of cells exposed to the combination of ESE-16 and QUER showed the least suppression of VEGF expression of all treated cell cultures (approximately 15 pg/ml). No statistically significant differences in VEGF content were observed. VEGF content for all samples are listed in Table 4.2.

Table 4.2: Vascular endothelial growth factor (VEGF) content of **MCF-7** cell culture supernatants exposed to the combinations of oestrone analogues and quercetin (QUER) for 8 h under hypoxic conditions. Cell supernatants incubated under normoxic conditions were used as positive control. Results are presented as mean ± standard error of the mean. Two independent experiments were performed.

	VEGF concentration (pg/ml)
Control	87.40 ± 40.46
Vehicle control	22.89 ± 5.15
Positive control	14.54 ± 1.66
ESE-15-ol	12.56 ± 0.46
ESE-16	13.09 ± 0.91
QUER	11.71 ± 0.58
ESE-15-ol+QUER	12.99 ± 0.50
ESE-16+QUER	14.58 ± 1.16

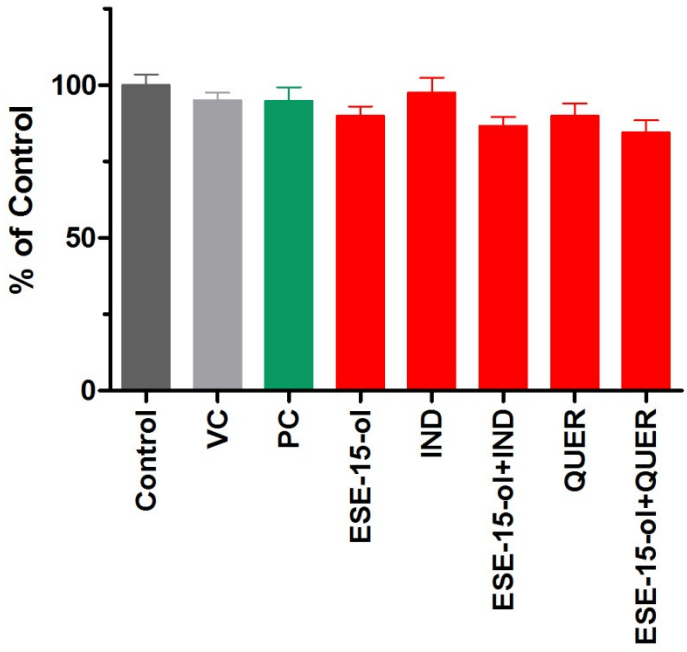

Figure 4.4: Vascular endothelial growth factor (VEGF) content of **MDA-MB-231** cell culture supernatants exposed to the combinations of ESE-15-ol (123 nM) and indinavir (IND, 55 µM) or quercetin (QUER, 0.64 µM) under hypoxic conditions for 8 h. Control indicates untreated cells cultured under hypoxic conditions. PC indicates untreated cells cultured under normoxic conditions. VC indicates DMSO-treated cells cultured under hypoxic conditions. Error bars represent SEM. No statistically significant difference was observed.

n = 2

The effect of oestrone analogues and selected combinations of oestrone analogues with glycolysis inhibitors on the VEGF expression of MDA-MB-231 cell cultures are shown in Figure 4.4. The VEGF content of cell culture supernatants obtained from MDA-MB-231 cells incubated under hypoxic conditions (1.1% O_2 for 8 h) were approximately 50 pg/ml higher than that of cell culture supernatants obtained from cells incubated under normoxic conditions (5% $CO_2$with approximately 21% O_2 for 8 h) indicating that VEGF expression was induced under hypoxic conditions. Supernates collected from untreated cells incubated under normoxic conditions served as positive control. The VEGF content of MDA-MB-231 cell culture supernatants were not greatly affected by the treatments (Figure 4.4): the greatest decrease in VEGF content (approximately 101 pg/ml) was observed where cells were exposed to the combination of ESE-15-ol and QUER. No statistically significant changes to VEGF content were observed. VEGF content for all samples are listed in Table 4.3.

Table 4.3: Vascular endothelial growth factor (VEGF) content of **MDA-MB-231** cell culture supernatants following exposure to the combinations of oestrone analogues and indinavir (IND) or quercetin (QUER) for 8 h under hypoxic conditions. Cell supernatants incubated under normoxic conditions were used as positive control. Results are presented as mean ± standard error of the mean. Two independent experiments were performed.

	VEGF concentration (pg/ml)
Control	514.40 ± 21.27
Vehicle control	463.40 ± 38.35
Positive control	461.40 ± 43.44
ESE-15-ol (123 nM)	438.90 ± 41.02
IND (55 µM)	475.90 ± 47.60
ESE-15-ol+IND	422.00 ± 35.41
QUER (0.64 µM)	439.50 ± 45.30
ESE-5-ol+QUER	413.10 ± 41.61

4.4.2 Tube formation assay

The effect of the combinations of oestrone analogues and glycolysis inhibitors on the tube formation of EA.hy926 hybrid endothelial cells were assessed after 8 h exposure. The number of tubes formed as well as the length of tubes formed was also evaluated.

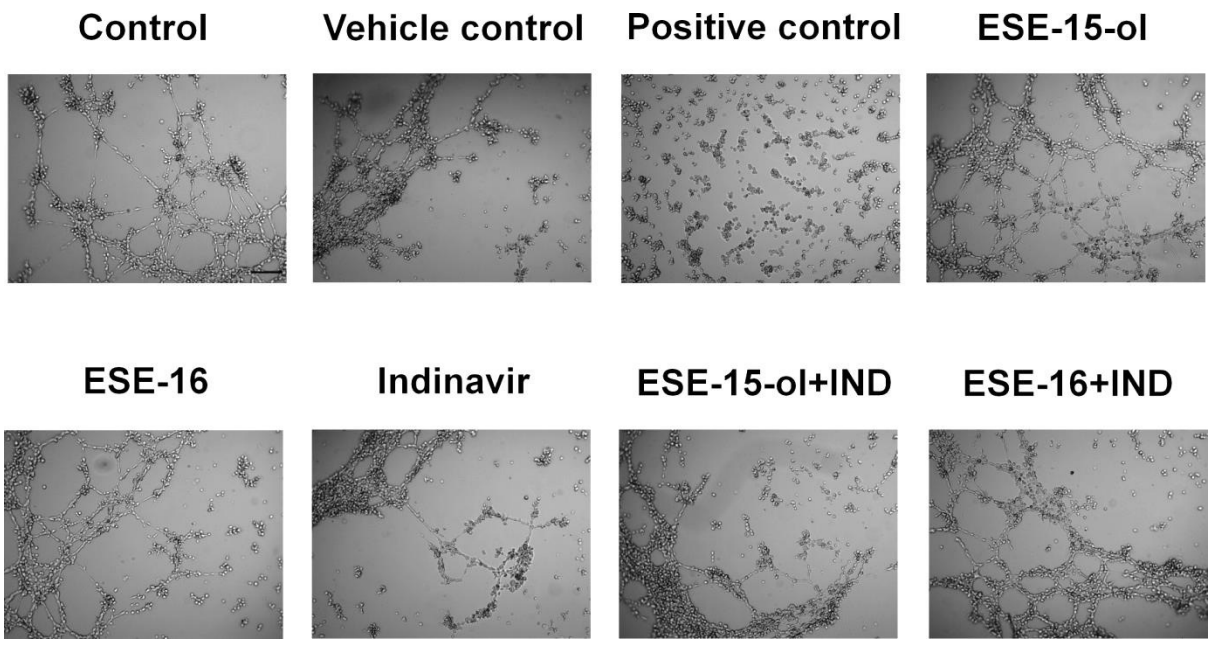

Figure 4.5: The effect of the combination of oestrone analogues, ESE-15-ol (70 nM) and ESE-16 (67 nM), and indinavir (IND, 115 µM) specific for **MCF-7** breast adenocarcinoma cells on the formation of tubes of **EA.hy926** hybrid endothelial cells after 8 h. 2-Methoxyestradiol (20 µM for 8 h) was used as positive control. Images are representative of one of five independent experiments. Scale bar in control image present 50 µm.

Table 4.4: The effect of the same combinations of oestrone analogues and indinavir (IND) shown in Figure 4.5 on the number of tubes and the length of the longest tube formed by **EA.hy926** hybrid endothelial cells after 8 h incubation. 2-Methoxyestradiol (20 µM for 8 h) was used as positive control. Results are presented as mean ± standard error of the mean. n = 5

	Number of tubes	Length of tubes (% of Control)
Control	13.50 ± 1.99	100.00 ± 7.04
Vehicle control	13.00 ± 1.39	98.67 ± 10.81
Positive control	8.40 ±2.13	60.75 ± 20.89
ESE-15-ol (70 nM)	11.00 ± 2.19	90.62 ± 10.04
ESE-16 (67 nM)	12.50 ± 2.06	75.99 ± 13.38
IND (115 µM)	12.70 ± 0.58	58.24 ± 13.61
ESE-15-ol+IND	9.70 ± 1.62	76.01 ± 12.28
ESE-16+IND	7.90 ± 2.19	74.16 ± 17.45

Where cells were treated with the known anti-angiogenic compound, 2ME, the formation of cell-cell connections and sprouting of endothelial cells were inhibited, indicating that the tube inhibition could be achieved (Figure 4.5). Reduction in both the number of tubes and tube length was also observed for 2ME-treated cells (Table 4.4). Inhibition of tube formation, the number of tubes formed and the length of tubes formed were observed where EA.hy926 cells were treated with IND. Combination treated cells formed fewer tubes than untreated cells as reflected in Table 4.4. A statistically significant reduction in the number of tubes formed or the length of the longest tube was not observed for any of the treated samples (Table 4.4).

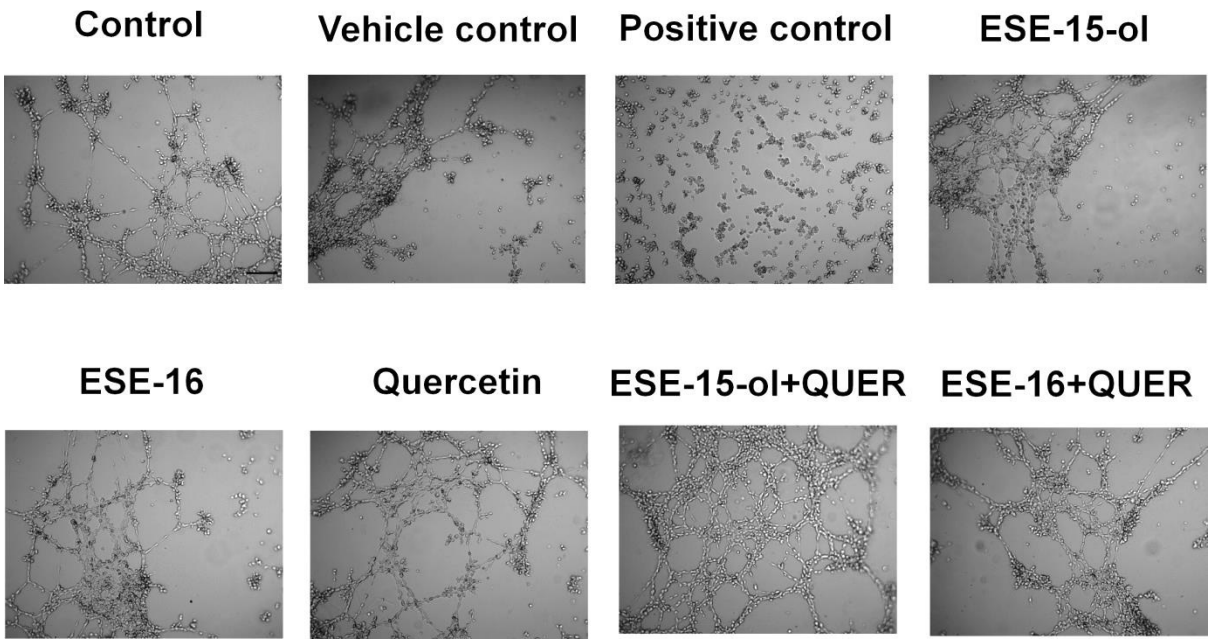

Figure 4.6: The effect of the combination of oestrone analogues, ESE-15-ol (17 nM) and ESE-16 (17 nM), and quercetin (QUER, 84 µM) specific for **MCF-7** breast adenocarcinoma cells on the formation of tubes by **EA.hy926** hybrid endothelial cells after 8 h incubation. 2-Methoxyestradiol (20 µM for 8 h) was used as positive control. Images are representative of one of five independent experiments. Scale bar in control image present 50 µm.

The formation of cell-cell connections and sprouting of EA.hy926 hybrid endothelial cells were inhibited after treatment with the anti-angiogenic compound 2ME indicating that inhibition of tube formation could be induced (Figure 4.6). The number of tubes formed as well as tube length was also reduced in 2ME-treated cells (Table 4.5). Treatment with the oestrone analogues limited the extent of tube formation of EA.hy926 hybrid endothelial cells. Cells which had not formed cell-cell connections were observed in these samples. A

polygonal tube network was formed where EA.hy926 hybrid endothelial cells were treated with QUER (84 µM). The combinations of oestrone analogues and QUER resulted in decreased number of tubes. A statistically significant reduction in the number of tubes formed or the length of the longest tube was not observed for any of the treated samples (Table 4.5).

Table 4.5: The effect of combinations of oestrone analogues and quercetin (QUER) shown in Figure 4.6 on the number of tubes and the length of the longest tube formed by **EA.hy926** hybrid endothelial cells after 8 h incubation. 2-Methoxyestradiol (20 µM for 8 h) was used as positive control. Results are presented as mean ± standard error of the mean. n = 5

	Number of tubes	**Length of tubes (% of Control)**
Control	13.50 ± 1.99	100.00 ± 7.04
Vehicle control	13.00 ± 1.39	98.67 ± 10.81
Positive control	8.40 ±2.13	60.75 ± 20.89
ESE-15-ol (17 nM)	10.40 ± 0.33	95.16 ± 8.73
ESE-16 (17 nM)	10.20 ± 1.37	98.10 ± 12.99
QUER (84 µM)	13.00 ± 0.69	95.68 ± 13.42
ESE-15-ol+QUER	10.60 ± 1.54	104.60 ± 10.43
ESE-16+QUER	11.00 ± 1.68	90.93 ± 19.19

Combinations specific for MDA-MB-231 breast adenocarcinoma cells were also assessed for effect on tube formation of EA.hy926 hybrid endothelial cells. The positive control, anti-angiogenic compound 2ME, inhibited tube formation indicating that the assay functioned correctly (Figure 4.7). Where cells were treated with ESE-15-ol the formation of a complex, polygonal tube network was limited. Tube number and length was also reduced by ESE-15-ol treatment. Treatment with the glycolysis inhibitor IND markedly reduced the number of cell-cell connections and sprouting of endothelial cells. The combination of ESE-15-ol and IND impeded the formation of a tube network with a reduction in the number of tubes and tube length observed. QUER-treated endothelial cells formed tube networks however the tube length was reduced in comparison to the control. The combination of ESE-15-ol and QUER reduced the complexity of the tube network as well as the number of tubes formed. A statistically significant reduction in the number of tubes formed or the length of the longest tube was not observed for any of the treated samples (Table 4.6).

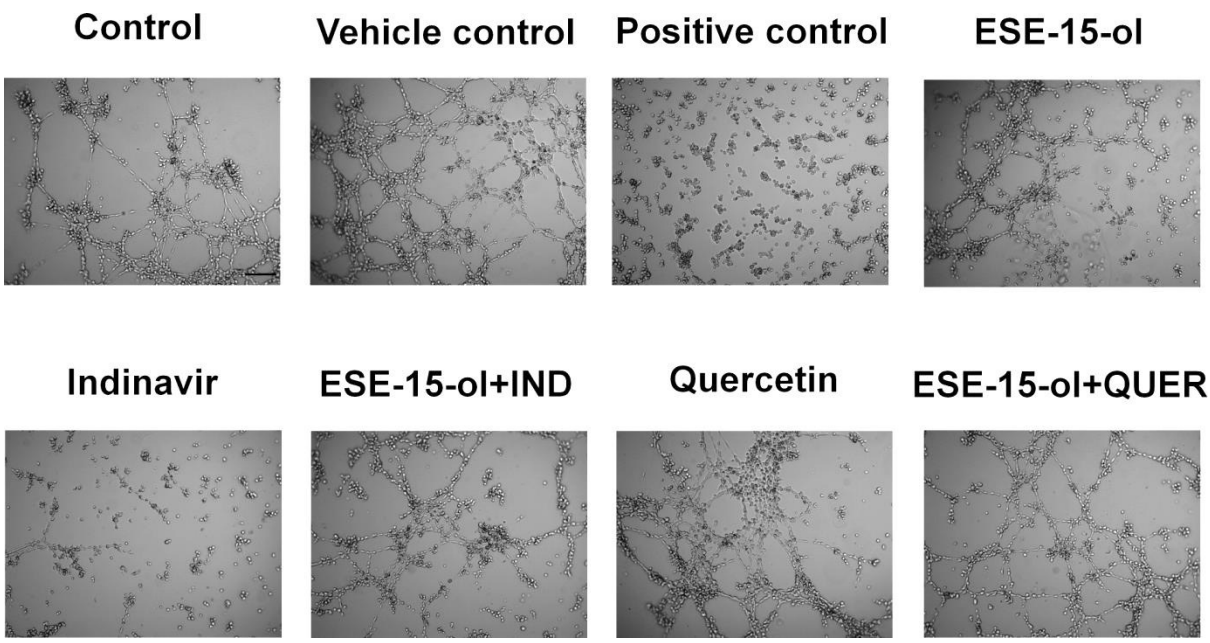

Figure 4.7: The effect of the combination of the oestrone analogueESE-15-ol (123 nM) and indinavir (IND, 55 µM) and quercetin (QUER, 0.64 µM) specific for **MDA-MB-231** breast adenocarcinoma cells on the formation of tubes by **EA.hy926** hybrid endothelial cells after 8 h incubation. 2-Methoxyestradiol (20 µM for 8 h) was used as positive control. Images are representative of one of four independent experiments. Scale bar in control image present 50 µm.

Table 4.6: The effect of combinations of oestrone analogues and indinavir (IND) and quercetin (QUER) shown in Figure 4.7 on the number of tubes and the length by the longest tube formed of **EA.hy926** hybrid endothelial cells after 8 h. 2-Methoxyestradiol (20 µM for 8 h) was used as positive control. Results are presented as mean ± standard error of the mean. n = 4

	Number of tubes	Length of tubes (% of Control)
Control	15.75 ± 2.39	108.30 ± 7.24
Vehicle control	17.25 ± 1.75	117.30 ± 13.74
Positive control	9.75 ± 1.79	62.06 ± 20.65
ESE-15-ol (123 nM)	9.88 ± 1.23	70.03 ± 12.66
Indinavir (55 µM)	11.75 ± 1.05	80.96 ± 13.62
ESE-15-ol+IND	10.13 ± 1.07	80.62 ± 16.63
QUER (0.64 µM)	12.13 ± 3.35	86.44 ± 11.36
ESE-15-ol+QUER	11.50 ± 1.34	86.60 ± 14.94

4.4.3 Assessment of cell migration using the scratch assay

The effect of the combinations of oestrone analogues and glycolysis inhibitors on cell migration was measured with the scratch assay. After a scratch was created through an established monolayer of MCF-7 and MDA-MB-231 breast adenocarcinoma and EA.hy926 human hybrid endothelial cells, the cultures were exposed to selected combinations. After 18 h incubation time, the scratch surface area still uncovered by cells was measured as an indicator of cell migration. Microscopy images with the subsequent quantification of the uncovered surface area (four independent experiments) are shown in Figures 4.8 - 4.16.

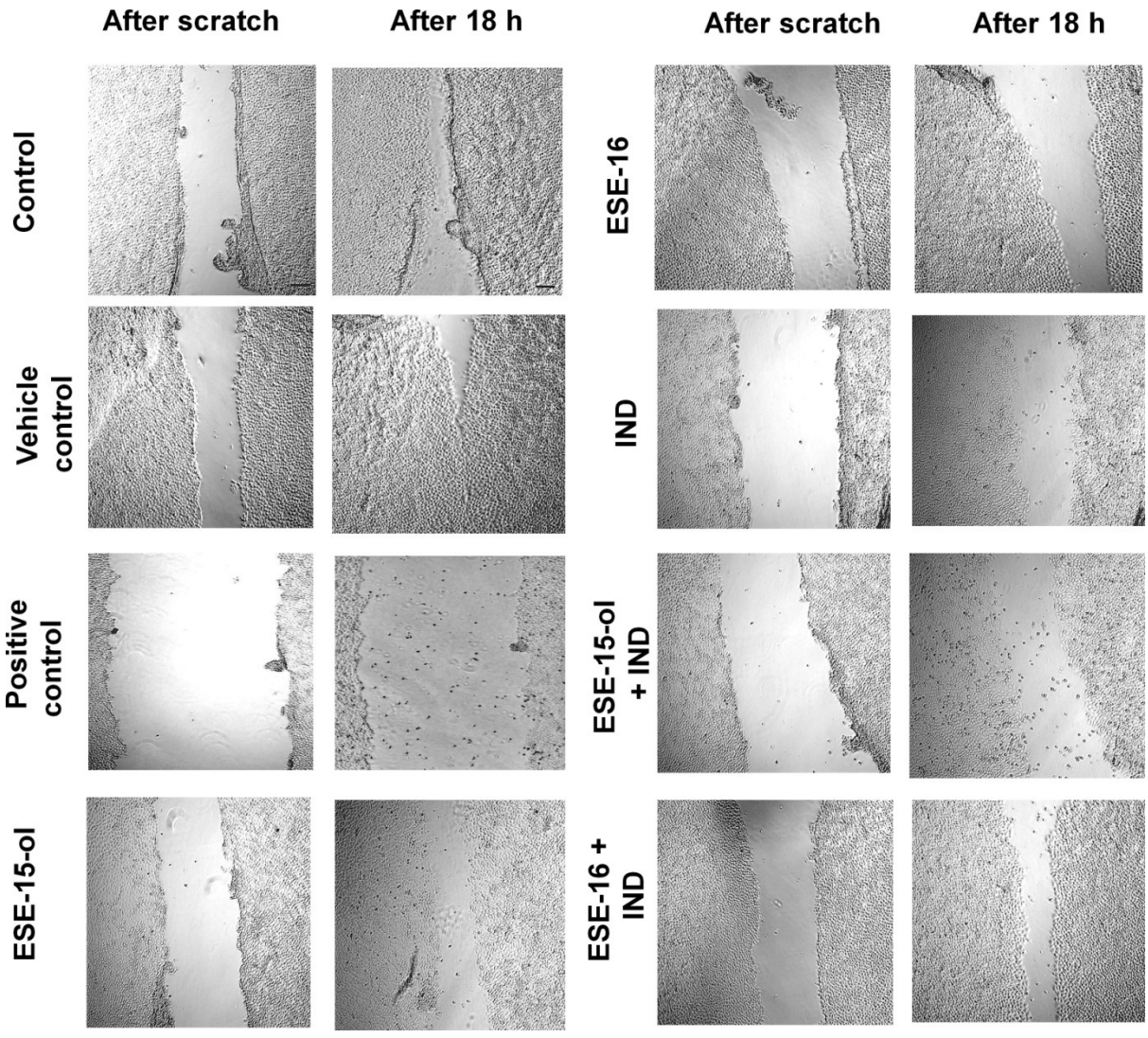

Figure 4.8: Cell migration studies on the **MCF-7** breast adenocarcinoma cells exposed to combinations of oestrone analogues, ESE-15-ol (70 nM) and ESE-16 (67 nM), and indinavir (IND, 115 µM) for 18 h. Actinomycin (40 nM for 18 h) was used as positive control. Images are representative of four independent experiments. Scale bars in control images present 50 µm.

Treatment with the positive control, actinomycin D, reduced the ability of MCF-7 breast adenocarcinoma and EA.hy926 hybrid endothelial cells to migrate into the exposed area, indicating that the assay functioned correctly (Figures 4.8 and 4.9).

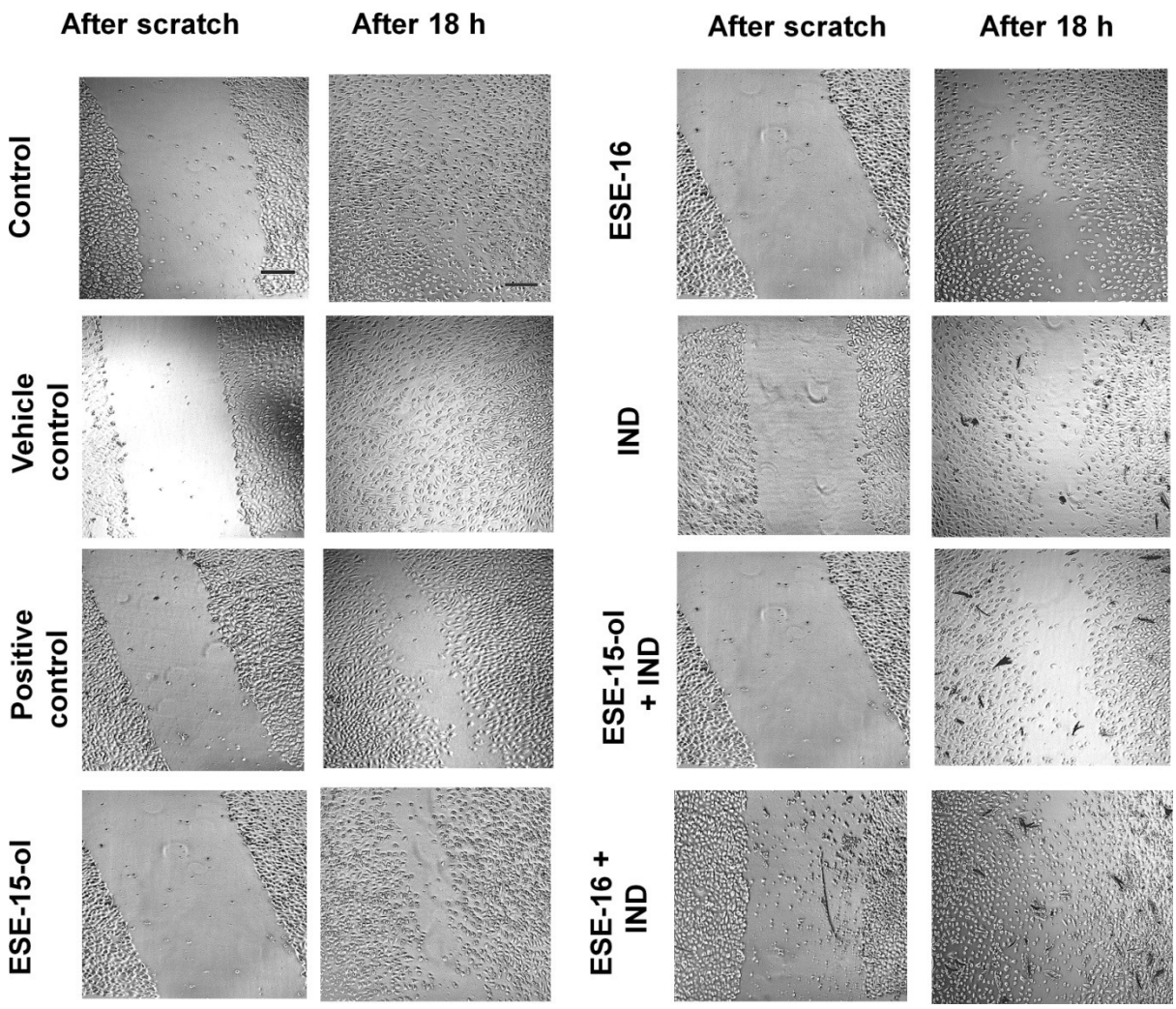

Figure 4.9: Cell migration studies on the **EA.hy926**hybrid endothelial cells exposed to combinations of oestrone analogues, ESE-15-ol (70 nM) and ESE-16 (67 nM), and indinavir (IND, 115 µM) for 18 h. Actinomycin (40 nM for 18 h) was used as positive control. Images are representative of four independent experiments. Scale bars in control images present 50 µm.

For MCF-7 breast adenocarcinoma cells treated with combinations of oestrone analogues and IND (115 µM), the exposed scratch area closure was reduced by approximately 50% compared to untreated controls (Figures 4.8 – 4.10). Limited cell migration into the exposed scratch area was observed when EA.hy926 hybrid endothelial cells were exposed to ESE-15-ol (70 nM) showing a 25% reduction in scratch area closure and the combination of ESE-

15-ol and IND (115 µM) with an approximate 18% reduction. The combination of ESE-16 (67 nM) and IND (115 µM) did not affect cell migration into the scratch area significantly.

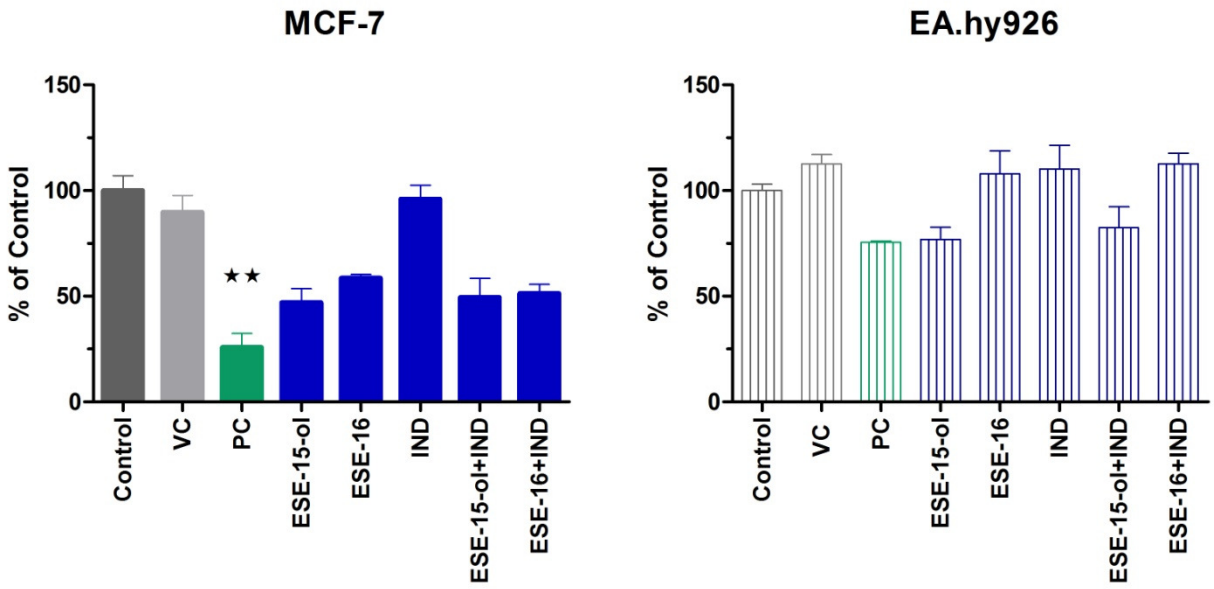

Figure4.10: Covered surface area remaining relative to untreated control after 18 h exposure to synergistic combinations of the oestrone analogues, ESE-15-ol (70 nM) and ESE-16 (67 nM), with indinavir (IND, 115 µM) on **MCF-7** breast adenocarcinoma and **EA.hy926** hybrid endothelial cell lines. VC indicates DMSO-treated cells. Actinomycin (40 nM for 18 h) was used as positive control.
n = 4; * p < 0.05** p < 0.01*** p < 0.001

Treatment with the positive control, actinomycin D, reduced the ability of MCF-7 breast adenocarcinoma and EA.hy926 hybrid endothelial cells to migrate into the exposed area, indicating that the assay functioned correctly (Figures 4.11 - 13). Where MCF-7 breast adenocarcinoma cells were treated with combinations of oestrone analogues and QUER, the ability of cells to migrate into the exposed area was greatly reduced (Figures 4.11 and 4.13). This effect was most prominent were cells were treated with ESE-15-ol (17 nM) and QUER (84 µM). Exposure of EA.hy926 hybrid endothelial cells to the same combinations resulted in a less pronounced inhibitory effect on the cell migration with ESE-16 (17 nM) alone significantly increased endothelial cell migration after 18 h. Of the drug combinations, the greatest reduction in covered surface area (approximately 10% reduction) was observed where cells were treated with the combination of ESE-15-ol and QUER.

No statistically significant differences between the untreated control and treatment groups were observed.

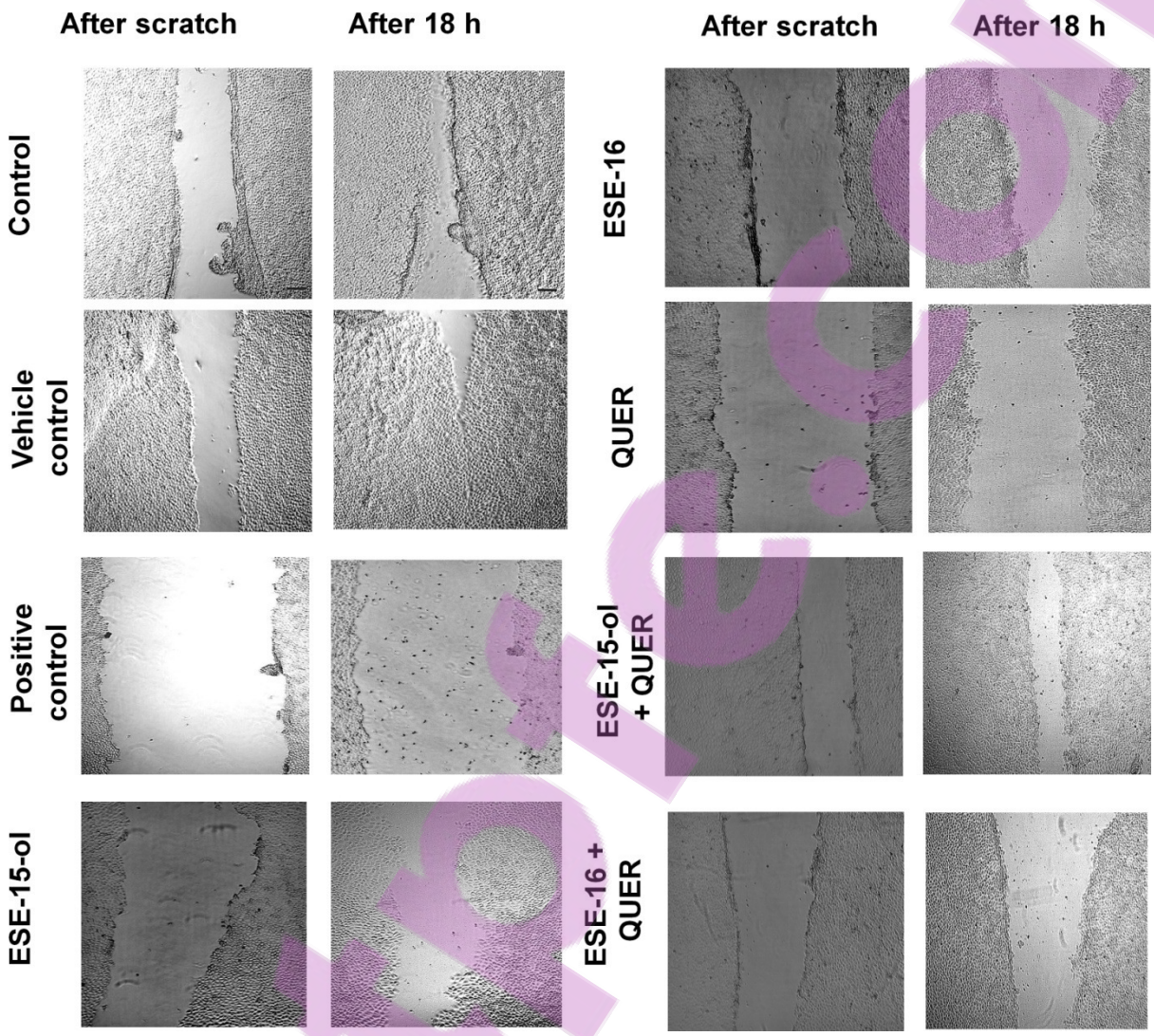

Figure 4.11: Cell migration studies on the **MCF-7**breast adenocarcinoma cells exposed to combinations of oestrone analogues, ESE-15-ol (17 nM) and ESE-16 (17 nM) and quercetin (QUER, 84 µM) for 18 h. Actinomycin (40 nM for 18 h) was used as positive control. Images are representative of four independent experiments. Scale bars in control images present 50 µm.

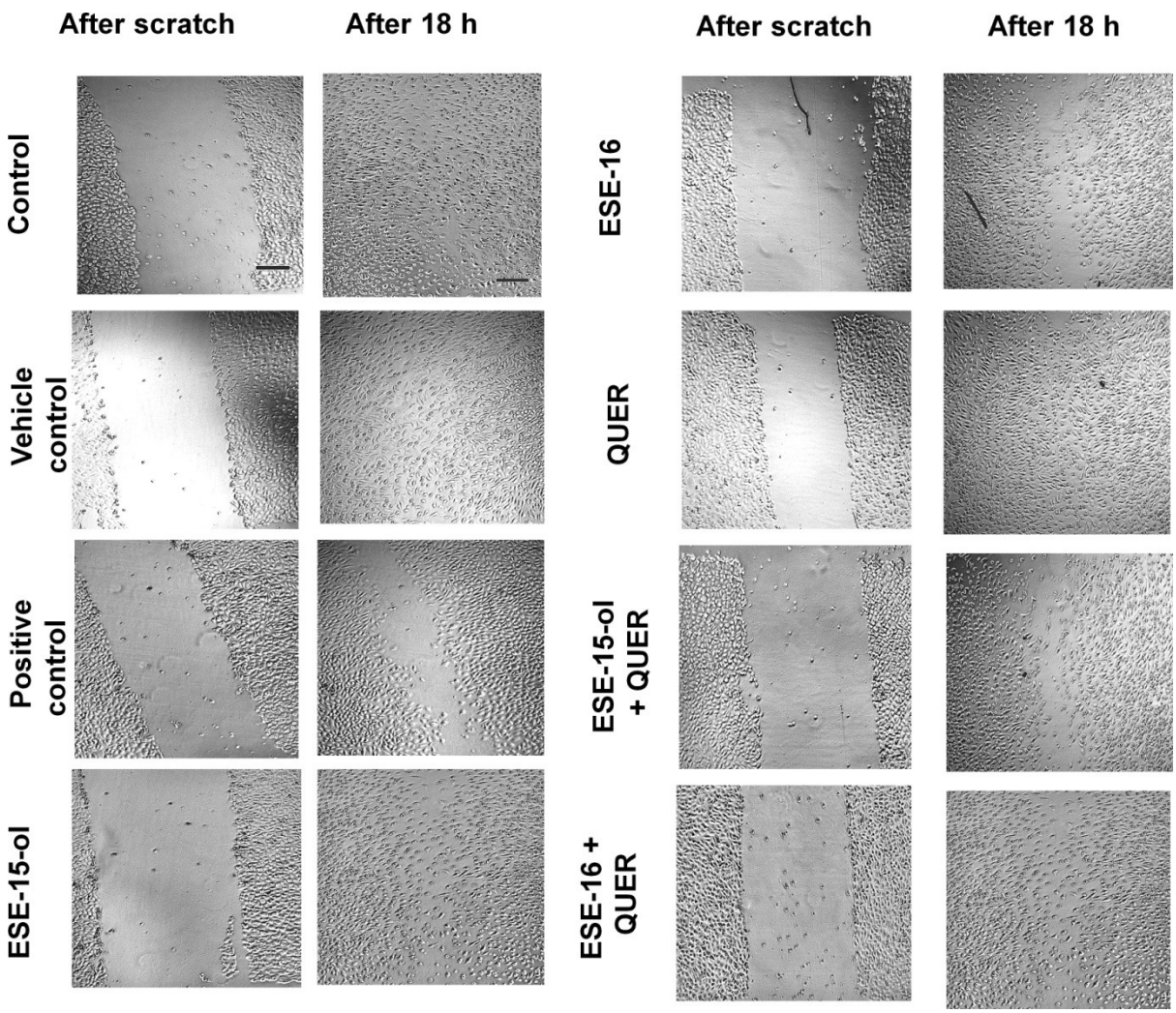

Figure 4.12: Cell migration studies on the **EA.hy926**hybrid endothelial cells exposed to combinations of oestrone analogues, ESE-15-ol (17 nM) and ESE-16 (17 nM) and quercetin (QUER, 84 µM) for 18 h. Actinomycin (40 nM for 18 h) was used as positive control. Images are representative of four independent experiments. Scale bars in control images present 50 µm.

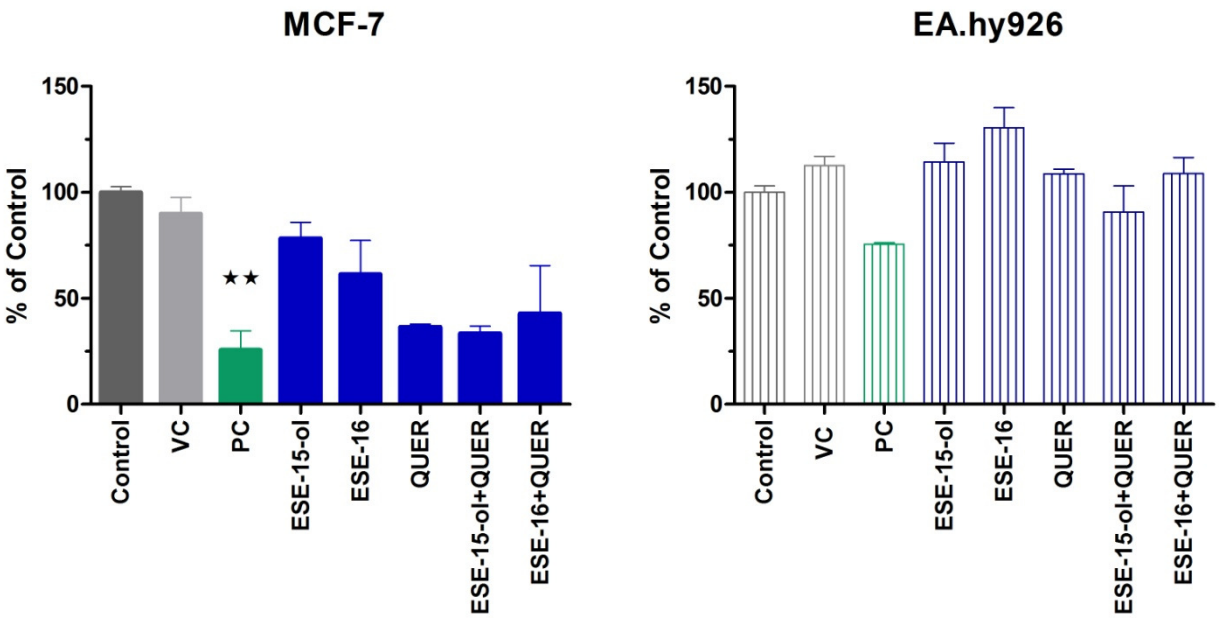

Figure 4.13: Covered surface area remaining relative to untreated control after 18 h exposure to synergistic combinations of the oestrone analogues, ESE-15-ol (17 nM) and ESE-16 (17 nM), with quercetin (QUER, 84 µM) on **MCF-7** breast adenocarcinoma and **EA.hy926** hybrid endothelial cell lines. VC indicates DMSO-treated cells. Actinomycin (40 nM for 18 h) was used as positive control.
n = 3;* $p < 0.05$** $p < 0.01$ *** $p < 0.001$

Where MDA-MB-231 breast adenocarcinoma and EA.hy926 hybrid endothelial cells were treated with the positive control, actinomycin D, a marked reduction in the ability of cells to migrate into the exposed area were observed, indicating that the assay functioned correctly (Figures 4.14 - 4.16). The reduced ability of the cells to migrate was not statistically significant.

When MDA-MB-231 breast adenocarcinoma cells were exposed to the combination of ESE-15-ol (123 nM) and IND (55 µM), a 40% reduction in cell migration into the exposed area was observed (Figures 4.14 and 4.16). Similarly treatment with the combination of ESE-15-ol (123 nM) and QUER (0.64 µM) limited the migration of MDA-MB-231 cells into the scratch area. A similar trend was observed where EA.hy926 hybrid endothelial cells were treated with the same combinations. The ability of EA.hy926 cells to migrate into the exposed area was significantly limited when exposed to ESE-15-ol (123 nM). No statistically significant differences between the untreated control and treatment groups were observed.

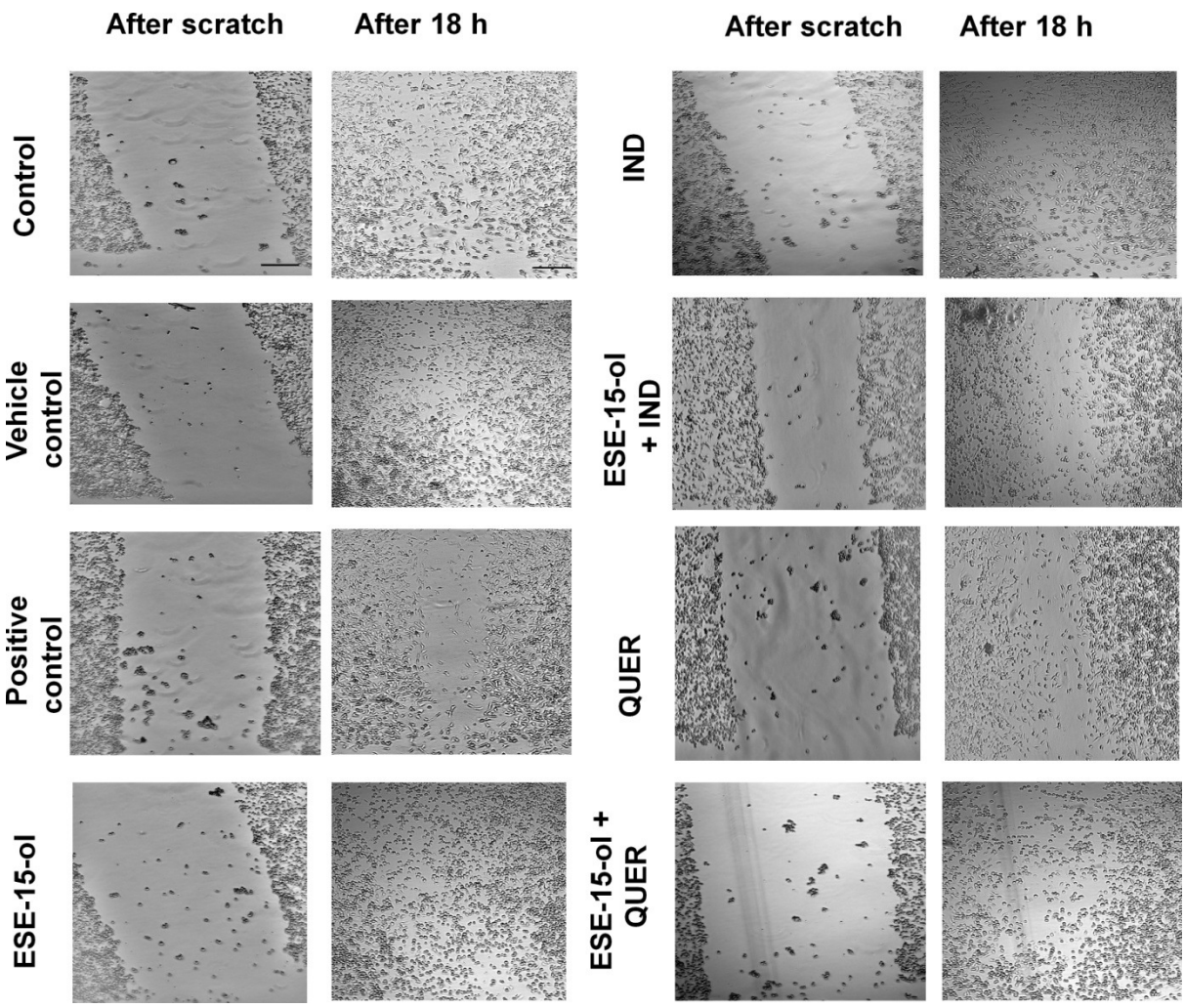

Figure 4.14: Cell migration studies on the **MDA-MB-231** breast adenocarcinoma cells exposed to combinations of the oestrone analogue ESE-15-ol (234 nM) and indinavir (IND, 55 μM) or quercetin (QUER, 0.64 μM) for 18 h. Actinomycin (40 nM for 18 h) was used as positive control. Images are representative of four independent experiments. Scale bars in control images present 50 μm.

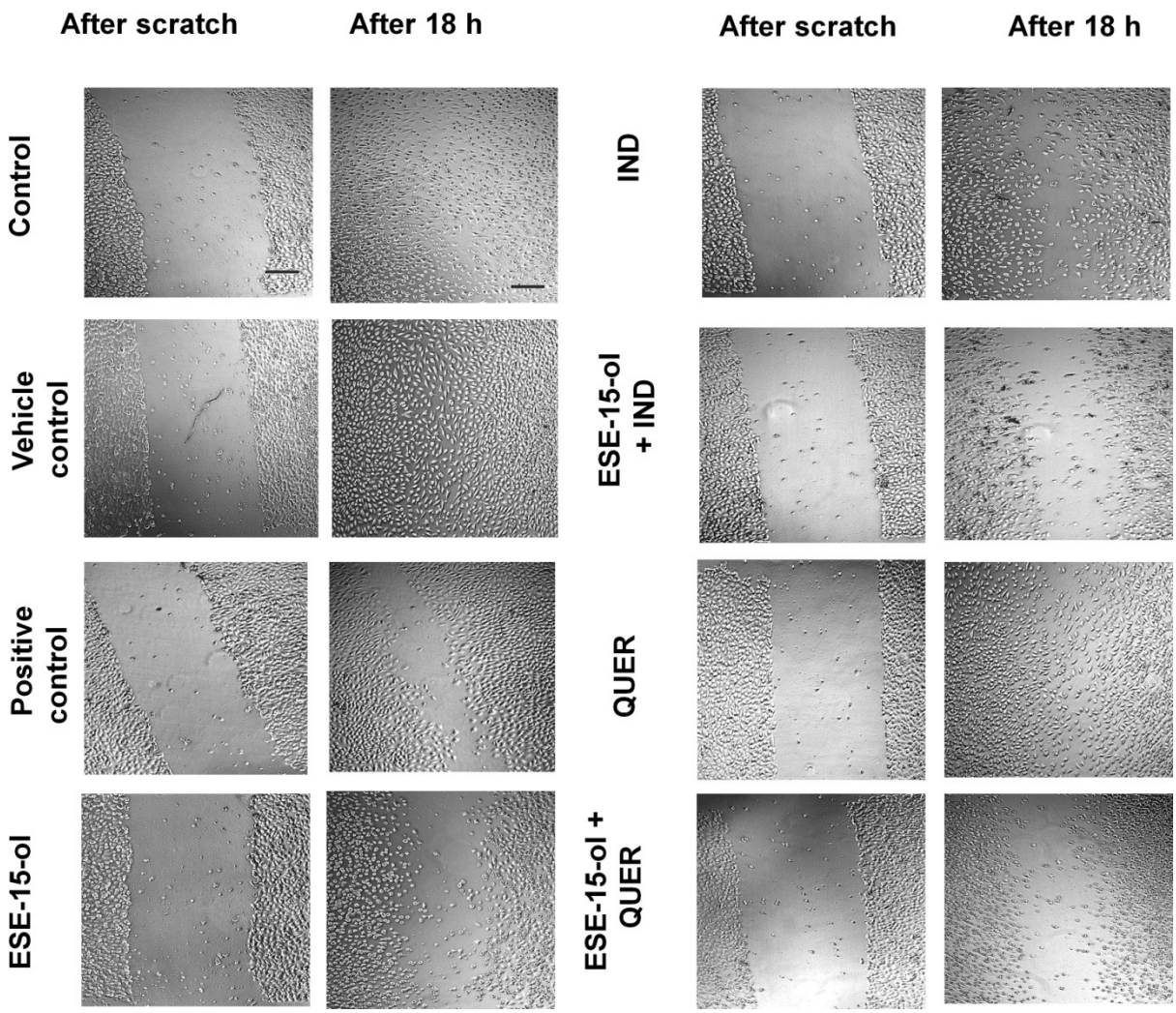

Figure 4.15: Cell migration studies on the **EA.hy926** hybrid endothelial cells exposed to combinations of the oestrone analogue ESE-15-ol (123 nM) and indinavir (IND, 55 μM) or quercetin (QUER, 0.64 μM) for 18 h. Actinomycin (40 nM for 18 h) was used as positive control. Images are representative of four independent experiments. Scale bars in control images present 50 μm.

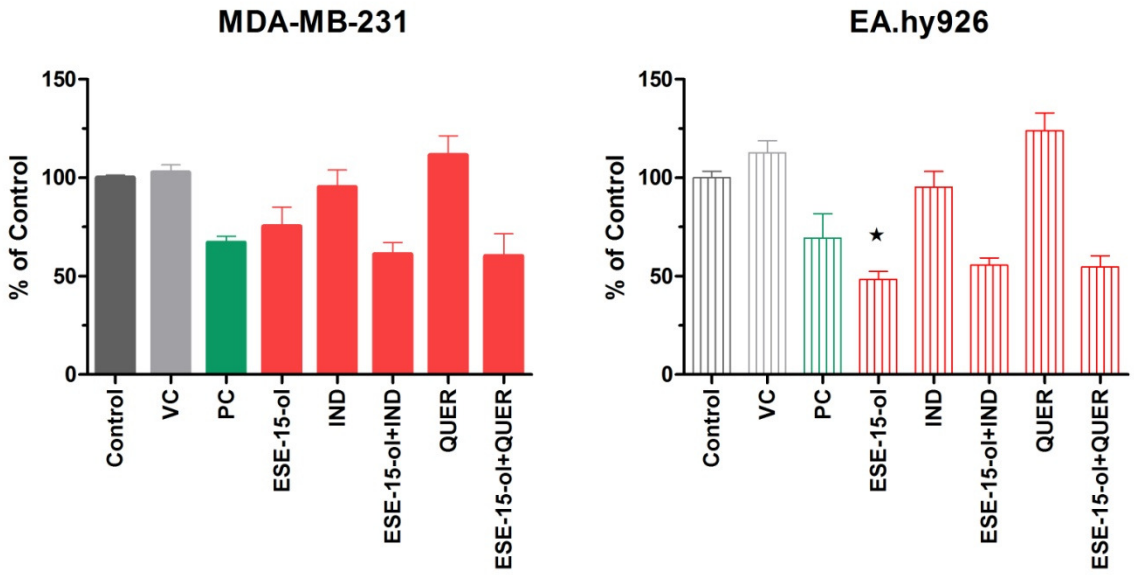

Figure 4.16: Covered surface area remaining relative to untreated control after 18 h exposure to synergistic combinations of the oestrone analogue ESE-15-ol (123 nM) and indinavir (IND, 55 µM) or quercetin (QUER, 0.64 µM) on **MDA-MB-231** breast adenocarcinoma and **EA.hy926** hybrid endothelial cell lines. VC indicates DMSO-treated cells.Actinomycin (40 nM for 18 h) was used as positive control.

n = 3;* $p < 0.05$** $p < 0.01$ *** $p < 0.001$

4.5 Discussion

The majority of breast cancer-related deaths occur after metastasis has taken place (O'Shaughnessy, 2005). The potential anti-angiogenic properties of combinations of oestrone analogues and glycolysis inhibitors were investigated using *in vitro* assays. As a 'gold standard' for angiogenesis assays has not yet been identified, the complex process of angiogenesis is best studied using a number of techniques (Staton *et al.*, 2009).

Tumour-angiogenesis result in the formation of abnormal blood vessels (Baish and Jain, 2000). It has been demonstrated that vasculature networks resulting from tumour angiogenesis often lack pericytes and remain dependent on VEGF for survival (Benjamin *et al.*, 1999). The vessels are often formed not only by endothelial cells but also cancer cells, termed 'vasculogenic mimicry', resulting in the formation of fractal vasculature (Baish and Jain, 2000). The effective supply of oxygen is not supported by this chaotic vasculature, promoting further hypoxia (Helmlinger *et al.*, 1997). The prevailing hypoxic conditions affect the release of pro-angiogenic factors and may therefore offer a survival advantage to cells more prone to metastasis (Carmeliet and Jain, 2000).

Recently classical chemotherapeutic agents, including microtubule-targeting agents and topoisomerase I inhibitors, which have been successfully used to inhibit proliferation of tumourigenic tissue have been shown to inhibit angiogenesis (Semenza, 2009). The anti-angiogenic effects of microtubule-targeting agents specifically are due to inhibition of HIF-1α. (Escuin *et al.*, 2005). Indeed, 2ME has been shown to down-regulate expression of VEGF (Banerjeei *et al.*, 2000; Chauhan *et al.*, 2002).

VEGF expression is a marker for metastatic potential (Zhang *et al.*, 2010). The expression of VEGF by the metastatic MDA-MB-231 breast adenocarcinoma cell line is therefore expected to be greater than that of the non-metastatic MCF-7 breast adenocarcinoma cells. In the present study conditioned medium from untreated MDA-MB-231 cells showed a VEGF concentration of approximately 520 pg/ml (Table 4.4), whereas the VEGF concentration of conditioned medium from untreated MCF-7 cells was approximately 84 pg/ml (Tables 4.2 and 4.3). This correlates to published reports as the VEGF concentration in MDA-MB-231 (Liu and Mueller, 2006) and MCF-7 cells (Cascio *et al.*, 2010).

In both cell lines tested treatment with the oestrone analogues resulted in reduced VEGF concentrations. This effect was most pronounced where MCF-7 cells were exposed to ESE-16 (70 nM, as used in combination with IND)(Figure 4.3). Decreased VEGF secretion as a result of ESE-16 treatment has been previously reported (Stander *et al.*, 2013). The oestrone derivatives may therefore abrogate early stages of angiogenesis.

Where oestrone analogues were combined with IND, VEGF expression was further attenuated. On the MCF-7 cells the effect was most pronounced where the combination of ESE-16 and IND was used (Table 4.1). Where MDA-MB-231 cells were exposed to the combination of ESE-15-ol and IND, the VEGF concentration was synergistically reduced (Table 4.3). Treatment of MCF-7 cells with IND (115 µM for 8 h) resulted in extensive but non-significant reduction in measured VEGF concentration. A similar reduction in VEGF expression was observed where MDA-MB-231 cells were treated with IND (55 µM for 8 h) alone.

This conflicts with published reports on the effect of IND on VEGF generation (Esposito *et al.*, 2006; Simone *et al.*, 2007). This may be explained by cell line specific responses and difference in treatment periods. The effect of IND on VEGF may also be concentration-dependent effect. Furthermore, in the present study two independent experiments with internal duplicates were assessed; a larger sample size may reveal a different trend.

Where combinations of oestrone analogues and QUER were used, reduced VEGF content was detected in cell culture supernatants prepared from MCF-7 and MDA-MB-231 breast

adenocarcinoma cells. QUER (84 µM for 8 h) had a greater inhibitory effect on the production of VEGF than either of the oestrone analogues used alone in MCF-7 cells (Table 4.2). However, the greatest reduction in VEGF concentration in conditioned medium prepared from MDA-MB-321 breast adenocarcinoma cells were detected after exposure to the combination of ESE-15-ol (123 nM) and QUER (0.64 µM) for 8 h (Table 4.3). The low concentration of QUER used had a similar inhibitory effect on the production of VEGF in the MDA-MB-231 cells as ESE-15-ol by itself. The reduction in VEGF concentration observed implies a synergistic, cell line-specific interaction between QUER and ESE-15-ol. The observed reduction in VEGF concentration was not statistically significant.

The inhibitory effect of QUER on VEGF production confirms published results. Reduction of VEGF secretion of human acute promyelyticleukaemia cells was observed after QUER treatment (Zhong *et al.*, 2006). In tamoxifen-resistant MCF-7 breast adenocarcinoma cells, QUER (30 µM for 24 h) significantly reduced VEGF secretion and transcription of the *VEGF* gene (Oh *et al.*, 2010). Conflicting reports demonstrating induction of VEGF secretion by QUER have also been published (Kaneuchi *et al.*, 2003; Jeon *et al.*, 2007).

The conflicting reports on the effect of IND and QUER on VEGF secretion impedes comparison with the present study. In the present study IND and QUER reduced VEGF secretion by MCF-7 and MDA-MB-231 breast adenocarcinoma cells. Few of the published articles reported assessment of VEGF secretion of tumourigenic cells under hypoxic conditions, as used in the present study. Furthermore, several of the aforementioned studies assessed VEGF production by endothelial cells and not tumourigenic cells. It is well known that a hypoxic tumour microenvironment is required for the initiation of tumour angiogenesis (Bergers and Benjamin, 2003; Semenza, 2015). This lends credibility to the assessment of VEGF production by tumourigenic cells under hypoxic conditions.

The results from *in vivo* studies would provide the most accurate account of the effect of experimental compounds on angiogenesis factors and the angiogenic process as a whole, as no adjustments are required to accurately mimic the tumour microenvironment. Additionally the influence of physiological factors which are absent in the *in vitro* setting would be observed. Numerous *in vivo* angiogenesis models have been established including the chick chorioallantoic membrane and corneal micropocket assays. Unfortunately these assays are complicated by inherent variation in animals translating to large variability in results obtained necessitating the use of large numbers of animals (Auerbach *et al.*, 2003). *In lieu* of *in vivo* studies numerous *in vitro* angiogenesis models have been developed which may be used as screening tools before moving on to *in vivo* testing.

Assessing the effect of an experimental compound on endothelial tube formation is a widely-used indicator of anti-angiogenic properties (Madri *et al.*, 1988). The formation of these tube networks aided by an extracellular matrix such as Matrigel is considered to be representative of *in vivo* tube formation (Auerbach *et al.*, 2003). Sequential steps in the formation of tube networks of EA.hy926 cells have been identified: initially cells flatten and projections appear (referred to as sprouts); then cells migrate to form cell-cell connections resulting in polygonal networks of increasing complexity (Aranda and Owen, 2009).

In the present study the effect of combinations of oestrone analogues and glycolysis inhibitors on the tube formation of EA.hy926 hybrid endothelial cells were investigated using the Matrigel-based assay. Untreated control samples showed the typical formation of complex polygonal networks of tubes. Cells treated with 2ME (20 µM for 8 h) showed some tube formation, but limited cell-cell connections were observed (Figure 4.5). The number of tubes formed in 2ME-treated cells as well as the length of the tubes was markedly reduced in comparison to the untreated control. This provided an indication of anti-angiogenic activity.

The effect of the oestrone analogues on endothelial tube formation has not yet been reported. ESE-15-ol appears to have a concentration-dependent effect as inhibition of tube formation, accompanied by reduction in the number of tubes formed and the tube length, was only observed at the highest concentration tested (123 nM)(Figure 4.7). A similar trend was seen as tube formation was only affected where 67 nM of ESE-16 was used (Figure 4.5) suggesting that ESE-16 has a superior inhibitory effect on endothelial tube formation. As inhibition of endothelial tube formation is considered to be a good indicator of anti-angiogenic potential (Madri *et al.*, 1988), ESE-16 seems to have greater potential as anti-angiogenic agent.

Where EA.hy926 hybrid endothelial cells were exposed to the combinations of oestrone analogues and IND selected for synergy against MCF-7 cells, inhibition of tube formation was observed (Figure 4.5). This was most prominent in cells exposed to IND (115 µM) and the combination of ESE-15-ol (70 nM) and IND (115 µM). Even though polygonal networks did establish after 8 h of drug combination exposure, a reduction in tube number and tube length was observed indicating anti-angiogenic potential of these combinations. However, the effect of IND on the number of tubes and the tube length was greater than that of the selected drug combinations.

The reduced concentration of IND (55 µM) required in combination with ESE-15-ol (123 nM) on the MDA-MB-231 cell line inhibited the formation of tubes as well as cell-cell connections (Figure 4.7). The anti-angiogenic effect was enhanced where the combination of ESE-15-ol

and IND was used: even though a polygonal network was established, it lacked the multi-cell wall as seen in the untreated control.

Previous studies have reported that the tube formation of HUVEC cells was stimulated in terms of number of tubes as well as tube length after IND treatment (1 – 50 µM for 18 h) (Simone *et al.*, 2007). It has been suggested that the seeding density used may influence the results obtained (Aranda and Owen, 2009). In the study by Simone and colleagues HUVEC cells were seeded at 2 x 10^4 cells/well, a seeding density similar to the seeding density used in the present study. The lowest concentration of IND used in the present study, 55 µM as required for synergistic drug combinations against the MDA-MB-231 cell line, is higher than that used by Simone and colleagues and may therefore indicate a concentration dependent effect of IND on tube formation. Unfortunately few reports have been published on the effect of IND on endothelial tube formation.

In EA.hy926 cells treated with QUER (84 µM) the formation of a tubule network did not appear to be inhibited (Figure 4.6). Indeed, QUER treatment did not affect the number of tubes formed or the tube length significantly. Where QUER (84 µM) was combined with ESE-15-ol (17 nM) or ESE-16 (17 nM) the effect was not enhanced, as indicated by the complexity of the tube network formed as well as the number of tubes and tube length calculated.

The formation of a complex polygonal tube network seemed impeded by QUER (0.64 µM) as unconnected cells were observed after 8 h (Figure 4.7). A slight reduction in the number of tubes formed as well as in tube length was seen in these samples. The addition of ESE-15-ol (123 nM) did not increase the inhibitory effect of QUER. The results obtained in the present study conflicts with previously published reports on the effect of QUER on endothelial tube formation (Igura *et al.*, 2001; Tan *et al.*, 2003). It may be argued that the disparity between the results of the present study and published reports are due to differences in the origin endothelial cell lines used and subtle experimental differences.

Of the *in vitro* assays developed to study the migration of cells, the modified Boyden chamber model is most often used (Auerbach *et al.*, 2003). However, accurate quantification of migrated cells is challenging and the assay employs a foreign matrix, i.e. a filter, through which cells must migrate (Auerbach *et al.*, 2003; Staton *et al.*, 2009). To aid in the quantification of cell migration, the use of wounded cell monolayers may be employed (Auerbach *et al.*, 2003). In order to limit the effect of cell proliferation, the use of low serum concentrations is recommended (Liang *et al.*, 2007).

In the present study the migration of cells into the scratch area was most impeded where MCF-7 breast adenocarcinoma cells were exposed to ESE-15-ol (70 nM) and the combination of ESE-15-ol and IND (115 µM)(Figures 4.8 and 4.10). IND (115 µM) caused only a slight reduction in cell migration of MCF-7 cells. The migration of EA.hy926 hybrid endothelial cells were inhibited to the greatest extent by the combination of ESE-15-ol and IND. Where MDA-MB-231 breast adenocarcinoma cells were treated with ESE-15-ol (123 nM) and the combination of ESE-15-ol (123 nM) and IND (55 µM) a similar reduction in cell migration was observed (Figures 4.14 and 4.16). This inhibition effect was exaggerated where EA.hy926 endothelial cells were treated with ESE-15-ol (123 nM) and IND (55 µM).The effect of IND (55 µM) on the migration of MDA-MB-231 and EA.hy926 cells were comparable to that observed in the MCF-7 cell line.

The effect of ESE-16 (67 nM) on the migration of MCF-7 breast adenocarcinoma and EA.hy926 endothelial cells was less pronounced (Figures 4.8 and 4.10). Treatment of MCF-7 cells with ESE-16 resulted in approximately 40% decrease in the surface area covered by migrating cells. Where ESE-16 was combined with IND (115 µM) a 50% reduction in cell migration of MCF-7 cells was observed. However, in the EA.hy926 hybrid endothelial cell line no reduction in the migratory ability of the cells was observed with exposure to ESE-16 or the combination of ESE-16 and IND.

No reports describing the effect of ESE-15-ol and ESE-16 on cell migration have been published to date.

IND (10 µM for 5 h) has been shown to inhibit the migration of HUVEC cells stimulated by basic fibroblast growth factor in a Boyden chamber model (Ensoli, 2002), confirming data obtained in the present study. *In vitro* assays used to detect the effect of an experimental compound on cell invasion differ from cell migration assays in the coating used as matrix: for cell migration studies Boyden chambers are often coated with collagen to aid in cell adhesion (Thompson *et al.*, 1991), whereas Matrigel-coated filters, to stimulate the basement membrane, are commonly used for cell invasion studies (Albini *et al.*, 1987). Numerous studies assessed cell invasion after IND treatment and reported that IND effectively inhibits cell invasion (Ensoli, 2002; Sgadari *et al.*, 2002).

The considerably decreased concentrations of the oestrone analogues were required for combination with QUER on the MCF-7 breast adenocarcinoma cell line reduced the cell migration of MCF-7 cells slightly. Interestingly the different concentrations of ESE-16 required (67 nM required for combinations with IND or 17 nM required for combinations with QUER) resulted in comparable suppression (approximately 40%) of cell migration of MCF-7 cells (Figures 4.11 and 4.13). Where ESE-15-ol (17 nM) or ESE-16 (17 nM) were combined

with QUER (84 µM) considerable inhibition of cell migration was observed for MCF-7 cells. A similar, yet less pronounced, trend was seen in the EA.hy926 endothelial cell line. This inhibitory effect seems to be largely due to QUER: where MCF-7 cells were exposed to QUER only, an extensive reduction in cell migration was observed. The combination of ESE-15-ol and QUER resulted in superior inhibition of cell migration of MCF-7 breast adenocarcinoma and EA.hy926 hybrid endothelial cells in comparison to the combination of ESE-16 and QUER.

A conflicting trend was observed for QUER on the MDA-MB-231 cell line: the migration of MDA-MB-231 breast adenocarcinoma and EA.hy926 endothelial cells were enhanced by QUER (0.64 µM) treatment (Figures 4.14 and 4.16). However, in both cell lines the addition of ESE-15-ol (123 nM) to QUER resulted in suppressed cell migration. This effect was synergistic as it was greater than the effect demonstrated by the compounds separately.

In accordance with results obtained for QUER (84 µM required for combinations on the MCF-7 cell line) published studies report reduced cell migration after QUER treatment. Where a scratch assay was used to assess the effect of QUER (1.5 – 100 µM for 16 h) on the migration of bovine aorta endothelial cells, a dose-dependent decrease in cell migration was observed (Igura *et al.*, 2001). QUER (25 – 100 µM for 8 h) has been demonstrated to inhibit cell migration using a modified Boyden chamber (Tan *et al.*, 2003). At concentrations as low as 10 nM QUER reduced the number of migrated bovine post-capillary coronary venular endothelial cells in a modified Boyden chamber model after 4 h (Donnini *et al.*, 2006). The migration of B16-BL6 murine melanoma cells were reduced after treatment with QUER (10 µM for 6 h)(Caltagirone *et al.*, 2000). QUER has been shown to inhibit cell migration of the human 143B osteosarcoma cell line (Berndt *et al.*, 2013).

Taken together, the results from the angiogenesis assays performed during the present study indicate that the combinations of oestrone analogues and IND or QUER have anti-angiogenic potential. Data indicate that both early and late stages of angiogenesis are inhibited by the combinations.

The anti-angiogenic properties of protease inhibitors, such as IND, have been established. It has been demonstrated that IND affects early angiogenesis through inhibition of matrix metalloprotease-2 activation (Esposito *et al.*, 2006). Even though IND treatment has not been shown to reduce proliferation of endothelial cells, inhibition of cell invasion by IND treatment has been demonstrated (Sgadari *et al.*, 2002; Esposito *et al.*, 2006). *In vivo* inhibition of tumour growth of xenografts of human lung, breast, or colon adenocarcinoma due to reduced vessel formation has also been reported in response to IND treatment (Sgadari *et al.*, 2003).

The combination of oestrone analogues and IND may result in inhibition of angiogenesis at the early stages through inhibition of VEGF secretion. This effect may be attributed addition of the oestrone analogues as IND reportedly elevates VEGF production (Simone *et al.*, 2007). Furthermore the formation of complex polygonal tube networks was inhibited, especially by the combination of ESE-15-ol and IND. This same drug combination also demonstrated suppressed cell migration of breast adenocarcinoma and endothelial cell lines.

QUER abrogates the process of angiogenesis at various steps. It has been shown that QUER inhibits early angiogenesis through reducing the expression of HIF-1α (Du *et al.*, 2000; Wilson and Poellinger, 2002; Oh *et al.*, 2010). In addition, QUER has been demonstrated to impede the activation of matrix metalloprotease-2 (Tan *et al.*, 2003) and reduce VEGF production (Zhong *et al.*, 2006; Oh *et al.*, 2010). The later stages of angiogenesis are also affected by QUER: inhibition of cell migration has been demonstrated after treatment with QUER (Igura *et al.*, 2001; Donnini *et al.*, 2006).

Data obtained from the present study suggests that the combinations of oestrone analogues and QUER may act as an anti-angiogenic drug combination. This is supported with data indicating the abrogation of the early stages of angiogenesis measured as reduced VEGF production and that QUER limited endothelial cell tube formation combined with extensive suppression of cell migration of the two tested cell lines MCF-7 and MDA-MB-231 breast adenocarcinoma and EA.hy926 endothelial cells was also observed.

In conclusion, the results obtained in the present study indicate that combinations of oestrone analogues with IND or QUER have possible anti-angiogenic potential as shown by *in vitro* assessment. The *in vivo* anti-angiogenic potential of these combinations should be confirmed using *in vivo* angiogenesis models.Data thus indicate that the synergistic combinations of oestrone analogues, ESE-15-ol and ESE-16, with the glycolysis inhibitors IND and QUER induce the cell death in MCF-7 and MDA-MB231 breast adenocarcinoma cell lines through various intracellular mechanisms. In addition, these combinations, especially the combination of ESE-15-ol and indinavir, show potential as anti-angiogenic agents. This may indicate application of these combinations as anti-cancer therapy with anti-angiogenic potential.

Chapter 5: Concluding discussion

In the clinical setting the greatest success in the treatment of malignancies has been achieved using combinations of effective chemotherapeutic agents with different mechanisms of action. The present study aimed at identifying synergistic combinations of anti-mitotic oestrone analogues and glycolysis inhibitors using *in vitro* breast cancer models.

5.1 Identification of synergistic combinations

The use of combinations of chemotherapeutic agents in the clinical setting was introduced by Frei and colleagues in the 1960's (Frei *et al.*, 1961a). This strategy allowed for lower concentrations of each agent to be used resulting in a more favourable adverse side effect profile. Moreover, as agents with different mechanisms of action were combined, the risk for development of chemo-resistance was reduced (Frei *et al.*, 1961a; Greco *et al.*, 1996; Chou, 2006).

Various *in vitro* models for the identification of synergy between two or more compounds have been proposed which include the use of isobolograms (Martinez-Irujo *et al.*, 1996), software packages to calculate combination index values (Chou and Talalay, 1984) and formula's utilising the shift in IC_{50} concentrations of the test compounds (Garbutcheon-Singh *et al.*, 2014). When compounds to be combined are not approximately equipotent, as in the present study, a checkerboard assay approach is recommended (Chou, 2010).

Stage 1 of the present study aimed at identifying synergistic combinations of two potent anti-mitotic oestrone analogues, ESE-15-ol and ESE-16, with each of six glycolysis inhibitors. ESE-15-ol and ESE-16 were *in silico* designed based on the structure of the potent anti-cancer agent 2ME (Stander *et al.*, 2011). The addition of a sulfamoylmoeity is proposed to improve on the poor pharmacokinetic properties of 2ME (Elger *et al.*, 1995; Stander *et al.*, 2011).

In addition to the characteristic increased rate of proliferation of malignant cells, these cells also exhibit a preference for aerobic glycolysis for the production of ATP, even in the presence of oxygen (Hanahan and Weinberg, 2000; Hanahan and Weinberg, 2011). Many cancer cells are known to over-express hexokinase responsible for the enzymatic conversion of glucose to glucose-6-phosphate in the first step of aerobic glycolysis (Bustamante and Pedersen, 1977; Rempel *et al.*, 1996). Elevated expression of glucose transporters to supply in the increased demand for glucose have also been observed in cancer cells (Grover-McKay *et al.*, 1998). The preference for aerobic glycolysis imparts an

evolutionary advantage to cancer cells: the production of lactic acid as a waste product of glycolysis acidifies the tumour microenvironment favouring mutagenesis (Yuan *et al.*, 2000).

The following glycolysis inhibitors were selected for this study:

1. Inhibitors of the hexokinase enzyme
    a. The glucose analogue 2-deoxyglucose (2DG)
    b. The small molecule 3- bromopyruvate (3-BrPA)
    c. The anti-spermatogenic compound lonidamine (LON)

2. Inhibitors of glucose transporters
    a. The small molecule fasentin (FAS)
    b. The flavonoid quercetin (QUER)
    c. The HIV protease inhibitor indinavir (IND)

In the present study CalcuSYN software, that uses the Median Effect equation of Chou and Talalay (Chou and Talalay, 1984), was used to identify synergistic combinations of the oestrone analogues and glycolysis inhibitorsfrom cytotoxicity data collected using *in vitro* models of breast cancer representing the most commonly diagnosed phenotypic subtypes of breast cancer. The combinations tested were based on the initial concentrations of each compound which inhibited the growth of the breast cancer cell lines by 50%. This identified drug combinations specific for each cell line. For example the most promising combination of ESE-15-ol and IND for MCF-7 breast adenocarcinoma cell line comprised of 70 nM ESE-15-ol and 115 µM IND, whereas 123 nM ESE-15-ol and 55 µM IND was required for synergy on the MDA-MB-231 breast adenocarcinoma cell line. The differences in synergistic drug combinations identified for the phenotypically different breast cancer subtypes allude to different biochemical pathway dominance thereby providing different susceptible drug targets responding differently to the specific treatment combinations required for greatest effect.

No synergistic combinations were identified for the SK-Br3 cell line, an *in vitro* model of Her2/neu positive breast cancer. In the clinical setting the recommended treatment for Her2/neu phenotypic subtype is a combination of a Her2-targeting humanised, monoclonal antibody and conventional small molecule chemotherapeutic agents (Slamon *et al.*, 2001). As there is no evidence currently suggesting that the oestrone analogues or glycolysis inhibitors specifically target the Her2/neu positive breast cancer, greater activity against the SK-Br3 cell line may be attained with a combination that includes a selective anti-Her2/neu agent.

Based on available clinical safety data, combinations of oestrone analogues and IND or QUER were selected for further investigation. Combinations of the oestrone analogues and these two glycolysis inhibitors were determined to act synergistically on the MCF-7 oestrogen receptor-positive breast cancer cell line as well as the MDA-MB-231 triple negative breast cancer cell line. Indinavir has been used in the treatment of human immunodeficiency virus infections and doses of up to 400 mg twice daily is reportedly well-tolerated (Cressey *et al.*, 2011). Quercetin is a natural flavanoid occurring in many foods with a daily dietary intake estimated at 20 to 100 mg with no side effects (Küuhnau, 1976; Leth and Justesen, 1998). In order to assess the potential of these glycolysis inhibitors in drug combinations for chemotherapeutic treatment, various *in vitro* assays were employed to elucidate mechanistic aspects of the cytotoxicity and potential anti-angiogenic properties of the most effective combinations as identified for each cell line.

5.2 Evaluation of toxicity sequence

Several assays were employed during Stage 2 of the present study in an attempt to track the sequence of toxicity induced following exposure to the combinations of the oestrone analogues and selected glycolysis inhibitors. It has been suggested that the sequence of toxicity occur in distinct stages progressing from transient events which require cell adaptation to pre-lethal events involving compromised intracellular homeostasis culminating in toxic, irreversible events (van Tonder *et al.*, 2013). Many of these techniques detect transient responses, such as fluctuations in the mitochondrial membrane potential and activation of caspases, and as and as these events are sequential but overlapping, the time points selected for the analysis of these responses must be well chosen.

The assays conducted during Stage 2 of the study were aimed at detecting different aspects of toxicity at various stages (Figure 5.1). To this end, the level of the anti-oxidant marker GSH was measured after 6 h exposure as indicator of early, transient events in the sequence of toxicity. As indicators of pre-lethal events the effects of the selected synergistic combinations on the induction of autophagy after 24 h, effects on ultrastructure after 24 h and fluctuations in the mitochondrial membrane potential after 24 and 48 h were assessed. Finally toxic, irreversible events were investigated by evaluating the activation of the caspase cascade after 24 and 48 h, morphological changes after 72 h and mode of cell death induced after 72 h.

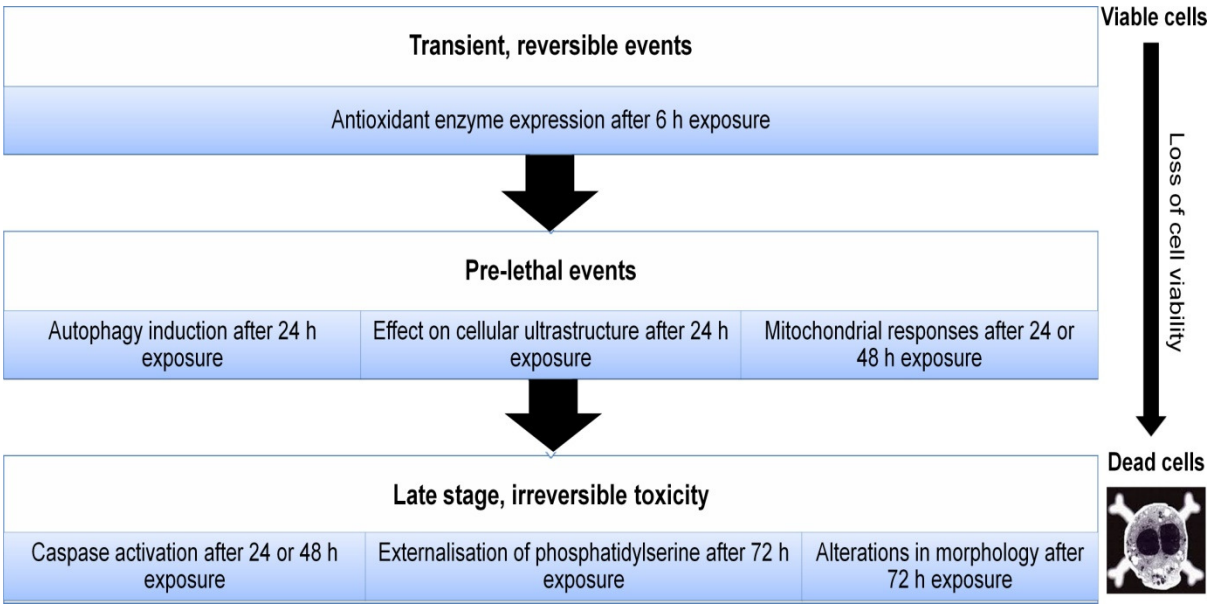

Figure 5.1: The *in vitro* assays used in the study to detect cellular changes indicative of the three stages of toxicity. Transient, reversible events were detected using anti-oxidant levels after 6 h exposure to the drug combinations. Pre-lethal events induced by the drug combinations were assessed by studying the induction of autophagy and cellular ultrastructure after 24 h and mitochondrial responses after 24 and 48 h exposure. The induction of late stage, irreversible toxicity was evaluated by the activation of the caspase cascade after 24 and 48 h, mode of cell death induced after 72 h and morphological changes induced after 72 h.
From (van Tonder *et al.*, 2013) with modifications. (http://cdn.intechopen.com/pdfs/41961/InTechPre_clinical_assessment_of_the_potential_intrinsic_hepatotoxicity_of_candidate_drugs.pdf)
Image titled 'The real face of cell death' used with permission from D Coletti.

It must be considered that synchronised cell populations were not used in the present study. The doubling time of a cell line is an indication of the time required for a tumour in an *in vivo* environment or cell population in an *in vitro* environment to double in size (Begg *et al.*, 1985). The average reported doubling time of MCF-7 breast adenocarcinoma cells is 35 h (Sutherland *et al.*, 1983; Barnes *et al.*, 2001; Kimura *et al.*, 2010), 29 h for MDA-MB-231 breast adenocarcinoma cells (Reddel *et al.*, 1985; Glunde *et al.*, 2004; Kimura *et al.*, 2010) and approximately 20 h for MCF-12A non-tumourigenic cells (Pauley *et al.*, 1993; Glunde *et al.*, 2004). Intracellular changes indicative of irreversible, toxic response is reportedly most accurately detected after exposure of 48 – 96 h (Monks *et al.*, 1991). As the initial cell population was not synchronised it is expected that some cells would be in more advanced stages of the cell cycle at the start of experiments, potentially confounding results. However,

even in non-synchronised populations of MCF-7, MDA-MB-231 and MCF-12A cells a minimum of one cell cycle for most cell culture would be completed in 72 h.

From the data obtained during the study a preliminary sequence of toxicity induced by combinations of oestrone analogues and IND or QUER were proposed (Figures 3.40 and 3.41). The results obtained during the present study are supported by published data about the effect of the oestrone analogues and the glycolysis inhibitors. Using published data on a number of intracellular parameters to support results from the present study a more detailed mechanism of action can be proposed for combinations with oestrone analogues and the two glycolysis inhibitors, IND and QUER.

Increased production of ROS in the mitochondria will occur following the attenuation of ATP synthesis (Apostolova *et al.*, 2011). The inhibition of aerobic glycolysis by IND (Hresko and Hruz, 2011) and QUER (Lang and Racker, 1974) would thus result in depletion of ATP initiating production of ROS. Generation of ROS is an indicator of early toxicity (Zamzami *et al.*, 1995). Results from the present study suggest that the combinations of oestrone analogues and glycolysis inhibitors induce the production of ROS after only 6 h exposure. It has been suggested that elevated levels of ROS may initiate intracellular adaptive mechanisms such as autophagy (Scherz-Shouval and Elazar, 2007).

The catabolic process of autophagy is a crucial pro-survival pathway activated under conditions of nutrient-deprivation as it allows the generation of amino acids from dysfunctional organelles and other non-essential intracellular components that can be used to generate ATP (Mizushima, 2005; Jin and White, 2007). Numerous techniques may be employed to detect the effect of a treatment on autophagy in intracellular systems. It has been suggested that more than one technique must be employed in order to confirm the induction of autophagy (Klionsky *et al.*, 2012).The most sensitive indicators of autophagy are the various molecular makers of autophagy, including LC3-II (Klionsky *et al.*, 2008).

In the present study both morphological studies using TEM were performed and LC3-II expression was detected using Western blot after 24 h drug combination exposure. It has been recommended that any marker of autophagy must be assessed at more than one time point so as to determine the effect of a treatment on autophagic flux (Klionsky *et al.*, 2008). However, due to the number of samples and financial implications involved, LC3-II expression was only assessed after 24 h treatment during the present study. Therefore the effect of the drug combinations on autophagy at other time points during the sequence of toxicity cannot be concluded. Evaluation of LC3-II expression at various times following exposure to the drug combinations is recommended for further studies.

Increased expression of LC3-II was not observed when MCF-7 or MDA-MB-231 breast adenocarcinoma cells were treated with ESE-15-ol (70 nM required for synergistic drug combinations with IND on MFC-7 cells, 17 nM required for synergistic drug combinations with QUER on MCF-7 cells or 123 nM required for synergistic drug combinations on MDA-MB-231 cells). However, data from the present study showed that treatment with ESE-16 (67 nM required for combinations with IND or 17 nM required for combinations with QUER) resulted in elevated expression of LC3-II, suggesting induction of autophagy. This is supports previously published reports on the effect of ESE-15-ol and ESE-16 on the induction of autophagy (Nkandeu *et al.*, 2013; Theron *et al.*, 2013; Wolmarans *et al.*, 2014).

The glycolysis inhibitors IND and QUER were observed to elevate levels of LC3-II expression in the present study indicative of the induction of autophagy. The ability of these glycolysis inhibitors to induce autophagy has been previously reported (McLean *et al.*, 2009; Klappan *et al.*, 2012) and has been proposed to promote cell survival (Gills *et al.*, 2007; Kim *et al.*, 2013).

From the data obtained from analysis of LC3-II expression after 24 h exposure, suppression of autophagy induced by IND was observed in both MCF-7 and MDA-MB-231 breast adenocarcinoma cell lines by the addition of the oestrone analogues. Similar trends were observed where MCF-7 cells were treated with combinations of oestrone analogues and QUER. However, in the MDA-MB-231 triple negative breast adenocarcinoma cell line slight elevation of LC3-II expression was observed where cells were treated with a combination of ESE-15-ol and QUER. This elevation was not significant and did not exceed the level of LC3-II in the untreated control cells.

It has been suggested that autophagy may present a pro-survival mechanism in cancer cells (Gu *et al.*, 2015). In this scenario autophagy may protect malignant cells from pro-death signals under conditions of nutrient deprivation or in response to limited cellular damage induced by anti-cancer agents (Shintani and Klionsky, 2004). This has been demonstrated in studies where pre-treatment with autophagy inhibitors resulted in increased cell death (Wang *et al.*, 2011; Kim *et al.*, 2013). Indeed, it has been demonstrated that autophagy induced by QUER fulfils a pro-survival role (Kim *et al.*, 2013) and similarly nelfinavir, a protease inhibitor like IND, induces protective autophagy (Gills *et al.*, 2007). It is therefore not surprising that numerous inhibitors of autophagy, including inhibitors of the mammalian target of rapamycin (mTOR)(Kahan and Camardo, 2001) and defrolimus (Rizzieri *et al.*, 2008), are currently under development as adjunct chemotherapy. When synergistic combinations of oestrone analogues and glycolysis inhibitors were used, LC3-II expression was reduced in comparison to IND- and QUER-treated samples. Thus the inhibition of IND- and QUER-

induced autophagy observed in the present study where cells where treated with synergistic drug combinations may sensitise tumourigenic cells to cell death.

Initiation of autophagic activity by IND and QUER is associated with stimulation of ER stress (Zha *et al.*, 2011; Klappan *et al.*, 2012). The ER is involved in the synthesis, folding, trafficking and post-translational modification of most proteins (Kim *et al.*, 2008; Martinon, 2012). Not only is the generation of receptors on cell surfaces dependent on the proper function of the ER, but it is also involved in the maintenance of the intracellular calcium ion balance (Martinon, 2012). Conditions known to stimulate ER stress include hypoxia and nutrient deprivation and may result in formation of misfolded proteins and the accumulation of unfolded proteins (Lee and Hendershot, 2006). ER stress may induce the 'unfolded protein response' (UPR), ER associated degradation or apoptosis (Hitomi *et al.*, 2004). As a protective mechanism, UPR aims to restore homeostasis through activation of the proteasome or autophagy to remove the improperly formed proteins (Schleicher *et al.*, 2010).

Prolonged ER stress has been shown to culminate in cell death via apoptosis or autophagy (Ma *et al.*, 2002; Rao *et al.*, 2006). Nuclear fragmentation and condensation has been observed in human neuroblastoma SK-N-SH cells treated with a known inducer of ER stress, tunicamycin (Imaizumi *et al.*, 2001). The induction of apoptosis observed after ER stress have been attributed to the activation of caspase 4 and the downstream activation of executioner caspases (Hitomi *et al.*, 2004).

Stimulation of autophagy in response to prolonged ER stress may be the result of phosphorylation of eukaryotic translation initiation factor 2α (eIF2α) by RNA-dependent protein kinase-like ER kinase (PERK)(Kouroku *et al.*, 2006). Autophosphorylation of PERK in response to ER stress results in the activation of eIF2α and reduction in protein translation (Harding *et al.*, 1999). Phosphorylated eIF2α has been demonstrated to upregulate expression of Atg12, a member of the Atg5-Atg12-Atg16 complex required for the conversion of LC3-I to LC3-II (Kouroku *et al.*, 2006). As both IND and QUER were shown to increase expression of LC3-II in the present study, the possible induction of an ER stress response should not be excluded.

Evidence suggests that the oestrone analogues may also induce ER stress. The oestrone analogues have been reported to increase aggresome formation (Nkandeu *et al.*, 2013; Theron *et al.*, 2013; Wolmarans *et al.*, 2014). Misfolded accumulated proteins in the cytoplasm are transported to the microtubule organising centre where the misfolded proteins are sequestered into a structure referred to as the aggresome (Garcia-Mata *et al.*, 2002). It

has been suggested that some of these aggresomes are degraded by lysosomes during autophagy and therefore accumulation of aggresomes may suggest induction of autophagy (Taylor *et al.*, 2003). Therefore the oestrone analogues may impede the proper folding of proteins resulting in the induction of ER stress. This is supported by the elevation in caspase 4 expression observed after treatment with ESE-16 (Stander *et al.*, 2013).

Moreover, the oestrone analogues may affect heat shock proteins (HSPs), which are crucial to protein folding, trafficking, secretion and degradation as well as in cell survival (Lianos *et al.*, 2015). The expression of HSPs is induced by numerous stress and environmentally unfavourable conditions including hypoxia, nutrient deprivation and exposure to cytotoxic chemicals (Wang *et al.*, 2014). Over-expression of HSP70 prevents the accumulation of aggresomes associated with the induction of ER stress (Garcia-Mata *et al.*, 2002). Attenuation of the activity of HSP70 would therefore render the cell susceptible to pro-death stimuli.

Previous studies have shown that numerous members of the HSP70 family were down-regulated in MCF-7 and MDA-MB-231 cells in response to treatment with ESE-16 (Stander *et al.*, 2013). Data on the effect of IND on the expression of HSP70 is lacking; over-expression of HSP70 has been demonstrated following treatment with the protease inhibitor ritonavir (Kraus *et al.*, 2008). However, QUER is a known HSP70 inhibitor (Yang *et al.*, 2003). Under conditions of stress this would translate as sensitivity to pro-death signals.

Therefore it seems likely that ER stress is involved in the sequence of toxicity induced following exposure to oestrone analogues and glycolysis inhibitors. It is recommended that effect of the combinations of oestrone analogues and glycolysis inhibitors on ER stress be elucidated by assessing the expression of phosphorylated PERK and phosphorylated eIF2α by Western blotting (Harding *et al.*, 1999). Evaluation of downstream effects such as aggresome formation should also be considered (Garcia-Mata *et al.*, 2002).

As the mitochondria is central to the production of ATP as well as induction of cell death, assessment of the effects of novel treatment strategies on the mitochondria are crucial. Mitochondrial effects can be classified as indicators of pre-lethal events in the sequence of toxicity (van Tonder *et al.*, 2013). During the present study mitochondrial membrane potential was assessed after 24 and 48 h. Overall treatment with synergistic drug combinations of oestrone analogues and IND resulted in hyperpolarisation of the mitochondrial membrane, whereas depolarisation of the mitochondrial membrane potential was observed when cells were treated with synergistic drug combinations of oestrone analogues and QUER.

Hyperpolarisation of the mitochondrial membrane potential is associated with the inhibition of ATP synthesis (Kalbáčová *et al.*, 2003). Inhibition of glucose transporters by IND will result in depleted intracellular glucose concentrations and subsequent inhibition of ATP production (Murata *et al.*, 2002; Hresko and Hruz, 2011). Mitochondrial dysfunction as a result of IND treatment has been reported (Matarrese *et al.*, 2003). The addition of oestrone analogues to IND exacerbated the hyperpolarisation observed and may therefore account for synergistic interaction.

Dissipation of the mitochondrial membrane potential occurs as a result of the increased permeability of the outer mitochondrial membrane (Tsujimoto and Shimizu, 2007). The increased permeability is due to the opening of the mitochondrial membrane permeability transition pore and results in the release of apoptogenic factors such as cytochrome *c* (Vander Heiden *et al.*, 1997; Osellame *et al.*, 2012). Depolarisation of the mitochondrial membrane potential as a result of exposure to QUER or the combinations of oestrone analogues and QUER therefore suggests the involvement of the mitochondria in the induction of cell death.

The balance between pro-apoptotic members of the family, such as Bax and Bak, and pro-survival members, including Bcl-2 and Bcl-$X_{L,}$ is involved in the regulation of cell death (Vander Heiden and Thompson, 1999). It has been suggested that pro-apoptotic Bax facilitates the release of cytochrome *c* from the mitochondrial inter-membrane space without dissipation of the mitochondrial membrane potential (Rosse *et al.*, 1998; Desagher and Martinou, 2000). In contrast, pro-survival Bcl-2 inhibits the release of apoptogenic cytochrome *c* from the mitochondria (Kluck *et al.*, 1997).

Published reports indicate that the oestrone analogues influence the balance between the pro-apoptotic and pro-survival Bcl-2 family members in favour of cell death induction. Phosphorylation of pro-survival Bcl-2 was observed after treatment with ESE-15-ol and ESE-16 (Stander *et al.*, 2012, 2013). Phosphorylation of Bcl-2 has been reported to limit its anti-apoptotic role, thus promoting cell death (Haldar *et al.*, 1995). Induction of autophagy has also been reported to occur as a result of phosphorylation of Bcl-2 (Wei *et al.*, 2008).

Reports have shown that IND does not affect the levels of Bcl-2 or Bax in lymphocytes (Matarrese *et al.*, 2003). However, the effect of IND on the expression of Bcl-2 and Bax in malignant cells has not been described. In response to QUER treatment decreased expression of anti-apoptotic Bcl-2 and elevation of pro-apoptotic Bax levels have been observed (Granado-Serrano *et al.*, 2006; Duo *et al.*, 2012). Therefore, the role of the Bcl-2 family in the sequence of toxicity induced by the synergistic drug combinations of oestrone analogues and glycolysis inhibitors warrants further investigation.

In the present study significant elevation in activity of caspases 3/7, -8 and -9 was not detected for any treatment groups after 24 or 48 h treatment. However, the slight increase in the activity of caspase 8 in MCF-7 cells treated with combinations of ESE-15-ol and IND for 24 h suggests the activation of the extrinsic pathway, whereas the slightly increased activity of caspase 9 in cells treated with combinations with QUER indicates the involvement of the intrinsic pathway. However, despite using a standardised cell number for the assays, protein standardisation was not performed in the assays used for the detection of caspase activity which limits the conclusions which may be drawn from the data obtained from these assays. Furthermore, the activation of a limited number of caspases determined in the present study does not preclude the involvement of alternative caspases such as caspase 4 and -6. To investigate the role of ER stress, it is recommended that the effect of the synergistic drug combinations on the activity of caspase 4 is evaluated as cell death due to ER stress has been associated with the activation of caspase 4 (Hitomi *et al.*, 2004).

As final parameter of irreversible toxicity evaluated during the study, the mode of cell death induced by treatment with the combinations of oestrone analogues and glycolysis inhibitors were determined after 72 h treatment. Data indicate that apoptotic and necrotic cell death was induced by the combinations after 72 h. This was observed in the MCF-7 and MDA-MB-231 breast adenocarcinoma cell lines as well as in the non-tumourigenic MCF-12A breast cell line.

During the unregulated process of necrosis, cytoplasmic contents are released into the extracellular environment resulting in the recruitment of inflammatory cells. The subsequent inflammation may cause damage to the surrounding tissue which is undesirable in the milieu of cancer treatment (Willingham, 1999). After MCF-7 or MDA-MB-231 breast adenocarcinoma cells were treated with cell line-specific combinations of ESE-15-ol and IND for 72 h, approximately 12% of the cell population was positively stained for propidium iodide, an indicator of compromised membrane integrity, while staining negative for the selective phosphatidylserine antibody annexin V-FITC. The use of this combination will thus result in the induction of apoptotic cell death while limiting the incidence of necrotic cell death.

From the data obtained during the study and published reports on the *in vitro* effects of the oestrone analogues and the glycolysis inhibitors on a number of intracellular parameters the sequence of toxicity induced by combinations on oestrone analogues and glycolysis inhibitors is proposed in Figures 5.2 and 5.3.

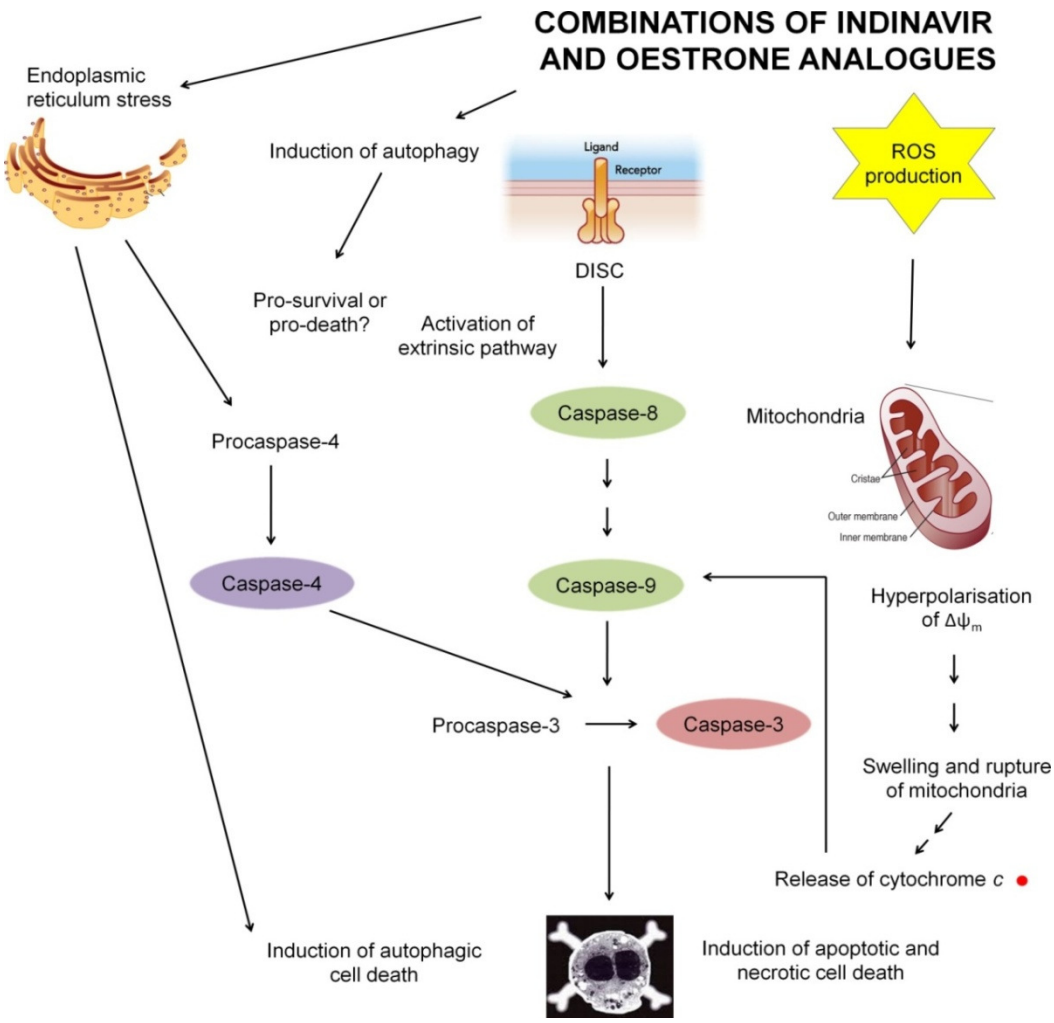

Figure 5.2: The proposed sequence of toxicity induced by synergistic drug combinations of oestrone analogues and indinavir from data obtained from the present study and published reports. Treatment with the combinations of oestrone analogues and indinavir result in production of ROS. Inhibition of ATP synthesis causes hyperpolarisation of the mitochondrial membrane potential resulting in swelling and eventual rupture of the mitochondria. The extrinsic pathway of apoptosis is activated by the synergistic drug combination as indicated by the activation of caspase 8 and downstream activation of caspase 3. Apoptotic and necrotic cell death follow. Results from the present study do not support the induction of autophagy after 24 h treatment. According to literature the oestrone analogues may induce endoplasmic reticulum stress resulting in the activation of caspase 4 and induction of apoptotic and autophagic cell death.

Structures of DISC from Sendoel and Hengartner, 2014. (Sendoel and Hengartner, 2014) with modifications. Creative Commons Attribution License (CC-BY-2.0). Structures of mitochondria and endoplasmic reticulum by Darryl Leja, NHGRI, www.genome.gov. Accessed September 2015.

Image titled 'The real face of cell death' used with permission from D Coletti.

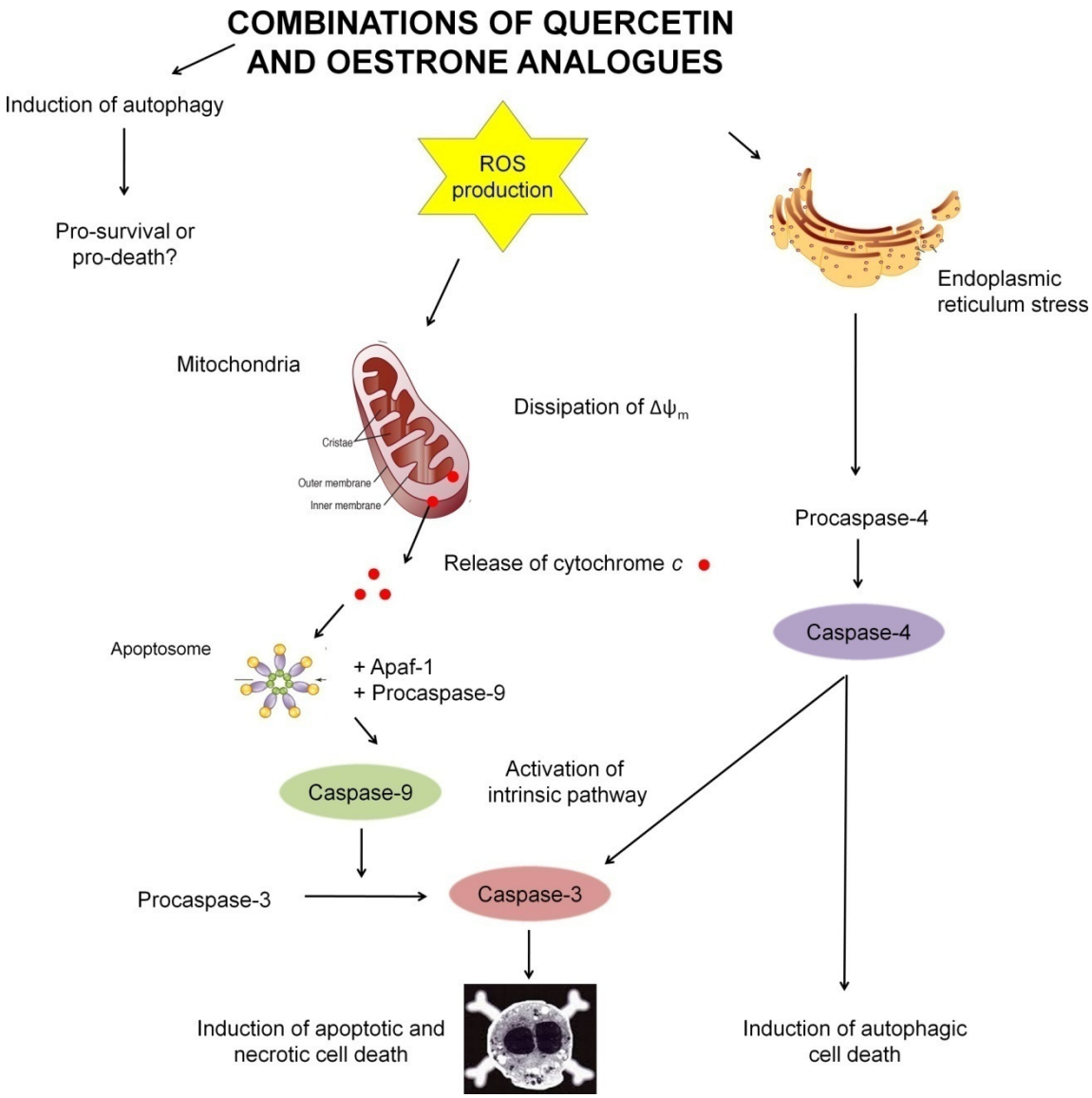

Figure 5.3: The proposed sequence of toxicity induced by combinations of oestrone analogues and quercetin from data obtained from the present study and published reports. Treatment with the synergistic drug combinations of oestrone analogues and quercetin result in generation of ROS leading to depolarisation of the mitochondrial membrane potential and activation of the intrinsic pathway of apoptosis. The activation of caspase 9 leads to the activation of caspase 3 and induction of apoptotic and necrotic cell death. Results from the present study do not support the induction of autophagy after 24 h treatment. According to literature the oestrone analogues may induce endoplasmic reticulum stress resulting in the activation of caspase 4 and induction of apoptotic and autophagic cell death.

Structures of apoptosome from Sendoel and Hengartner, 2014. (Sendoel and Hengartner, 2014) with modifications. Creative Commons Attribution License (CC-BY-2.0). Structures of mitochondria and endoplasmic reticulum by Darryl Leja, NHGRI, www.genome.gov. Accessed September 2015. Image titled 'The real face of cell death' used with permission from D Coletti.

Reports of *in vitro* studies have demonstrated anti-angiogenic properties for quercetin (Tan *et al.*, 2003; Oh *et al.*, 2010) and indinavir (Sgadari *et al.*, 2002). In order to obtain a more detailed mechanistic profile of the combinations of oestrone analogues and IND or QUER the anti-angiogenic properties of the synergistic drug combinations were investigated.

5.3 Anti-angiogenic assessment of the selected combinations

The induction of angiogenesis ensures the survival of cells within tumours under conditions of hypoxia (Kumar and Choi, 2015). The process of tumour neovascularisation is reputed to be initiated with the formation of the HIF-1 complex which induces the transcription of pro-angiogenic factors including vascular endothelial growth factor (Ryan *et al.*, 1998; Hitchon and El-Gabalawy, 2004). Once endothelial cells from closely located blood vessels are liberated from the basement membrane by matrix metalloproteases, they migrate toward the tumour in the direction of pro-angiogenic factors gradient (Bergers and Benjamin, 2003; Carmeliet and Jain, 2011). During the process of angiogenesis tube formation and cell migration occur interchangeably (Auerbach *et al.*, 2003).

The angiogenic potential of a tumour is directly associated with its metastatic potential (Folkman, 1971). As angiogenesis is not an ongoing process in healthy adults, inhibition of this process is a relatively selective target for cancer therapy (Cook and Figg, 2010). A number of anti-angiogenic treatments have undergone clinical testing including the multikinase inhibitor sorafenib (Cheng *et al.*, 2009), the kinase inhibitor imatinib (Druker *et al.*, 2006), the anti-VEGF monoclonal antibody bevacizumab (Sandler *et al.*, 2006) and the notorious anti-angiogenic agent thalidomide (Rajkumar *et al.*, 2006). The enhanced therapeutic efficacy obtained with anti-angiogenic treatment is often at the risk of increased toxicity (Rajkumar *et al.*, 2006; Sandler *et al.*, 2006).

The release of VEGF from a tumour under hypoxic conditions is reported to be one of the first steps in the process of angiogenesis and is associated with tumour progression (Wenger, 2002; Zhang *et al.*, 2010). In the present study the effect of synergistic combinations of oestrone analogues and glycolysis inhibitors were assessed on the secretion of VEGF from breast adenocarcinoma cells. All tested combinations successfully reduced the VEGF concentration in conditioned medium from drug combination treated relative to untreated MCF-7 or MDA-MB-231 breast adenocarcinoma cells suggesting at least some anti-metastatic potential.

Endothelial cells are central to the process of tumour angiogenesis as these cells form new vessels (Hanahan and Folkman, 1996). A great advantage to the use of anti-angiogenic

agents is that the untransformed, proliferating endothelial cells often targeted by anti-angiogenic agents present a selective target as endothelial cells in unaffected areas are mostly in a dormant state (Kerbel, 1991). Furthermore, the low mutation rate of endothelial cells does not encourage the development of drug resistance: where a potent angiogenesis inhibitor was administered intermittently to tumour-bearing mice, drug resistance was not observed (Boehm *et al.*, 1997).

It has been suggested that the administration schedule of chemotherapeutics may be manipulated to target endothelial cells, and thus tumour vasculature, through the administration of continuous, low-dose chemotherapy (Browder *et al.*, 2000). This strategy, in contrast to conventional chemotherapy where a bolus dose is administered followed by a recovery period, would prevent the recovery of tumour cells after treatment with chemotherapy (Kerbel *et al.*, 2000). This has been demonstrated *in vivo* where an 'anti-angiogenic schedule' of cyclophosphamide resulted in enhanced eradication of drug resistant tumours (Browder *et al.*, 2000). These results were repeated in neuroblastoma xenografts exposed to the combination of low dose vinblastine and a specific angiogenic agent where extensive tumour regression was observed (Klement *et al.*, 2000). Surprisingly during the 6 month treatment period drug resistance did not develop and the low doses of the compounds used translated into in absence of toxicity (Klement *et al.*, 2000).

Evaluation of the effect of the combinations of oestrone analogues with IND or QUER on the ability of EA.hy926 hybrid endothelial cell line to form tubule networks after 8 h revealed decreased complexity of tube networks, reduced number of tubes formed as well as a reduction in the length of the longest tubes. The ability of EA.hy926 hybrid endothelial cells to migrate into a scratch zone through an established almost confluent culture was reduced after exposure to the selected synergistic drug combinations. A similar reduced ability of MCF-7 and MDA-MB-231 breast adenocarcinoma cells to migrate into a scratch zone was observed. These effects were most pronounced with combinations of ESE-15-ol and IND. The results from these *in vitro* assays suggest that the combinations of oestrone analogues and glycolysis inhibitors affect the process of tumour angiogenesis, or potentially cell migration, at different stages.

It was initially believed that resistance to anti-angiogenic therapy was unlikely due to the genome stability of endothelial cells (Kerbel, 1991; Folkman *et al.*, 2000). However, transient efficacy of anti-angiogenic agents have been reported using *in vivo* models (Klement *et al.*, 2000). It has been suggested that the greatest success will be obtained with combinations of agents targeting both angiogenesis and the enhanced proliferation rate of cancer cells simultaneously (Teicher *et al.*, 1992). Results from the present study suggest that the

synergistic combinations of oestrone analogues and glycolysis inhibitors do have the potential of inhibiting the proliferation of cancer cells as well as the formation of tumour vasculature.

5.4 Future directions

During preclinical evaluation of potential therapeutic agents a number of parameters must be adequately and appropriately assessed to ascertain suitability for clinical development. Preclinical *in vitro* testing is required to obtain sufficient data to warrant *in vivo* testing of a limited number of potential therapeutic agents (Ruiz-Garcia *et al.*, 2008). In the present study the number of synergistic combinations between oestrone analogues and glycolysis inhibitors was reduced to six potential combinations.

In order to clarify the intracellular effects of the identified combinations of oestrone analogues and glycolysis inhibitors the following steps are recommended:

1. *Autophagy studies.* Due to the large sample size, time- and financial constraints, a time course evaluation of LC3-II expression was not conducted in the present study. In order to fully elucidate the role of autophagy in the sequence of toxicity, it is recommended that the expression of LC3-II is assessed at both earlier and later time points than the 24 h used in the present study.
2. *Caspase activation studies.* In the present study the activity of caspase 8 as indicator of the involvement of the extrinsic pathway, the activity of caspase 9 as indicator of the role of the intrinsic pathway and the activity of caspases 3/7 were assessed. Significant activity of these caspases were not observed, which may suggest the involvement of alternative caspases or may be an experimental artefact as the results were not standardised to protein concentration but relied on the use of the same cell number to perform the assays. It is therefore recommended that the activation of the caspase cascade be assessed in greater detail with the added evaluation of the activation of alternative caspases such as caspases 4 and -6.
3. *Elucidation of the involvement of ER stress.* Published reports on the oestrone analogues suggest the induction of ER stress (Nkandeu *et al.*, 2013; Stander *et al.*, 2013; Theron *et al.*, 2013; Wolmarans *et al.*, 2014). The confirmation of the role of ER stress induced by the synergistic drug combinations may explain the absence of caspase activity even though apoptotic cell death was observed as ER stress induces apoptosis through the activation of caspase 4. Furthermore, it will provide insight into the role of autophagy in the sequence of toxicity induced by these

combinations as ER stress has been associated with the induction of apoptosis and autophagy (Hitomi *et al.*, 2004; Schleicher *et al.*, 2010).

4. *Further anti-angiogenic studies.* The *in vitro* angiogenesis studies performed in the present study provide the first proof that the synergistic combinations of oestrone analogues and glycolysis inhibitors have anti-angiogenic properties. However, these studies quantified the effect of the combinations on specific, isolated parameters of angiogenesis, and cannot elucidate the effect of the physiological environment on the observed anti-angiogenic efficacy. It is therefore recommended that *in vivo* angiogenesis models, such as the chorioallantoic membrane assay or Matrigel-plug assay, are used to confirm the anti-angiogenic properties observed.
5. *Toxicity studies.* These are described in detail below.

Throughout the study the various parameters of toxic events were assessed not only on the breast adenocarcinoma cell lines, but also in the MCF-12A non-tumourigenic cell line. The MCF-12A non-tumourigenic cell line was established from breast tissue obtained from a mammoplasty which became immortal after exposure to high temperatures. The immortalisation of this cell line allowed for the study of neoplastic transformation in normal epithelial cells which had previously not been possible (Pauley *et al.*, 1993). Numerous non-tumourigenic cell lines have been established using transfection or chemicals (Chou, 1989). Even though such *in vitro* systems provide valuable information on the potential toxicity of experimental treatments, the complete effect can only be assessed in an intact organism where system integration and pharmacokinetic and pharmacodynamic influences are involved (Bhogal *et al.*, 2005).

Ex vivo studies have been used to assess the effects of the oestrone analogues on erythrocytes and platelets and no signs of toxicity were observed (Repsold *et al.*, 2014a; Repsold *et al.*, 2014b). Clinical safety data on IND indicate that the concentrations used in the present study is physiologically achievable with a tolerable side effect profile(La Porte *et al.*, 2006). It is therefore recommended that potential toxicity of the synergistic combinations identified in the present study should be assessed using *ex vivo* studies and if results are favourable, *in vivo* testing may be initiated.

Obtaining a balance between efficacy and toxicity of anti-cancer therapy is the goal of the rational use of chemotherapeutics. This equilibrium is well illustrated by the use of thalidomide. Thalidomide is most infamous for inducing teratogenic effects including phocomelia (McBride, 1961; Lenz *et al.*, 1962). However, the potent anti-angiogenic properties of thalidomide have resulted in its reintroduction as anti-cancer agent (D'Amato *et al.*, 1994b; Singhal *et al.*, 1999). Currently the use of thalidomide is closely regulated by

stringent prescribing protocols (Kumar *et al.*, 2002). The successful use of chemotherapeutic agents may therefore rely on obtaining the balance between efficacy and toxicity in a population where the therapeutic benefit outweighs the risk of treatment.

5.5 Conclusion

During this study, synergistic combinations of two *in silico* designed oestrone analogues, ESE-15-ol and ESE-16, and six glycolysis inhibitors were successfully assayed. Synergistic combinations specific for the oestrogen receptor-positive MCF-7 breast adenocarcinoma cell line or MDA-MB-231 the metastatictriple negative, breast adenocarcinoma cell line were identified using multiple checkerboard type concentration combination assays. The most promising of these synergistic drug combinations were selected taking into account published safety data of the glycolysis inhibitors. Synergistic combinations of the oestrone analogues and antiretroviral protease inhibitor indinavir or the flavonoid quercetin were then investigated using *in vitro* models to establish the sequence of toxicity induced by each combination and finally *in vitro* evaluated for potential anti-angiogenic properties.

Data indicate that combinations of the oestrone analogue ESE-15-ol and IND is most promising based on the following observations:

1. Production of reactive oxygen species
2. Inhibition of ATP synthase, as indicated by hyperpolarisation of the mitochondrial membrane potential
3. Induction of cell death predominantly via apoptosis
4. Inhibition of angiogenesis by decreasing secretion of vascular endothelial growth factor
5. Limits formation of endothelial tubule networks and cell migration

An advantage of the combination of ESE-15-ol and IND is that it shows activity against the *in vitro* model of triple negative breast cancer. Triple negative breast cancer generally responds poorly to chemotherapeutic treatment and thus is generally associated with poor prognosis (Meyer *et al.*, 1977; Wirapati *et al.*, 2008). As the clinical safety profile of IND has been established, the next step in investigating the clinical potential of this combination would be to assess the *in vivo* safety of ESE-15-ol in appropriate rodent models.

In conclusion, the aims and objectives for this study were achieved using various *in vitro* methods and resulted in the identification of synergistic combinations of ESE-15-ol, a

synthetic oestrone analogue, and indinavir, a HIV protease inhibitor, which show potential anti-metastatic activity that could be used for treatment of breast cancer.

More effective treatment of malignancies will evolve from the use of drugs in available synergistic combinations that target different intracellular pathways.

References

AARONSON, S. A. 1991. Growth Factors and Cancer. *Science,* 254**,** 1146-53.

ABRAMSON, V. G.; LEHMANN, B. D.; BALLINGER, T. J. & PIETENPOL, J. A. 2015. Subtyping of Triple-Negative Breast Cancer: Implications for Therapy. *Cancer,* 121**,** 8-16.

AFT, R.; ZHANG, F. & GIUS, D. 2002. Evaluation of 2-Deoxy-D-Glucose as a Chemotherapeutic Agent: Mechanism of Cell Death. *Br J Cancer,* 87**,** 805-12.

AHLBERG, K.; EKMAN, T.; GASTON-JOHANSSON, F. & MOCK, V. 2003. Assessment and Management of Cancer-Related Fatigue in Adults. *Lancet,* 362**,** 640-50.

AKBAS, S. H.; TIMUR, M. & OZBEN, T. 2005. The Effect of Quercetin on Topotecan Cytotoxicity in MCF-7 and MDA-MB-231 Human Breast Cancer Cells 1. *J Surg Res,* 125**,** 49-55.

ALBINI, A.; IWAMOTO, Y.; KLEINMAN, H. K.; MARTIN, G. R.; AARONSON, S. A.; KOZLOWSKI, J. M. & MCEWAN, R. N. 1987. A Rapid in Vitro Assay for Quantitating the Invasive Potential of Tumor Cells. *Cancer Res,* 47**,** 3239-45.

APOSTOLOVA, N.; BLAS-GARCÍA, A. & ESPLUGUES, J. V. 2011. Mitochondrial Interference by Anti-HIV Drugs: Mechanisms Beyond Pol-Γ Inhibition. *Trends Pharmacol Sci,* 32**,** 715-25.

ARANDA, E. & OWEN, G. I. 2009. A Semi-Quantitative Assay to Screen for Angiogenic Compounds and Compounds with Angiogenic Potential Using the EA.Hy926 Endothelial Cell Line. *Biol Res,* 42**,** 377-89.

ARTEMOV, D.; BHUJWALLA, Z. M.; PILATUS, U. & GLICKSON, J. D. 1998. Two-Compartment Model for Determination of Glycolytic Rates of Solid Tumors by in Vivo13C NMR Spectroscopy. *NMR in Biomed,* 11**,** 395-404.

ATCHLEY, D. P.; ALBARRACIN, C. T.; LOPEZ, A.; VALERO, V.; AMOS, C. I.; GONZALEZ-ANGULO, A. M.; HORTOBAGYI, G. N. & ARUN, B. K. 2008. Clinical and Pathologic Characteristics of Patients with BRCA-Positive and BRCA-Negative Breast Cancer. *J Clin Oncol,* 26**,** 4282-88.

ATTALLA, H.; MÄKELÄ, T. P.; ADLERCREUTZ, H. & ANDERSSON, L. C. 1996. 2-Methoxyestradiol Arrests Cells in Mitosis without Depolymerizing Tubulin. *Biochem Biophys Res Comm,* 228**,** 467-73.

AUBRY, J.-P.; BLAECKE, A.; LECOANET-HENCHOZ, S.; JEANNIN, P.; HERBAULT, N.; CARON, G.; MOINE, V. & BONNEFOY, J.-Y. 1999. Annexin V Used for Measuring Apoptosis in the Early Events of Cellular Cytotoxicity. *Cytometry,* 37**,** 197-204.

AUERBACH, R.; LEWIS, R.; SHINNERS, B.; KUBAI, L. & AKHTAR, N. 2003. Angiogenesis Assays: A Critical Overview. *Clin Chem,* 49**,** 32-40.

BADLEY, A. 2005. In Vitro and in Vivo Effects of HIV Protease Inhibitors on Apoptosis. *Cell Death Differ,* 12**,** 924-31.

BAI, X.; KINNEY, W. H.; SU, W.-L.; BAI, A.; OVRUTSKY, A. R.; HONDA, J. R.; NETEA, M. G.; HENAO-TAMAYO, M.; ORDWAY, D. J. & DINARELLO, C. A. 2015. Caspase-3-Independent

Apoptotic Pathways Contribute to Interleukin-32γ-Mediated Control of Mycobacterium Tuberculosis Infection in THP-1 Cells. *BMC Microbiol,* 15**,** 39.

BAISH, J. W. & JAIN, R. K. 2000. Fractals and Cancer. *Cancer Res,* 60**,** 3683-88.

BAKER, S.; MARKOWITZ, S.; FEARON, E.; WILLSON, J. & VOGELSTEIN, B. 1990. Suppression of Human Colorectal Carcinoma Cell Growth by Wild-Type P53. *Science,* 249**,** 912-15.

BALENDIRAN, G. K.; DABUR, R. & FRASER, D. 2004. The Role of Glutathione in Cancer. *Cell Biochem Funct,* 22**,** 343-52.

BALLARD-BARBASH, R.; SCHATZKIN, A.; CARTER, C. L.; KANNEL, W. B.; KREGER, B. E.; D'AGOSTINO, R. B.; SPLANSKY, G. L.; ANDERSON, K. M. & HELSEL, W. E. 1990. Body Fat Distribution and Breast Cancer in the Framingham Study. *J Natl Cancer Inst,* 82**,** 286-90.

BANERJEEI, S. K.; ZOUBINE, M. N.; SARKAR, D. K.; WESTON, A. P.; SHAH, J. H. & CAMPBELL, D. R. 2000. 2-Methoxyestradiol Blocks Estrogen-Induced Rat Pituitary Tumor Growth and Tumor Angiogenesis: Possible Role of Vascular Endothelial Growth Factor. *Anticancer Res,* 20**,** 2641-45.

BARAN, I.; GANEA, C.; URSU, I.; BARAN, V.; CALINESCU, O.; IFTIME, A.; UNGUREANU, R. & TOFOLEAN, I. 2011. Fluorescence Properties of Quercetin in Human Leukemia Jurkat T-Cells. *Rom J Phys,* 56**,** 388-98.

BARANSKA, P.; JERCZYNSKA, H.; PAWLOWSKA, Z.; KOZIOLKIEWICZ, W. & CIERNIEWSKI, C. S. 2005. Expression of Integrins and Adhesive Properties of Human Endothelial Cell Line EA.Hy 926. *Cancer Genomics-Proteomics,* 2**,** 265-69.

BARGMANN, C. I.; HUNG, M.-C. & WEINBERG, R. A. 1986. The Neu Oncogene Encodes an Epidermal Growth Factor Receptor-Related Protein. *Nature,* 319**,** 226-30.

BARNES, J. A.; DIX, D. J.; COLLINS, B. W.; LUFT, C. & ALLEN, J. W. 2001. Expression of Inducible Hsp70 Enhances the Proliferation of MCF-7 Breast Cancer Cells and Protects against the Cytotoxic Effects of Hyperthermia. *Cell Stress Chaperones,* 6**,** 316-25.

BARTH, S.; GLICK, D. & MACLEOD, K. F. 2010. Autophagy: Assays and Artifacts. *J Pathol,* 221**,** 117-24.

BARTLETT, N. L.; LUM, B. L.; FISHER, G. A.; BROPHY, N. A.; EHSAN, M. N.; HALSEY, J. & SIKIC, B. I. 1994. Phase I Trial of Doxorubicin with Cyclosporine as a Modulator of Multidrug Resistance. *J Clin Oncol,* 12**,** 835-42.

BASU, A.; CASTLE, V. P.; BOUZIANE, M.; BHALLA, K. & HALDAR, S. 2006. Crosstalk between Extrinsic and Intrinsic Cell Death Pathways in Pancreatic Cancer: Synergistic Action of Estrogen Metabolite and Ligands of Death Receptor Family. *Cancer Res,* 66**,** 4309-18.

BEGG, A.; MCNALLY, N.; SHRIEVE, D. & KARCHE, H. 1985. A Method to Measure the Duration of DNA Synthesis and the Potential Doubling Time from Single Sample. *Cytometry,* 6**,** 620-26.

BENJAMIN, L. E.; GOLIJANIN, D.; ITIN, A.; PODE, D. & KESHET, E. 1999. Selective Ablation of Immature Blood Vessels in Established Human Tumors Follows Vascular Endothelial Growth Factor Withdrawal. *J Clin Invest,* 103**,** 159.

BERGERS, G. & BENJAMIN, L. E. 2003. Tumorigenesis and the Angiogenic Switch. *Nat Rev Cancer,* 3**,** 401-10.

BERNDT, K.; CAMPANILE, C.; MUFF, R.; STREHLER, E.; BORN, W. & FUCHS, B. 2013. Evaluation of Quercetin as a Potential Drug in Osteosarcoma Treatment. *Anticancer Res,* 33**,** 1297-306.

BERNSTEIN, L.; HENDERSON, B. E.; HANISCH, R.; SULLIVAN-HALLEY, J. & ROSS, R. K. 1994. Physical Exercise and Reduced Risk of Breast Cancer in Young Women. *J Natl Cancer Inst,* 86**,** 1403-08.

BEUTNER, G.; RÜCK, A.; RIEDE, B. & BRDICZKA, D. 1998. Complexes between Porin, Hexokinase, Mitochondrial Creatine Kinase and Adenylate Translocator Display Properties of the Permeability Transition Pore. Implication for Regulation of Permeability Transition by the Kinases. *BBA - Biomembranes,* 1368**,** 7-18.

BHOGAL, N.; GRINDON, C.; COMBES, R. & BALLS, M. 2005. Toxicity Testing: Creating a Revolution Based on New Technologies. *Trends Biotechnol,* 23**,** 299-307.

BHUTIA, S. K.; MUKHOPADHYAY, S.; SINHA, N.; DAS, D. N.; PANDA, P. K.; PATRA, S. K.; MAITI, T. K.; MANDAL, M.; DENT, P.; WANG, X.-Y.; DAS, S. K.; SARKAR, D. & FISHER, P. B. 2013. Autophagy: Cancer's Friend or Foe? *Adv Cancer Res,* 118**,** 61-95.

BISHOP, J. M. 1982. Oncogenes. *Sci Am,* 246**,** 80.

BISHOP, J. M. 1985. Viral Oncogenes. *Cell,* 42**,** 23-38.

BLISS, C. I. 1939. The Toxicity of Poisons Applied Jointly. *Ann App Biol,* 26**,** 585-615.

BLOOM, H. & RICHARDSON, W. 1957. Histological Grading and Prognosis in Breast Cancer: A Study of 1409 Cases of Which 359 Have Been Followed for 15 Years. *Br J Cancer,* 11**,** 359.

BOEHM, T.; FOLKMAN, J.; BROWDER, T. & O'REILLY, M. S. 1997. Antiangiogenic Therapy of Experimental Cancer Does Not Induce Acquired Drug Resistance. *Nature,* 390**,** 404-07.

BONADONNA, G.; VALAGUSSA, P.; MOLITERNI, A.; ZAMBETTI, M. & BRAMBILLA, C. 1995. Adjuvant Cyclophosphamide, Methotrexate, and Fluorouracil in Node-Positive Breast Cancer — the Results of 20 Years of Follow-Up. *N Engl J Med,* 332**,** 901-06.

BOSSY-WETZEL, E.; NEWMEYER, D. D. & GREEN, D. R. 1998. Mitochondrial Cytochrome C Release in Apoptosis Occurs Upstream of DEVD-Specific Caspase Activation and Independently of Mitochondrial Transmembrane Depolarization. *EMBO J,* 17**,** 37-49.

BOUÏS, D.; HOSPERS, G. A.; MEIJER, C.; MOLEMA, G. & MULDER, N. H. 2001. Endothelium in Vitro: A Review of Human Vascular Endothelial Cell Lines for Blood Vessel-Related Research. *Angiogenesis,* 4**,** 91-102.

BRAND, M. D.; CHIEN, L.-F.; AINSCOW, E. K.; ROLFE, D. F. & PORTER, R. K. 1994. The Causes and Functions of Mitochondrial Proton Leak. *BBA-Bioenergetics,* 1187**,** 132-39.

BRANDMANN, M.; TULPULE, K.; SCHMIDT, M. M. & DRINGEN, R. 2012. The Antiretroviral Protease Inhibitors Indinavir and Nelfinavir Stimulate MRP1-Mediated GSH Export from Cultured Brain Astrocytes. *J Neurochem,* 120**,** 78-92.

BRÖKER, L. E.; KRUYT, F. A. & GIACCONE, G. 2005. Cell Death Independent of Caspases: A Review. *Clin Cancer Res,* 11**,** 3155-62.

BROWDER, T.; BUTTERFIELD, C. E.; KRÄLING, B. M.; SHI, B.; MARSHALL, B.; O'REILLY, M. S. & FOLKMAN, J. 2000. Antiangiogenic Scheduling of Chemotherapy Improves Efficacy against Experimental Drug-Resistant Cancer. *Cancer Res,* 60**,** 1878-86.

BU, S. Z.; HUANG, Q.; JIANG, Y. M.; MIN, H. B.; HOU, Y.; GUO, Z. Y.; WEI, J. F.; WANG, J. W.; NI, X. & ZHENG, S. S. 2006. P38 Mitogen-Activated Protein Kinases Is Required for Counteraction of 2-Methoxyestradiol to Estradiol-Stimulated Cell Proliferation and Induction of Apoptosis in Ovarian Carcinoma Cells Via Phosphorylation Bcl-2. *Apoptosis,* 11**,** 413-25.

BUCHKOVICH, K.; DUFFY, L. A. & HARLOW, E. 1989. The Retinoblastoma Protein Is Phosphorylated During Specific Phases of the Cell Cycle. *Cell,* 58**,** 1097-105.

BUSTAMANTE, E. & PEDERSEN, P. L. 1977. High Aerobic Glycolysis of Rat Hepatoma Cells in Culture: Role of Mitochondrial Hexokinase. *Proc Natl Acad Sci,* 74**,** 3735-39.

BYRSKI, T.; HUZARSKI, T.; DENT, R.; MARCZYK, E.; JASIOWKA, M.; GRONWALD, J.; JAKUBOWICZ, J.; CYBULSKI, C.; WISNIOWSKI, R.; GODLEWSKI, D.; LUBINSKI, J. & NAROD, S. A. 2014. Pathologic Complete Response to Neoadjuvant Cisplatin in BRCA1-Positive Breast Cancer Patients. *Breast Cancer Res Treat,* 147**,** 401-05.

CAI, F. F.; KOHLER, C.; ZHANG, B.; CHEN, W. J.; BAREKATI, Z.; GARRITSEN, H. S. P.; LENNER, P.; TONIOLO, P.; ZHANG, J. J. & ZHONG, X. Y. 2011. Mutations of Mitochondrial DNA as Potential Biomarkers in Breast Cancer. *Anticancer Res,* 31**,** 4267-71.

CAILLEAU, R.; YOUNG, R.; OLIVE, M. & REEVES, W. 1974. Breast Tumor Cell Lines from Pleural Effusions. *J Natl Cancer Inst,* 53**,** 661-74.

CALTAGIRONE, S.; ROSSI, C.; POGGI, A.; RANELLETTI, F. O.; NATALI, P. G.; BRUNETTI, M.; AIELLO, F. B. & PIANTELLI, M. 2000. Flavonoids Apigenin and Quercetin Inhibit Melanoma Growth and Metastatic Potential. *Int J Cancer,* 87**,** 595-600.

CAO, G.; SOFIC, E. & PRIOR, R. L. 1997. Antioxidant and Prooxidant Behavior of Flavonoids: Structure-Activity Relationships. *Free Radic Biol Med,* 22**,** 749-60.

CAO, J.; LIU, Y.; JIA, L.; ZHOU, H.-M.; KONG, Y.; YANG, G.; JIANG, L.-P.; LI, Q.-J. & ZHONG, L.-F. 2007. Curcumin Induces Apoptosis through Mitochondrial Hyperpolarization and MtDNA Damage in Human Hepatoma G2 Cells. *Free Radic Biol Med,* 43**,** 968-75.

CARMELIET, P. & JAIN, R. K. 2000. Angiogenesis in Cancer and Other Diseases. *Nature,* 407**,** 249-57.

CARMELIET, P. & JAIN, R. K. 2011. Molecular Mechanisms and Clinical Applications of Angiogenesis. *Nature,* 473**,** 298-307.

CARTER, P.; PRESTA, L.; GORMAN, C. M.; RIDGWAY, J.; HENNER, D.; WONG, W.; ROWLAND, A. M.; KOTTS, C.; CARVER, M. E. & SHEPARD, H. M. 1992. Humanization of an Anti-P185her2 Antibody for Human Cancer Therapy. *Proc Natl Acad Sci,* 89**,** 4285-89.

CASCIO, S.; D'ANDREA, A.; FERLA, R.; SURMACZ, E.; GULOTTA, E.; AMODEO, V.; BAZAN, V.; GEBBIA, N. & RUSSO, A. 2010. Mir-20b Modulates Vegf Expression by Targeting HIF-1α and Stat3 in Mcf-7 Breast Cancer Cells. *J Cell Physiol,* 224**,** 242-49.

CHANDELE, A.; PRASAD, V.; JAGTAP, J. C.; SHUKLA, R. & SHASTRY, P. R. 2004. Upregulation of Survivin in G2/M Cells and Inhibition of Caspase 9 Activity Enhances Resistance in Staurosporine-Induced Apoptosis. *Neoplasia,* 6**,** 29-40.

CHATTERJEE, A.; CHANG, X.; NAGPAL, J.; CHANG, S.; UPADHYAY, S.; CALIFANO, J.; TRINK, B. & SIDRANSKY, D. 2008. Targeting Human 8-Oxoguanine DNA Glycosylase to Mitochondria

Protects Cells from 2-Methoxyestradiol-Induced-Mitochondria-Dependent Apoptosis. *Oncogene,* 27**,** 3710-20.

CHAUHAN, D.; CATLEY, L.; HIDESHIMA, T.; LI, G.; LEBLANC, R.; GUPTA, D.; SATTLER, M.; RICHARDSON, P.; SCHLOSSMAN, R. L.; PODAR, K.; WELLER, E.; MUNSHI, N. & ANDERSON, K. C. 2002. 2-Methoxyestradiol Overcomes Drug Resistance in Multiple Myeloma Cells. *Blood,* 100**,** 2187-94.

CHAVAN, S.; KODOTH, S.; PAHWA, R. & PAHWA, S. 2001. The HIV Protease Inhibitor Indinavir Inhibits Cell-Cycle Progression in Vitro in Lymphocytes of HIV-Infected and Uninfected Individuals. *Blood,* 98**,** 383-89.

CHEN, X. & THIBEAULT, S. Effect of Dmso Concentration, Cell Density and Needle Gauge on the Viability of Cryopreserved Cells in Three Dimensional Hyaluronan Hydrogel. Engineering in Medicine and Biology Society (EMBC), 2013 35th Annual International Conference of the IEEE, 2013 Osaka, Japan. IEEE, 6228-31.

CHENG, A.-L.; KANG, Y.-K.; CHEN, Z.; TSAO, C.-J.; QIN, S.; KIM, J. S.; LUO, R.; FENG, J.; YE, S.; YANG, T.-S.; XU, J.; SUN, Y.; LIANG, H.; LIU, J.; WANG, J.; TAK, W. Y.; PAN, H.; BUROCK, K.; ZOU, J.; VOLIOTIS, D. & GUAN, Z. 2009. Efficacy and Safety of Sorafenib in Patients in the Asia-Pacific Region with Advanced Hepatocellular Carcinoma: A Phase III Randomised, Double-Blind, Placebo-Controlled Trial. *Lancet Oncol,* 10**,** 25-34.

CHENG, G.; ZIELONKA, J.; DRANKA, B. P.; MCALLISTER, D.; MACKINNON, A. C.; JOSEPH, J. & KALYANARAMAN, B. 2012. Mitochondria-Targeted Drugs Synergize with 2-Deoxyglucose to Trigger Breast Cancer Cell Death. *Cancer Res,* 72**,** 2634-44.

CHERRA, S. J.; KULICH, S. M.; UECHI, G.; BALASUBRAMANI, M.; MOUNTZOURIS, J.; DAY, B. W. & CHU, C. T. 2010. Regulation of the Autophagy Protein LC3 by Phosphorylation. *J Cell Biol,* 190**,** 533-39.

CHIEN, S.-Y.; WU, Y.-C.; CHUNG, J.-G.; YANG, J.-S.; LU, H.-F.; TSOU, M.-F.; WOOD, W.; KUO, S.-J. & CHEN, D.-R. 2009. Quercetin-Induced Apoptosis Acts through Mitochondrial- and Caspase-3-Dependent Pathways in Human Breast Cancer MDA-MB-231 Cells. *Hum Exp Toxicol,* 28**,** 493-503.

CHIPUK, J. E. & GREEN, D. R. 2005. Do Inducers of Apoptosis Trigger Caspase-Independent Cell Death? *Nat Rev Mol Cell Biol,* 6**,** 268-75.

CHOI, C.-H. 2005. Abc Transporters as Multidrug Resistance Mechanisms and the Development of Chemosensitizers for Their Reversal. *Cancer Cell Int,* 5**,** 30.

CHOI, J.-A.; KIM, J.-Y.; LEE, J.-Y.; KANG, C.-M.; KWON, H.-J.; YOO, Y.-D.; KIM, T.-W.; LEE, Y.-S. & LEE, S.-J. 2001. Induction of Cell Cycle Arrest and Apoptosis in Human Breast Cancer Cells by Quercetin. *Int J Oncol,* 19**,** 837-44.

CHOKUNONGA, E.; LEVY, L. M.; BASSETT, M. T.; BOROK, M. Z.; MAUCHAZA, B. G.; CHIRENJE, M. Z. & PARKIN, D. M. 1999. Aids and Cancer in Africa: The Evolving Epidemic in Zimbabwe. *Aids,* 13**,** 2583-88.

CHOU, C.-C.; YANG, J.-S.; LU, H.-F.; IP, S.-W.; LO, C.; WU, C.-C.; LIN, J.-P.; TANG, N.-Y.; CHUNG, J.-G.; CHOU, M.-J.; TENG, Y.-H. & CHEN, D.-R. 2010. Quercetin-Mediated Cell Cycle Arrest

and Apoptosis Involving Activation of a Caspase Cascade through the Mitochondrial Pathway in Human Breast Cancer MCF-7 Cells. *Arch Pharm Res,* 33**,** 1181-91.

CHOU, J. Y. 1989. Minireview: Differentiated Mammalian Cell Lines Immortalized by Temperature Sensitive Tumor Viruses. *Mol Endocrinol,* 3**,** 1511-14.

CHOU, T.-C. 2010. Drug Combination Studies and Their Synergy Quantification Using the Chou-Talalay Method. *Cancer Res,* 70**,** 440-46.

CHOU, T. C. 2006. Theoretical Basis, Experimental Design, and Computerized Simulation of Synergism and Antagonism in Drug Combination Studies. *Pharmacol Rev,* 58**,** 621-81.

CHOU, T. C. & TALALAY, P. 1984. Quantitative Analysis of Dose-Effect Relationships: The Combined Effects of Multiple Drugs or Enzyme Inhibitors. *Adv Enzyme Regul,* 22**,** 27-55.

CHU, C. T. 2006. Autophagic Stress in Neuronal Injury and Disease. *J Neuropath Exp Neur,* 65**,** 423.

COHEN, G. 1997. Caspases: The Executioners of Apoptosis. *Biochem J,* 326**,** 1-16.

COOK, K. M. & FIGG, W. D. 2010. Angiogenesis Inhibitors: Current Strategies and Future Prospects. *CA: Cancer J Clin,* 60**,** 222-43.

CREGAN, S. P.; FORTIN, A.; MACLAURIN, J. G.; CALLAGHAN, S. M.; CECCONI, F.; YU, S.-W.; DAWSON, T. M.; DAWSON, V. L.; PARK, D. S.; KROEMER, G. & SLACK, R. S. 2002. Apoptosis-Inducing Factor Is Involved in the Regulation of Caspase-Independent Neuronal Cell Death. *J Cell Biol,* 158**,** 507-17.

CRESSEY, T. R.; URIEN, S.; HIRT, D.; HALUE, G.; TECHAPORNROONG, M.; BOWONWATANUWONG, C.; LEENASIRIMAKUL, P.; TRELUYER, J.-M.; JOURDAIN, G. & LALLEMANT, M. 2011. Influence of Body Weight on Achieving Indinavir Concentrations within Its Therapeutic Window in HIV-Infected Thai Patients Receiving Indinavir Boosted with Ritonavir. *Ther Drug Monit,* 33**,** 25-31.

CUERVO, A. M. & DICE, J. F. 1998. Lysosomes, a Meeting Point of Proteins, Chaperones, and Proteases. *J Mol Med,* 76**,** 6-12.

CUSHMAN, M.; HE, H.-M.; KATZENELLENBOGEN, J. A.; LIN, C. M. & HAMEL, E. 1995. Synthesis, Antitubulin and Antimitotic Activity, and Cytotoxicity of Analogs of 2-Methoxyestradiol, an Endogenous Mammalian Metabolite of Estradiol That Inhibits Tubulin Polymerization by Binding to the Colchicine Binding Site. *J Med Chem,* 38**,** 2041-49.

CUSHMAN, M.; HE, H.-M.; KATZENELLENBOGEN, J. A.; VARMA, R. K.; HAMEL, E.; LIN, C. M.; RAM, S. & SACHDEVA, Y. P. 1997. Synthesis of Analogs of 2-Methoxyestradiol with Enhanced Inhibitory Effects on Tubulin Polymerization and Cancer Cell Growth. *J Med Chem,* 40**,** 2323-34.

CUZICK, J.; SESTAK, I.; BAUM, M.; BUZDAR, A.; HOWELL, A.; DOWSETT, M. & FORBES, J. F. 2010. Effect of Anastrozole and Tamoxifen as Adjuvant Treatment for Early-Stage Breast Cancer: 10-Year Analysis of the ATAC Trial. *Lancet Oncol,* 11**,** 1135-41.

CZENE, K.; LICHTENSTEIN, P. & HEMMINKI, K. 2002. Environmental and Heritable Causes of Cancer among 9.6 Million Individuals in the Swedish Family-Cancer Database. *Int J Cancer,* 99**,** 260-66.

D'AMATO, R. J.; LIN, C. M.; FLYNN, E.; FOLKMAN, J. & HAMEL, E. 1994a. 2-Methoxyestradiol, an Endogenous Mammalian Metabolite, Inhibits Tubulin Polymerization by Interacting at the Colchicine Site. *Proc Natl Acad Sci,* 91**,** 3964-68.

D'AMATO, R. J.; LOUGHNAN, M. S.; FLYNN, E. & FOLKMAN, J. 1994b. Thalidomide Is an Inhibitor of Angiogenesis. *Proc Natl Acad Sci,* 91**,** 4082-85.

D ARCHIVIO, M.; FILESI, C.; DI BENEDETTO, R.; GARGIULO, R.; GIOVANNINI, C. & MASELLA, R. 2007. Polyphenols, Dietary Sources and Bioavailability. *Ann I Super Sanita,* 43**,** 348.

DA VIOLANTE, G.; ZERROUK, N.; RICHARD, I.; PROVOT, G.; CHAUMEIL, J. C. & ARNAUD, P. 2002. Evaluation of the Cytotoxicity Effect of Dimethyl Sulfoxide (DMSO) on CACO2/TC7 Colon Tumor Cell Cultures. *Biol Pharm Bull,* 25**,** 1600-03.

DANAEI, G.; VANDER HOORN, S.; LOPEZ, A. D.; MURRAY, C. J. L. & EZZATI, M. 2005. Causes of Cancer in the World: Comparative Risk Assessment of Nine Behavioural and Environmental Risk Factors. *Lancet,* 366**,** 1784-93.

DE LENA, M.; LORUSSO, V.; LATORRE, A.; FANIZZA, G.; GARGANO, G.; CAPORUSSO, L.; GUIDA, M.; CATINO, A.; CRUCITTA, E.; SAMBIASI, D. & MAZZEI, A. 2001. Paclitaxel, Cisplatin and Lonidamine in Advanced Ovarian Cancer. A Phase II Study. *Eur J Cancer,* 37**,** 364-68.

DEGENHARDT, K.; MATHEW, R.; BEAUDOIN, B.; BRAY, K.; ANDERSON, D.; CHEN, G.; MUKHERJEE, C.; SHI, Y.; GÉLINAS, C. & FAN, Y. 2006. Autophagy Promotes Tumor Cell Survival and Restricts Necrosis, Inflammation, and Tumorigenesis. *Cancer Cell,* 10**,** 51-64.

DEGTEREV, A.; BOYCE, M. & YUAN, J. 2003. A Decade of Caspases. *Oncogene,* 22**,** 8543-67.

DELEO, A. B.; JAY, G.; APPELLA, E.; DUBOIS, G. C.; LAW, L. W. & OLD, L. J. 1979. Detection of a Transformation-Related Antigen in Chemically Induced Sarcomas and Other Transformed Cells of the Mouse. *Proc Natl Acad Sci,* 76**,** 2420-24.

DENT, R.; TRUDEAU, M.; PRITCHARD, K. I.; HANNA, W. M.; KAHN, H. K.; SAWKA, C. A.; LICKLEY, L. A.; RAWLINSON, E.; SUN, P. & NAROD, S. A. 2007. Triple-Negative Breast Cancer: Clinical Features and Patterns of Recurrence. *Clin Cancer Res,* 13**,** 4429-34.

DESAGHER, S. & MARTINOU, J.-C. 2000. Mitochondria as the Central Control Point of Apoptosis. *Trends Cell Biol,* 10**,** 369-77.

DISTLER, J. H.; WENGER, R. H.; GASSMANN, M.; KUROWSKA, M.; HIRTH, A.; GAY, S. & DISTLER, O. 2004. Physiologic Responses to Hypoxia and Implications for Hypoxia-Inducible Factors in the Pathogenesis of Rheumatoid Arthritis. *Arthritis Rheum,* 50**,** 10-23.

DJAVAHERI-MERGNY, M.; AMELOTTI, M.; MATHIEU, J.; BESANÇON, F.; BAUVY, C.; SOUQUÈRE, S.; PIERRON, G. & CODOGNO, P. 2006. NF-Kb Activation Represses Tumor Necrosis Factor-A-Induced Autophagy. *J Biol Chem,* 281**,** 30373-82.

DOBOS, J.; TÍMÁR, J.; BOCSI, J.; BURIÁN, Z.; NAGY, K.; BARNA, G.; PETÁK, I. & LADÁNYI, A. 2004. In Vitro and in Vivo Antitumor Effect of 2-Methoxyestradiol on Human Melanoma. *Int J Cancer,* 112**,** 771-76.

DOGLIOTTI, L.; DANESE, S.; BERRUTI, A.; ZOLA, P.; BUNIVA, T.; BOTTINI, A.; RICHIARDI, G.; MORO, G.; FARRIS, A. & BAU, M. 1998. Cisplatin, Epirubicin, and Lonidamine Combination

Regimen as First-Line Chemotherapy for Metastatic Breast Cancer: A Pilot Study. *Cancer Chemother Pharmacol,* 41**,** 333-38.

DONNINI, S.; FINETTI, F.; LUSINI, L.; MORBIDELLI, L.; CHEYNIER, V.; BARRON, D.; WILLIAMSON, G.; WALTENBERGER, J. & ZICHE, M. 2006. Divergent Effects of Quercetin Conjugates on Angiogenesis. *Br J Nutr,* 95**,** 1016-23.

DRUKER, B. J.; GUILHOT, F.; O'BRIEN, S. G.; GATHMANN, I.; KANTARJIAN, H.; GATTERMANN, N.; DEININGER, M. W. N.; SILVER, R. T.; GOLDMAN, J. M.; STONE, R. M.; CERVANTES, F.; HOCHHAUS, A.; POWELL, B. L.; GABRILOVE, J. L.; ROUSSELOT, P.; REIFFERS, J.; CORNELISSEN, J. J.; HUGHES, T.; AGIS, H.; FISCHER, T.; VERHOEF, G.; SHEPHERD, J.; SAGLIO, G.; GRATWOHL, A.; NIELSEN, J. L.; RADICH, J. P.; SIMONSSON, B.; TAYLOR, K.; BACCARANI, M.; SO, C.; LETVAK, L. & LARSON, R. A. 2006. Five-Year Follow-up of Patients Receiving Imatinib for Chronic Myeloid Leukemia. *N Engl J Med,* 355**,** 2408-17.

DU, C.; FANG, M.; LI, Y.; LI, L. & WANG, X. 2000. Smac, a Mitochondrial Protein That Promotes Cytochrome C–Dependent Caspase Activation by Eliminating Iap Inhibition. *Cell,* 102**,** 33-42.

DUCHEN, M. R. 2004. Mitochondria in Health and Disease: Perspectives on a New Mitochondrial Biology. *Mol Aspects Med,* 25**,** 365-451.

DUDAK, S. D.; LOPEZ, A.; BLOCK, N. L. & LOKESHWAR, B. L. 1996. Enhancement of Radiation Response of Prostatic Carcinoma by Lonidamine. *Anticancer Res,* 16**,** 3665-71.

DUO, J.; YING, G.-G.; WANG, G.-W. & ZHANG, L. 2012. Quercetin Inhibits Human Breast Cancer Cell Proliferation and Induces Apoptosis Via Bcl-2 and Bax Regulation. *Mol Med Rep,* 5**,** 1453-56.

DWARAKANATH, B.; SINGH, D.; BANERJI, A. K.; SARIN, R.; VENKATARAMANA, N.; JALALI, R.; VISHWANATH, P.; MOHANTI, B.; TRIPATHI, R. & KALIA, V. 2009. Clinical Studies for Improving Radiotherapy with 2-Deoxy-D-Glucose: Present Status and Future Prospects. *J Cancer Res Ther,* 5**,** 21.

EARLY BREAST CANCER TRIALISTS' COLLABORATIVE, G. 1998. Polychemotherapy for Early Breast Cancer: An Overview of the Randomised Trials. *Lancet,* 352**,** 930-42.

EDGELL, C.; MCDONALD, C. C. & GRAHAM, J. B. 1983. Permanent Cell Line Expressing Human Factor VIII-Related Antigen Established by Hybridization. *Proc Natl Acad Sci,* 80**,** 3734-37.

EGERT, S.; WOLFFRAM, S.; BOSY-WESTPHAL, A.; BOESCH-SAADATMANDI, C.; WAGNER, A. E.; FRANK, J.; RIMBACH, G. & MUELLER, M. J. 2008. Daily Quercetin Supplementation Dose-Dependently Increases Plasma Quercetin Concentrations in Healthy Humans. *J Nutr,* 138**,** 1615-21.

EISENBERG-LERNER, A.; BIALIK, S.; SIMON, H. & KIMCHI, A. 2009. Life and Death Partners: Apoptosis, Autophagy and the Cross-Talk between Them. *Cell Death Differ,* 16**,** 966-75.

ELGER, W.; SCHWARZ, S.; HEDDEN, A.; REDDERSEN, G. & SCHNEIDER, B. 1995. Sulfamates of Various Estrogens Are Prodrugs with Increased Systemic and Reduced Hepatic Estrogenicity at Oral Application. *J Steroid Biochem Mol Biol,* 55**,** 395-403.

ELIYAHU, D.; MICHALOVITZ, D.; ELIYAHU, S.; PINHASI-KIMHI, O. & OREN, M. 1989. Wild-Type P53 Can Inhibit Oncogene-Mediated Focus Formation. *Proc Natl Acad Sci,* 86**,** 8763-67.

ELLSWORTH, R. E.; DECEWICZ, D. J.; SHRIVER, C. D. & ELLSWORTH, D. L. 2010. Breast Cancer in the Personal Genomics Era. *Curr Genomics,* 11**,** 146-61.

EMEIS, J. & EDGELL, C. 1988. Fibrinolytic Properties of a Human Endothelial Hybrid Cell Line (EA. Hy 926). *Blood,* 71**,** 1669-75.

ENSOLI, B. 2002. Use of Inhibitors of the Protease of the Human Immunodeficiency Virus (HIV) to Block Cell Migration and/or Invasion, Tissue Infiltration and Oedema for the Therapy of Diseases Associated Therewith. Google Patents.

ESCUIN, D.; KLINE, E. R. & GIANNAKAKOU, P. 2005. Both Microtubule-Stabilizing and Microtubule-Destabilizing Drugs Inhibit Hypoxia-Inducible Factor-1α Accumulation and Activity by Disrupting Microtubule Function. *Cancer Res,* 65**,** 9021-28.

ESKELINEN, E.-L. 2008. To Be or Not to Be? Examples of Incorrect Identification of Autophagic Compartments in Conventional Transmission Electron Microscopy of Mammalian Cells. *Autophagy,* 4**,** 257-60.

ESPOSITO, V.; PALESCANDOLO, E.; SPUGNINI, E. P.; MONTESARCHIO, V.; DE LUCA, A.; CARDILLO, I.; CORTESE, G.; BALDI, A. & CHIRIANNI, A. 2006. Evaluation of Antitumoral Properties of the Protease Inhibitor Indinavir in a Murine Model of Hepatocarcinoma. *Clin Cancer Res,* 12**,** 2634-39.

ESPOSTI, M. D. & DIVE, C. 2003. Mitochondrial Membrane Permeabilisation by Bax/Bak. *Biochem Biophys Res Comm,* 304**,** 455-61.

EXTERMANN, M.; BOLER, I.; REICH, R. R.; LYMAN, G. H.; BROWN, R. H.; DEFELICE, J.; LEVINE, R. M.; LUBINER, E. T.; REYES, P.; SCHREIBER, F. J. & BALDUCCI, L. 2012. Predicting the Risk of Chemotherapy Toxicity in Older Patients: The Chemotherapy Risk Assessment Scale for High-Age Patients (Crash) Score. *Cancer,* 118**,** 3377-86.

FADOK, V. A.; VOELKER, D. R.; CAMPBELL, P. A.; COHEN, J. J.; BRATTON, D. L. & HENSON, P. M. 1992. Exposure of Phosphatidylserine on the Surface of Apoptotic Lymphocytes Triggers Specific Recognition and Removal by Macrophages. *J Immunol,* 148**,** 2207-16.

FALLAHI-SICHANI, M.; HONARNEJAD, S.; HEISER, L. M.; GRAY, J. W. & SORGER, P. K. 2013. Metrics Other Than Potency Reveal Systematic Variation in Responses to Cancer Drugs. *Nat Chem Biol,* 9**,** 708-14.

FALLETI, M. G.; SANFILIPPO, A.; MARUFF, P.; WEIH, L. & PHILLIPS, K.-A. 2005. The Nature and Severity of Cognitive Impairment Associated with Adjuvant Chemotherapy in Women with Breast Cancer: A Meta-Analysis of the Current Literature. *Brain Cognition,* 59**,** 60-70.

FANG, Y.-Z.; YANG, S. & WU, G. 2002. Free Radicals, Antioxidants, and Nutrition. *Nutrition,* 18**,** 872-79.

FENDLY, B. M.; WINGET, M.; HUDZIAK, R. M.; LIPARI, M. T.; NAPIER, M. A. & ULLRICH, A. 1990. Characterization of Murine Monoclonal Antibodies Reactive to Either the Human Epidermal Growth Factor Receptor or Her2/Neu Gene Product. *Cancer Res,* 50**,** 1550-58.

FERLAY, J.; SOERJOMATARAM, I.; DIKSHIT, R.; ESER, S.; MATHERS, C.; REBELO, M.; PARKIN, D. M.; FORMAN, D. & BRAY, F. 2015. Cancer Incidence and Mortality Worldwide: Sources, Methods and Major Patterns in Globocan 2012. *Int J Cancer,* 136**,** E359-E86.

FERNANDES, R. S. & COTTER, T. G. 1994. Apoptosis or Necrosis: Intracellular Levels of Glutathione Influence Mode of Cell Death. *Biochem Pharmacol,* 48**,** 675-81.

FERNÁNDEZ-CHECA, J. & KAPLOWITZ, N. 1990. The Use of Monochlorobimane to Determine Hepatic GSH Levels and Synthesis. *Anal Biochem,* 190**,** 212-19.

FERRARO-PEYRET, C.; QUEMENEUR, L.; FLACHER, M.; REVILLARD, J.-P. & GENESTIER, L. 2002. Caspase-Independent Phosphatidylserine Exposure During Apoptosis of Primary T Lymphocytes. *J Immunol,* 169**,** 4805-10.

FERRY, D. R.; SMITH, A.; MALKHANDI, J.; FYFE, D. W.; ANDERSON, D.; BAKER, J. & KERR, D. 1996. Phase I Clinical Trial of the Flavonoid Quercetin: Pharmacokinetics and Evidence for in Vivo Tyrosine Kinase Inhibition. *Clin Cancer Res,* 2**,** 659-68.

FIGUEROA-MAGALHÃES, M. C.; JELOVAC, D.; CONNOLLY, R. M. & WOLFF, A. C. 2014. Treatment of Her2-Positive Breast Cancer. *Breast J,* 23**,** 128-36.

FISHER, B.; COSTANTINO, J.; REDMOND, C.; POISSON, R.; BOWMAN, D.; COUTURE, J.; DIMITROV, N. V.; WOLMARK, N.; WICKERHAM, D. L.; FISHER, E. R.; MARGOLESE, R.; ROBIDOUX, A.; SHIBATA, H.; TERZ, J.; PATERSON, A. H. G.; FELDMAN, M. I.; FARRAR, W.; EVANS, J.; LICKLEY, H. L. & KETNER, M. 1989. A Randomized Clinical Trial Evaluating Tamoxifen in the Treatment of Patients with Node-Negative Breast Cancer Who Have Estrogen-Receptor–Positive Tumors. *N Engl J Med,* 320**,** 479-84.

FISHER, B.; DIGNAM, J.; EMIR, B.; BRYANT, J.; DECILLIS, A.; WOLMARK, N.; WICKERHAM, D. L.; DIMITROV, N. V.; ABRAMSON, N.; ATKINS, J. N.; SHIBATA, H.; DESCHENES, L. & MARGOLESE, R. G. 1997. Tamoxifen and Chemotherapy for Lymph Node-Negative, Estrogen Receptor-Positive Breast Cancer. *J Natl Cancer Inst,* 89**,** 1673-82.

FISHER, B.; JEONG, J.-H.; BRYANT, J.; ANDERSON, S.; DIGNAM, J.; FISHER, E. R. & WOLMARK, N. 2004. Treatment of Lymph-Node-Negative, Oestrogen-Receptor-Positive Breast Cancer: Long-Term Findings from National Surgical Adjuvant Breast and Bowel Project Randomised Clinical Trials. *Lancet,* 364**,** 858-68.

FISHER, E.; OSBORNE, C. K.; MCGUIRE, W.; REDMOND, C.; KNIGHT, W., III; FISHER, B.; BANNAYAN, G.; WALDER, A.; GREGORY, E.; JACOBSEN, A.; QUEEN, D.; BENNETT, D. & FORD, H. 1981. Correlation of Primary Breast Cancer Histopathology and Estrogen Receptor Content. *Breast Cancer Res Treat,* 1**,** 37-41.

FITZGERALD, J. B.; SCHOEBERL, B.; NIELSEN, U. B. & SORGER, P. K. 2006. Systems Biology and Combination Therapy in the Quest for Clinical Efficacy. *Nat Chem Biol,* 2**,** 458-66.

FLORIDI, A.; BRUNO, T.; MICCADEI, S.; FANCIULLI, M.; FEDERICO, A. & PAGGI, M. G. 1998. Enhancement of Doxorubicin Content by the Antitumor Drug Lonidamine in Resistant Ehrlich Ascites Tumor Cells through Modulation of Energy Metabolism. *Biochem Pharmacol,* 56**,** 841-49.

FLORIDI, A.; DEMARTINO, C.; MARCANTE, M. L.; APOLLONJ, C.; SCORZA BARCELLONA, P. & SILVESTRINI, B. 1981a. Morphological and Biochemical Modifications of Rat Germ Cell Mitochondria Induced by New Antispermatogenic Compounds: Studies in Vivo and in Vitro. *Exp Mol Pathol,* 35**,** 314-31.

FLORIDI, A.; PAGGI, M. G.; D'ATRI, S.; DE MARTINO, C.; MARCANTE, M. L.; SILVESTRINI, B. & CAPUTO, A. 1981b. Effect of Lonidamine on the Energy Metabolism of Ehrlich Ascites Tumor Cells. *Cancer Res,* 41**,** 4661-66.

FOLKMAN, J. 1971. Tumor Angiogenesis: Therapeutic Implications. *N Engl J Med,* 285**,** 1182-86.

FOLKMAN, J. 2003. Angiogenesis and Apoptosis. *Semin Cancer Biol,* 13**,** 159-67.

FOLKMAN, J.; HAHNFELDT, P. & HLATKY, L. 2000. Cancer: Looking Outside the Genome. *Nat Rev Mol Cell Biol,* 1**,** 76-79.

FREI, E. 1972. Combination Cancer Therapy: Presidential Address. *Cancer Res,* 32**,** 2593-607.

FREI, E.; FREIREICH, E. J.; GEHAN, E.; PINKEL, D.; HOLLAND, J. F.; SELAWRY, O.; HAURANI, F.; SPURR, C. L.; HAYES, D. M. & JAMES, G. W. 1961a. Studies of Sequential and Combination Antimetabolite Therapy in Acute Leukemia: 6-Mercaptopurine and Methotrexate. *Blood,* 18**,** 431-54.

FREI, E.; FREIREICH, E. J.; GEHAN, E.; PINKEL, D.; HOLLAND, J. F.; SELAWRY, O.; HAURANI, F.; SPURR, C. L.; HAYES, D. M.; JAMES, G. W.; ROTHBERG, H.; SODEE, D. B.; RUNDLES, R. W.; SCHROEDER, L. R.; HOOGSTRATEN, B.; WOLMAN, I. J.; TRAGGIS, D. G.; COOPER, T.; GENDEL, B. R.; EBAUGH, F. & TAYLOR, R. 1961b. Studies of Sequential and Combination Antimetabolite Therapy in Acute Leukemia: 6-Mercaptopurine and Methotrexate. *Blood,* 18**,** 431-54.

FREI, W. 1913. Versuche Über Kombination Von Desinfektionsmitteln. *Z Hyg Infektionskr,* 75**,** 433-96.

FRIED, M. 1965. Cell-Transforming Ability of a Temperature-Sensitive Mutant of Polyoma Virus. *Proc Natl Acad Sci,* 53**,** 486.

FRIEND, C.; SCHER, W.; HOLLAND, J. & SATO, T. 1971. Hemoglobin Synthesis in Murine Virus-Induced Leukemic Cells in Vitro: Stimulation of Erythroid Differentiation by Dimethyl Sulfoxide. *Proc Natl Acad Sci,* 68**,** 378-82.

FUKUMURA, D.; XAVIER, R.; SUGIURA, T.; CHEN, Y.; PARK, E.-C.; LU, N.; SELIG, M.; NIELSEN, G.; TAKSIR, T.; JAIN, R. K. & SEED, B. 1998. Tumor Induction of VEGF Promoter Activity in Stromal Cells. *Cell,* 94**,** 715-25.

GALLUZZI, L.; AARONSON, S. A.; ABRAMS, J.; ALNEMRI, E. S.; ANDREWS, D. W.; BAEHRECKE, E. H.; BAZAN, N. G.; BLAGOSKLONNY, M. V.; BLOMGREN, K.; BORNER, C.; BREDESEN, D. E.; BRENNER, C.; CASTEDO, M.; CIDLOWSKI, J. A.; CIECHANOVER, A.; COHEN, G. M.; DE LAURENZI, V.; DE MARIA, R.; DESHMUKH, M.; DYNLACHT, B. D.; EL-DEIRY, W. S.; FLAVELL, R. A.; FULDA, S.; GARRIDO, C.; GOLSTEIN, P.; GOUGEON, M. L.; GREEN, D. R.; GRONEMEYER, H.; HAJNOCZKY, G.; HARDWICK, J. M.; HENGARTNER, M. O.; ICHIJO, H.; JAATTELA, M.; KEPP, O.; KIMCHI, A.; KLIONSKY, D. J.; KNIGHT, R. A.; KORNBLUTH, S.; KUMAR, S.; LEVINE, B.; LIPTON, S. A.; LUGLI, E.; MADEO, F.; MALORNI, W.; MARINE, J. C.; MARTIN, S. J.; MEDEMA, J. P.; MEHLEN, P.; MELINO, G.; MOLL, U. M.; MORSELLI, E.; NAGATA, S.; NICHOLSON, D. W.; NICOTERA, P.; NUNEZ, G.; OREN, M.; PENNINGER, J.; PERVAIZ, S.; PETER, M. E.; PIACENTINI, M.; PREHN, J. H. M.; PUTHALAKATH, H.; RABINOVICH, G. A.; RIZZUTO, R.; RODRIGUES, C. M. P.;

RUBINSZTEIN, D. C.; RUDEL, T.; SCORRANO, L.; SIMON, H. U.; STELLER, H.; TSCHOPP, J.; TSUJIMOTO, Y.; VANDENABEELE, P.; VITALE, I.; VOUSDEN, K. H.; YOULE, R. J.; YUAN, J.; ZHIVOTOVSKY, B. & KROEMER, G. 2009. Guidelines for the Use and Interpretation of Assays for Monitoring Cell Death in Higher Eukaryotes. *Cell Death Differ,* 16**,** 1093-107.

GAN, D.; ZENG, X.; LIU, R. H. & YE, H. 2015. Potential Mechanism of Mycelium Polysaccharide from Pholiota Dinghuensis Bi in Regulating the Proliferation and Apoptosis of Human Breast Cancer MCF-7 Cells through P38/MAPK Pathway. *J Funct Foods,* 12**,** 375-88.

GANAPATHY-KANNIAPPAN, S.; GESCHWIND, J.-F. H.; KUNJITHAPATHAM, R.; BUIJS, M.; SYED, L. H.; RAO, P. P.; OTA, S. & VALI, M. 2010. The Pyruvic Acid Analog 3-Bromopyruvate Interferes with the Tetrazolium Reagent Mts in the Evaluation of Cytotoxicity. *Assay Drug Dev Technol,* 8**,** 258-62.

GAO, N.; RAHMANI, M.; DENT, P. & GRANT, S. 2005. 2-Methoxyestradiol-Induced Apoptosis in Human Leukemia Cells Proceeds through a Reactive Oxygen Species and Akt-Dependent Process. *Oncogene,* 24**,** 3797-809.

GARBUTCHEON-SINGH, K. B.; HARPER, B. W.; MYERS, S. & ALDRICH-WRIGHT, J. R. 2014. Combination Studies of Platinum (II)-Based Metallointercalators with Buthionine-S, R-Sulfoximine, 3-Bromopyruvate, Cisplatin or Carboplatin. *Metallomics,* 6**,** 126-31.

GARCIA-MATA, R.; GAO, Y. S. & SZTUL, E. 2002. Hassles with Taking out the Garbage: Aggravating Aggresomes. *Traffic,* 3**,** 388-96.

GATENBY, R. A.; GAWLINSKI, E. T.; GMITRO, A. F.; KAYLOR, B. & GILLIES, R. J. 2006. Acid-Mediated Tumor Invasion: A Multidisciplinary Study. *Cancer Res,* 66**,** 5216-23.

GATENBY, R. A. & GILLIES, R. J. 2004. Why Do Cancers Have High Aerobic Glycolysis? *Nat Rev Cancer,* 4**,** 891-99.

GATENBY, R. A. & GILLIES, R. J. 2007. Glycolysis in Cancer: A Potential Target for Therapy. *Int J Biochem Cell B,* 39**,** 1358-66.

GEKELER, V.; EPPLE, J.; KLEYMANN, G. & PROBST, H. 1993. Selective and Synchronous Activation of Early-S-Phase Replicons of Ehrlich Ascites Cells. *Mol Cell Biol,* 13**,** 5020-33.

GESCHWIND, J.-F.; GEORGIADES, C. S.; KO, Y. H. & PEDERSEN, P. L. 2004. Recently Elucidated Energy Catabolism Pathways Provide Opportunities for Novel Treatments in Hepatocellular Carcinoma. *Expert Rev Anticancer Ther,* 4**,** 449-57.

GESCHWIND, J.-F. H.; KO, Y. H.; TORBENSON, M. S.; MAGEE, C. & PEDERSEN, P. L. 2002. Novel Therapy for Liver Cancer: Direct Intraarterial Injection of a Potent Inhibitor of ATP Production. *Cancer Res,* 62**,** 3909-13.

GHIBELLI, L.; MENGONI, F.; LICHTNER, M.; COPPOLA, S.; DE NICOLA, M.; BERGAMASCHI, A.; MASTROIANNI, C. & VULLO, V. 2003. Anti-Apoptotic Effect of HIV Protease Inhibitors Via Direct Inhibition of Calpain. *Biochem Pharmacol,* 66**,** 1505-12.

GIACCIA, A. J. 1996. Hypoxic Stress Proteins: Survival of the Fittest. *Semin Radiat Oncol,* 6**,** 46-58.

GILLS, J. J.; LOPICCOLO, J.; TSURUTANI, J.; SHOEMAKER, R. H.; BEST, C. J. M.; ABU-ASAB, M. S.; BOROJERDI, J.; WARFEL, N. A.; GARDNER, E. R.; DANISH, M.; HOLLANDER, M. C.;

KAWABATA, S.; TSOKOS, M.; FIGG, W. D.; STEEG, P. S. & DENNIS, P. A. 2007. Nelfinavir, a Lead HIV Protease Inhibitor, Is a Broad-Spectrum, Anticancer Agent That Induces Endoplasmic Reticulum Stress, Autophagy, and Apoptosis in Vitro and in Vivo. *Clin Cancer Res,* 13**,** 5183-94.

GIMBRONE, M. A.; LEAPMAN, S. B.; COTRAN, R. S. & FOLKMAN, J. 1972. Tumor Dormancy in Vivo by Prevention of Neovascularization. *J Exp Med,* 136**,** 261-76.

GLOSSMANN, H.; PRESEK, P. & EIGENBRODT, E. 1981. Quercetin Inhibits Tyrosine Phosphorylation by the Cyclic Nucleotide-Independent, Transforming Protein Kinase, PP60SRC. *Naunyn-Schmiedebergs Arch Pharmacol,* 317**,** 100-02.

GLUNDE, K.; JIE, C. & BHUJWALLA, Z. M. 2004. Molecular Causes of the Aberrant Choline Phospholipid Metabolism in Breast Cancer. *Cancer Res,* 64**,** 4270-76.

GOLDHIRSCH, A.; INGLE, J. N.; GELBER, R. D.; COATES, A. S.; THÜRLIMANN, B.; SENN, H.-J. & MEMBERS, P. 2009. Thresholds for Therapies: Highlights of the St Gallen International Expert Consensus on the Primary Therapy of Early Breast Cancer 2009. *Ann Oncol,* 20**,** 1319-29.

GOMEZ, D.; ALONSO, D.; YOSHIJI, H. & THORGEIRSSON, U. 1997. Tissue Inhibitors of Metalloproteinases: Structure, Regulation and Biological Functions. *Eur J Cell Biol,* 74**,** 111-22.

GONDA, T. J.; SHEINESS, D. K. & BISHOP, J. M. 1982. Transcripts from the Cellular Homologs of Retroviral Oncogenes: Distribution among Chicken Tissues. *Mol Cell Biol,* 2**,** 617-24.

GOTTESMAN, M. M.; FOJO, T. & BATES, S. E. 2002. Multidrug Resistance in Cancer: Role of ATP-Dependent Transporters. *Nat Rev Cancer,* 2**,** 48-58.

GOTTESMAN, M. M. & PASTAN, I. 1993. Biochemistry of Multidrug Resistance Mediated by the Multidrug Transporter. *Ann Rev Biochem,* 62**,** 385-427.

GOTTLOB, K.; MAJEWSKI, N.; KENNEDY, S.; KANDEL, E.; ROBEY, R. B. & HAY, N. 2001. Inhibition of Early Apoptotic Events by AKT/PKB Is Dependent on the First Committed Step of Glycolysis and Mitochondrial Hexokinase. *Genes Dev,* 15**,** 1406-18.

GRANADO-SERRANO, A. B.; MARTÍN, M. A.; BRAVO, L.; GOYA, L. & RAMOS, S. 2006. Quercetin Induces Apoptosis Via Caspase Activation, Regulation of Bcl-2, and Inhibition of PI-3-Kinase/Akt and ERK Pathways in a Human Hepatoma Cell Line (HepG2). *J Nutr,* 136**,** 2715-21.

GRAVANCE, C. G.; GARNER, D. L.; BAUMBER, J. & BALL, B. A. 2000. Assessment of Equine Sperm Mitochondrial Function Using JC-1. *Theriogenology,* 53**,** 1691-703.

GRECO, W. R.; FAESSEL, H. & LEVASSEUR, L. 1996. The Search for Cytotoxic Synergy between Anticancer Agents: A Case of Dorothy and the Ruby Slippers? *J Natl Cancer Inst,* 88**,** 699-700.

GREEN, D. R. & REED, J. C. 1998. Mitochondria and Apoptosis. *Science,* 281**,** 1309.

GREVER, M. R.; SCHEPARTZ, S. A. & CHABNER, B. A. 1992. The National Cancer Institute: Cancer Drug Discovery and Development Program. *Semin Oncol,* 19**,** 622-38.

GROVER-MCKAY, M.; WALSH, S. A.; SEFTOR, E. A.; THOMAS, P. A. & HENDRIX, M. J. 1998. Role for Glucose Transporter 1 Protein in Human Breast Cancer. *Pathol Oncol Res,* 4**,** 115-20.

GU, Y.; LI, P.; PENG, F.; ZHANG, M.; ZHANG, Y.; LIANG, H.; ZHAO, W.; QI, L.; WANG, H. & WANG, C. 2015. Autophagy-Related Prognostic Signature for Breast Cancer. *Mol Carcinog,* DOI: 10.1002/mc.22278.

GUKOVSKAYA, A. S. & GUKOVSKY, I. 2012. Autophagy and Pancreatitis. *Am J Physiol Gastrointest Liver Physiol,* 303**,** G993-G1003.

GWAK, H.; HAEGEMAN, G.; TSANG, B. K. & SONG, Y. S. 2014. Cancer-Specific Interruption of Glucose Metabolism by Resveratrol Is Mediated through Inhibition of AKT/GLUT1 Axis in Ovarian Cancer Cells. *Mol Carcinog,* DOI: 10.1002/mc.22227.

HAHN, W. C.; COUNTER, C. M.; LUNDBERG, A. S.; BEIJERSBERGEN, R. L.; BROOKS, M. W. & WEINBERG, R. A. 1999. Creation of Human Tumour Cells with Defined Genetic Elements. *Nature,* 400**,** 464.

HAHN, W. C. & WEINBERG, R. A. 2002. Rules for Making Human Tumor Cells. *N Engl J Med,* 347**,** 1593-603.

HAKEM, R.; HAKEM, A.; DUNCAN, G. S.; HENDERSON, J. T.; WOO, M.; SOENGAS, M. S.; ELIA, A.; DE LA POMPA, J. L.; KAGI, D. & KHOO, W. 1998. Differential Requirement for Caspase 9 in Apoptotic Pathways in Vivo. *Cell,* 94**,** 339-52.

HALDAR, S.; JENA, N. & CROCE, C. M. 1995. Inactivation of Bcl-2 by Phosphorylation. *Proc Natl Acad Sci,* 92**,** 4507-11.

HALSTED, W. S. 1898. I. A Clinical and Histological Study of Certain Adenocarcinomata of the Breast: And a Brief Consideration of the Supraclavicular Operation and of the Results of Operations for Cancer of the Breast from 1889 to 1898 at the Johns Hopkins Hospital. *Ann Surg,* 28**,** 557.

HANAHAN, D. & FOLKMAN, J. 1996. Patterns and Emerging Mechanisms of the Angiogenic Switch During Tumorigenesis. *Cell,* 86**,** 353-64.

HANAHAN, D. & WEINBERG, R. A. 2000. The Hallmarks of Cancer. *Cell,* 100**,** 57-70.

HANAHAN, D. & WEINBERG, ROBERT A. 2011. Hallmarks of Cancer: The Next Generation. *Cell,* 144**,** 646-74.

HARDING, H. P.; ZHANG, Y. & RON, D. 1999. Protein Translation and Folding Are Coupled by an Endoplasmic-Reticulum-Resident Kinase. *Nature,* 397**,** 271-74.

HARRIS, H. 1971. The Croonian Lecture, 1971: Cell Fusion and the Analysis of Malignancy. *P Roy Soc Lond B Bio***,** 1-20.

HARVEY, H. A.; LIPTON, A.; MAX, D. T.; PEARLMAN, H. G.; DIAZ-PERCHES, R. & DE LA GARZA, J. 1985. Medical Castration Produced by the Gnrh Analogue Leuprolide to Treat Metastatic Breast Cancer. *J Clin Oncol,* 3**,** 1068-72.

HELMLINGER, G.; YUAN, F.; DELLIAN, M. & JAIN, R. K. 1997. Interstitial Ph and PO2 Gradients in Solid Tumors in Vivo: High-Resolution Measurements Reveal a Lack of Correlation. *Nat Med,* 3**,** 177-82.

HIGGINS, C. F. 1991. Molecular Basis of Multidrug Resistance Mediated by P-Glycoprotein. *Curr Opin Biotech,* 2**,** 278-81.

HIGGINS, P. J. 2002. Pai-1 Gene as a Target for Breast Cancer Therapy. DTIC Document.

HITCHON, C. A. & EL-GABALAWY, H. S. 2004. Oxidation in Rheumatoid Arthritis. *Arthritis Res Ther,* 6**,** 265-78.

HITOMI, J.; KATAYAMA, T.; EGUCHI, Y.; KUDO, T.; TANIGUCHI, M.; KOYAMA, Y.; MANABE, T.; YAMAGISHI, S.; BANDO, Y.; IMAIZUMI, K.; TSUJIMOTO, Y. & TOHYAMA, M. 2004. Involvement of Caspase-4 in Endoplasmic Reticulum Stress-Induced Apoptosis and Aβ-Induced Cell Death. *J Cell Biol,* 165**,** 347-56.

HORISBERGER, M. & ROSSET, J. 1977. Colloidal Gold, a Useful Marker for Transmission and Scanning Electron Microscopy. *J Histochem Cytochem,* 25**,** 295-305.

HOWLADER, N.; NOONE, A.; KRAPCHO, M.; GARSHELL, J.; NEYMAN, N.; ALTEKRUSE, S.; KOSARY, C.; YU, M.; RUHL, J. & TATALOVICH, Z. 2013. Seer Cancer Statistics Review, 1975-2010. [Based on the November 2012 Seer Data Submission, Posted to the Seer Web Site, April 2013.]. Bethesda, MD: National Cancer Institute.

HRESKO, R. C. & HRUZ, P. W. 2011. HIV Protease Inhibitors Act as Competitive Inhibitors of the Cytoplasmic Glucose Binding Site of GLUTs with Differing Affinities for GLUT1 and GLUT4. *PloS one,* 6**,** e25237.

HURRIA, A.; TOGAWA, K.; MOHILE, S. G.; OWUSU, C.; KLEPIN, H. D.; GROSS, C. P.; LICHTMAN, S. M.; GAJRA, A.; BHATIA, S.; KATHERIA, V.; KLAPPER, S.; HANSEN, K.; RAMANI, R.; LACHS, M.; WONG, F. L. & TEW, W. P. 2011. Predicting Chemotherapy Toxicity in Older Adults with Cancer: A Prospective Multicenter Study. *J Clin Oncol,* 29**,** 3457-65.

HÜTTEMANN, M.; LEE, I.; PECINOVA, A.; PECINA, P.; PRZYKLENK, K. & DOAN, J. 2008. Regulation of Oxidative Phosphorylation, the Mitochondrial Membrane Potential, and Their Role in Human Disease. *J Bioenerg Biomembr,* 40**,** 445-56.

IGURA, K.; OHTA, T.; KURODA, Y. & KAJI, K. 2001. Resveratrol and Quercetin Inhibit Angiogenesis in Vitro. *Cancer Lett,* 171**,** 11-16.

IHRLUND, L. S.; HERNLUND, E.; KHAN, O. & SHOSHAN, M. C. 2008. 3-Bromopyruvate as Inhibitor of Tumour Cell Energy Metabolism and Chemopotentiator of Platinum Drugs. *Mol Oncol,* 2**,** 94-101.

IMAIZUMI, K.; MIYOSHI, K.; KATAYAMA, T.; YONEDA, T.; TANIGUCHI, M.; KUDO, T. & TOHYAMA, M. 2001. The Unfolded Protein Response and Alzheimer's Disease. *BBA-Mol Basis Dis,* 1536**,** 85-96.

INAI, Y.; YABUKI, M.; KANNO, T.; AKIYAMA, J.; YASUDA, T. & UTSUMI, K. 1997. Valinomycin Induces Apoptosis of Ascites Hepatoma Cells (AH-130) in Relation to Mitochondrial Membrane Potential. *Cell Struct Funct,* 22**,** 555-63.

JAATTELA, M. & TSCHOPP, J. 2003. Caspase-Independent Cell Death in T Lymphocytes. *Nat Immunol,* 4**,** 416-23.

JAIN, R. K. 2001. Delivery of Molecular and Cellular Medicine to Solid Tumors1. *Adv Drug Deliv Rev,* 46**,** 149-68.

JAKUBOWICZ-GIL, J.; LANGNER, E.; WERTEL, I.; PIERSIAK, T. & RZESKI, W. 2010. Temozolomide, Quercetin and Cell Death in the Moggccm Astrocytoma Cell Line. *Chem Biol Interact,* 188**,** 190-203.

JAMES, J.; MURRY, D.; TRESTON, A.; STORNIOLO, A.; SLEDGE, G.; SIDOR, C. & MILLER, K. 2007. Phase I Safety, Pharmacokinetic and Pharmacodynamic Studies of 2-Methoxyestradiol Alone or in Combination with Docetaxel in Patients with Locally Recurrent or Metastatic Breast Cancer. *Invest New Drug,* 25**,** 41-48.

JÄNICKE, R. 2009. MCF-7 Breast Carcinoma Cells Do Not Express Caspase-3. *Breast Cancer Res Treat,* 117**,** 219-21.

JÄNICKE, R. U.; SPRENGART, M. L.; WATI, M. R. & PORTER, A. G. 1998. Caspase-3 Is Required for DNA Fragmentation and Morphological Changes Associated with Apoptosis. *J Biol Chem,* 273**,** 9357-60.

JEON, H.; KIM, H.; CHOI, D.; KIM, D.; PARK, S.-Y.; KIM, Y.-J.; KIM, Y. M. & JUNG, Y. 2007. Quercetin Activates an Angiogenic Pathway, Hypoxia Inducible Factor (HIF)-1-Vascular Endothelial Growth Factor, by Inhibiting HIF-Prolyl Hydroxylase: A Structural Analysis of Quercetin for Inhibiting HIF-Prolyl Hydroxylase. *Mol Pharmacol,* 71**,** 1676-84.

JIANG, B.; HEBERT, V. Y.; LI, Y.; MATHIS, J. M.; ALEXANDER, J. S. & DUGAS, T. R. 2007. HIV Antiretroviral Drug Combination Induces Endothelial Mitochondrial Dysfunction and Reactive Oxygen Species Production, but Not Apoptosis. *Toxicol App Pharmacol,* 224**,** 60-71.

JIN, S.; DIPAOLA, R. S.; MATHEW, R. & WHITE, E. 2007. Metabolic Catastrophe as a Means to Cancer Cell Death. *J Cell Sci,* 120**,** 379-83.

JIN, S. & WHITE, E. 2007. Role of Autophagy in Cancer: Management of Metabolic Stress. *Autophagy,* 3**,** 28-31.

JONES, P. T.; DEAR, P. H.; FOOTE, J.; NEUBERGER, M. S. & WINTER, G. 1986. Replacing the Complementarity-Determining Regions in a Human Antibody with Those from a Mouse. *Nature,* 321**,** 522-25.

JULIANO, R. L. & LING, V. 1976. A Surface Glycoprotein Modulating Drug Permeability in Chinese Hamster Ovary Cell Mutants. *BBA - Biomembranes,* 455**,** 152-62.

KABEYA, Y.; MIZUSHIMA, N.; UENO, T.; YAMAMOTO, A.; KIRISAKO, T.; NODA, T.; KOMINAMI, E.; OHSUMI, Y. & YOSHIMORI, T. 2000. LC3, a Mammalian Homologue of Yeast APG8P, Is Localized in Autophagosome Membranes after Processing. *EMBO J,* 19**,** 5720-28.

KAHAN, B. D. & CAMARDO, J. S. 2001. Rapamycin: Clinical Results and Future Opportunities1. *Transplantation,* 72**,** 1181-93.

KALBÁČOVÁ, M.; VRBACKÝ, M.; DRAHOTA, Z. & MĚLKOVÁ, Z. 2003. Comparison of the Effect of Mitochondrial Inhibitors on Mitochondrial Membrane Potential in Two Different Cell Lines Using Flow Cytometry and Spectrofluorometry. *Cytometry A,* 52**,** 110-16.

KAMADA, S.; WASHIDA, M.; HASEGAWA, J.-I.; KUSANO, H.; FUNAHASHI, Y. & TSUJIMOTO, Y. 1997. Involvement of Caspase-4 (-Like) Protease in Fas-Mediated Apoptotic Pathway. *Oncogene,* 15**,** 285-90.

KAMENCIC, H.; LYON, A.; PATERSON, P. G. & JUURLINK, B. H. 2000a. Monochlorobimane Fluorometric Method to Measure Tissue Glutathione. *Anal Biochem,* 286**,** 35-37.

KAMENCIC, H.; LYON, A.; PATERSON, P. G. & JUURLINK, B. H. J. 2000b. Monochlorobimane Fluorometric Method to Measure Tissue Glutathione. *Anal Biochem,* 286**,** 35-37.

KANEUCHI, M.; SASAKI, M.; TANAKA, Y.; SAKURAGI, N.; FUJIMOTO, S. & DAHIYA, R. 2003. Quercetin Regulates Growth of Ishikawa Cells through the Suppression of EGF and Cyclin D1. *Int J Oncol,* 22**,** 159-64.

KANG, H. T. & HWANG, E. S. 2006. 2-Deoxyglucose: An Anticancer and Antiviral Therapeutic, but Not Any More a Low Glucose Mimetic. *Life Sci,* 78**,** 1392-99.

KAPLAN, O.; NAVON, G.; LYON, R. C.; FAUSTINO, P. J.; STRAKA, E. J. & COHEN, J. S. 1990. Effects of 2-Deoxyglucose on Drug-Sensitive and Drug-Resistant Human Breast Cancer Cells: Toxicity and Magnetic Resonance Spectroscopy Studies of Metabolism. *Cancer Res,* 50**,** 544-51.

KARNOVKSY, M. J. 1965. A Formaldehyde Glutaraldehyde Fixative of High Osmolality for Use in Electron Microscopy. *J Cell Biol,* 27**,** 137-39.

KERBEL, R. S. 1991. Inhibition of Tumor Angiogenesis as a Strategy to Circumvent Acquired Resistance to Anti-Cancer Therapeutic Agents. *BioEssays,* 13**,** 31-36.

KERBEL, R. S.; VILORIA-PETIT, A.; KLEMENT, G. & RAK, J. 2000. 'Accidental' Anti-Angiogenic Drugs: Anti-Oncogene Directed Signal Transduction Inhibitors and Conventional Chemotherapeutic Agents as Examples. *Eur J Cancer,* 36**,** 1248-57.

KIETZMANN, T.; CORNESSE, Y.; BRECHTEL, K.; MODARESSI, S. & JUNGERMANN, K. 2001. Perivenous Expression of the Mrna of the Three Hypoxia-Inducible Factor A-Subunits, HIF1α, HIF2α and HIF3α, in Rat Liver. *Biochem. J,* 354**,** 531-37.

KIM, H.; MOON, J. Y.; AHN, K. S. & CHO, S. K. 2013. Quercetin Induces Mitochondrial Mediated Apoptosis and Protective Autophagy in Human Glioblastoma U373MG Cells. *Oxid Med Cell Longev,* 2013.

KIM, I.; XU, W. & REED, J. C. 2008. Cell Death and Endoplasmic Reticulum Stress: Disease Relevance and Therapeutic Opportunities. *Nat Rev Drug Discov,* 7**,** 1013-30.

KIMURA, F.; IWAYA, K.; KAWAGUCHI, T.; KAISE, H.; YAMADA, K.; MUKAI, K.; MATSUBARA, O.; IKEDA, N. & KOHNO, N. 2010. Epidermal Growth Factor-Dependent Enhancement of Invasiveness of Squamous Cell Carcinoma of the Breast. *Cancer Sci,* 101**,** 1133-40.

KIOKA, N.; HOSOKAWA, N.; KOMANO, T.; HIRAYOSHI, K.; NAGATE, K. & UEDA, K. 1992. Quercetin, a Bioflavonoid, Inhibits the Increase of Human Multidrug Resistance Gene (MDR1) Expression Caused by Arsenite. *FEBS Lett,* 301**,** 307-09.

KIRSCH, D. G.; DOSEFF, A.; CHAU, B. N.; LIM, D.-S.; DE SOUZA-PINTO, N. C.; HANSFORD, R.; KASTAN, M. B.; LAZEBNIK, Y. A. & HARDWICK, J. M. 1999. Caspase-3-Dependent Cleavage of Bcl-2 Promotes Release of Cytochrome C. *J Biol Chem,* 274**,** 21155-61.

KISCHKEL, F. C.; LAWRENCE, D. A.; TINEL, A.; LEBLANC, H.; VIRMANI, A.; SCHOW, P.; GAZDAR, A.; BLENIS, J.; ARNOTT, D. & ASHKENAZI, A. 2001. Death Receptor Recruitment

of Endogenous Caspase-10 and Apoptosis Initiation in the Absence of Caspase-8. *J Biol Chem,* 276**,** 46639-46.

KIŠŠOVÁ, I.; DEFFIEU, M.; SAMOKHVALOV, V.; VELOURS, G.; BESSOULE, J.-J.; MANON, S. & CAMOUGRAND, N. 2006. Lipid Oxidation and Autophagy in Yeast. *Free Radic Biol Med,* 41**,** 1655-61.

KLAPPAN, A.; HONES, S.; MYLONAS, I. & BRÜNING, A. 2012. Proteasome Inhibition by Quercetin Triggers Macroautophagy and Blocks MTOR Activity. *Histochem Cell Biol,* 137**,** 25-36.

KLAUBER, N.; PARANGI, S.; FLYNN, E.; HAMEL, E. & D'AMATO, R. J. 1997. Inhibition of Angiogenesis and Breast Cancer in Mice by the Microtubule Inhibitors 2-Methoxyestradiol and Taxol. *Cancer Res,* 57**,** 81-86.

KLEMENT, G.; BARUCHEL, S.; RAK, J.; MAN, S.; CLARK, K.; HICKLIN, D. J.; BOHLEN, P. & KERBEL, R. S. 2000. Continuous Low-Dose Therapy with Vinblastine and Vegf Receptor-2 Antibody Induces Sustained Tumor Regression without Overt Toxicity. *J Clin Invest,* 105**,** R15.

KLIONSKY, D. J. 2005. The Molecular Machinery of Autophagy: Unanswered Questions. *J Cell Sci,* 118**,** 7-18.

KLIONSKY, D. J.; ABDALLA, F. C.; ABELIOVICH, H.; ABRAHAM, R. T.; ACEVEDO-AROZENA, A.; ADELI, K.; AGHOLME, L.; AGNELLO, M.; AGOSTINIS, P. & AGUIRRE-GHISO, J. A. 2012. Guidelines for the Use and Interpretation of Assays for Monitoring Autophagy. *Autophagy,* 8**,** 445-544.

KLIONSKY, D. J.; ABELIOVICH, H.; AGOSTINIS, P.; AGRAWAL, D. K.; ALIEV, G.; ASKEW, D. S.; BABA, M.; BAEHRECKE, E. H.; BAHR, B. A.; BALLABIO, A.; BAMBER, B. A.; BASSHAM, D. C.; BERGAMINI, E.; BI, X.; BIARD-PIECHACZYK, M.; BLUM, J. S.; BREDESEN, D. E.; BRODSKY, J. L.; BRUMELL, J. H.; BRUNK, U. T.; BURSCH, W.; CAMOUGRAND, N.; CEBOLLERO, E.; CECCONI, F.; CHEN, Y.; CHIN, L.-S.; CHOI, A.; CHU, C. T.; CHUNG, J.; CLARK, R. S. B.; CLARKE, P. G. H.; CLARKE, S. G.; CLAVE, C.; CLEVELAND, J. L.; CODOGNO, P.; COLOMBO, M. I.; COTO-MONTES, A.; CREGG, J. M.; CUERVO, A. M.; DEBNATH, J.; DENNIS, P. B.; DENNIS, P. A.; DEMARCHI, F.; DERETIC, V.; DEVENISH, R. J.; DI SANO, F.; DICE, J. F.; DISTELHORST, C. W.; DINESH-KUMAR, S. P.; EISSA, N. T.; DIFIGLIA, M.; DJAVAHERI-MERGNY, M.; DORSEY, F. C.; DRÖGE, W.; DRON, M.; DUNN, J. W. A.; DUSZENKO, M.; ELAZAR, Z.; ESCLATINE, A.; ESKELINEN, E.-L.; FÉSÜS, L.; FINLEY, K. D.; FUENTES, J. M.; FUEYO-MARGARETO, J.; FUJISAKI, K.; GALLIOT, B.; GAO, F.-B.; GEWIRTZ, D. A.; GIBSON, S. B.; GOHLA, A.; GOLDBERG, A. L.; GONZALEZ, R.; GONZÁLEZ-ESTÉVEZ, C.; GORSKI, S. M.; GOTTLIEB, R. A.; HÄUSSINGER, D.; HE, Y.-W.; HEIDENREICH, K.; HILL, J. A.; HØYER-HANSEN, M.; HU, X.; HUANG, W.-P.; IWASAKI, A.; JÄÄTTELÄ, M.; JACKSON, W. T.; JIANG, X.; JIN, S. V.; JOHANSEN, T.; JUNG, J. U.; KADOWAKI, M.; KANG, C.; KELEKAR, A.; KESSEL, D. H.; KIEL, J. A. K. W.; KIM, H. P.; KIMCHI, A.; KINSELLA, T. J.; KISELYOV, K.; KITAMOTO, K.; KNECHT, E.*, et al.* 2008. Guidelines for the Use and Interpretation of Assays for Monitoring Autophagy in Higher Eukaryotes. *Autophagy,* 4**,** 151-75.

KLUCK, R. M.; BOSSY-WETZEL, E.; GREEN, D. R. & NEWMEYER, D. D. 1997. The Release of Cytochrome C from Mitochondria: A Primary Site for Bcl-2 Regulation of Apoptosis. *Science,* 275**,** 1132-36.

KNUDSON, A. G. 1971. Mutation and Cancer: Statistical Study of Retinoblastoma. *Proc Natl Acad Sci,* 68**,** 820-23.

KNUDSON, A. G. & STRONS, L. C. 1972. Mutation and Cancer: A Model for Wilms' Tumor of the Kidney. *J Natl Cancer Inst,* 48**,** 313-24.

KO, Y.; VERHOEVEN, H.; LEE, M.; CORBIN, D.; VOGL, T. & PEDERSEN, P. 2012. A Translational Study “Case Report” on the Small Molecule “Energy Blocker” 3-Bromopyruvate (3BP) as a Potent Anticancer Agent: From Bench Side to Bedside. *J Bioenerg Biomembr,* 44**,** 163-70.

KO, Y. H.; PEDERSEN, P. L. & GESCHWIND, J. F. 2001. Glucose Catabolism in the Rabbit VX2 Tumor Model for Liver Cancer: Characterization and Targeting Hexokinase. *Cancer Lett,* 173**,** 83-91.

KO, Y. H.; SMITH, B. L.; WANG, Y.; POMPER, M. G.; RINI, D. A.; TORBENSON, M. S.; HULLIHEN, J. & PEDERSEN, P. L. 2004. Advanced Cancers: Eradication in All Cases Using 3-Bromopyruvate Therapy to Deplete Atp. *Biochem Biophys Res Comm,* 324**,** 269-75.

KOBOLDT, D. C.; FULTON, R. S.; MCLELLAN, M. D.; SCHMIDT, H.; KALICKI-VEIZER, J.; MCMICHAEL, J. F.; FULTON, L. L.; DOOLING, D. J.; DING, L.; MARDIS, E. R.; WILSON, R. K.; ALLY, A.; BALASUNDARAM, M.; BUTTERFIELD, Y. S. N.; CARLSEN, R.; CARTER, C.; CHU, A.; CHUAH, E.; CHUN, H.-J. E.; COOPE, R. J. N.; DHALLA, N.; GUIN, R.; HIRST, C.; HIRST, M.; HOLT, R. A.; LEE, D.; LI, H. I.; MAYO, M.; MOORE, R. A.; MUNGALL, A. J.; PLEASANCE, E.; ROBERTSON, A. G.; SCHEIN, J. E.; SHAFIEI, A.; SIPAHIMALANI, P.; SLOBODAN, J. R.; STOLL, D.; TAM, A.; THIESSEN, N.; VARHOL, R. J.; WYE, N.; ZENG, T.; ZHAO, Y.; BIROL, I.; JONES, S. J. M.; MARRA, M. A.; CHERNIACK, A. D.; SAKSENA, G.; ONOFRIO, R. C.; PHO, N. H.; CARTER, S. L.; SCHUMACHER, S. E.; TABAK, B.; HERNANDEZ, B.; GENTRY, J.; NGUYEN, H.; CRENSHAW, A.; ARDLIE, K.; BEROUKHIM, R.; WINCKLER, W.; GETZ, G.; GABRIEL, S. B.; MEYERSON, M.; CHIN, L.; PARK, P. J.; KUCHERLAPATI, R.; HOADLEY, K. A.; AUMAN, J. T.; FAN, C.; TURMAN, Y. J.; YAN SHI15; LI, L.; TOPAL, M. D.; HE, X.; CHAO, H.-H.; PRAT, A.; SILVA, G. O.; IGLESIA, M. D.; ZHAO, W.; USARY, J.; BERG, J. S.; ADAMS, M.; BOOKER, J.; WU, J.; GULABANI, A.; BODENHEIMER, T.; HOYLE, A. P.; SIMONS, J. V.; SOLOWAY, M. G.; MOSE, L. E.; JEFFERYS, S. R.; BALU, S.; PARKER, J. S.; HAYES, D. N.; PEROU, C. M.; MALIK, S.; MAHURKAR, S.; SHEN, H.; WEISENBERGER, D. J.; TRICHE JR, T., *et al.* 2012. Comprehensive Molecular Portraits of Human Breast Tumours. *Nature,* 490**,** 61-70.

KOKAI, Y.; MYERS, J. N.; WADA, T.; BROWN, V. I.; LEVEA, C. M.; DAVIS, J. G.; DOBASHI, K. & GREENE, M. I. 1989. Synergistic Interaction of P185c-Neu and the EGF Receptor Leads to Transformation of Rodent Fibroblasts. *Cell,* 58**,** 287-92.

KOOPMAN, G.; REUTELINGSPERGER, C.; KUIJTEN, G.; KEEHNEN, R.; PALS, S. & VAN OERS, M. 1994. Annexin V for Flow Cytometric Detection of Phosphatidylserine Expression on B Cells Undergoing Apoptosis. *Blood,* 84**,** 1415-20.

KOUROKU, Y.; FUJITA, E.; TANIDA, I.; UENO, T.; ISOAI, A.; KUMAGAI, H.; OGAWA, S.; KAUFMAN, R. J.; KOMINAMI, E. & MOMOI, T. 2006. ER Stress (PERK//EIF2[Alpha] Phosphorylation) Mediates the Polyglutamine-Induced LC3 Conversion, an Essential Step for Autophagy Formation. *Cell Death Differ,* 14**,** 230-39.

KOVÁCS, J.; LÁSZLÓ, L. & KOVÁCS, A. L. 1988. Regression of Autophagic Vacuoles in Pancreatic Acinar, Seminal Vesicle Epithelial, and Liver Parenchymal Cells: A Comparative Morphometric Study of the Effect of Vinblastine and Leupeptin Followed by Cycloheximide Treatment. *Exp Cell Res,* 174**,** 244-51.

KRAUS, M.; MALENKE, E.; GOGEL, J.; MÜLLER, H.; RÜCKRICH, T.; OVERKLEEFT, H.; OVAA, H.; KOSCIELNIAK, E.; HARTMANN, J. T. & DRIESSEN, C. 2008. Ritonavir Induces Endoplasmic Reticulum Stress and Sensitizes Sarcoma Cells toward Bortezomib-Induced Apoptosis. *Mol Cancer Ther,* 7**,** 1940-48.

KUMAR, H. & CHOI, D.-K. 2015. Hypoxia Inducible Factor Pathway and Physiological Adaptation: A Cell Survival Pathway? *Mediat Inflamm,* DOI: 10.1155/2015/584758.

KUMAR, S.; WITZIG, T. & RAJKUMAR, S. 2002. Thalidomide as an Anti-Cancer Agent. *J Cell Mol Med,* 6**,** 160-74.

KÜUHNAU, J. 1976. The Flavonoids. A Class of Semi-Essential Food Components. *World Rev Nutr Diet,* 24**,** 117-91.

KWABI-ADDO, B.; WANG, J.; ERDEM, H.; VAID, A.; CASTRO, P.; AYALA, G. & ITTMANN, M. 2004. The Expression of SPROUTY1, an Inhibitor of Fibroblast Growth Factor Signal Transduction, Is Decreased in Human Prostate Cancer. *Cancer Res,* 64**,** 4728-35.

KWON, O.; ECK, P.; CHEN, S.; CORPE, C. P.; LEE, J.-H.; KRUHLAK, M. & LEVINE, M. 2007. Inhibition of the Intestinal Glucose Transporter GLUT2 by Flavonoids. *FASEB J,* 21**,** 366-77.

LA PORTE, C.; BACK, D.; BLASCHKE, T.; BOUCHER, C.; FLETCHER, C.; FLEXNER, C.; GERBER, J.; KASHUBA, A.; SCHAPIRO, J. & BURGER, D. 2006. Updated Guideline to Perform Therapeutic Drug Monitoring for Antiretroviral Agents. *Rev in Antivir Ther,* 3**,** 4-14.

LAGATHU, C.; EUSTACE, B.; PROT, M.; FRANTZ, D.; GU, Y.; BASTARD, J.-P.; MAACHI, M.; AZOULAY, S.; BRIGGS, M. & CARON, M. 2007. Some Hiv Antiretrovirals Increase Oxidative Stress and Alter Chemokine, Cytokine or Adiponectin Production in Human Adipocytes and Macrophages. *Antivir Ther,* 12**,** 489.

LAKHANI, N. J.; SARKAR, M. A.; VENITZ, J. & FIGG, W. D. 2003. 2-Methoxyestradiol, a Promising Anticancer Agent. *Pharmacother,* 23**,** 165-72.

LAND, H.; PARADA, L. F. & WEINBERG, R. A. 1982. Tumorigenic Conversion of Primary Embryo Fibroblasts Requires at Least Two Cooperating Oncogenes. *Nature,* 304**,** 596-602.

LANG, D. R. & RACKER, E. 1974. Effects of Quercetin and F1 Inhibitor on Mitochondrial ATPase and Energy-Linked Reactions in Submitochondrial Particles. *BBA - Bioenergetics,* 333**,** 180-86.

LAUGHTON, M. J.; HALLIWELL, B.; EVANS, P. J.; ROBIN, J. & HOULT, S. 1989. Antioxidant and Pro-Oxidant Actions of the Plant Phenolics Quercetin, Gossypol and Myricetin: Effects on Lipid Peroxidation, Hydroxyl Radical Generation and Bleomycin-Dependent Damage to DNA. *Biochem Pharmacol,* 38**,** 2859-65.

LAVALLEE, T. M.; ZHAN, X. H.; HERBSTRITT, C. J.; KOUGH, E. C.; GREEN, S. J. & PRIBLUDA, V. S. 2002. 2-Methoxyestradiol Inhibits Proliferation and Induces Apoptosis Independently of Estrogen Receptors A and B. *Cancer Res,* 62**,** 3691-97.

LAVALLEE, T. M.; ZHAN, X. H.; JOHNSON, M. S.; HERBSTRITT, C. J.; SWARTZ, G.; WILLIAMS, M. S.; HEMBROUGH, W. A.; GREEN, S. J. & PRIBLUDA, V. S. 2003a. 2-Methoxyestradiol up-Regulates Death Receptor 5 and Induces Apoptosis through Activation of the Extrinsic Pathway. *Cancer Res,* 63**,** 468-75.

LAVALLEE, T. M.; ZHAN, X. H.; JOHNSON, M. S.; HERBSTRITT, C. J.; SWARTZ, G.; WILLIAMS, M. S.; HEMBROUGH, W. A.; GREEN, S. J. & PRIBLUDA, V. S. 2003b. 2-Methoxyestradiol up-Regulates Death Receptor 5 and Induces Apoptosis through Activation of the Extrinsic Pathway. *Cancer Res,* 63**,** 468-75.

LE DRAN, H.-F. 1757. *Memoire Avec Un Precis De Plusieurs Observations Sur Le Cancer*.

LEBBÉ, C.; BLUM, L.; PELLET, C.; BLANCHARD, G.; VÉROLA, O.; MOREL, P.; DANNE, O. & CALVO, F. 1998. Clinical and Biological Impact of Antiretroviral Therapy with Protease Inhibitors on Hiv-Related Kaposi's Sarcoma. *Aids,* 12**,** F45-F49.

LEDOUX, S.; YANG, R.; FRIEDLANDER, G. & LAOUARI, D. 2003. Glucose Depletion Enhances P-Glycoprotein Expression in Hepatoma Cells: Role of Endoplasmic Reticulum Stress Response. *Cancer Res,* 63**,** 7284-90.

LEE, A. S. & HENDERSHOT, L. M. 2006. Er Stress and Cancer. *Cancer Biol Ther,* 5**,** 721-22.

LEE, E. A.; KEUTMANN, M. K.; DOWLING, M. L.; HARRIS, E.; CHAN, G. & KAO, G. D. 2004. Inactivation of the Mitotic Checkpoint as a Determinant of the Efficacy of Microtubule-Targeted Drugs in Killing Human Cancer Cells. *Mol Cancer Ther,* 3**,** 661-69.

LEE, J.-C.; KIM, J.; PARK, J.-K.; CHUNG, G.-H. & JANG, Y.-S. 2003. The Antioxidant, Rather Than Prooxidant, Activities of Quercetin on Normal Cells:: Quercetin Protects Mouse Thymocytes from Glucose Oxidase-Mediated Apoptosis. *Exp Cell Res,* 291**,** 386-97.

LEE, S. I. 2010. Drug Interaction: Focusing on Response Surface Models. *Korean J Anesthesiol,* 58**,** 421-34.

LEIS JR, H. P. 1981. The Surgeon's Role in Breast Cancer: Changing Concepts. *Breast Cancer Res Treat,* 1**,** 5-15.

LEMASTERS, J. J.; NIEMINEN, A.-L.; QIAN, T.; TROST, L. C.; ELMORE, S. P.; NISHIMURA, Y.; CROWE, R. A.; CASCIO, W. E.; BRADHAM, C. A. & BRENNER, D. A. 1998. The Mitochondrial Permeability Transition in Cell Death: A Common Mechanism in Necrosis, Apoptosis and Autophagy. *BBA-Bioenergetics,* 1366**,** 177-96.

LENZ, W.; PFEIFFER, R. A.; KOSENOW, W. & HAYMAN, D. 1962. Thalidomide and Congenital Abnormalities. *Lancet,* 279**,** 45-46.

LETH, T. & JUSTESEN, U. 1998. Analysis of Flavonoids in Fruits, Vegetables and Beverages by HPLC-UV and LC-MS and Estimation of the Total Daily Flavonoid Intake in Denmark. *Polyphenols in food***,** 39-40.

LEVINE, A. J. 1997. P53, the Cellular Gatekeeper for Growth and Division. *Cell,* 88**,** 323-31.

LI, C. I.; DALING, J. R. & MALONE, K. E. 2003. Incidence of Invasive Breast Cancer by Hormone Receptor Status from 1992 to 1998. *J Clin Oncol,* 21**,** 28-34.

LI, H.; ZHU, H.; XU, C.-J. & YUAN, J. 1998. Cleavage of BID by Caspase 8 Mediates the Mitochondrial Damage in the Fas Pathway of Apoptosis. *Cell,* 94**,** 491-501.

LI, P.; NIJHAWAN, D.; BUDIHARDJO, I.; SRINIVASULA, S. M.; AHMAD, M.; ALNEMRI, E. S. & WANG, X. 1997. Cytochrome C and dATP-Dependent Formation of APAF-1/Caspase-9 Complex Initiates an Apoptotic Protease Cascade. *Cell,* 91**,** 479-89.

LIANG, C.-C.; PARK, A. Y. & GUAN, J.-L. 2007. In Vitro Scratch Assay: A Convenient and Inexpensive Method for Analysis of Cell Migration in Vitro. *Nat Protoc,* 2**,** 329-33.

LIANG, Y.; YAN, C. & SCHOR, N. F. 2001. Apoptosis in the Absence of Caspase 3. *Oncogene,* 20**,** 6570-78.

LIANOS, G. D.; ALEXIOU, G. A.; MANGANO, A.; MANGANO, A.; RAUSEI, S.; BONI, L.; DIONIGI, G. & ROUKOS, D. H. 2015. The Role of Heat Shock Proteins in Cancer. *Cancer Lett,* 360**,** 114-18.

LICHTENSTEIN, P.; HOLM, N. V.; VERKASALO, P. K.; ILIADOU, A.; KAPRIO, J.; KOSKENVUO, M.; PUKKALA, E.; SKYTTHE, A. & HEMMINKI, K. 2000. Environmental and Heritable Factors in the Causation of Cancer — Analyses of Cohorts of Twins from Sweden, Denmark, and Finland. *N Engl J Med,* 343**,** 78-85.

LIOU, W.; GEUZE, H. & SLOT, J. 1996. Improving Structural Integrity of Cryosections for Immunogold Labeling. *Histochem Cell Biol,* 106**,** 41-58.

LIPPMAN, M.; BOLAN, G. & HUFF, K. 1976. The Effects of Estrogens and Antiestrogens on Hormone-Responsive Human Breast Cancer in Long-Term Tissue Culture. *Cancer Res,* 36**,** 4595-601.

LIU, X.; KIM, C. N.; YANG, J.; JEMMERSON, R. & WANG, X. 1996. Induction of Apoptotic Program in Cell-Free Extracts: Requirement for Datp and Cytochrome C. *Cell,* 86**,** 147-57.

LIU, Y. & MUELLER, B. M. 2006. Protease-Activated Receptor-2 Regulates Vascular Endothelial Growth Factor Expression in MDA-MB-231 Cells Via Mapk Pathways. *Biochem Biophys Res Comm,* 344**,** 1263-70.

LIU, Y.; ZHANG, W.; CAO, Y.; LIU, Y.; BERGMEIER, S. & CHEN, X. 2010. Small Compound Inhibitors of Basal Glucose Transport Inhibit Cell Proliferation and Induce Apoptosis in Cancer Cells Via Glucose-Deprivation-Like Mechanisms. *Cancer Lett,* 298**,** 176-85.

LIU, Z.; ZHANG, Y.-Y.; ZHANG, Q.-W.; ZHAO, S.-R.; WU, C.-Z.; CHENG, X.; JIANG, C.-C.; JIANG, Z.-W. & LIU, H. 2014. 3-Bromopyruvate Induces Apoptosis in Breast Cancer Cells by Downregulating MCL-1 through the PI3k/Akt Signaling Pathway. *Anti-cancer Drug,* 25**,** 447-55.

LO, S.-C.; WANG, Y.; WEBER, M.; LARSON, J. L.; SCEARCE-LEVIE, K. & SHENG, M. 2015. Caspase-3 Deficiency Results in Disrupted Synaptic Homeostasis and Impaired Attention Control. *J Neurosci,* 35**,** 2118-32.

LO, T. L.; YUSOFF, P.; FONG, C. W.; GUO, K.; MCCAW, B. J.; PHILLIPS, W. A.; YANG, H.; WONG, E. S. M.; LEONG, H. F. & ZENG, Q. 2004. The Ras/Mitogen-Activated Protein Kinase

Pathway Inhibitor and Likely Tumor Suppressor Proteins, SPROUTY 1 and SPROUT 2 Are Deregulated in Breast Cancer. *Cancer Res,* 64**,** 6127-36.

LOEWE, S. 1953. The Problem of Synergism and Antagonism of Combined Drugs. *Arzneimittelforchung,* 3**,** 285-90.

LONGNECKER, M. P.; BERLIN, J. A.; ORZA, M. J. & CHALMERS, T. C. 1988. A Meta-Analysis of Alcohol Consumption in Relation to Risk of Breast Cancer. *JAMA,* 260**,** 652-56.

LOPEZ, M.; CARPANO, S.; DILAURO, L.; CHIATTI, L.; VICI, P.; CAVALIERE, F.; GENTILE, P. & CITRO, G. 1995. Clinical Modulation of Epirubicin Resistance by Lonidamine in Patients with Advanced Soft-Tissue Sarcomas. *Int J Oncol,* 6**,** 363-67.

LORIZIO, W.; WU, A. B.; BEATTIE, M.; RUGO, H.; TCHU, S.; KERLIKOWSKE, K. & ZIV, E. 2012. Clinical and Biomarker Predictors of Side Effects from Tamoxifen. *Breast Cancer Res Treat,* 132**,** 1107-18.

LUMACHI, F.; BRUNELLO, A.; MARUZZO, M.; BASSO, U. & MM BASSO, S. 2013. Treatment of Estrogen Receptor-Positive Breast Cancer. *Curr Med Chem,* 20**,** 596-604.

LUMACHI, F.; LUISETTO, G.; M.M. BASSO, S.; BASSO, U.; BRUNELLO, A. & CAMOZZI, V. 2011. Endocrine Therapy of Breast Cancer. *Curr Med Chem,* 18**,** 513-22.

LUQMANI, Y. 2005. Mechanisms of Drug Resistance in Cancer Chemotherapy. *Med Princ Pract,* 14**,** 35-48.

LY, J. D.; GRUBB, D. & LAWEN, A. 2003. The Mitochondrial Membrane Potential (Δψm) in Apoptosis; an Update. *Apoptosis,* 8**,** 115-28.

LYDEN, D.; HATTORI, K.; DIAS, S.; COSTA, C.; BLAIKIE, P.; BUTROS, L.; CHADBURN, A.; HEISSIG, B.; MARKS, W. & WITTE, L. 2001. Impaired Recruitment of Bone-Marrow–Derived Endothelial and Hematopoietic Precursor Cells Blocks Tumor Angiogenesis and Growth. *Nat Med,* 7**,** 1194-201.

MA, Y.; BREWER, J. W.; ALAN DIEHL, J. & HENDERSHOT, L. M. 2002. Two Distinct Stress Signaling Pathways Converge Upon the CHOP Promoter During the Mammalian Unfolded Protein Response. *J Mol Biol,* 318**,** 1351-65.

MACMAHON, B.; COLE, P.; LIN, T. M.; LOWE, C. R.; MIRRA, A. P.; RAVNIHAR, B.; SALBER, E. J.; VALAORAS, V. G. & YUASA, S. 1970. Age at First Birth and Breast Cancer Risk. *Bull World Health Organ,* 43**,** 209-21.

MADDEN, S. L.; COOK, D. M.; MORRIS, J. F.; GASHLER, A.; SUKHATME, V. P. & III, F. J. R. 1991. Transcriptional Repression Mediated by the WT1 Wilms Tumor Gene Product. *Science,* 253**,** 1550-53.

MADRI, J. A.; PRATT, B. M. & TUCKER, A. M. 1988. Phenotypic Modulation of Endothelial Cells by Transforming Growth Factor-Beta Depends Upon the Composition and Organization of the Extracellular Matrix. *J Cell Biol,* 106**,** 1375-84.

MAHER, J.; KRISHAN, A. & LAMPIDIS, T. 2004. Greater Cell Cycle Inhibition and Cytotoxicity Induced by 2-Deoxy-D-Glucose in Tumor Cells Treated under Hypoxic Vs Aerobic Conditions. *Cancer Chemother Pharmacol,* 53**,** 116-22.

MARTINET, W.; DE MEYER, G. R.; ANDRIES, L.; HERMAN, A. G. & KOCKX, M. M. 2006a. In Situ Detection of Starvation-Induced Autophagy. *J Histochem Cytochem,* 54**,** 85-96.

MARTINET, W.; MEYER, G. R. D.; ANDRIES, L.; HERMAN, A. G. & KOCKX, M. M. 2006b. Detection of Autophagy in Tissue by Standard Immunohistochemistry: Possibilities and Limitations. *Autophagy,* 2**,** 55-57.

MARTINEZ-IRUJO, J. J.; VILLAHERMOSA, M. L.; ALBERDI, E. & SANTIAGO, E. 1996. A Checkerboard Method to Evaluate Interactions between Drugs. *Biochem Pharmacol,* 51**,** 635-44.

MARTÍNEZ-ZAGUILÁN, R.; SEFTOR, E.; SEFTOR, R. B.; CHU, Y.-W.; GILLIES, R. & HENDRIX, M. C. 1996. Acidic Ph Enhances the Invasive Behavior of Human Melanoma Cells. *Clin Exp Metastas,* 14**,** 176-86.

MARTINON, F. 2012. Targeting Endoplasmic Reticulum Signaling Pathways in Cancer. *Acta Oncol,* 51**,** 822-30.

MASCHEK, G.; SAVARAJ, N.; PRIEBE, W.; BRAUNSCHWEIGER, P.; HAMILTON, K.; TIDMARSH, G. F.; DE YOUNG, L. R. & LAMPIDIS, T. J. 2004. 2-Deoxy-D-Glucose Increases the Efficacy of Adriamycin and Paclitaxel in Human Osteosarcoma and Non-Small Cell Lung Cancers in Vivo. *Cancer Res,* 64**,** 31-34.

MATARRESE, P.; GAMBARDELLA, L.; CASSONE, A.; VELLA, S.; CAUDA, R. & MALORNI, W. 2003. Mitochondrial Membrane Hyperpolarization Hijacks Activated T Lymphocytes toward the Apoptotic-Prone Phenotype: Homeostatic Mechanisms of Hiv Protease Inhibitors. *J Immunol,* 170**,** 6006-15.

MATHUPALA, S.; REMPEL, A. & PEDERSEN, P. 1997a. Aberrant Glycolytic Metabolism of Cancer Cells: A Remarkable Coordination of Genetic, Transcriptional, Post-Translational, and Mutational Events That Lead to a Critical Role for Type II Hexokinase. *J Bioenerg Biomembr,* 29**,** 339-43.

MATHUPALA, S. P.; HEESE, C. & PEDERSEN, P. L. 1997b. Glucose Catabolism in Cancer Cells: The Type II Hexokinase Promoter Contains Functionally Active Response Elements for the Tumor Suppressor P53. *J Biol Chem,* 272**,** 22776-80.

MATSUYAMA, S.; LLOPIS, J.; DEVERAUX, Q. L.; TSIEN, R. Y. & REED, J. C. 2000. Changes in Intramitochondrial and Cytosolic Ph: Early Events That Modulate Caspase Activation During Apoptosis. *Nat Cell Biol,* 2**,** 318-25.

MCBRIDE, W. G. 1961. Thalidomide and Congenital Abnormalities. *Lancet,* 278**,** 1358.

MCGUIRE, W.; HORWITZ, K.; PEARSON, O. & SEGALOFF, A. 1977. Current Status of Estrogen and Progesterone Receptors in Breast Cancer. *Cancer,* 39**,** 2934-47.

MCLEAN, K.; VANDEVEN, N. A.; SORENSON, D. R.; DAUDI, S. & LIU, J. R. 2009. The HIV Protease Inhibitor Saquinavir Induces Endoplasmic Reticulum Stress, Autophagy, and Apoptosis in Ovarian Cancer Cells. *Gynecol Oncol,* 112**,** 623-30.

MEDEMA, J. P.; SCAFFIDI, C.; KISCHKEL, F. C.; SHEVCHENKO, A.; MANN, M.; KRAMMER, P. H. & PETER, M. E. 1997. Flice Is Activated by Association with the CD95 Death-Inducing Signaling Complex (DISC). *EMBO J,* 16**,** 2794-804.

MEMETO, T.; VANA, J. & BEDWANA, R. 1980. Management and Survival of Female Breast Cancer. *Cancer,* 45**,** 2917-24.

MERLIN, J.-L.; BARBERI-HEYOB, M. & BACHMANN, N. 2002. In Vitro Comparative Evaluation of Trastuzumab (Herceptin®) Combined with Paclitaxel (Taxol®) or Docetaxel (Taxotere®) in Her2-Expressing Human Breast Cancer Cell Lines. *Ann Oncol,* 13**,** 1743-48.

METODIEWA, D.; JAISWAL, A. K.; CENAS, N.; DICKANCAITÉ, E. & SEGURA-AGUILAR, J. 1999. Quercetin May Act as a Cytotoxic Prooxidant after Its Metabolic Activation to Semiquinone and Quinoidal Product. *Free Radic Biol Med,* 26**,** 107-16.

MEYER, J. S.; RAMANATH RAO, B.; STEVENS, S. C. & WHITE, W. L. 1977. Low Incidence of Estrogen Receptor in Breast Carcinomas with Rapid Rates of Cellular Replication. *Cancer,* 40**,** 2290-98.

MGBAKOR, A. C.; OGBONNA, A. O.; ORANUSI, K. C. & AZIKE, J. E. 2014. Cancer Management in Africa: The Burden of Late Presentation and the Case for Cancer Awareness. *Int J Pharm Med Sci,* 4**,** 10-16.

MIKI, Y.; SWENSEN, J.; SHATTUCK-EIDENS, D.; FUTREAL, P. A.; HARSHMAN, K.; TAVTIGIAN, S.; LIU, Q.; COCHRAN, C.; BENNETT, L. M. & DING, W. 1994. A Strong Candidate for the Breast and Ovarian Cancer Susceptibility Gene BRCA1. *Science,* 266**,** 66-71.

MILANE, L.; DUAN, Z. & AMIJI, M. 2011. Therapeutic Efficacy and Safety of Paclitaxel/Lonidamine Loaded EGFR-Targeted Nanoparticles for the Treatment of Multi-Drug Resistant Cancer. *PloS one,* 6**,** e24075.

MILLER, E. G. 1975. Stimulation of Nuclear Poly (Adenosine Diphosphate-Ribose) Polymerase Activity from HeLa Cells by Endonucleases. *BBA-Nucleic Acids Prot Synth,* 395**,** 191-200.

MIZUSHIMA, N. 2005. The Pleiotropic Role of Autophagy: From Protein Metabolism to Bactericide. *Cell Death Differ,* 12**,** 1535-41.

MONINI, P.; SGADARI, C.; GROSSO, M. G.; BELLINO, S.; DI BIAGIO, A.; TOSCHI, E.; BACIGALUPO, I.; SABBATUCCI, M.; CENCIONI, G. & SALVI, E. 2009. Clinical Course of Classic Kaposi's Sarcoma in HIV-Negative Patients Treated with the HIV Protease Inhibitor Indinavir. *Aids,* 23**,** 534-38.

MONKS, A.; SCUDIERO, D.; SKEHAN, P.; SHOEMAKER, R.; PAULL, K.; VISTICA, D.; HOSE, C.; LANGLEY, J.; CRONISE, P. & VAIGRO-WOLFF, A. 1991. Feasibility of a High-Flux Anticancer Drug Screen Using a Diverse Panel of Cultured Human Tumor Cell Lines. *J Natl Cancer Inst,* 83**,** 757-66.

MONSUEZ, J.-J.; CHARNIOT, J.-C.; VIGNAT, N. & ARTIGOU, J.-Y. 2010. Cardiac Side-Effects of Cancer Chemotherapy. *Int J Cardiol,* 144**,** 3-15.

MOYNAHAN, M. E.; CHIU, J. W.; KOLLER, B. H. & JASIN, M. 1999. BRCA1 Controls Homology-Directed DNA Repair. *Mol Cell,* 4**,** 511-18.

MUKHOPADHYAY, T. & ROTH, J. A. 1997. Induction of Apoptosis in Human Lung Cancer Cells after Wild-Type P53 Activation by Methoxyestradiol. *Oncogene,* 14**,** 379-84.

MULLIGAN, K.; GRUNFELD, C.; TAI, V. W.; ALGREN, H.; PANG, M.; CHERNOFF, D. N.; LO, J. C. & SCHAMBELAN, M. 2000. Hyperlipidemia and Insulin Resistance Are Induced by Protease

Inhibitors Independent of Changes in Body Composition in Patients with HIV Infection. *J Acquir Immune Defic Syndr,* 23**,** 35-43.

MURATA, H.; HRUZ, P. W. & MUECKLER, M. 2002. Indinavir Inhibits the Glucose Transporter Isoform GLUT4 at Physiologic Concentrations. *Aids,* 16**,** 859-63.

NAKADA, H. I. & WICK, A. N. 1956. Galactose Metabolism by the Isolated Rat Diaphragm. *Am J Physiol - Legacy Content,* 185**,** 23-26.

NAKAMURA, Y.; ISHIMITSU, S. & TONOGAI, Y. 2000. Effects of Quercetin and Rutin on Serum and Hepatic Lipid Concentrations, Fecal Steroid Excretion and Serum Antioxidant Properties. *J Health Sci,* 46**,** 229-40.

NGUYEN, T. T. T.; TRAN, E.; NGUYEN, T. H.; DO, P. T.; HUYNH, T. H. & HUYNH, H. 2004. The Role of Activated MEK-ERK Pathway in Quercetin-Induced Growth Inhibition and Apoptosis in A549 Lung Cancer Cells. *Carcinogenesis,* 25**,** 647-59.

NICHOLLS, D. G. 1977. The Effective Proton Conductance of the Inner Membrane of Mitochondria from Brown Adipose Tissue. *Eur J Biochem,* 77**,** 349-56.

NIFLI, A.-P.; THEODOROPOULOS, P. A.; MUNIER, S.; CASTAGNINO, C.; ROUSSAKIS, E.; KATERINOPOULOS, H. E.; VERCAUTEREN, J. & CASTANAS, E. 2007. Quercetin Exhibits a Specific Fluorescence in Cellular Milieu: A Valuable Tool for the Study of Its Intracellular Distribution. *Journal of agricultural and food chemistry,* 55**,** 2873-78.

NISHIMURO, H.; OHNISHI, H.; SATO, M.; OHNISHI-KAMEYAMA, M.; MATSUNAGA, I.; NAITO, S.; IPPOUSHI, K.; OIKE, H.; NAGATA, T. & AKASAKA, H. 2015. Estimated Daily Intake and Seasonal Food Sources of Quercetin in Japan. *Nutrients,* 7**,** 2345-58.

NIXON, R. A. 2007. Autophagy, Amyloidogenesis and Alzheimer Disease. *J Cell Sci,* 120**,** 4081-91.

NIZAMUTDINOVA, I. T.; LEE, G. W.; SON, K. H.; JEON, S. J.; KANG, S. S.; KIM, Y. S.; LEE, J. H.; SEO, H. G.; CHANG, K. C. & KIM, H. J. 2008. Tanshinone I Effectively Induces Apoptosis in Estrogen Receptor-Positive (MCF-7) and Estrogen Receptor-Negative (MDA-MB-231) Breast Cancer Cells. *Int J Oncol,* 33**,** 485-91.

NKANDEU, D. S.; MQOCO, T. V.; VISAGIE, M. H.; STANDER, B. A.; WOLMARANS, E.; CRONJE, M. J. & JOUBERT, A. M. 2013. In Vitro Changes in Mitochondrial Potential, Aggresome Formation and Caspase Activity by a Novel 17-B-Estradiol Analogue in Breast Adenocarcinoma Cells. *Cell Biochem Funct,* 31**,** 566-74.

NUALART, F.; GARCIA, M. D. L. A.; MEDINA, R. A. & OWEN, G. I. 2009. Glucose Transporters in Sex Steroid Hormone Related Cancer. *Curr Vasc Pharmacol,* 7**,** 534-48.

NUYDENS, R.; NOVALBOS, J.; DISPERSYN, G.; WEBER, C.; BORGERS, M. & GEERTS, H. 1999. A Rapid Method for the Evaluation of Compounds with Mitochondria-Protective Properties. *J Neurosci Methods,* 92**,** 153-59.

O'BRIEN, P. J.; IRWIN, W.; DIAZ, D.; HOWARD-COFIELD, E.; KREJSA, C. M.; SLAUGHTER, M. R.; GAO, B.; KALUDERCIC, N.; ANGELINE, A.; BERNARDI, P.; BRAIN, P. & HOUGHAM, C. 2006. High Concordance of Drug-Induced Human Hepatotoxicity with in Vitro Cytotoxicity Measured in a Novel Cell-Based Model Using High Content Screening. *Arch Toxicol,* 80**,** 580-604.

O'SHAUGHNESSY, J. 2005. Extending Survival with Chemotherapy in Metastatic Breast Cancer. *Oncologist,* 10**,** 20-29.

OCAÑA, A.; FREEDMAN, O.; AMIR, E.; SERUGA, B. & PANDIELLA, A. 2014. Biological Insights into Effective and Antagonistic Combinations of Targeted Agents with Chemotherapy in Solid Tumors. *Cancer Metastas Rev,* 33**,** 295-307.

OH, S. J.; KIM, O.; LEE, J. S.; KIM, J.-A.; KIM, M. R.; CHOI, H. S.; SHIM, J.-H.; KANG, K. W. & KIM, Y. C. 2010. Inhibition of Angiogenesis by Quercetin in Tamoxifen-Resistant Breast Cancer Cells. *Food Chem Toxicol,* 48**,** 3227-34.

OSELLAME, L. D.; BLACKER, T. S. & DUCHEN, M. R. 2012. Cellular and Molecular Mechanisms of Mitochondrial Function. *Best Pract Res Clin Endocrinol Metab,* 26**,** 711-23.

PAFFENBARGER, R. S.; KAMPERT, J. B. & CHANG, H. G. 1980. Characteristics That Predict Risk of Breast Cancer before and after the Menopause. *Am J Epidemiol,* 112**,** 258-68.

PALELLA JR, F. J.; DELANEY, K. M.; MOORMAN, A. C.; LOVELESS, M. O.; FUHRER, J.; SATTEN, G. A.; ASCHMAN, D. J. & HOLMBERG, S. D. 1998. Declining Morbidity and Mortality among Patients with Advanced Human Immunodeficiency Virus Infection. *N Engl J Med,* 338**,** 853-60.

PANDURI, V.; WEITZMAN, S. A.; CHANDEL, N. S. & KAMP, D. W. 2004. Mitochondrial-Derived Free Radicals Mediate Asbestos-Induced Alveolar Epithelial Cell Apoptosis. *Am J Physiol Lung Cell Mol Physiol,* 286**,** L1220-L27.

PANG, X.; LI, K.; WEI, L.; HUANG, Y.; SU, M.; WANG, L.; CAO, H. & CHEN, T. 2015. Il-8 Inhibits the Apoptosis of MCF-7 Human Breast Cancer Cells by up-Regulating Bcl-2 and Down-Regulating Caspase-3. *Xi Bao Yu Fen Zi Mian Yi Xue Za Zhi,* 31**,** 307-11.

PAPATHANASSIU, A. E.; MACDONALD, N. J.; EMLET, D. R. & VU, H. A. 2011. Antitumor Activity of Efrapeptins, Alone or in Combination with 2-Deoxyglucose, in Breast Cancer in Vitro and in Vivo. *Cell Stress Chaperones,* 16**,** 181-93.

PARK, C.; SO, H.-S.; SHIN, C.-H.; BAEK, S.-H.; MOON, B.-S.; SHIN, S.-H.; LEE, H.-S.; LEE, D.-W. & PARK, R. 2003. Quercetin Protects the Hydrogen Peroxide-Induced Apoptosis Via Inhibition of Mitochondrial Dysfuntion in H9C2 Cardiomyoblast Cells. *Biochem Pharmacol,* 66**,** 1287-95.

PARKIN, D. M.; BRAY, F.; FERLAY, J. & JEMAL, A. 2014. Cancer in Africa 2012. *Cancer Epidem Biomarkers Prevent,* 23**,** 953-66.

PARKIN, D. M.; WABINGA, H.; NAMBOOZE, S. & WABWIRE-MANGEN, F. 1999. AIDS-Related Cancers in Africa: Maturation of the Epidemic in Uganda. *Aids,* 13**,** 2563-70.

PASQUIER, E.; CARRÉ, M.; POURROY, B.; CAMOIN, L.; REBAÏ, O.; BRIAND, C. & BRAGUER, D. 2004. Antiangiogenic Activity of Paclitaxel Is Associated with Its Cytostatic Effect, Mediated by the Initiation but Not Completion of a Mitochondrial Apoptotic Signaling Pathway. *Mol Cancer Ther,* 3**,** 1301-10.

PAULEY, R. J.; PAINE, T. J. & SOULE, H. D. 1993. Immortal Human Mammary Epithelial Cell Sublines. Google Patents.

PEGRAM, M. D.; KONECNY, G. E.; O'CALLAGHAN, C.; BERYT, M.; PIETRAS, R. & SLAMON, D. J. 2004. Rational Combinations of Trastuzumab with Chemotherapeutic Drugs Used in the Treatment of Breast Cancer. *J Natl Cancer Inst,* 96**,** 739-49.

PELICANO, H.; MARTIN, D.; XU, R., AND & HUANG, P. 2006. Glycolysis Inhibition for Anticancer Treatment. *Oncogene,* 25**,** 4633-46.

PENNOCK, G. D.; DALTON, W. S.; ROESKE, W. R.; APPLETON, C. P.; MOSLEY, K.; PLEZIA, P.; MILLER, T. P. & SALMON, S. E. 1991. Systemic Toxic Effects Associated with High-Dose Verapamil Infusion and Chemotherapy Administration. *J Natl Cancer Inst,* 83**,** 105-10.

PEREZ, E. A. 2007. Safety Profiles of Tamoxifen and the Aromatase Inhibitors in Adjuvant Therapy of Hormone-Responsive Early Breast Cancer. *Ann Oncol,* 18**,** viii26-viii35.

PERONA, R. 2006. Cell Signalling: Growth Factors and Tyrosine Kinase Receptors. *Clin Transl Oncol,* 8**,** 77-82.

PEROU, C. M.; SORLIE, T.; EISEN, M. B.; VAN DE RIJN, M.; JEFFREY, S. S.; REES, C. A.; POLLACK, J. R.; ROSS, D. T.; JOHNSEN, H.; AKSLEN, L. A.; FLUGE, O.; PERGAMENSCHIKOV, A.; WILLIAMS, C.; ZHU, S. X.; LONNING, P. E.; BORRESEN-DALE, A.-L.; BROWN, P. O. & BOTSTEIN, D. 2000. Molecular Portraits of Human Breast Tumours. *Nature,* 406**,** 747-52.

PERRY, S. W.; NORMAN, J. P.; BARBIERI, J.; BROWN, E. B. & GELBARD, H. A. 2011. Mitochondrial Membrane Potential Probes and the Proton Gradient: A Practical Usage Guide. *Biotechniques,* 50**,** 98-115.

PIKE, M. C.; GERKINS, V. R.; CASAGRANDE, J. T.; GRAY, G. E.; BROWN, J. & HENDERSON, B. E. 1979. The Hormonal Basis of Breast Cancer. *Natl Cancer Inst Monogr***,** 187-93.

PIPER, R. C. & KATZMANN, D. J. 2007. Biogenesis and Function of Multivesicular Bodies. *Annu Rev Cell Dev Biol,* 23**,** 519.

PLENDERLEITH, I. H. 1990. Treating the Treatment: Toxicity of Cancer Chemotherapy. *Can Fam Physician,* 36**,** 1827.

PORTER, A. G. & JÄNICKE, R. U. 1999. Emerging Roles of Caspase-3 in Apoptosis. *Cell Death Differ,* 6**,** 99-104.

PRESS, M. F.; BERNSTEIN, L.; THOMAS, P. A.; MEISNER, L. F.; ZHOU, J. Y.; MA, Y.; HUNG, G.; ROBINSON, R. A.; HARRIS, C.; EL-NAGGAR, A.; SLAMON, D. J.; PHILLIPS, R. N.; ROSS, J. S.; WOLMAN, S. R. & FLOM, K. J. 1997. Her-2/Neu Gene Amplification Characterized by Fluorescence in Situ Hybridization: Poor Prognosis in Node-Negative Breast Carcinomas. *J Clin Oncol,* 15**,** 2894-904.

RAEZ, L. E.; PAPADOPOULOS, K.; RICART, A. D.; CHIOREAN, E. G.; DIPAOLA, R. S.; STEIN, M. N.; LIMA, C. M. R.; SCHLESSELMAN, J. J.; TOLBA, K. & LANGMUIR, V. K. 2013. A Phase I Dose-Escalation Trial of 2-Deoxy-D-Glucose Alone or Combined with Docetaxel in Patients with Advanced Solid Tumors. *Cancer Chemother Pharmacol,* 71**,** 523-30.

RAJKUMAR, S. V.; BLOOD, E.; VESOLE, D.; FONSECA, R. & GREIPP, P. R. 2006. Phase Iii Clinical Trial of Thalidomide Plus Dexamethasone Compared with Dexamethasone Alone in Newly

Diagnosed Multiple Myeloma: A Clinical Trial Coordinated by the Eastern Cooperative Oncology Group. *J Clin Oncol,* 24**,** 431-36.

RAK, J.; JOANNE, L. Y.; KLEMENT, G. & KERBEL, R. S. 2000. Oncogenes and Angiogenesis: Signaling Three-Dimensional Tumor Growth. *J Invest Dermatol Symp Proc,* 5**,** 24-33.

RAMOS, A. M. & ALLER, P. 2008. Quercetin Decreases Intracellular Gsh Content and Potentiates the Apoptotic Action of the Antileukemic Drug Arsenic Trioxide in Human Leukemia Cell Lines. *Biochem Pharmacol,* 75**,** 1912-23.

RAO, R.; NIAZI, K.; MOLLAHAN, P.; MAO, X.; CRIPPEN, D.; POKSAY, K.; CHEN, S. & BREDESEN, D. 2006. Coupling Endoplasmic Reticulum Stress to the Cell-Death Program: A Novel HSP90-Independent Role for the Small Chaperone Protein P23. *Cell Death Differ,* 13**,** 415-25.

RAPP, U. R.; GOLDSBOROUGH, M. D.; MARK, G. E.; BONNER, T. I.; GROFFEN, J.; REYNOLDS, F. H. & STEPHENSON, J. R. 1983. Structure and Biological Activity of V-Raf, a Unique Oncogene Transduced by a Retrovirus. *Proc Natl Acad Sci,* 80**,** 4218-22.

REDDEL, R. R.; MURPHY, L. C.; HALL, R. E. & SUTHERLAND, R. L. 1985. Differential Sensitivity of Human Breast Cancer Cell Lines to the Growth-Inhibitory Effects of Tamoxifen. *Cancer Res,* 45**,** 1525-31.

REEF, S.; ZALCKVAR, E.; SHIFMAN, O.; BIALIK, S.; SABANAY, H.; OREN, M. & KIMCHI, A. 2006. A Short Mitochondrial Form of P19ARF Induces Autophagy and Caspase-Independent Cell Death. *Mol Cell,* 22**,** 463-75.

REERS, M.; SMITH, T. W. & CHEN, L. B. 1991. J-Aggregate Formation of a Carbocyanine as a Quantitative Fluorescent Indicator of Membrane Potential. *Biochem,* 30**,** 4480-86.

REMPEL, A.; MATHUPALA, S. P.; GRIFFIN, C. A.; HAWKINS, A. L. & PEDERSEN, P. L. 1996. Glucose Catabolism in Cancer Cells: Amplification of the Gene Encoding Type II Hexokinase. *Cancer Res,* 56**,** 2468-71.

REPSOLD, L.; MQOCO, T.; WOLMARANS, E.; NKANDEU, S.; THERON, J.; PIORKOWSKI, T.; DU TOIT, P.; VAN PAPENDORP, D. & JOUBERT, A. M. 2014a. Ultrastructural Changes of Erythrocytes in Whole Blood after Exposure to Prospective in Silico-Designed Anticancer Agents: A Qualitative Case Study. *Biol Res,* 47**,** 39.

REPSOLD, L.; PRETORIUS, E. & JOUBERT, A. M. 2014b. An Estrogen Analogue and Promising Anticancer Agent Refrains from Inducing Morphological Damage and Reactive Oxygen Species Generation in Erythrocytes, Fibrin and Platelets: A Pilot Study. *Cancer Cell Int,* 14**,** 48.

REYNOLDS, E. S. 1963. The Use of Lead Citrate at High Ph as an Electron-Opaque Stain in Electron Microscopy. *J Cell Biol,* 17**,** 208-12.

RIEBER, M. & STRASBERG-RIEBER, M. 2014. P53 Inactivation Decreases Dependence on Estrogen/ERK Signalling for Proliferation but Promotes EMT and Susceptility to 3-Bromopyruvate in ERα+ Breast Cancer MCF-7 Cells. *Biochem Pharmacol,* 88**,** 169-77.

RIEDINGER, H.-J.; GEKELER, V. & PROBST, H. 1992. Reversible Shutdown of Replicon Initiation by Transient Hypoxia in Ehrlich Ascites Cells. *Eur J Biochem,* 210**,** 389-98.

RIGANTI, C.; MINI, E. & NOBILI, S. 2015. Editorial: "Multidrug Resistance in Cancer: Pharmacological Strategies from Basic Research to Clinical Issues". *Front Oncol,* 5.

RISAU, W. & FLAMME, I. 1995. Vasculogenesis. *Annu Rev Cell Dev Biol,* 11**,** 73-91.

RIVENZON-SEGAL, D.; BOLDIN-ADAMSKY, S.; SEGER, D.; SEGER, R. & DEGANI, H. 2003. Glycolysis and Glucose Transporter 1 as Markers of Response to Hormonal Therapy in Breast Cancer. *Int J Cancer,* 107**,** 177-82.

RIZZIERI, D. A.; FELDMAN, E.; DIPERSIO, J. F.; GABRAIL, N.; STOCK, W.; STRAIR, R.; RIVERA, V. M.; ALBITAR, M.; BEDROSIAN, C. L. & GILES, F. J. 2008. A Phase 2 Clinical Trial of Deforolimus (AP23573, MK-8669), a Novel Mammalian Target of Rapamycin Inhibitor, in Patients with Relapsed or Refractory Hematologic Malignancies. *Clin Cancer Res,* 14**,** 2756-62.

ROGERS, S.; MACHEDA, M. L.; DOCHERTY, S. E.; CARTY, M. D.; HENDERSON, M. A.; SOELLER, W. C.; GIBBS, E. M.; JAMES, D. E. & BEST, J. D. 2002. Identification of a Novel Glucose Transporter-Like Protein—GLUT-12. *Am J Physiol Endocrinol Metab,* 282**,** E733-E38.

ROSBE, K. W.; BRANN, T. W.; HOLDEN, S. A.; TEICHER, B. A. & FREI III, E. 1989. Effect of Lonidamine on the Cytotoxicity of Four Alkylating Agents in Vitro. *Cancer Chemother Pharmacol,* 25**,** 32-36.

ROSS, J. A. & KASUM, C. M. 2002. Dietary Flavonoids: Bioavailability, Metabolic Effects, and Safety. *Annu Rev Nutr,* 22**,** 19-34.

ROSS, J. S.; FLETCHER, J. A.; LINETTE, G. P.; STEC, J.; CLARK, E.; AYERS, M.; SYMMANS, W. F.; PUSZTAI, L. & BLOOM, K. J. 2003. The Her-2/Neu Gene and Protein in Breast Cancer 2003: Biomarker and Target of Therapy. *Oncologist,* 8**,** 307-25.

ROSSE, T.; OLIVIER, R.; MONNEY, L.; RAGER, M.; CONUS, S.; FELLAY, I.; JANSEN, B. & BORNER, C. 1998. Bcl-2 Prolongs Cell Survival after Bax-Induced Release of Cytochrome C. *Nature,* 391**,** 496-99.

ROTHMAN, J. E. & WIELAND, F. T. 1996. Protein Sorting by Transport Vesicles. *Science,* 272**,** 227+.

RUIZ-GARCIA, A.; BERMEJO, M.; MOSS, A. & CASABO, V. G. 2008. Pharmacokinetics in Drug Discovery. *J Pharm Sci,* 97**,** 654-90.

RULEY, H. E. 1983. Adenovirus Early Region 1a Enables Viral and Cellular Transforming Genes to Transform Primary Cells in Culture. *Nature,* 304**,** 602-06.

RYAN, H. E.; LO, J. & JOHNSON, R. S. 1998. HIF-1α Is Required for Solid Tumor Formation and Embryonic Vascularization. *EMBO J,* 17**,** 3005-15.

SAGER, R.; TANAKA, K.; LAU, C. C.; EBINA, Y. & ANISOWICZ, A. 1983. Resistance of Human Cells to Tumorigenesis Induced by Cloned Transforming Genes. *Proc Natl Acad Sci,* 80**,** 7601-05.

SALAMA, S. A.; KAMEL, M. W.; BOTTING, S.; SALIH, S. M.; BORAHAY, M. A.; HAMED, A. A.; KILIC, G. S.; SAEED, M.; WILLIAMS, M. Y. & DIAZ-ARRASTIA, C. R. 2009. Catechol-O-Methyltransferase Expression and 2-Methoxyestradiol Affect Microtubule Dynamics and Modify Steroid Receptor Signaling in Leiomyoma Cells. *PloS one,* 4**,** e7356.

SAMBO, L.; DANGOU, J.; ADEBAMOWO, C.; ALBRECHT, C.; GOMBÉ-MBALAWA, C.; NGOMA, T.; MOETI, M. & SAMBO, B. 2012. Cancer in Africa: A Preventable Public Health Crisis. *African Journal of Cancer,* 4**,** 127-36.

SANCHEZ-ALCAZAR, J.; AULT, J.; KHODJAKOV, A. & SCHNEIDER, E. 2000. Increased Mitochondrial Cytochrome C Levels and Mitochondrial Hyperpolarization Precede Camptothecin-Induced Apoptosis in Jurkat Cells. *Cell Death Differ,* 7**,** 1090-100.

SANDLER, A.; GRAY, R.; PERRY, M. C.; BRAHMER, J.; SCHILLER, J. H.; DOWLATI, A.; LILENBAUM, R. & JOHNSON, D. H. 2006. Paclitaxel–Carboplatin Alone or with Bevacizumab for Non–Small-Cell Lung Cancer. *N Engl J Med,* 355**,** 2542-50.

SAOTOME, K.; MORITA, H. & UMEDA, M. 1989. Cytotoxicity Test with Simplified Crystal Violet Staining Method Using Microtitre Plates and Its Application to Injection Drugs. *Toxicol in Vitro,* 3**,** 317-21.

SATTLER, M.; QUINNAN, L. R.; PRIDE, Y. B.; GRAMLICH, J. L.; CHU, S. C.; EVEN, G. C.; KRAEFT, S.-K.; CHEN, L. B. & SALGIA, R. 2003. 2-Methoxyestradiol Alters Cell Motility, Migration, and Adhesion. *Blood,* 102**,** 289-96.

SCAFFIDI, C.; FULDA, S.; SRINIVASAN, A.; FRIESEN, C.; LI, F.; TOMASELLI, K. J.; DEBATIN, K. M.; KRAMMER, P. H. & PETER, M. E. 1998. Two CD95 (APO-1/Fas) Signaling Pathways. *EMBO J,* 17**,** 1675-87.

SCHAAPVELD, M.; VISSER, O.; LOUWMAN, M. J.; DE VRIES, E. G. E.; WILLEMSE, P. H. B.; OTTER, R.; VAN DER GRAAF, W. T. A.; COEBERGH, J.-W. W. & VAN LEEUWEN, F. E. 2008. Risk of New Primary Nonbreast Cancers after Breast Cancer Treatment: A Dutch Population-Based Study. *J Clin Oncol,* 26**,** 1239-46.

SCHAEFER, N. G.; GESCHWIND, J. F.; ENGLES, J.; BUCHANAN, J. W. & WAHL, R. L. 2012. Systemic Administration of 3-Bromopyruvate in Treating Disseminated Aggressive Lymphoma. *Transl Res,* 159**,** 51-57.

SCHENDEL, S. L.; XIE, Z.; MONTAL, M. O.; MATSUYAMA, S.; MONTAL, M. & REED, J. C. 1997. Channel Formation by Antiapoptotic Protein Bcl-2. *Proc Natl Acad Sci,* 94**,** 5113-18.

SCHERZ-SHOUVAL, R. & ELAZAR, Z. 2007. Ros, Mitochondria and the Regulation of Autophagy. *Trends Cell Biol,* 17**,** 422-27.

SCHIMMER, A. D.; THOMAS, M. P.; HURREN, R.; GRONDA, M.; PELLECCHIA, M.; POND, G. R.; KONOPLEVA, M.; GURFINKEL, D.; MAWJI, I. A.; BROWN, E. & REED, J. C. 2006. Identification of Small Molecules That Sensitize Resistant Tumor Cells to Tumor Necrosis Factor-Family Death Receptors. *Cancer Res,* 66**,** 2367-75.

SCHLEICHER, S. M.; MORETTI, L.; VARKI, V. & LU, B. 2010. Progress in the Unraveling of the Endoplasmic Reticulum Stress/Autophagy Pathway and Cancer: Implications for Future Therapeutic Approaches. *Drug Resist Update,* 13**,** 79-86.

SCHMITT, C. A. 2003. Senescence, Apoptosis and Therapy—Cutting the Lifelines of Cancer. *Nat Rev Cancer,* 3**,** 286-95.

SCHOLL, S.; BEUZEBOC, P. & POUILLART, P. 2001. Targeting Her2 in Other Tumor Types. *Ann Oncol,* 12**,** S81-S87.

SCHORNACK, P. A. & GILLIES, R. J. 2003. Contributions of Cell Metabolism and H+ Diffusion to the Acidic Ph of Tumors. *Neoplasia,* 5**,** 135-45.

SCHUMACHER, G.; KATAOKA, M.; ROTH, J. A. & MUKHOPADHYAY, T. 1999. Potent Antitumor Activity of 2-Methoxyestradiol in Human Pancreatic Cancer Cell Lines. *Clin Cancer Res,* 5**,** 493-99.

SCHWARTZ, D. L.; RAJENDRAN, J.; YUEH, B. & ET AL. 2004. FDG-Pet Prediction of Head and Neck Squamous Cell Cancer Outcomes. *Arch Otolaryngol Head Neck Surg,* 130**,** 1361-67.

SCHWARZBACH, M. H.; HINZ, U.; DIMITRAKOPOULOU-STRAUSS, A.; WILLEKE, F.; CARDONA, S.; MECHTERSHEIMER, G.; LEHNERT, T.; STRAUSS, L. G.; HERFARTH, C. & BÜCHLER, M. W. 2005. Prognostic Significance of Preoperative [18-F] Fluorodeoxyglucose (FDG) Positron Emission Tomography (Pet) Imaging in Patients with Resectable Soft Tissue Sarcomas. *Ann Surg,* 241**,** 286.

SCHWEICHEL, J. U. & MERKER, H. J. 1973. The Morphology of Various Types of Cell Death in Prenatal Tissues. *Teratology,* 7**,** 253-66.

SEEGERS, J. C.; AVELING, M.-L.; VAN ASWEGEN, C. H.; CROSS, M.; KOCH, F. & JOUBERT, W. S. 1989. The Cytotoxic Effects of Estradiol-17β, Catecholestradiols and Methoxyestradiols on Dividing MCF-7 and HeLa Cells. *J Steroid Biochem,* 32**,** 797-809.

SEEGERS, J. C.; LOTTERING, M.-L.; GROBLER, C. J. S.; VAN PAPENDORP, D. H.; HABBERSETT, R. C.; SHOU, Y. & LEHNERT, B. E. 1997. The Mammalian Metabolite, 2-Methoxyestradiol, Affects P53 Levels and Apoptosis Induction in Transformed Cells but Not in Normal Cells. *J Steroid Biochem Mol Biol,* 62**,** 253-67.

SEMENZA, G. L. 2009. Defining the Role of Hypoxia-Inducible Factor 1 in Cancer Biology and Therapeutics. *Oncogene,* 29**,** 625-34.

SEMENZA, G. L. 2015. The Hypoxic Tumor Microenvironment: A Driving Force for Breast Cancer Progression. *BBA - Mol Cell Res,* DOI: 10.1016/j.bbamcr.2015.05.036.

SENDOEL, A. & HENGARTNER, M. O. 2014. Apoptotic Cell Death under Hypoxia. *Physiology,* 29**,** 168-76.

SERRAINO, D. 1999. The Spectrum of AIDS-Associated Cancers in Africa. *Aids,* 13**,** 2589-90.

SESHADRI, R.; FIRGAIRA, F. A.; HORSFALL, D. J.; MCCAUL, K.; SETLUR, V. & KITCHEN, P. 1993. Clinical Significance of Her-2/Neu Oncogene Amplification in Primary Breast Cancer. The South Australian Breast Cancer Study Group. *J Clin Oncol,* 11**,** 1936-42.

SGADARI, C.; BARILLARI, G.; TOSCHI, E.; CARLEI, D.; BACIGALUPO, I.; BACCARINI, S.; PALLADINO, C.; LEONE, P.; BUGARINI, R.; MALAVASI, L.; CAFARO, A.; FALCHI, M.; VALDEMBRI, D.; REZZA, G.; BUSSOLINO, F.; MONINI, P. & ENSOLI, B. 2002. HIV Protease Inhibitors Are Potent Anti-Angiogenic Molecules and Promote Regression of Kaposi Sarcoma. *Nat Med,* 8**,** 225-32.

SGADARI, C.; MONINI, P.; BARILLARI, G. & ENSOLI, B. 2003. Use of HIV Protease Inhibitors to Block Kaposi's Sarcoma and Tumour Growth. *Lancet Oncol,* 4**,** 537-47.

SHAPIRO, S. 1997. Periodic Screening for Breast Cancer: The HIP Randomized Controlled Trial. *JNCI Monographs,* 1997**,** 27-30.

SHI, X. & WANG, L. 2012. Treatment for Triple-Negative Breast Cancer. *Chin Ger J Clin Oncol,* 11**,** 539-43.

SHINTANI, T. & KLIONSKY, D. J. 2004. Autophagy in Health and Disease: A Double-Edged Sword. *Science,* 306**,** 990-95.

SIEGEL, R. L.; MILLER, K. D. & JEMAL, A. 2015. Cancer Statistics, 2015. *CA: Cancer J Clin,* 65**,** 5-29.

SIMONE, N. D.; SANTIS, M. D.; TAMBURRINI, E.; NICUOLO, F. D.; LUCIA, M. B.; RICCARDI, P.; D'IPPOLITO, S.; CAUDA, R. & CARUSO, A. 2007. Effects of Antiretroviral Therapy on Tube-Like Network Formation of Human Endothelial Cells. *Biol Pharm Bull,* 30**,** 982-84.

SINGH, D.; BANERJI, A. K.; DWARAKANATH, B. S.; TRIPATHI, R. P.; GUPTA, J. P.; MATHEW, T. L.; RAVINDRANATH, T. & JAIN, V. 2005. Optimizing Cancer Radiotherapy with 2-Deoxy-D-Glucose. *Strahlenther Onkol,* 181**,** 507-14.

SINGHAL, S.; MEHTA, J.; DESIKAN, R.; AYERS, D.; ROBERSON, P.; EDDLEMON, P.; MUNSHI, N.; ANAISSIE, E.; WILSON, C.; DHODAPKAR, M.; ZELDIS, J.; SIEGEL, D.; CROWLEY, J. & BARLOGIE, B. 1999. Antitumor Activity of Thalidomide in Refractory Multiple Myeloma. *N Engl J Med,* 341**,** 1565-71.

SLAMON, D. J.; CLARK, G. M.; WONG, S. G.; LEVIN, W. J.; ULLRICH, A. & MCGUIRE, W. L. 1987. Human Breast Cancer: Correlation of Relapse and Survival with Amplification of the Her-2/Neu Oncogene. *Science,* 235**,** 177-82.

SLAMON, D. J.; LEYLAND-JONES, B.; SHAK, S.; FUCHS, H.; PATON, V.; BAJAMONDE, A.; FLEMING, T.; EIERMANN, W.; WOLTER, J. & PEGRAM, M. 2001. Use of Chemotherapy Plus a Monoclonal Antibody against Her2 for Metastatic Breast Cancer That Overexpresses Her2. *N Engl J Med,* 344**,** 783-92.

SLEE, E. A.; HARTE, M. T.; KLUCK, R. M.; WOLF, B. B.; CASIANO, C. A.; NEWMEYER, D. D.; WANG, H.-G.; REED, J. C.; NICHOLSON, D. W. & ALNEMRI, E. S. 1999. Ordering the Cytochrome C–Initiated Caspase Cascade: Hierarchical Activation of Caspases-2,-3,-6,-7,-8, and-10 in a Caspase-9–Dependent Manner. *J Cell Biol,* 144**,** 281-92.

SPUGNINI, E. P.; ESPOSITO, V.; GROEGER, A. M.; CASSANDRO, R.; ONORI, N.; CHIRIANNI, A. & BALDI, A. 2006. Effects of Indinavir in a Preliminary Phase I Study on Dogs with Stage Iii Slenic Hemangiosarcoma. *In Vivo,* 20**,** 125-27.

STANDER, A.; JOUBERT, F. & JOUBERT, A. 2011. Docking, Synthesis, and in Vitro Evaluation of Antimitotic Estrone Analogs. *Chem Biol Drug Des,* 77**,** 173-81.

STANDER, B. A.; JOUBERT, F.; TU, C.; SIPPEL, K. H.; MCKENNA, R. & JOUBERT, A. M. 2012. In Vitro Evaluation of ESE-15-OL, an Estradiol Analogue with Nanomolar Antimitotic and Carbonic Anhydrase Inhibitory Activity. *PloS one,* 7**,** e52205.

STANDER, B. A.; JOUBERT, F.; TU, C.; SIPPEL, K. H.; MCKENNA, R. & JOUBERT, A. M. 2013. Signaling Pathways of ESE-16, an Antimitotic and Anticarbonic Anhydrase Estradiol Analog, in Breast Cancer Cells. *PloS one,* 8**,** e53853.

STATON, C. A.; REED, M. W. & BROWN, N. J. 2009. A Critical Analysis of Current in Vitro and in Vivo Angiogenesis Assays. *Int J Exp Pathol,* 90**,** 195-221.

STENNICKE, H. R. & SALVESEN, G. S. 1999. Caspase Assays. *Methods Enzymol,* 322**,** 91-100.

STEVENSON, M. & VOLSKY, D. J. 1986. Activated V-Myc and V-Ras Oncogenes Do Not Transform Normal Human Lymphocytes. *Mol Cell Biol,* 6**,** 3410-17.

STEWART, E. A. & NOWAK, R. A. 1996. Leiomyoma-Related Bleeding: A Classic Hypothesis Updated for the Molecular Era. *Hum Reprod Update,* 2**,** 295-306.

SUI, D. & WILSON, J. E. 1997. Structural Determinants for the Intracellular Localization of the Isozymes of Mammalian Hexokinase: Intracellular Localization of Fusion Constructs Incorporating Structural Elements from the Hexokinase Isozymes and the Green Fluorescent Protein. *Arch Biochem Biophys,* 345**,** 111-25.

SUOLINNA, E.-M.; BUCHSBAUM, R. N. & RACKER, E. 1975. The Effect of Flavonoids on Aerobic Glycolysis and Growth of Tumor Cells. *Cancer Res,* 35**,** 1865-72.

SUTER, T. M.; PROCTER, M.; VAN VELDHUISEN, D. J.; MUSCHOLL, M.; BERGH, J.; CARLOMAGNO, C.; PERREN, T.; PASSALACQUA, R.; BIGHIN, C.; KLIJN, J. G. M.; AGEEV, F. T.; HITRE, E.; GROETZ, J.; IWATA, H.; KNAP, M.; GNANT, M.; MUEHLBAUER, S.; SPENCE, A.; GELBER, R. D. & PICCART-GEBHART, M. J. 2007. Trastuzumab-Associated Cardiac Adverse Effects in the Herceptin Adjuvant Trial. *J Clin Oncol,* 25**,** 3859-65.

SUTHERLAND, R. L.; HALL, R. E. & TAYLOR, I. W. 1983. Cell Proliferation Kinetics of MCF-7 Human Mammary Carcinoma Cells in Culture and Effects of Tamoxifen on Exponentially Growing and Plateau-Phase Cells. *Cancer Res,* 43**,** 3998-4006.

SUZUKI, Y.; IMAI, Y.; NAKAYAMA, H.; TAKAHASHI, K.; TAKIO, K. & TAKAHASHI, R. 2001. A Serine Protease, HTRA2, Is Released from the Mitochondria and Interacts with XIAP, Inducing Cell Death. *Mol Cell,* 8**,** 613-21.

SWEENEY, C.; LIU, G.; YIANNOUTSOS, C.; KOLESAR, J.; HORVATH, D.; STAAB, M. J.; FIFE, K.; ARMSTRONG, V.; TRESTON, A. & SIDOR, C. 2005. A Phase II Multicenter, Randomized, Double-Blind, Safety Trial Assessing the Pharmacokinetics, Pharmacodynamics, and Efficacy of Oral 2-Methoxyestradiol Capsules in Hormone-Refractory Prostate Cancer. *Clin Cancer Res,* 11**,** 6625-33.

SZABADKAI, G. & DUCHEN, M. 2010. Roles of Mitochondria in Human Disease. *Essays Biochem,* 47.

TALANIAN, R. V.; QUINLAN, C.; TRAUTZ, S.; HACKETT, M. C.; MANKOVICH, J. A.; BANACH, D.; GHAYUR, T.; BRADY, K. D. & WONG, W. W. 1997. Substrate Specificities of Caspase Family Proteases. *J Biol Chem,* 272**,** 9677-82.

TAN, W.-F.; LIN, L.-P.; LI, M.-H.; ZHANG, Y.-X.; TONG, Y.-G.; XIAO, D. & DING, J. 2003. Quercetin, a Dietary-Derived Flavonoid, Possesses Antiangiogenic Potential. *Eur J Pharmacol,* 459**,** 255-62.

TANAKA, K.; IWAMOTO, S.; GON, G.; NOHARA, T.; IWAMOTO, M. & TANIGAWA, N. 2000. Expression of Survivin and Its Relationship to Loss of Apoptosis in Breast Carcinomas. *Clin Cancer Res,* 6**,** 127-34.

TANG, S.-W.; DUCROUX, A.; JEANG, K.-T. & NEUVEUT, C. 2012. Impact of Cellular Autophagy on Viruses: Insights from Hepatitis B Virus and Human Retroviruses. *J. Biomed. Sci,* 19**,** 92.

TAYLOR, J. P.; TANAKA, F.; ROBITSCHEK, J.; SANDOVAL, C. M.; TAYE, A.; MARKOVIC-PLESE, S. & FISCHBECK, K. H. 2003. Aggresomes Protect Cells by Enhancing the Degradation of Toxic Polyglutamine-Containing Protein. *Hum Mol Gen,* 12**,** 749-57.

TEICHER, B. A.; SOTOMAYOR, E. A. & HUANG, Z. D. 1992. Antiangiogenic Agents Potentiate Cytotoxic Cancer Therapies against Primary and Metastatic Disease. *Cancer Res,* 52**,** 6702-04.

TEVAARWERK, A. J.; HOLEN, K. D.; ALBERTI, D. B.; SIDOR, C.; ARNOTT, J.; QUON, C.; WILDING, G. & LIU, G. 2009. Phase I Trial of 2-Methoxyestradiol Nanocrystal Dispersion in Advanced Solid Malignancies. *Clin Cancer Res,* 15**,** 1460-65.

TEWARI, M.; QUAN, L. T.; O'ROURKE, K.; DESNOYERS, S.; ZENG, Z.; BEIDLER, D. R.; POIRIER, G. G.; SALVESEN, G. S. & DIXIT, V. M. 1995. YAMA/CPP32β, a Mammalian Homolog of CED-3, Is a Crma-Inhibitable Protease That Cleaves the Death Substrate Poly(ADP-Ribose) Polymerase. *Cell,* 81**,** 801-09.

THERON, A. E.; NOLTE, E. M.; LAFANECHÈRE, L. & JOUBERT, A. M. 2013. Molecular Crosstalk between Apoptosis and Autophagy Induced by a Novel 2-Methoxyestradiol Analogue in Cervical Adenocarcinoma Cells. *Cancer Cell Int,* 13**,** 87.

THOMPSON, E. W.; NAKAMURA, S.; SHIMA, T. B.; MELCHIORI, A.; MARTIN, G. R.; ZAKI SALAHUDDIN, S.; GALLO, R. C. & ALBINI, A. 1991. Supernatants of Acquired Immunodeficiency Syndrome-Related Kaposi's Sarcoma Cells Induce Endothelial Cell Chemotaxis and Invasiveness. *Cancer Res,* 51**,** 2670-76.

TINLEY, T. L.; LEAL, R. M.; RANDALL-HLUBEK, D. A.; CESSAC, J. W.; WILKENS, L. R.; RAO, P. N. & MOOBERRY, S. L. 2003. Novel 2-Methoxyestradiol Analogues with Antitumor Activity. *Cancer Res,* 63**,** 1538-49.

TREMPE, G. & FOGH, J. 1973. Variation in Characteristics of Human Tumor-Cell Lines Derived from Similar Tumors. *In Vitro-Journal Of The Tissue Culture Association,* 8**,** 433-&.

TSAO, H.; GOEL, V.; WU, H.; YANG, G. & HALUSKA, F. G. 2004. Genetic Interaction between NRAS and BRAF Mutations and PTEN/MMAC1 Inactivation in Melanoma. *J Invest Dermatol,* 122**,** 337-41.

TSUJIMOTO, Y. & SHIMIZU, S. 2007. Role of the Mitochondrial Membrane Permeability Transition in Cell Death. *Apoptosis,* 12**,** 835-40.

TSUKAMOTO, A.; KANEKO, Y.; YOSHIDA, T.; HAN, K.; ICHINOSE, M. & KIMURA, S. 1998. 2-Methoxyestradiol, an Endogenous Metabolite of Estrogen, Enhances Apoptosis and B-Galactosidase Expression in Vascular Endothelial Cells. *Biochem Biophys Res Comm,* 248**,** 9-12.

TSURUO, T.; IIDA, H.; TSUKAGOSHI, S. & SAKURAI, Y. 1981. Overcoming of Vincristine Resistance in P388 Leukemia in Vivo and in Vitro through Enhanced Cytotoxicity of Vincristine and Vinblastine by Verapamil. *Cancer Res,* 41**,** 1967-72.

TSURUO, T.; IIDA, H.; TSUKAGOSHI, S. & SAKURAI, Y. 1982. Increased Accumulation of Vincristine and Adriamycin in Drug-Resistant P388 Tumor Cells Following Incubation with Calcium Antagonists and Calmodulin Inhibitors. *Cancer Res,* 42**,** 4730-33.

TURRENS, J. F. 2003. Mitochondrial Formation of Reactive Oxygen Species. *J Physiol,* 552**,** 335-44.

TUTT, A.; ROBSON, M.; GARBER, J. E.; DOMCHEK, S. M.; AUDEH, M. W.; WEITZEL, J. N.; FRIEDLANDER, M.; ARUN, B.; LOMAN, N. & SCHMUTZLER, R. K. 2010. Oral Poly (Adp-Ribose) Polymerase Inhibitor Olaparib in Patients with BRCA1 or BRCA2 Mutations and Advanced Breast Cancer: A Proof-of-Concept Trial. *Lancet,* 376**,** 235-44.

TWENTYMAN, P.; FOX, N. & WHITE, D. 1987. Cyclosporin a and Its Analogues as Modifiers of Adriamycin and Vincristine Resistance in a Multi-Drug Resistant Human Lung Cancer Cell Line. *Br J Cancer,* 56**,** 55.

VALAGUSSA, P.; BONADONNA, G. & VERONESI, U. 1978. Patterns of Relapse and Survival Following Radical Mastectomy. Analysis of 716 Consecutive Patients. *Cancer,* 41**,** 1170-78.

VAN TONDER, A.; JOUBERT, A. M. & CROMARTY, A. D. 2015. Limitations of the 3-(4, 5-Dimethylthiazol-2-Yl)-2, 5-Diphenyl-2h-Tetrazolium Bromide (MTT) Assay When Compared to Three Commonly Used Cell Enumeration Assays. *BMC Res Notes,* 8**,** 47.

VAN TONDER, J. J.; GULUMIAN, M.; CROMARTY, A. D. & STEENKAMP, V. 2014. In Vitro Effect of N-Acetylcysteine on Hepatocyte Injury Caused by Dichlorodiphenyltrichloroethane and Its Metabolites. *Hum Exp Toxicol,* 33**,** 41-53.

VAN TONDER, J. J.; GULUMIAN, M. & STEENKAMP, V. 2013. *Pre-Clinical Assessment of the Potential Intrinsic Hepatotoxicity of Candidate Drugs*, INTECH Open Access Publisher.

VANAJA, S. K.; RATHINAM, V. A. K. & FITZGERALD, K. A. 2015. Mechanisms of Inflammasome Activation: Recent Advances and Novel Insights. *Trends Cell Biol,* 25**,** 308-15.

VANDER HEIDEN, M. G.; CHANDEL, N. S.; SCHUMACKER, P. T. & THOMPSON, C. B. 1999. Bcl-Xl Prevents Cell Death Following Growth Factor Withdrawal by Facilitating Mitochondrial Atp/Adp Exchange. *Mol Cell,* 3**,** 159-67.

VANDER HEIDEN, M. G.; CHANDEL, N. S.; WILLIAMSON, E. K.; SCHUMACKER, P. T. & THOMPSON, C. B. 1997. Bcl-XL Regulates the Membrane Potential and Volume Homeostasis of Mitochondria. *Cell,* 91**,** 627-37.

VANDER HEIDEN, M. G. & THOMPSON, C. B. 1999. Bcl-2 Proteins: Regulators of Apoptosis or of Mitochondrial Homeostasis? *Nat Cell Biol,* 1**,** E209-E16.

VENNSTROM, B.; SHEINESS, D.; ZABIELSKI, J. & BISHOP, J. M. 1982. Isolation and Characterization of C-Myc, a Cellular Homolog of the Oncogene (V-Myc) of Avian Myelocytomatosis Virus Strain 29. *J Virol,* 42**,** 773-79.

VERA, J. C.; REYES, A. M.; VELÁSQUEZ, F. V.; RIVAS, C. I.; ZHANG, R. H.; STROBEL, P.; SLEBE, J. C.; NÚÑEZ-ALARCÓN, J. & GOLDE, D. W. 2001. Direct Inhibition of the Hexose Transporter GLUT1 by Tyrosine Kinase Inhibitors. *Biochem,* 40**,** 777-90.

VERGARAJAUREGUI, S.; CONNELLY, P. S.; DANIELS, M. P. & PUERTOLLANO, R. 2008. Autophagic Dysfunction in Mucolipidosis Type IV Patients. *Hum Mol Gen,* 17**,** 2723-37.

VERHAGEN, A. M.; EKERT, P. G.; PAKUSCH, M.; SILKE, J.; CONNOLLY, L. M.; REID, G. E.; MORITZ, R. L.; SIMPSON, R. J. & VAUX, D. L. 2000. Identification of Diablo, a Mammalian Protein That Promotes Apoptosis by Binding to and Antagonizing IAP Proteins. *Cell,* 102**,** 43-53.

VERMA, N. K. & ROSHAN, A. 2015. Liposomes: A Targeted Drug Delivery System- a Review. *Acta Med Sci,* 2**,** 6.

VERONESI, U.; CASCINELLI, N.; MARIANI, L.; GRECO, M.; SACCOZZI, R.; LUINI, A.; AGUILAR, M. & MARUBINI, E. 2002. Twenty-Year Follow-up of a Randomized Study Comparing Breast-Conserving Surgery with Radical Mastectomy for Early Breast Cancer. *N Engl J Med,* 347**,** 1227-32.

VERONESI, U.; SACCOZZI, R.; DEL VECCHIO, M.; BANFI, A.; CLEMENTE, C.; DE LENA, M.; GALLUS, G.; GRECO, M.; LUINI, A.; MARUBINI, E.; MUSCOLINO, G.; RILKE, F.; SALVADORI, B.; ZECCHINI, A. & ZUCALI, R. 1981. Comparing Radical Mastectomy with Quadrantectomy, Axillary Dissection, and Radiotherapy in Patients with Small Cancers of the Breast. *N Engl J Med,* 305**,** 6-11.

VICHAI, V. & KIRTIKARA, K. 2006. Sulforhodamine B Colorimetric Assay for Cytotoxicity Screening. *Nat Protoc,* 1**,** 1112-6.

VIJAYANATHAN, V.; VENKITESWARAN, S.; NAIR, S. K.; VERMA, A.; THOMAS, T.; ZHU, B. T. & THOMAS, T. 2006. Physiologic Levels of 2-Methoxyestradiol Interfere with Nongenomic Signaling of 17β-Estradiol in Human Breast Cancer Cells. *Clin Cancer Res,* 12**,** 2038-48.

VODUC, K. D.; CHEANG, M. C. U.; TYLDESLEY, S.; GELMON, K.; NIELSEN, T. O. & KENNECKE, H. 2010. Breast Cancer Subtypes and the Risk of Local and Regional Relapse. *J Clin Oncol,* 28**,** 1684-91.

WALLACE, K. & STARKOV, A. 2000. Mitochondrial Targets of Drug Toxicity. *Annu Rev Pharmacol Toxicol,* 40**,** 353-88.

WANEBO, C. K.; JOHNSON, K. G.; SATO, K. & THORSLUND, T. W. 1968. Breast Cancer after Exposure to the Atomic Bombings of Hiroshima and Nagasaki. *N Engl J Med,* 279**,** 667-71.

WANG, C. & KURZER, M. S. 1997. Phytoestrogen Concentration Determines Effects on DNA Synthesis in Human Breast Cancer Cells. *Nutr Cancer,* 28**,** 236-47.

WANG, K.; LIU, R.; LI, J.; MAO, J.; LEI, Y.; WU, J.; ZENG, J.; ZHANG, T.; WU, H.; CHEN, L.; HUANG, C. & WEI, Y. 2011. Quercetin Induces Protective Autophagy in Gastric Cancer Cells: Involvement of AKT-MTOR- and Hypoxia-Induced Factor 1α-Mediated Signaling. *Autophagy,* 7**,** 966-78.

WANG, R.; WANG, X.; LI, B.; LIN, F.; DONG, K.; GAO, P. & ZHANG, H.-Z. 2009a. Tumor-Specific Adenovirus-Mediated Puma Gene Transfer Using the Survivin Promoter Enhances Radiosensitivity of Breast Cancer Cells In vitro and In vivo. *Breast Cancer Res Treat,* 117**,** 45-54.

WANG, X.; CHAI, H.; LIN, P. H.; YAO, Q. & CHEN, C. 2009b. Roles and Mechanisms of Human Immunodeficiency Virus Protease Inhibitor Ritonavir and Other Anti-Human

Immunodeficiency Virus Drugs in Endothelial Dysfunction of Porcine Pulmonary Arteries and Human Pulmonary Artery Endothelial Cells. *Am J Pathol,* 174**,** 771-81.

WANG, X.; CHEN, M.; ZHOU, J. & ZHANG, X. 2014. HSP27, 70 and 90, Anti-Apoptotic Proteins, in Clinical Cancer Therapy *Int J Oncol,* 45**,** 18-30.

WARBURG, O.; POSENER, K. & NEGELEIN, E. 1924. Ueber Den Stoffwechsel Der Tumoren. *Biochem Z,* 152**,** 319-44.

WEHNER, E. 2003. PlasDIC, an Innovative Relief Contrast for Routine Observation in Cell Biology. *Imaging Microsc,* 4**,** 23.

WEI, Y.; PATTINGRE, S.; SINHA, S.; BASSIK, M. & LEVINE, B. 2008. JNK1-Mediated Phosphorylation of Bcl-2 Regulates Starvation-Induced Autophagy. *Mol Cell,* 30**,** 678-88.

WEIDNER, N.; CARROLL, P.; FLAX, J.; BLUMENFELD, W. & FOLKMAN, J. 1993. Tumor Angiogenesis Correlates with Metastasis in Invasive Prostate Carcinoma. *Am J Pathol,* 143**,** 401.

WEIDNER, N.; FOLKMAN, J.; POZZA, F.; BEVILACQUA, P.; ALLRED, E. N.; MOORE, D. H.; MELI, S. & GASPARINI, G. 1992. Tumor Angiogenesis: A New Significant and Independent Prognostic Indicator in Early-Stage Breast Carcinoma. *J Natl Cancer Inst,* 84**,** 1875-87.

WEIGELT, B.; BAEHNER, F. L. & REIS-FILHO, J. S. 2010. The Contribution of Gene Expression Profiling to Breast Cancer Classification, Prognostication and Prediction: A Retrospective of the Last Decade. *J Pathol,* 220**,** 263-80.

WEINBERG, R. A. 1991. Tumor Suppressor Genes. *Science,* 254**,** 1138-46.

WENGER, R. H. 2002. Cellular Adaptation to Hypoxia: O2-Sensing Protein Hydroxylases, Hypoxia-Inducible Transcription Factors, and O2-Regulated Gene Expression. *FASEB J,* 16**,** 1151-62.

WICK, A. N.; DRURY, D. R.; NAKADA, H. I. & WOLFE, J. B. 1957. Localization of the Primary Metabolic Block Produced by 2-Deoxyglucose. *J Biol Chem,* 224**,** 963-69.

WILLINGHAM, M. C. 1999. Cytochemical Methods for the Detection of Apoptosis. *J Histochem Cytochem,* 47**,** 1101-09.

WILSON, J. E. 2003. Isozymes of Mammalian Hexokinase: Structure, Subcellular Localization and Metabolic Function. *J Exp Biol,* 206**,** 2049-57.

WILSON, W. J. & POELLINGER, L. 2002. The Dietary Flavonoid Quercetin Modulates HIF-1α Activity in Endothelial Cells. *Biochem Biophys Res Comm,* 293**,** 446-50.

WIRAPATI, P.; SOTIRIOU, C.; KUNKEL, S.; FARMER, P.; PRADERVAND, S.; HAIBE-KAINS, B.; DESMEDT, C.; IGNATIADIS, M.; SENGSTAG, T. & SCHUTZ, F. 2008. Meta-Analysis of Gene Expression Profiles in Breast Cancer: Toward a Unified Understanding of Breast Cancer Subtyping and Prognosis Signatures. *Breast Cancer Res,* 10**,** R65.

WOLF, S.; BARTON, D.; KOTTSCHADE, L.; GROTHEY, A. & LOPRINZI, C. 2008. Chemotherapy-Induced Peripheral Neuropathy: Prevention and Treatment Strategies. *Eur J Cancer,* 44**,** 1507-15.

WOLMARANS, E.; MQOCO, T. V.; STANDER, A.; NKANDEU, S. D.; SIPPEL, K.; MCKENNA, R. & JOUBERT, A. 2014. Novel Estradiol Analogue Induces Apoptosis and Autophagy in Esophageal Carcinoma Cells. *Cell Mol Biol Lett,* 19**,** 98-115.

WOO, M.; HAKEM, R.; SOENGAS, M. S.; DUNCAN, G. S.; SHAHINIAN, A.; KÄGI, D.; HAKEM, A.; MCCURRACH, M.; KHOO, W. & KAUFMAN, S. A. 1998. Essential Contribution of Caspase 3/CPP32 to Apoptosis and Its Associated Nuclear Changes. *Genes Dev,* 12**,** 806-19.

WOOD, T. E.; DALILI, S.; SIMPSON, C. D.; HURREN, R.; MAO, X.; SAIZ, F. S.; GRONDA, M.; EBERHARD, Y.; MINDEN, M. D. & BILAN, P. J. 2008. A Novel Inhibitor of Glucose Uptake Sensitizes Cells to Fas-Induced Cell Death. *Mol Cancer Ther,* 7**,** 3546-55.

WOOD, T. E.; DALILI, S.; SIMPSON, C. D.; SUKHAI, M. A.; HURREN, R.; ANYIWE, K.; MAO, X.; SAIZ, F. S.; GRONDA, M. & EBERHARD, Y. 2010. Selective Inhibition of Histone Deacetylases Sensitizes Malignant Cells to Death Receptor Ligands. *Mol Cancer Ther,* 9**,** 246-56.

WOOSTER, R.; BIGNELL, G.; LANCASTER, J.; SWIFT, S.; SEAL, S.; MANGION, J.; COLLINS, N.; GREGORY, S.; GUMBS, C.; MICKLEM, G.; BARFOOT, R.; HAMOUDI, R.; PATEL, S.; RICES, C.; BIGGS, P.; HASHIM, Y.; SMITH, A.; CONNOR, F.; ARASON, A.; GUDMUNDSSON, J.; FICENEC, D.; KELSELL, D.; FORD, T. D.; TIMOTHY BISHOP, D.; SPURR, N. K.; PONDER, B. A. J.; EELES, R.; PETO, J.; DEVILEE, P.; CORNELISSE, C.; LYNCH, H.; NAROD, S.; LENOIR, G.; EGILSSON, V.; BJORK BARKADOTTIR, R.; EASTON, D. F.; BENTLEY, D. R.; FUTREAL, P. A.; ASHWORTH, A. & STRATTON, M. R. 1995. Identification of the Breast Cancer Susceptibility Gene BRCA2. *Nature,* 378**,** 789-92.

WYLLIE, A. H.; KERR, J. F. R. & CURRIE, A. R. 1980. Cell Death: The Significance of Apoptosis. *In:* G.H. BOURNE, J. F. D. & JEON, K. W. (eds.) *Int Rev Cytol.* Academic Press.

XIAO-MING, Y. 2000. Signal Transduction Mediated by Bid, a Pro-Death Bcl-2 Family Proteins, Connects the Death Receptor and Mitochondria Apoptosis Pathways. *Cell Res,* 10**,** 161-67.

XU, R.-H.; PELICANO, H.; ZHOU, Y.; CAREW, J. S.; FENG, L.; BHALLA, K. N.; KEATING, M. J. & HUANG, P. 2005. Inhibition of Glycolysis in Cancer Cells: A Novel Strategy to Overcome Drug Resistance Associated with Mitochondrial Respiratory Defect and Hypoxia. *Cancer Res,* 65**,** 613-21.

YANG, C. W.; LI, C.; JUNG, J. Y.; SHIN, S. J.; CHOI, B. S.; LIM, S. W.; SUN, B. K.; KIM, Y. S.; KIM, J.; CHANG, Y. S. & BANG, B. K. 2003. Preconditioning with Erythropoietin Protects against Subsequent Ischemia-Reperfusion Injury in Rat Kidney. *FASEB J,* 17**,** 1754-55.

YANG, J. & LIU, X. 1997. Prevention of Apoptosis by Bcl-2: Release of Cytochrome C from Mitochondria Blocked. *Science,* 275**,** 1129.

YANG, Y.; IKEZOE, T.; TAKEUCHI, T.; ADACHI, Y.; OHTSUKI, Y.; TAKEUCHI, S.; KOEFFLER, H. P. & TAGUCHI, H. 2005. HIV-1 Protease Inhibitor Induces Growth Arrest and Apoptosis of Human Prostate Cancer LNCAP Cells in Vitro and in Vivo in Conjunction with Blockade of Androgen Receptor STAT3 and AKT Signaling. *Cancer Sci,* 96**,** 425-33.

YANG, Z. & KLIONSKY, D. J. 2010. Eaten Alive: A History of Macroautophagy. *Nat Cell Biol,* 12**,** 814-22.

YEH, C. C.; HOU, M. F.; WU, S. H.; TSAI, S. M.; LIN, S. K.; HOU, L. A.; MA, H. & TSAI, L. Y. 2006. A Study of Glutathione Status in the Blood and Tissues of Patients with Breast Cancer. *Cell Biochem Funct,* 24**,** 555-59.

YERUVA, L.; ELEGBEDE, J. A. & CARPER, S. W. 2008. Methyl Jasmonate Decreases Membrane Fluidity and Induces Apoptosis Via Tumor Necrosis Factor Receptor 1 in Breast Cancer Cells. *Anti-cancer Drug,* 19**,** 766-76.

YOSHIDA, M.; SAKAI, T.; HOSOKAWA, N.; MARUI, N.; MATSUMOTO, K.; FUJIOKA, A.; NISHINO, H. & AOIKE, A. 1990. The Effect of Quercetin on Cell Cycle Progression and Growth of Human Gastric Cancer Cells. *FEBS Lett,* 260**,** 10-13.

YOU, J.; HE, Z.; CHEN, L.; DENG, G.; LIU, W.; QIN, L.; QIU, F. & CHEN, X. 2010. CH05-10, a Novel Indinavir Analog, Is a Broad-Spectrum Antitumor Agent That Induces Cell Cycle Arrest, Apoptosis, Endoplasmic Reticulum Stress and Autophagy. *Cancer Sci,* 101**,** 2644-51.

YU, D.; WOLF, J. K.; SCANLON, M.; PRICE, J. E. & HUNG, M.-C. 1993. Enhanced C-ERBB-2/Neu Expression in Human Ovarian Cancer Cells Correlates with More Severe Malignancy That Can Be Suppressed by E1a. *Cancer Res,* 53**,** 891-98.

YU, S.-W.; WANG, H.; POITRAS, M. F.; COOMBS, C.; BOWERS, W. J.; FEDEROFF, H. J.; POIRIER, G. G.; DAWSON, T. M. & DAWSON, V. L. 2002. Mediation of Poly(ADP-Ribose) Polymerase-1-Dependent Cell Death by Apoptosis-Inducing Factor. *Science,* 297**,** 259-63.

YUAN, J.; NARAYANAN, L.; ROCKWELL, S. & GLAZER, P. M. 2000. Diminished DNA Repair and Elevated Mutagenesis in Mammalian Cells Exposed to Hypoxia and Low Ph. *Cancer Res,* 60**,** 4372-76.

YUAN, J.; SHAHAM, S.; LEDOUX, S.; ELLIS, H. M. & HORVITZ, H. R. 1993. The C. Elegans Cell Death Gene CED-3 Encodes a Protein Similar to Mammalian Interleukin-1β-Converting Enzyme. *Cell,* 75**,** 641-52.

YUE, C.-H.; CHIU, Y.-W.; TUNG, J.-N.; TZANG, B.-S.; SHIU, J.-J.; HUANG, W.-H.; LIU, J.-Y. & HWANG, J.-M. 2012. Expression of Protein Kinase C Alpha and the MZF-1 and ELK-1 Transcription Factors in Human Breast Cancer Cells. *Chin J Physiol,* 55**,** 31-36.

YUE, T.-L.; WANG, X.; LOUDEN, C. S.; GUPTA, S.; PILLARISETTI, K.; GU, J.-L.; HART, T. K.; LYSKO, P. G. & FEUERSTEIN, G. Z. 1997. 2-Methoxyestradiol, an Endogenous Estrogen Metabolite, Induces Apoptosis in Endothelial Cells and Inhibits Angiogenesis: Possible Role for Stress-Activated Protein Kinase Signaling Pathway and Fas Expression. *Mol Pharmacol,* 51**,** 951-62.

ZAMZAMI, N.; MARCHETTI, P.; CASTEDO, M.; DECAUDIN, D.; MACHO, A.; HIRSCH, T.; SUSIN, S. A.; PETIT, P. X.; MIGNOTTE, B. & KROEMER, G. 1995. Sequential Reduction of Mitochondrial Transmembrane Potential and Generation of Reactive Oxygen Species in Early Programmed Cell Death. *J Exp Med,* 182**,** 367-77.

ZHA, B. S.; STUDER, E. J.; ZHOU, H.; HYLEMON, P. B.; ZHA, W. & PANDAK, W. 2011. *Highly Active Antiretroviral Therapy (Haart) and Metabolic Complications*, INTECH Open Access Publisher.

ZHANG, F. & AFT, R. L. 2009. Chemosensitizing and Cytotoxic Effects of 2-Deoxy-D-Glucose on Breast Cancer Cells. *J Cancer Res Ther,* 5**,** 41.

ZHANG, J.; LU, A.; LI, L.; YUE, J. & LU, Y. 2010. P16 Modulates VEGF Expression Via Its Interaction with HIF-1α in Breast Cancer Cells. *Cancer Invest,* 28**,** 588-97.

ZHONG, L.; CHEN, F.-Y.; WANG, H.-R.; TEN, Y.; WANG, C. & OUYANG, R.-R. 2006. Effects of Quercetin on Morphology and Vegf Secretion of Leukemia Cells NB4 in Vitro. *Zhonghua Zhong Liu Za Zhi,* 28**,** 25-27.

ZHU, W.; QIN, W.; BRADLEY, P.; WESSEL, A.; PUCKETT, C. L. & SAUTER, E. R. 2005a. Mitochondrial DNA Mutations in Breast Cancer Tissue and in Matched Nipple Aspirate Fluid. *Carcinogenesis,* 26**,** 145-52.

ZHU, Z.; JIANG, W.; MCGINLEY, J. N. & THOMPSON, H. J. 2005b. 2-Deoxyglucose as an Energy Restriction Mimetic Agent: Effects on Mammary Carcinogenesis and on Mammary Tumor Cell Growth in Vitro. *Cancer Res,* 65**,** 7023-30.

Addendum 1: Approval letter from the Faculty of Health Sciences Research Ethics Committee of the University of Pretoria

The Research Ethics Committee, Faculty Health Sciences, University of Pretoria complies with ICH-GCP guidelines and has US Federal wide Assurance.
- FWA 00002567 Aperoved do 22 May 2002 and Expires 20 Oct 2016.
- IRB 0000 2235 IORG0001762 Approved do 13/04/2011 and Expires 13/04/2014.

UNIVERSITEIT VAN PRETORIA
UNIVERSITY OF PRETORIA
YUNIBESITHI YA PRETORIA

Faculty of Health Sciences Research Ethics Committee

7/08/2013

Approval Notice
New Application

Ethics Reference No.: 307/2013

Title: Exploit ng drug synergism to extend the application of oestrone analogues

Dear Ms Alet van Tonder

The **New Application** for your research received July 2013, was approved by the Faculty of Health Sciences Research Ethics Committee on the 7/08/2013.

Please note the following about your ethics approval:
- Ethics Approval is valid for 3 years.
- Please remember to use your protocol number (307/2013) on any documents or correspondence with the Research Ethics Committee regarding your research.
- Please note that the Research Ethics Committee may ask further questions, seek additional information, require further modification, or monitor the conduct of your research.

Ethics approval is subject to the following:
Standard Conditions:
- The ethics approval is conditional on the receipt of 6 monthly written Progress Reports, and
- The ethics approval is conditional on the research being conducted as stipulated by the details of all documents submitted to the Committee. In the event that a further need arises to change who the investigators are, the methods or any other aspect, such changes must be submitted as an Amendment for approval by the Committee.

The Faculty of Health Sciences Research Ethics Committee complies with the SA National Act 61 of 2003 as it pertains to health research and the United States Code of Federal Regulations Title 45 and 46. This committee abides by the ethical norms and principles for research, established by the Declaration of Helsinki, the South African Medical Research Council Guidelines as well as the Guidelines for Ethical Research: Principles Structures and Processes 2004 (Department of Health).

We wish you the best with your research.

Yours sincerely

Professor Werdie (CW) Van Staden
MBChB MMed(Psych) MD FCPsych FTCL UPLM
Chairperson: Faculty of Health Sciences Research Ethics Committee

☎ 012 354 1677 🖷 0866516047 ✉ deepeka.behari@up.ac.za 🌐 http://www.healthethics-up.co.za
✉ Private Bag X323, Arcadia, 0007 - 31 Bophelo Road, HW Snyman South Building Level 2, Room 2.33, Gezina, Pretoria

Addendum 2: User agreement for EA.hy926 hybrid endothelial cells

UNC
LINEBERGER COMPREHENSIVE CANCER CENTER
N.C. CANCER HOSPITAL

AGREEMENT For Single User Distribution of EA.hy926 CELLS

FROM: Steve Oglesbee representing Dr. Cora-Jean S. Edgell
TO: Dr AD Cromarty of the Pharmacology Department of the University of Pretoria, Pretoria, South Africa.
DATE: 30 January 2013
RE: General Terms for the Transfer of the EA.hy926 Cell Line

In order to avoid conflicts of interest, and because of potential commercial applications for this cell line, each investigator who requests EA.hy926 cells must agree to the conditions as specified below.

Please sign, make a copy for your own records, and return the original to the Tissue Culture Facility, attention Steve Oglesbee.

The EA.hy926 cells will be used in this lab for studies regarding:

cytotoxicity and angiogenesis studies.

The University of North Carolina at Chapel Hill and the Tissue Culture Facility are not-for-profit, and the use of this cell line or its derivatives are not allowed to be used for commercial purposes without prior successful negotiation and a signed licensing agreement between the appropriate party(s) and UNC. Any such agreement will be negotiated with the UNC Office of Technology Development (OTD). Use of this cell line by for-profit institutions for basic research and NOT FOR USE IN COMMERCIAL APPLICATIONS can also be accommodated but an additional fee will be imposed. (Please inquire about this specific situation).

I, Dr AD Cromarty, understand and agree with the above restrictions for use and subsequent distribution and I will be responsible for preventing this cell line from being passed on to other investigators outside my authority.

AD Cromarty

Signature:
Research Coordinator: Pharmacology Department University of Pretoria

Date: 30 January 2013

Addendum 3: Research outputs

National conference presentations

Van Tonder A, Jouber tAM, Cromarty AD. Die Sulforhodamien b sitotoksisiteitstoets in vergelyking met drie algemene sitotoksisiteitstoetse. Suid-Afrikaanse Akademie vir Wetenskap en Kuns, Potchefstroom. 5 October 2012.

Van Tonder A, Joubert AM, Cromarty AD. Comparison of four cytotoxicity assays and their interaction with glycolysis inhibitors. 46th Annual Congress of the South African Society of Basic and Clinical Pharmacology in association with the Department of Family Medicine and Toxicology Society of South Africa. Pretoria. 29 September – 2 October 2012.

Van Tonder A, Joubert AM, Cromarty AD. Combination of hexokinase inhibitors with oestrone analogues on the growth of MCF-7 breast adenocarcinoma cells. 41stConference of the Physiology Society of Southern Africa. 15 – 18 September 2013.

Van Tonder A, Joubert AM, Cromarty AD. Kombinasies van inhibeerders van glukosedraers en estroonanaloë op borskankersellyne.The Annual Congress of the Division Biological Sciences, Pretoria. 16 October 2013.

Van Tonder A, Joubert AM, Cromarty AD. Effects of synergistic combinations of oestrone analogues and quercetin on an *in vitro* breast cancer model.Pharmacology and Toxicology Congress, Johannesburg. 31 August – 2 September 2015.

International conference presentations

Van Tonder A, Joubert AM, Cromarty AD. Synergistic combinations between oestrone analogues and glycolysis inhibitors lonidamine and indinavir on MDA-MB-231 breast adenocarcinoma cells. 17th World Congress of Basic and Clinical Pharmacology, Cape Town. 13-18 July 2014.

Publications

Original research articles

Van Tonder A, Joubert AM, Cromarty AD. 2015. Limitations of the 3-(4,5-dimethylthiazol-2-yl)-2,5-diphenyl-2H-tetrazolium bromide (MTT) assay when compared to three commonly used cell enumeration assays. *BMC Res Notes,* 8 (47), 1-10.

Published conference abstracts

Van Tonder A, Joubert AM, Cromarty AD. 2014. Synergistic combinations between oestrone analogues and glycolysis inhibitors lonidamine and indinavir on MDA-MB-231 breast adenocarcinoma cells. *Basic Clin Pharmacol Toxicol,* 115, Supplement 1 abstract number 488.

Van Tonder A, Joubert AM, Cromarty AD. 2014. Combination of glucose transporter inhibitors and oestrone analogues on breast cancer cells. *S-Afr Tydskr Natuurwet Tegnol* 33(1). DOI: 10.4102/satnt.v33i1.1263.

Van Tonder A, Joubert AM, Cromarty AD. 2014. The Sulforhodamine B Assay in comparison with three commonly used cytotoxicity assays. *S-Afr Tydskr Natuurwet Tegnol* 33(1). DOI:10.4102/satnt.v33i1.1216.